



# Developmental Anatomy of Craniofacial Skin, Fat, and Fascia

# 11

Michael H. Carstens

## Introduction

Craniofacial skin is surprisingly diverse. Depending upon the tissue source, the cutaneous coverage of the head and neck has nine different developmental zones. Why should we care about the neuromeric map of skin? The primary importance of this topic is to understand the interactions between epithelium and mesenchyme so important in specifying dermal appendages, teeth, and membranous craniofacial bones and cartilages. It also lends itself to appreciating the pathology of syndromes in which mesenchymal defects are seen in association with characteristic cutaneous manifestations (e.g. the blue sclera of Osgood-Schlatter or the facial clefts seen in congenital ichthyosis). The neuromeric map of dermis (and neural crest) is fundamental to the assembly of the meninges and craniofacial blood vessels. Failure of fronto-orbital development seen in trigonocephaly involves interaction between caudal prosencephalic dermis, r1 dura and r1 neural crest. Associated problems with neural crest pericytes required for proper development of transdural blood vessels may contribute to the neuropathology (developmental delay) seen in this condition. Finally, our knowledge of anatomy is enriched when we understand the developmental diversity of human skin.

As we have previously seen, gastrulation creates a trilaminar embryo organized along its axis into neuromeric zones, beginning at r0-r1 (henceforth referred to as r1) and proceeding backwards. Endoderm and mesoderm associated with each neuromeric level share a common homeotic expression pattern. A primitive “fate map” is laid out which is roughly Cartesian in nature. Recall that the embryo at the end of gastrulation is an ovoid disc. Emanating from the midline, these mesomeric–endomeric “stripes” fan out from both sides beneath the epiblast.

Until now, nothing has been said about the post-gastrulation state of ectoderm. Recall that one is not permitted to use this term loosely. *Ectoderm is strictly those epiblast cells that remain behind after the process of gastrulation has been completed.* Thus, ectoderm, because it has not undergone gastrulation, is *not* intrinsically neuromeric. It will acquire a neuromeric definition by virtue of the mesenchyme which comes to lie beneath its surface. *Hox* genes expressed by dermis eventually appear in the epidermis. Because skin is a compound organ, with the epidermis derived from ectoderm or neural crest, and the dermis from either neural crest or mesoderm, we shall explore both layers separately, and then together.

## Non-neural Ectoderm

### Models of Ectodermal Organization

Gastrulation creates a trilaminar embryo. The process begins at level r0-r1 and proceeds caudally. The first wave of cells at day 14 displaces the hypoblast or primitive endoderm (tan) to become *definitive intraembryonic endoderm* (yellow). At 16 days a second wave pushes its way in between the epiblast and endoderm to create intraembryonic mesoderm, IEM (red). Residual epiblast is neural (pink), unless it receives signals from the underlying mesoderm, in which case it becomes non-neural ectoderm (blue). Hypoblast gets pushed out of the way to become *extraembryonic endoderm*, EEE; it forms the yolk sac from the outer wall of which develops *extra-embryonic mesoderm*, EEM. Blood islands in the EEM form the endothelial cells of the vascular system and the precursors of hematopoietic cells. EEM also spread dorsally over the top of the embryo, thereby becoming interposed between the extra-embryonic ectoderm, that is, the amnion, and the trophoblastic tissues. Since the vascular system develops in mesoderm, the continuity between the EEM and the IEM ensures connection with the placenta and establishes life support [1].

M. H. Carstens (✉)  
Wake Forest Institute of Regenerative Medicine, Wake Forest University, Winston-Salem, NC, USA  
e-mail: [mcarsten@wakehealth.edu](mailto:mcarsten@wakehealth.edu)

## Common Neural Plate Model: Neural Border Zone

In the model, a binary choice is made at the time of gastrulation, in which the embryonic ectoderm is subdivided into two domains: the non-neuronal ectoderm and neural ectoderm. They give rise to the epidermis and central nervous system (CNS), respectively. At the boundary between these two domains lies a third: the neural border zone (NBZ). This domain consists of two precursor fields which gives rise to two distinct cell populations. Within the NBZ, the neural crest region lies medial; lateral to it is pre-placodal region. These are established in response to signals mediated by BMPs, Wnt, and FGFs. The response of each territory to these signals is different. In the PPR, members of the Six and Eya families, neural crest-specific transcription factors, thus consolidating a placode development program. Next, the PPR becomes further subdivided into distinct placodal territory, each one with a specific menu of transcription factors that will lead to specific sensory tissue. Thus, pre-placodal region segregates into individual cranial placodes: the ade-

nohypophyseal, olfactory, lens, trigeminal, lateral line, otic, and epibranchial placodes (from anterior to posterior). Although these are critical for craniofacial development, they are not the end of the story. Another type of placode, found throughout the skin, is essential for the development of hair, and it is these epidermal placodes that we shall now direct our attention (Fig. 11.1).

## Binary Competence Model

Ectodermal development can be conceptualized by a binary competence model proposed by Schlosser et al., in which only neural ectoderm is competent to form neural crest, while only non-neural ectoderm is competent to develop into placodal fates. Furthermore, these fates depend upon the physical location of the target cells within the NNE [The reader is referred to Pathy, Pieper, and Schlosser for additional references.] (Fig. 11.2).

Prior to gastrulation, ectoderm is competent to generate all ectodermal fates, but during gastrulation the competence to form neural crest becomes restricted to dorsal ectoderm,

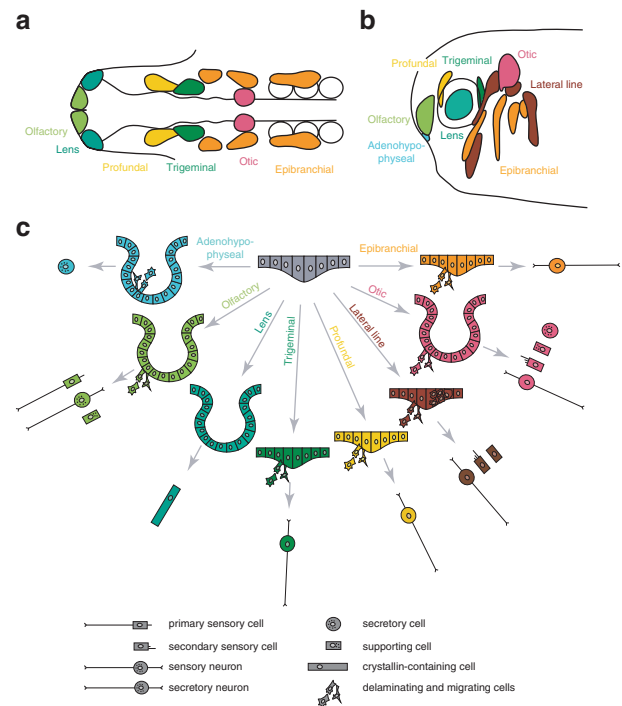
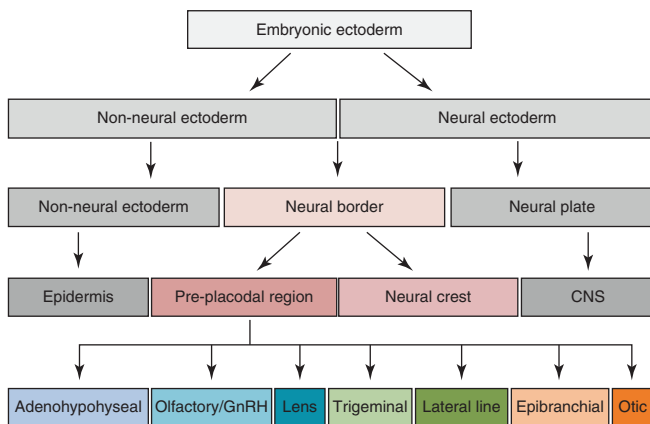


**Fig. 11.1** Placodeal development: common neural plate model. Gastrulation creates a trilaminar embryo. At its conclusion the ectoderm remaining behind, the epiblast, makes fundamental choices. As to a neural versus non-neural fate. Fundamental for production of skin is the distribution of 3 components. (1) Neural crest cells from r0 to r11 produce the pericytes and pigment of craniofacial skin. Neural crest from the remaining neuromeres is primarily pigmentary. (1) Non-neural crest ectomesenchymal precursors called pre-pericytes interact with mesoderm of the somites to produce the adipose tissues of the body. The remain of the body fascia and I and placodal precursors. (3) Placodal cells are positioned outboard to neural crest. There are two models of the distribution of organization placodes: (1) the common neural plate

model; and (2) the binary competence model. LEFT: Common neural plate assumes neural ectoderm subdivides between CNS and an intermediate neural border zone (IBZ) which is further divided into two strips with neural crest medial and placodes lateral. Epidermal NNE is considered distinct. RIGHT: Outboard NNE produces distinct craniofacial placodes which interacts with neural crest to form sensory ganglia of the face. Left: [Reprinted from Saint Jennet JP, Moody SA. Establishing the pre-placodal region and breaking it into placodes with distinct identities. *Dev Biol* 2014; 389(1): 13–27. With permission from Elsevier.]. Right: [Reprinted from Pathy C, Schlosser G, Shimeld SM. The evolutionary history of vertebrate placodes I: Cell type evolution. *Devel Biol* 2014; 389(1): 82–97. With permission from Elsevier]

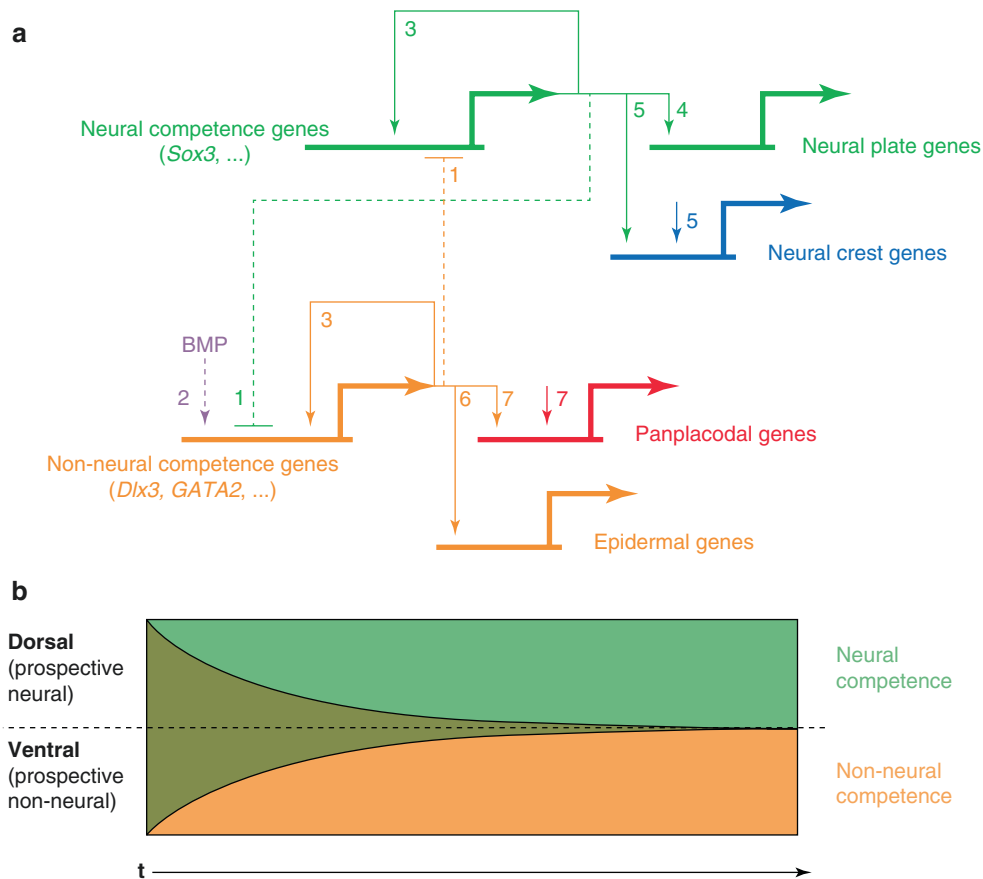


**Fig. 11.2** Model for regulation of ectodermal competence. **(a)** Genes that promote non-neural competence, including *Dlx3* and *GATA2* (orange), and those that promote non-neural competence, probably including *Sox3* (green), cross-repress each others transcription (1, broken lines indicate indirect effects). Expression of non-neural competence genes is initially dependent on BMP signaling (2). In the presence of BMP, transcription of non-neural competence genes is therefore promoted over neural competence genes, whereas the reverse is true in the absence of BMP. However, persistent expression of these genes may lead to their autoactivation (3), thereby making their expression resilient to repression and BMP independent. Neural competence factors promote transcription of neural plate genes (4) or, in the presence of

additional signals such as BMP, Wnt, and FGF (5), neural crest genes. Non-neural competence factors promote transcription of epidermal genes (6) or, in the presence of additional signals such as BMP inhibitors, FGFs, and Wnt inhibitors (7), panplacodal and placodal genes. **(b)** Owing to the dorsal secretion of BMP antagonists and crossrepressive interactions among competence genes, their initially overlapping expression domains will resolve into two distinct territories over time (t). [Reprinted from Pieper M, Ahrens K, Rink E, Peter A, Schlosser G. Differential distribution of competence for neural crest induction to non-neural and neural ectoderm. *Development* 2012; 139: 1175–1187. With permission from The Company of Biologists, Ltd.]

whereas the competence to express the panplacodal marker *Six1* becomes ventrally restricted. These changes parallel the dorsal restriction of neural competence, suggesting that, during gastrulation, two mutually exclusive competence territories are established: a dorsal neural territory that has *neural plate as a default state* but can be induced to form neural crest; and a ventral non-neural territory that has *epidermis as default state* but can be induced to form pre-placodal ectoderm. These findings confirm the predictions of the ‘binary competence model’; but do not support models according to which a common neural plate border state is first established from which neural crest and placodes are subsequently induced [1].

Although ectoderm from early gastrulae can form all ectodermal fates, it will preferentially differentiate into neural plate or neural crest rather than panplacodal fates if exposed to signals in the neural plate border region, indicating that *neural competence overrules non-neural competence*. This suggests, that neural competence is the default state.

The Schlosser model is as follows:

- In ventral ectoderm, BMP expression promotes the expression of non-neural competence genes (e.g. *Dlx3* and *GATA2*; see below), which repress neural competence genes.

- In dorsal ectoderm, BMP inhibition relieves this repression of neural competence genes.
- Transcriptional cross-repression between neural and non-neural competence factors ensures stable boundaries.
- At the beginning of gastrulation (stage 6), the expression of neural and non-neural competence genes is still labile and BMP dependent, and the entire ectoderm, therefore, maintains neural as well as non-neural competence.
- By the end of gastrulation (stage 7), however, their expression becomes stabilized and BMP independent, e.g. due to auto-activation.
- At neural plate stages (stage 8).
  - neural competence factors promote transcription of *neural plate genes* or—in the presence of signals such as BMP, Wnt, and FGF—*neural crest genes*.
  - non-neural competence factors promote transcription of epidermal or—in the presence of signals such as BMP inhibitors, FGFs and Wnt inhibitors—*panplacodal genes*, whereas.

In agreement with this model, it has recently been shown that induction of neural crest and neural plate requires low BMP levels during gastrulation [2], whereas induction of many ventral transcription factors, pre-placodal ectoderm and epidermis requires high BMP levels. From neural plate stages onwards, the expression of many ventrally localized transcription factors becomes BMP independent, and BMP requirements for neural crest and pan-placodal induction change. BMP inhibition is now required for the induction of pre-placodal ectoderm, whereas some BMP signaling is required for neural crest induction. Because BMP signaling recedes from the neural plate border from stage 13 onwards, these later phase BMP requirements also explain why stage 12 and stage 13 NBs provide better-inducing environments for neural crest and placodes.

### Epidermal Placodes: Origins

Hair is a defining characteristic of all mammals; it develops from a series of interactions between dermis and epidermis, the first step of which is the induction by the former of discrete epidermal placodes, one for each hair shaft. At the end of this chapter, we shall consider aspects of hair development and evolution but, for now, our focus is on the placodes themselves. Where did they come from? Preplacodal ectoderm directly abuts epidermal ectoderm. Neural crest cells and placodal cells both arise from the NBZ and likely share common characteristics. One possibility is that cells from the PPR have a previously unappreciated migratory ability and therefore distribute themselves into the epidermal ectoderm. Another (more likely) possibility is that placodal potential is intrinsic to all cells within the epidermal ectoderm and that

these make their appearance when appropriately stimulated from signals by mesenchymal cells in the dermis. Although hair distribution is generally uniform, unusual patterns are seen, characterized by the absence or excess of hair follicles. Such phenomena can be explained by either model but they can also occur as the result of localized deficits or excess of signals from the embryonic pre-dermal mesenchyme. In any case, the physical juxtaposition of epidermal ectoderm with the lateral region of the NBZ creates a situation in which transcription factors can have differential effects on primitive ectodermal cells depending on their physical location in the embryo.

The existence of cells with placodal potential in the epidermis thus has two different explanations, depending on one's model of ectodermal organization.

The common neural plate model presents a sorting-out in which neural crest genes with neural crest cells sort out with CNS genes and CNS cells. The so-called “third zone” or NBZ does not admix placodal genes with epidermal genes. The binary choice of NBZ cells to become neural crest versus placode cells depends on the physical location of the cells (with placodes being further lateral). This deficit means that either migration must occur, or the original model of segregation from the NBZ is incomplete (Fig. 11.1) (Saint Jenet, 2014).

The binary competence model also presents a binary choice in which neural crest genes sort out with neural plate cells and pan-placodal genes sort out with epidermal genes. The appearance of epidermal placodes during development can occur in two potential scenarios (Fig. 11.2) [3].

- Skin is a mixture of placodal (P) cells admixed with epidermal (E) cells. Thus, MSCs produce signals that selectively trigger the P cells and not the E cells.
- Placodal cells and epidermal cells are one and the same.
- The “decision” by a skin cell to adopt a P fate and become an epidermal placode is a matter of its immediate proximity to a local diffusion gradient of signals produced by MSCs.

### Phylogeny of Placodes

The evolution of placode faithfully reflects increasing degrees of genetic complexity. Innovations in ectodermal patterning came about from new mechanisms and the origin of new cell types (Fig. 11.3). Important nodes are numbered and the key depicts which characters can be traced to each node. Character origination events whose placement on the tree is controversial are indicated by a question mark. AP: anteroposterior; DV: dorsoventral; TF: transcription factor [4].

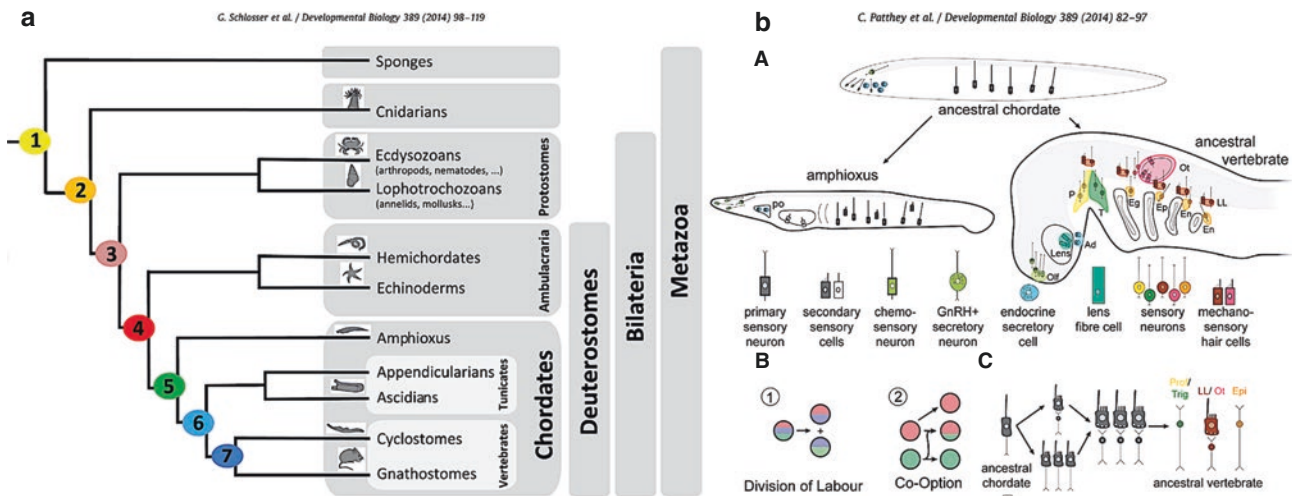


**Fig. 11.3** Phylogeny of placodes. Left (a): Evolutionary steps in placodal patterning and origin of new cell types. The important nodes are numbers: (1). Metazoa common ancestor (yellow) (2). Cnidarian-Bilateria common ancestor (orange) (3). Bilaterian common ancestor (pink) (4). Deuterostome common ancestor (red) (5). Chordate common ancestor (green) (6). Olfactores (tunicate+vertebrate) common ancestor (blue) (7). Vertebrate common ancestor (purple). Right (b): Evolution of placode-derived cell types. (A) Placode-related cell types are believed to be present in the chordate ancestor, and the cell types derived from them. (B) Novel cell types appear in two possible ways. In the process of *division of labor*, a cell type becomes two sister cell types by splitting part of the transcriptomes between the two daughter cell types. In the process of *gene network co-option*, a new cell type originates by merging the transcriptome of two existing cell types. (C) Scenarios for the evolution of somatosensory (SSN: trigeminal/profundal, otic/lateral line) and viscerosensory (VSN: epi-

branchial) neurons from a putative ciliated primary sensory neuron. (1) The primary sensory cell splits into a secondary sensory cell and an afferent neuron by segregation of functions. Resulting neurons and sensory cells become three distinct sister cells corresponding to the trigeminal/profundal, otic/lateral le, and epibranchial-derived neurons. (2), Three sister cell types first evolve as primary sensory neurons. Then the primary sensory cells split into secondary sensory cells and afferent neurons. Finally, in both scenarios, the secondary sensory cells of the trigeminal/profundal and epibranchial, but not otic/lateral line systems are lost. Left: [Reprinted from Schlosser G, Patthey C, Shimeld SM. The evolutionary history of vertebrate placodes II. Evolution of ectodermal patterning. *Devel Biol* 2014; 389(1): 98–119. With permission from Elsevier.]. Right: [Reprinted from Patthey C, Schlosser G, The evolutionary history of vertebrate placodes I: Cell type evolution. *Devel Biol* 2014; 389(1): 82–97. With permission from Elsevier]

### Summary of Placodal Evolution

#### 1. Metazoan common ancestor.

- Primitive genes involved in placode formation: *Eya*, *Six1/2*, *PaxB*.

#### 2. Cnidarian-bilaterian common ancestor.

- Most of the genes involved in placode development are present: *Six3/6*, *Six 4/5*, *Fox1*, *PitX*.
- Primary sensory cells (mechano-, chemo-, photo-receptors) with differentiation dependent on: *POU/IVM PaxB*, *Six1/2*, *Eya*.
- Neurosecretory cells present for the first time.
- Body axis determination depends on *Wnt*, *BMP*.
- Some regionalized expressions in the ectoderm of TFs (eg. *Hox*, *Six3/6*).

#### 3. Bilaterian common ancestor.

- Dorsal-ventral ectodermal patterning depending on TFs.
  - ventral: low *BMP* (*SoxB*),

- dorsal: high *BMP* (*Msx*, *Dlx*).

- CNS is centralized on the ventral side.
- AP ectodermal patterning: *Wnt*-dependent TFs.
  - anterior: *Six3/6*, *fezf*, *Emx*, *Otx*,
  - posterior: *Irxd*, *Gbx*, ***Hox***.
- Left-right patterning dependent on *Pitx*.

#### 4. Deuterostome common ancestor.

- Pharyngeal pouches: *Six1/2*, *Pax1/9*, *Eya*.

#### 5. Chordate common ancestor.

- Dorsoventral axis now inverts.
- Segregation of ectoderm.
  - dorsal neural ectoderm,
  - ventral: non-neural ectoderm,
  - neural ectoderm now contains *Pax6*, *Pax2/5/8*.
- Specialized border territory.
- Regionalized expression of *Pax6* and *Pax2/5/8*.
- New rostral neurosecretory area: *Six3/6*, *Pax1*, *Pit1*, *Lhx*, *Eye* (future).

6. Olfatores (Tunicates+Vertebrates) common ancestry.
  - Hair cell-like prototype secondary mechanosensory cells with cilium and microvillar collar.
  - New competence factors are recruited for non-neural ectoderm: *GATA1/2/3*.
  - New definition of roles for **FGF** and **BMP** in neural induction.
  - Non-neural border territory that is thickened: *Six1/2*, *Eya*, *Msx*, **Dlx**.
  - AP ectodermal programming now depends on Wnt, FGF, and RA.
  - New posterior ectodermal territories expressing: Fox, *Pax2/5/8*, *Six4/5*, *Eya*, *Islet*, *Six1/2* and **Eya** (anterior proto-placodal domain).
7. Vertebrate common ancestor.
  - New or highly developed cell types that are placode-specific:
    - neurosecretory cells of the adenohypophysis,
    - lens cells,
    - olfactory and vomeronasal receptors neurons,
    - somatosensory and viscerosensory neurons,
    - hair cells.
  - Recruitment of new competence factors for non-neural ectoderm: Fox.
  - **Neural crest cells** appear by recruitment of TFs from ectoderm (*AP2*) and mesoderm (*FoxD SoxE, Twist*).
  - Cranial placodes zones as focused areas of proliferating progenitor cells giving rise to cells and neurons.
  - **Cranial placodes proper**: adenohypophyseal, olfactory, lens, profundal (*V1*)/trigeminal (*V2-V3*), otic, lateral line, epibranchial.
  - New roles for *Six1/2* and *Eye* to control proliferation within placodes.
  - Recruitment of many AP-restricted TFs for new roles in placode specification.

## In Summation

The above discussion should make it clear that the human skin develops from several embryonic sources. The epidermis of the face is derived from non-neural ectoderm. Its adnexal elements develop either from a selective stimulus of epidermal cells by neural crest in the dermis or as a distinct population committed to a placodal fate. Facial dermis originated from neural crest, not mesoderm. Adnexal structures are distributed according to the neural crest coding of the trigeminal system, largely eschewing the *V1* distribution. Non-craniofacial epidermis is formed from non-neural ectoderm outlying the axial zones that give rise to neural crests and

placodes. It likewise contains cells with placodal competence. The dermis of this skin is mesodermal, arising from somites. Subcutaneous adipose tissue arises in all sites from mesenchymal precursors cells known as pre-pericytes. With these definitions and concepts in hand, we will now consider the components of the skin, subcutaneous tissues, and fascia.

---

## Skin: Epidermis and Appendages

Epidermis arises from two fundamentally different sources of tissue: brain and non-brain. Neural crest from the anterior forebrain (telencephalon) makes the frontonasal epidermis of the columella, nose, and forehead. All remaining epidermis of the face and body comes from the nonneural ectoderm in register with neuromeres from the hindbrain and backward.

---

## Sources of Epidermis: Neural Crest Versus Non-neural Ectoderm

### Neural Crest Epidermis

Recall that the forebrain, or prosencephalon, is constructed from developmental units called prosomeres. In the 2013 iteration of the Puelles model the anterior forebrain becomes telecephalon (the precursor of cortex), the eye fields, and the hypothalamus. These were formerly classified as prosomeres p6-p4 but the terminology has been dropped. Above anterior prosencephalon, *rostral neural folds* do not contain neural crest. Instead, they have specialized non-neural ectoderm (NNE), some of which form placodes and remainder frontonasal epidermis. The posterior prosencephalon develops from prosomeres p3 to p1 which contain prethalamus, thalamus, and post thalamus. Above the posterior prosencephalon, *caudal prosencephalic neural folds* contain neural crest (PNC) which produces the underlying frontonasal dermis. We shall describe how this lamination process happens shortly [Figs. 11.4, 11.5 and 11.6; neuromeric map showing prosencephalic non-neural ectoderm (epidermis) and prosencephalic neural crest (dermis)].

Because there the brain has no somatic sensory nerves forward from r1, all sensation for the frontonasal skin must come from *V1*. *The anatomic distribution of neural crest epidermis is defined by that of V1*. And because forebrain neural crest is incapable of forming blood vessels, the entire blood supply of this unique skin will come from arteries programmed by *V1* sensory nerves. Indeed, the St*V1* arterial system represents an evolutionary “add-on” to the primitive ophthalmic artery.

**Fig. 11.4** Neuromeric model consists of 6 prosomeres (p1-p6), 2 mesomeres (m1-m2), and 12 rhombomeres (r0-r11). Underlying notochord from r1 backward imposes homeotic identity for each segment. From rhombomere 2 forward the alternative no-hox homeotic genes define the neuromeres. Gastrulation exposes migrating cells to homeotic imprinting from the notochord. Mesoderm produced by this process will provide a definition for the overlying ectoderm of its specific zone. [Courtesy of Michael Carstens, MD]

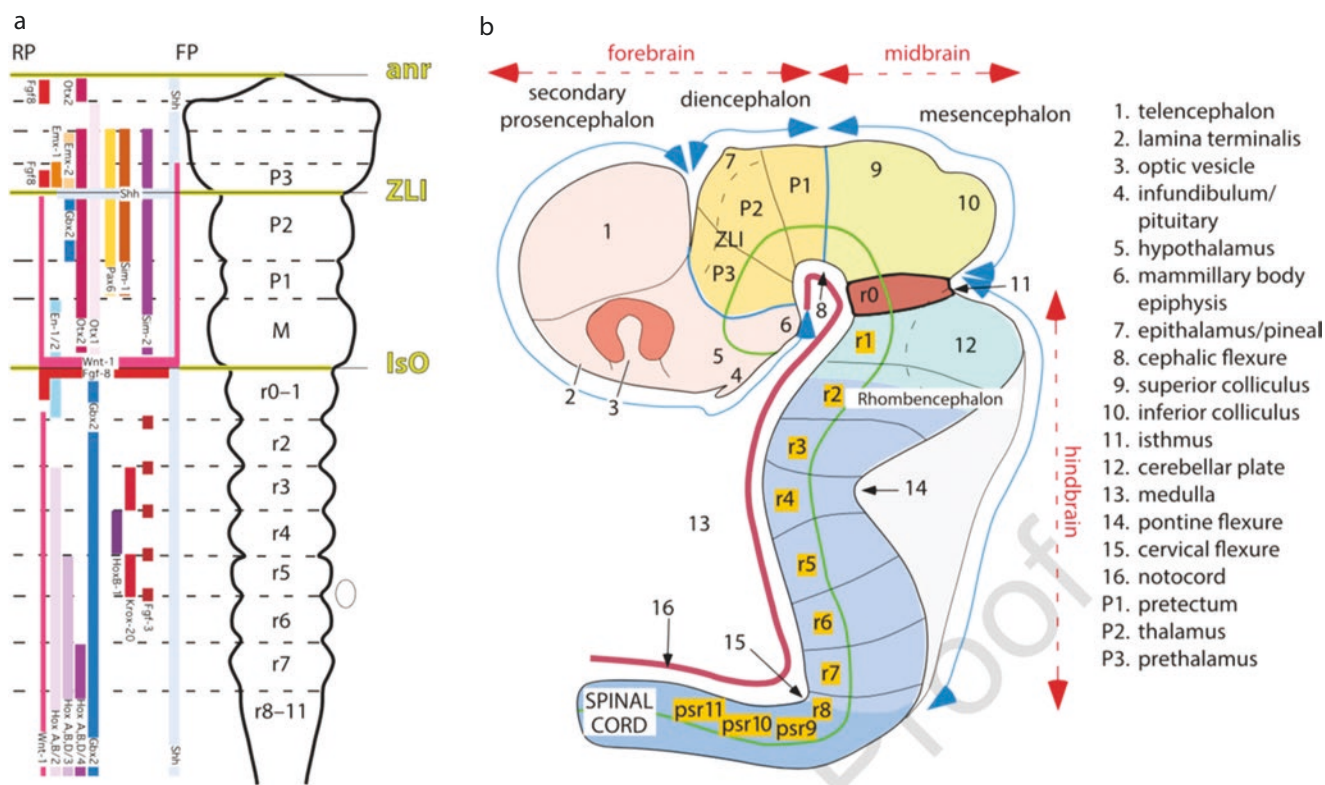
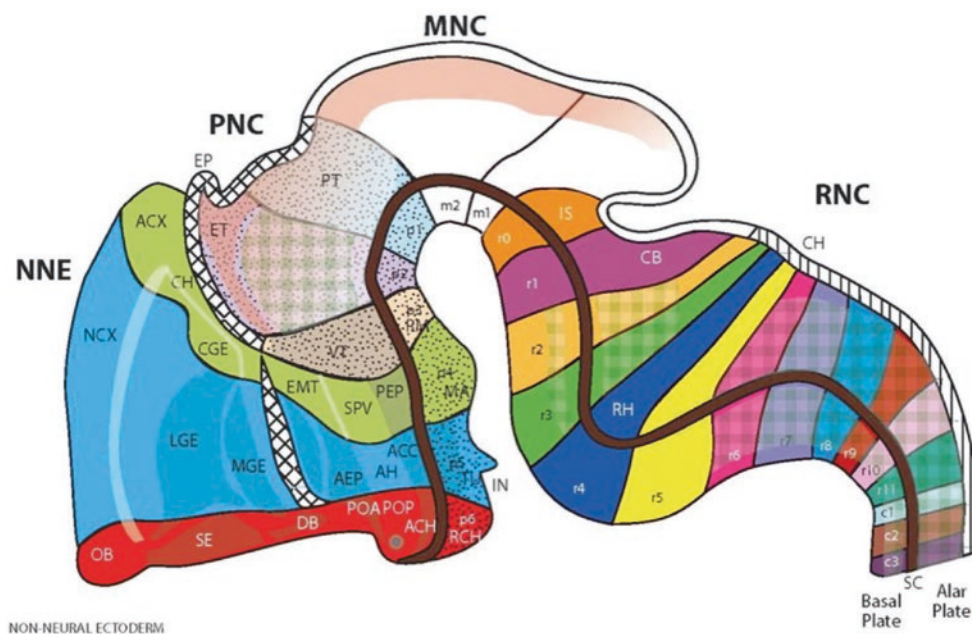


**Fig 11.5** Midbrain and forebrain maturation sequence. In the original Puelles model the maturation sequence of the midbrain and forebrain proceeds forward from r0. Developmental ES stages in the mouse correlate with Carnegie stages in humans.

- ES 8.5 = Stage 8 The neural plate induces an initially flat midbrain and forebrain. Note large size of the midbrain. Floor plate terminates at rostral hindbrain. Prechordal floorplate produces Sonic hedgehog (Shh). As stage 8 progresses, the forebrain and midbrain rise out of the plane and project forward. Isthmus not present.

- ES 10.5 = stage 12 Mesomeres and prosomeres are in place. Primary (mesencephalic) flexure positions head and face in front of rostral hindbrain, r1-r3. Shh localizes to rostral forebrain, p4-p6. Isthmus is now present.
- EX 12.5 = stage 16 Secondary (cervical flexure).

[Reprinted from Puelles L, Rubenstein JLR. Expression patterns of homeobox and other putative regulatory genes in the embryonic mouse forebrain suggest a neuromeric organization. *Trends Neurosci.* 1993;16(11): 472-479. With permission from Elsevier.]

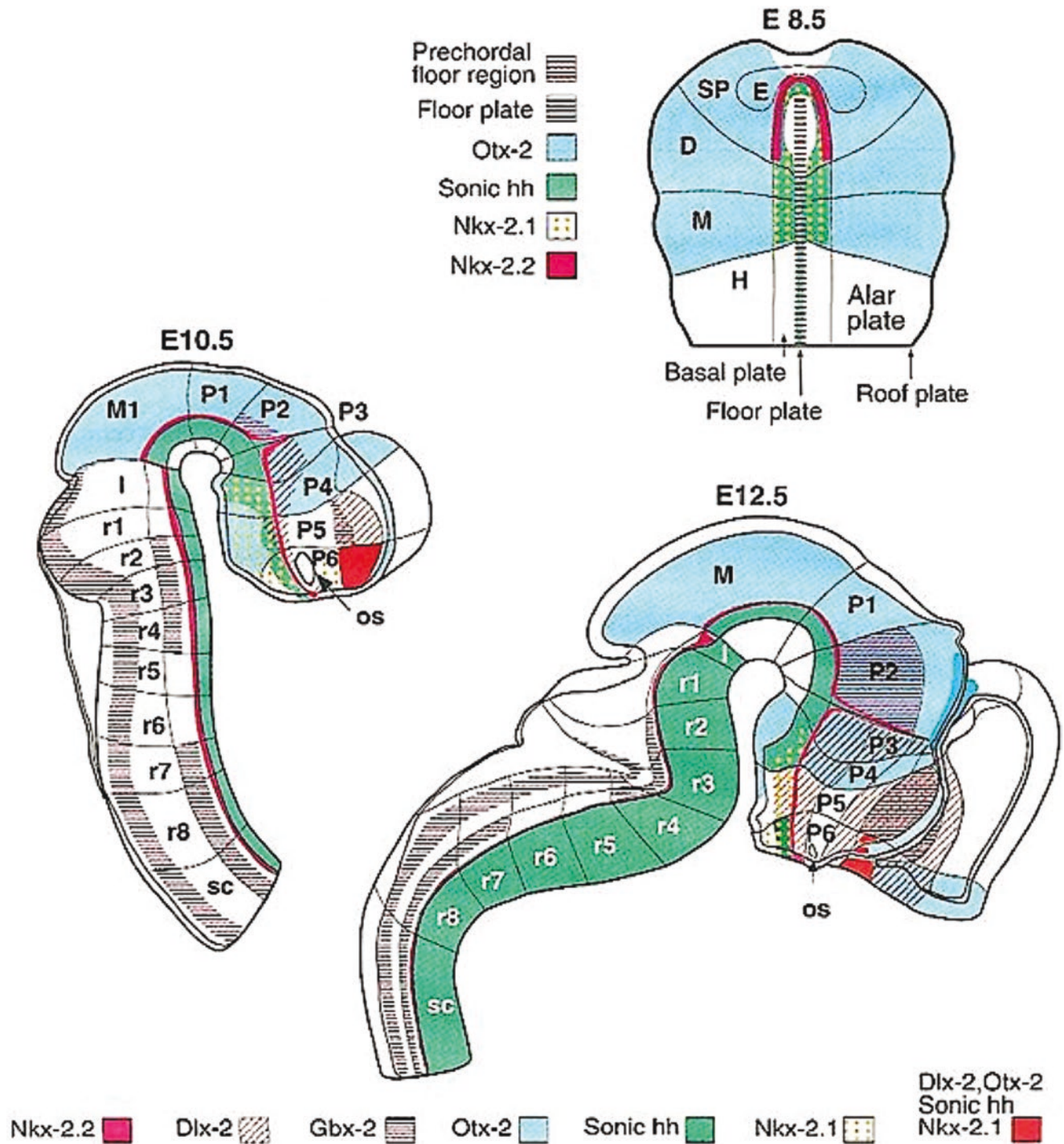


**Fig. 11.6 Embryonic brain regionalization explains the order of skin development.** Gene expression map supports the embryonic developmental sequence of mesoderm and neural crest migration. Note production by isthmus of *Wnt-1* and *Otx-2* for midbrain induction and *Fgf8* for cerebellum induction. Note that *Wnt-1* continues forward until

the p3 junction with secondary prosencephalon (the old p3-p4 junction). [Reprinted from Martinez S, Puelles E, Echevarria D. Ontogeny of the vertebrate nervous system. In: Galizia CG, Llego P-M (eds). Neurosciences. Berlin, Germany: Springer; 2013. with permission from Springer Nature]



## Ectodermal Epidermis

*Non-neural ectoderm* (NNE) produces epidermis covering the entire body except the frontonasal zone. NNE acquires its neuromeric identity indirectly as a consequence of gastrulation. These cell populations are sessile and do not enter the primitive streak thus, it has not come into contact with the notochord. Initially, it does not express homeotic genes. Later, under the influence of underlying mesoderm, positional *Hox* genes appear. Thus, *the neuromeric coding of the epidermis is dependent upon that of the dermis*. It is organized as *ectomeres* in register with the notochord from r1 backward. **Note:** The isthmus, r0, that lies in front of r1 and separates midbrain from hindbrain, produces prechordal mesendoderm and is not relevant for mapping of epidermis. The contribution of “pure” r1 non-neural ectoderm is probably limited to skin of the upper eyelid and the epithelium of the conjunctiva.

At the same time, important growth factors produced by epidermis are vital for the development of the dermis. Later in development, both skin and gut mucosa have important programming functions for their respective mesenchymal structures. Because dermis exists in equilibrium with epidermis, let’s explain why the skin-forming ectoderm represents “the layer left behind,” what is left over of the epiblast after gastrulation is complete.

### What Is the Origin of Ectoderm that Produces Epidermis?

During gastrulation, cells of the original primitive epiblast migrate through the primitive streak in two successive waves. The first population displaces the hypoblast laterally, creating two new structures. Cells remaining in the axial midline are known as the *mesendoderm*; these become the notochord, which in turn plays a crucial role in the organization of the overlying neural plate. Cells lateral to the midline produce the *definitive endoderm*. Following this, a second successive migration of epiblast cells exploits the potential space between epiblast and endoderm to create mesoderm. These newly-ingressed cells manufacture glycosaminoglycans retain water. The resultant edema separates the epiblast layer from endoderm, thus creating the space for mesoderm. Once gastrulation is complete, the remaining epiblast layer takes on a new name: ectoderm.

*The default expression of ectoderm, unless inhibited, is neural*. The next iteration of ectoderm is a gene-driven partition of the ectoderm into two distinct zones: *neural ectoderm*, which gives rise to the neural plate and future CNS and *non-neural ectoderm* (NNE), which gives rise to the

skin. The expression of neural fate is inhibited by two signals produced by mesoderm, BMP-4, and BMP-7. In the embryonic midline, Sonic hedgehog (*Shh*) produced by notochord antagonizes the inhibitory influence of BMP-4. This results in the induction of the floor plate. As one proceeds laterally from the midline, the *Shh* signal dies out; and the unopposed activity of BMP-4 and BMP-7 produced by the mesoderm results in NNE. Neural crest cells arise from the neural fold, an interface zone between NE and NNE.

## Development of Epidermis

At one month’s gestation the NNE is a thin layer of flat cells called *periderm*. Although the organization of underlying mesenchyme into a two-layered dermis does not take place until 12 weeks, a basement membrane layer that will give rise to postnatal epidermis and the more superficial periderm. The periderm reaches its apogee at ten weeks. Its main function is the exchange of water, electrolytes, and glucose with amniotic fluid. By sixteen weeks a basal germinative layer and an intermediate layer are identified. Periderm sloughs, producing squames in the amniotic fluid. These lead to the cellular debris seen covering the fetus at birth, the *vernix caseosa*.

As the germinative layer proliferates, successive layers of intermediate cells become interposed between it and the periderm. Initially, biosynthetic activity (as evidenced by glycogen granules) is present in all the layers but, over time, a reduction of activity occurs toward the surface leading to keratohyaline granules at 20 weeks (Fig. 11.7).

Differentiation of epidermal layers follows a spatio-temporal template. The cranial-caudal gradient reflects the spatial organization of the ectoderm after gastrulation is complete. The ectomeres overlying the pharyngeal arches develop before the cervical ectomeres. Thoracic epidermis matures before that of its lumbar counterpart. Furthermore, epidermal maturity follows the outward (ventral) development of neuro-angiosomes from the midline. Mid-axillary epidermis at any given neuromeric level matures before that of the ventral midline. Does this mean that epidermis is organized neuromerically? In a strict sense, it is not. The ectoderm remaining behind after the completion of gastrulation consists of broad geographic regions; these undoubtedly have differing genetic compositions. The epidermis overlying the future chest is distinct from that of the flanks. Furthermore, epidermal growth factors such as Fgf-8 exert a trophic effect on the underlying mesenchyme. When these are deficient, the skin itself is atrophic. This type of pathology is well illustrated by *cutis aplasia*.

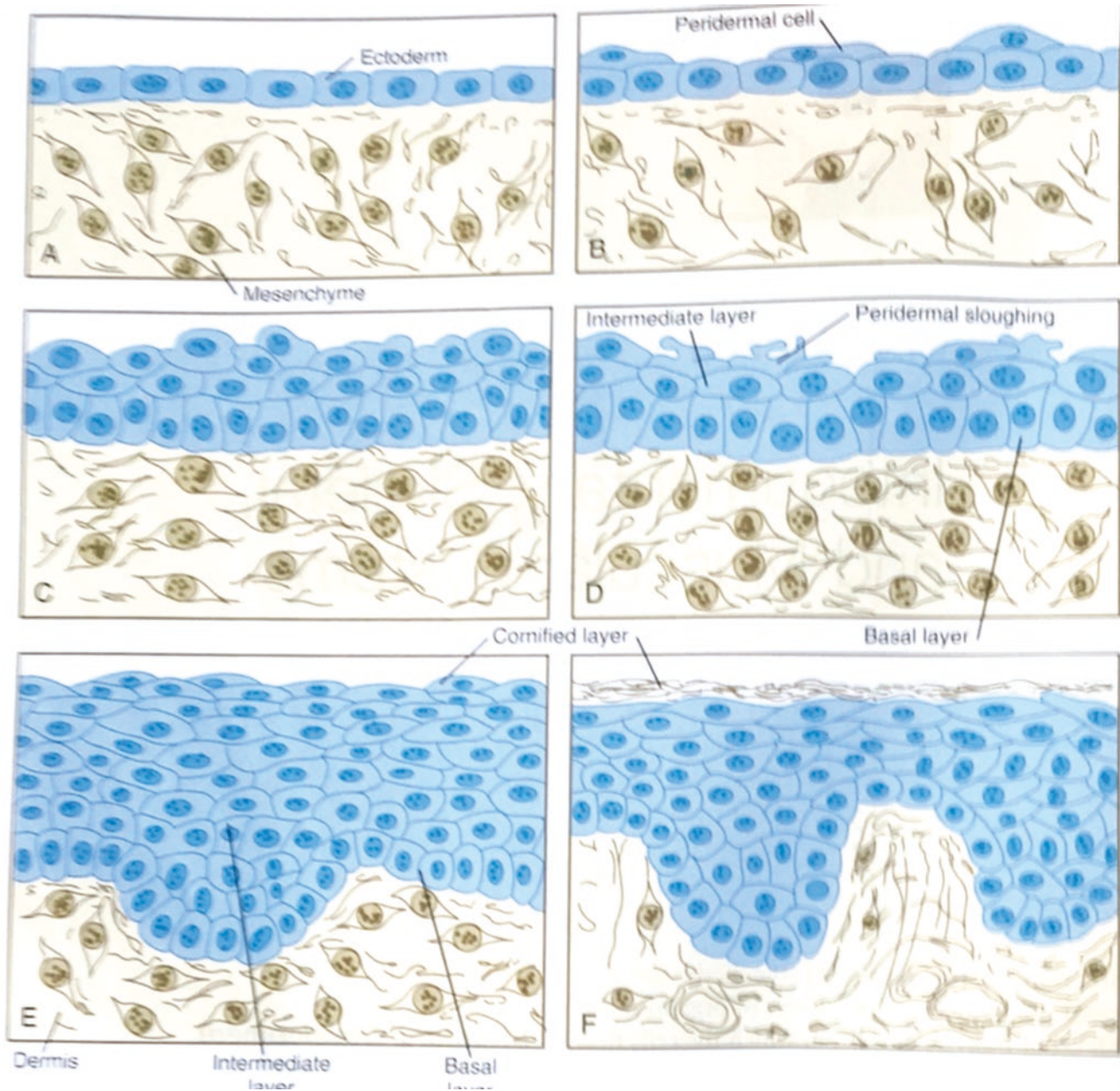


**Fig. 11.7** Histogenesis of human skin. (a) At one month non-neural ectoderm is single layer. (b) At two months flattened periderm cells appear on the surface of the NNE. (c) the NNE thickens. (d) The skin had three layers, a germinative, basal layer, an intermediate layer resulting from dividing stem cells in the basal layer, and periderm cells which

slough into the amniotic fluid. (e) Dermis is formally identified and the individual layers of epidermis are established. (f) Rete pegs are present. [Reprinted from Carlson BM. *Human Embryology and Developmental Biology*, sixth edition. St. Louis, MO: Elsevier; 2019. With permission from Elsevier]

## Components of Epidermis

The following specialized cells are present in epidermis. *Merkel cells* are modified keratinocytes found in the glabrous palms and soles. They appear at 8–12 weeks. Later on, they associate with dermal axon-Schwann cell complexes. *Langerhans cells* are derived from bone marrow. Development of hematopoietic population is very primitive,

and blood supply to skin via dermis is established by six weeks these cells appear in the epidermis as early as 6 weeks. Their function is immune surveillance. *Melanocytes* first appear in the cranial region at 8 weeks. The ratio of melanocytes to keratinocytes is controlled by the keratinocytes.

*Piloosebaceous units* appear at 9 weeks. They also follow a cranial-caudal developmental gradient. The *pre-germ* refers to localized collections of cells in the basal layer of epidermis. The *hair-germ* projects downward into mesenchyme.

Cells from the latter clump around the hair germ as the *dermal papilla*. Further downward growth of the hair germ engulfs the dermal papilla like a hand grasping a ball. This is the *bulbous peg*. Three attachments develop along the shaft: an upper apocrine gland (sometimes), a middle sebaceous gland, and a lower arrector pili muscle. These arise from mesenchyme under the influence of signals from differing regions of the shaft. Eccrine sweat glands arise when epidermal down-growths into dermis induce a mesenchymal *secretory coil*. Consider the remaining components of the skin and subcutaneous tissues.

---

## Skin: Dermis

Dermis is essential for epidermis. It provides physical support. The rete pegs are like Velcro® keeping the epidermis anchored. Ectoderm is incapable of making blood vessels. The subdermal plexus provides nutritional support. Innervation comes to the skin surface via the dermis, which also shelters. In reciprocal fashion, epidermis is essential for dermal development. It “instructs” underlying mesenchyme to become dermis.

Contact between epidermis and mesenchyme causes the latter to secrete a protein-rich matrix within which individual cell types develop. The matrix itself undergoes transformation with differential expression of glycosaminoglycans and collagens. At 3 months, major changes occur. Collagen becomes organized, epidermal appendages appear, and the neurovascular structures develop. Superficial dermal blood vessels result from the transformation of angiogenic MSCs. Nucleated RBCs appear at 6 weeks and the subpapillary plexus forms 2 weeks later. At 9–10 weeks a deeper *horizontal plexus* forms. Pericytes develop from neural crest MSCs. Capillary leak results in the pooling of extracellular proteinaceous fluid. MSCs organize around these pools forming encircling, interconnected channels. These will become lymphatics.

A great deal is known about epithelial-mesenchymal interactions. In the primordium of the face and limbs, chondrogenesis from MSCs within the dermis is prevented by the ectoderm. Dermal development also is epidermis dependent. Regional properties of dermis determine what appendages will be present or absent. At the same time, epidermis determines the morphology of the appendages and their cranial-caudal distribution.

---

## Neuromeric Identity of Skin: Dermatoma vs. Non-dermatoma

How do we assign skin a neuromeric identity? Is it embedded in the epidermis from the start or is it acquired from the underlying mesenchyme? Although epidermis has a regional

specification, *epidermis expresses homeobox gene products that originate in response to signals from dermis*. This makes intuitive sense because epidermis arises from those epiblast cells left behind after gastrulation has taken place. This “straggler” population is never been in physical contact with the primitive streak; thus, it has not been exposed to notochordal signals.

Epiblast “adventurer” cells that participate in gastrulation plunge down through the primitive node or streak, at which point they acquire the homeotic “bar code” of their neuromeric level of exit. Intraembryonic germ layers of endoderm and mesoderm will bear the same bar code. Thus, *the source material of dermis (mesoderm) imparts its neuromeric identity to the overlying epidermis*. Below the craniocervical junction, an orderly pattern of cutaneous innervation is seen along the dorsal (epaxial) skin, with the continuous representation of every neuromeric level, from c2 to s5.

This apparently tidy system has two anatomic problems. First, the innervation of craniofacial skin and mucosa has a *discontinuous* neuromeric pattern. Along the posterior scalp, ear, and lower jaw dermal zones originating from r3 hind-brain neural crest abut against dermis derived from cervical c2 to c3 paraxial mesoderm (PAM). Second, epaxial skin of the entire body has a continuous sensory innervation pattern representing all neuromeres from C2 to S5. In contrast, the hypaxial skin of the trunk has a *discontinuous* sensory innervation pattern, with neuromeres c5-t2 and l2 to s3 confined to the extremities. These apparent discrepancies can be readily understood using developmental principles (Figs. 11.8 and 11.9; neuromeric map of the skin).

Gastrulation is a very regular process. Initially, for every neuromere there is a corresponding swatch of mesoderm. Similarly, neural crest cells develop from every neuromeric level. Why then, is the sensory pattern of the head and neck discontinuous? Let’s begin by looking at classical teaching about somites. All somites are made up of paraxial mesoderm; they typically consist of three elements: (1) the *sclerotome* forms the axial skeleton, that is, the vertebra and rib; (2) the *myotome* forms the striated muscles of the body, with the exception of those developing from the first seven somitomeres; (3) and *dermatome* forms the neck, trunk, and extremities.

## The Mystery of the Fifth Somite

This orderly model applies only to somites from neuromeric level c2 backward. What makes the first five somites so special is that they are more primitive...they cannot produce the full complement of mesodermal structures. As one moves caudally from the first somite (S1), a progressively greater degree of specialization takes place. The occipital somites (S1-S4) contain the sclerotomes of the posterior cranial base

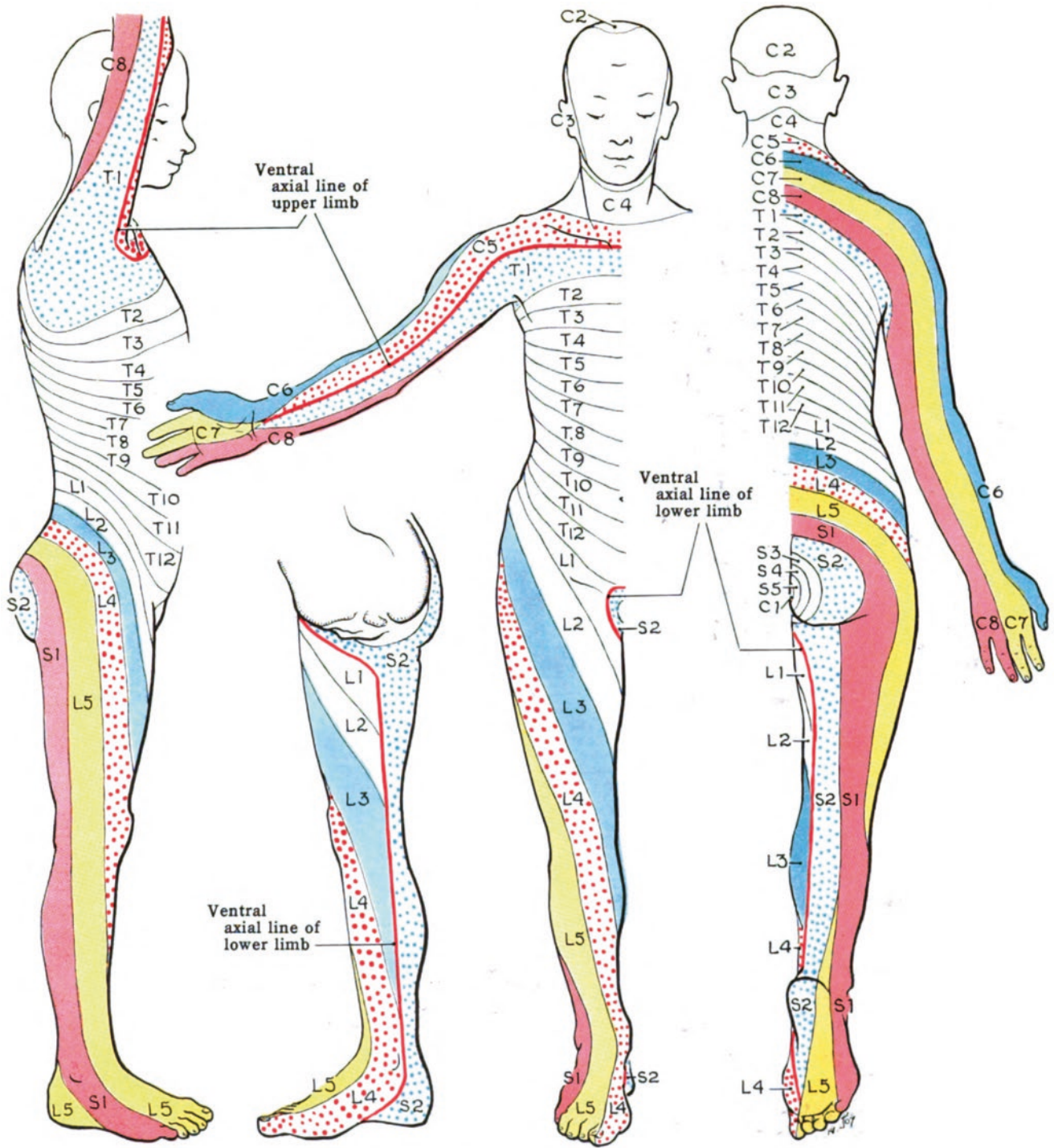


**Fig. 11.8** Dermatomal map. Note the absence of representation from c1. Hypaxial (ventral) cervical dermatomes are “stolen” at level c4 with c5-t1 reassigned to the upper extremity. Epaxial (dorsal) dermatomes

remain fully represented. The limbs are strictly hypaxial structures. [Reprinted from Wikimedia. Retrieved from: [https://commons.wikimedia.org/wiki/File:Grant\\_1962\\_663.png](https://commons.wikimedia.org/wiki/File:Grant_1962_663.png)]

and myotomes that give strictly ventral derivative; these create the hypaxial muscles of the tongue and the cucullaris complex. The occipital somites do not possess dermatomes.

This situation changes with the cervical somites. Somite 5 (neuromere c1) has a myotome with both ventral *and* dorsal

derivatives—it is responsible for epaxial muscles controlling extension of the craniovertebral joint. These are innervated by a dorsal branch of C1. Somite 5 does have a dermatome, but it has no specific representation on the skin of the neck (although it is depicted as contributing to the cervical plexus;

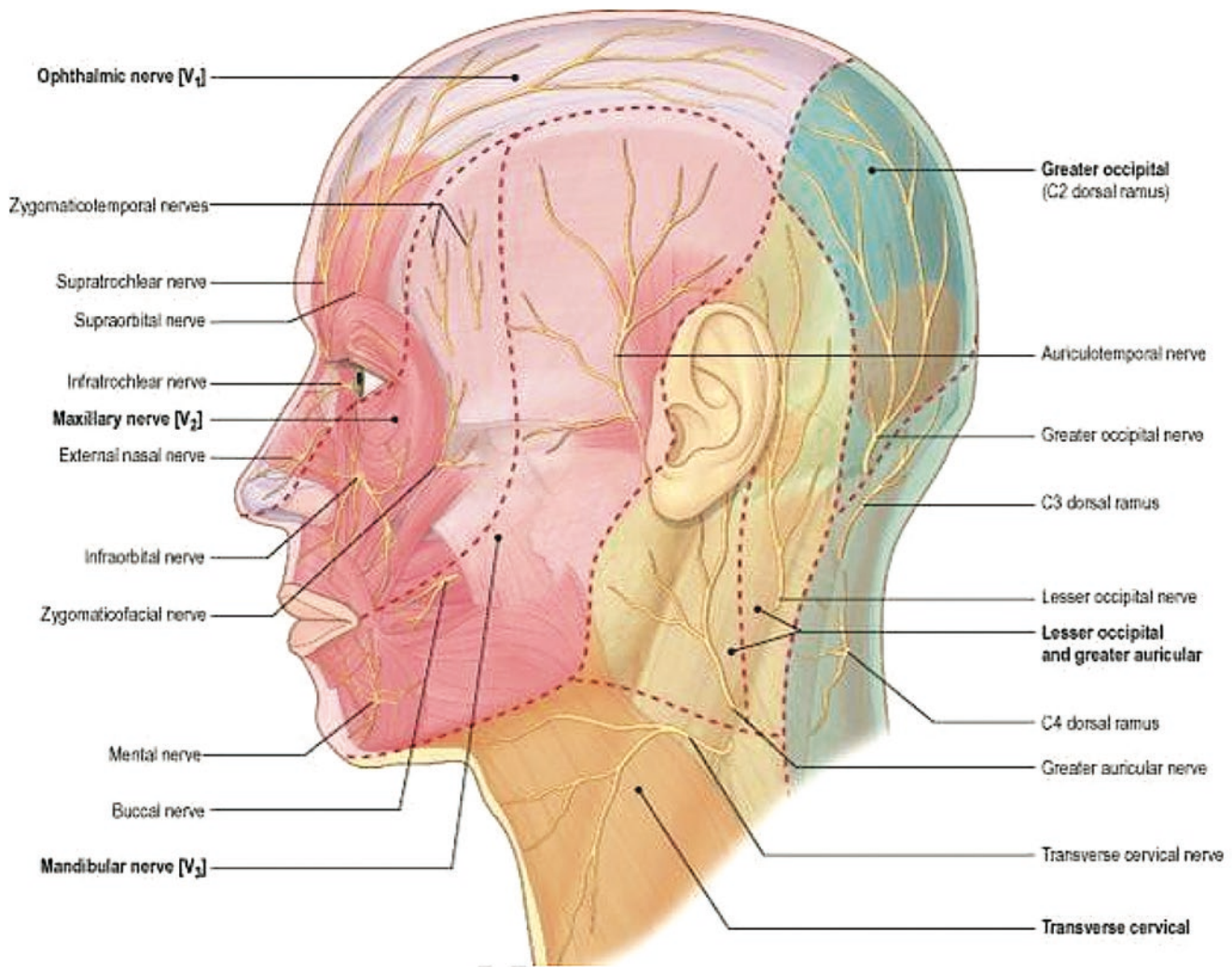


**Fig. 11.9** Cutaneous innervation of the head and neck. Each half of the neck four hypaxial zones supplied through the cervical plexus: transverse cervical (C2-C3) supraclavicular (C3-C4), greater auricular (C2-C3) to the ear, and lesser occipital (C2) to the scalp. There are two epaxial zones supplied by individual roots: greater occipital (C2-C3) to the interparietal scalp and dorsal roots C2-C8 to the midline of the neck.

Note the sharp divide between the hypaxial LON and the epaxial GON. [Modified from Drake R, Vogel AW, Mitchell AWM. *Head and Neck*. In: *Gray's Anatomy for Students*, third edition. Philadelphia, PA: Churchill-Livingstone. 2015: 924–1052. With permission from Elsevier]

more on this later). The true contribution of S 5 is to the dura sheath connecting atlas with foramen magnum. Somite 6 (neuromere c2) contains a complete dermatome serving both epaxial skin of the posterior scalp and hypaxial skin of the neck, as mapped out by distribution of the cervical plexus). It also produces local dura (Fig. 11.10 occipital somites).

One might ask, why are the “primitive somites” five in number? After all, mammals have four occipital somites. Why is our fifth somite anomalous? The answer has to do with the evolutionary relationship between birds and mammals. Avian embryos have, not four, but five occipital somites. Recall that occipital somites produce neither epaxial muscle nor dermis. Birds and mammals diverged from the reptilian line at about the same time, from a common ancestral form,

as yet unidentified, which possessed five occipital somites. But in the transition to the mammalian line, certain aspects of the ancestral pattern continued to persist at the level of S5. Our fifth somite behaves as if it were partly occipital and partly cervical—hence the failure to produce identifiable dermis. Mammalian neuroembryology thus recapitulates the original neuromeric arrangement of its precursor.

### **Dermatomes: How Zones of Hypaxial Dermis Are Stolen from the Trunk**

All students of anatomy are familiar with the dermatomal system. Epaxial dermis is rather boring, as all levels from

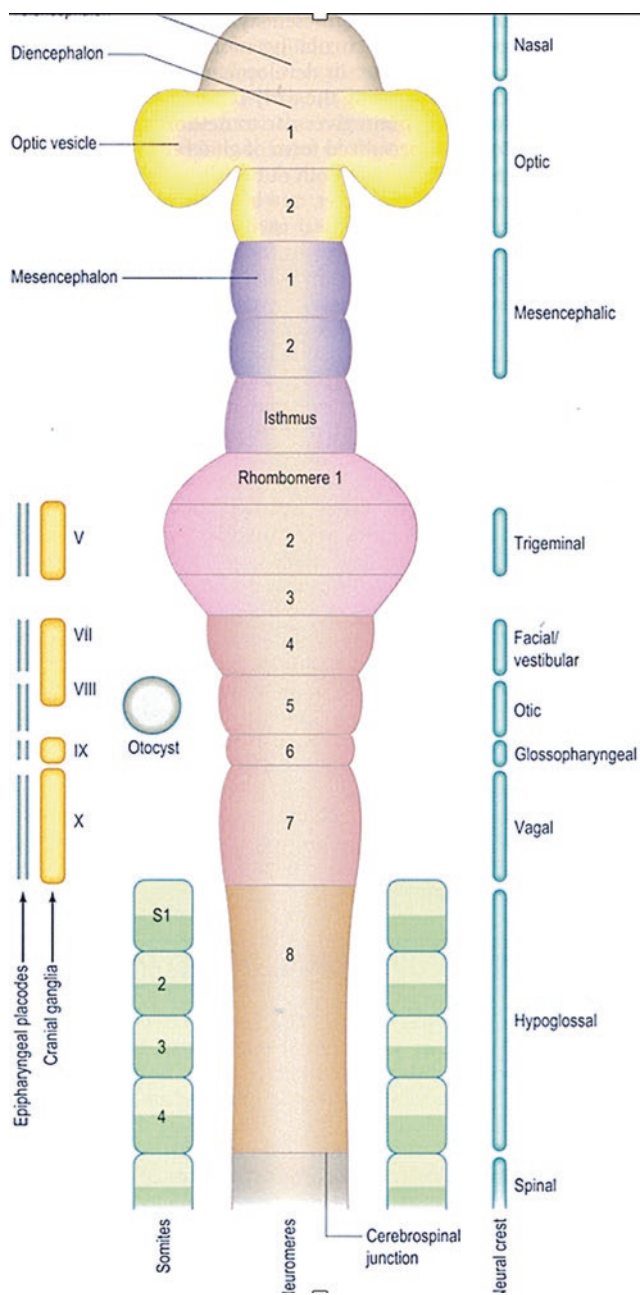


**Fig. 11.10 Isthmus rhombencephali.** Neuromeric map of O’Rahilly and Müller shows isthmus interposed between hindbrain and midbrain. It represents a secondary induction of r1. Isthmus neural folds do *not* produce neural crest. Basal floorplate of isthmus produces nucleus of trochlear nerve (CN IV). Midbrain has two neuromeres, m1 and m2. Basal plate of m1-m2 produces cerebral peduncles while *oculomotor nuclei* reside primarily in m2. Alar plate of isthmus and midbrain contain *mesencephalic nucleus of V* receiving fibers from V1-V3 for ocular and masticatory proprioception. Note: tactile fibers from V1-V3 are located at levels r1-r3. Nocioceptive fibers from V1-V3 refer to the *spinal nucleus of V*. [Reprinted from Lewis, Warren H (ed). *Gray’s Anatomy of the Human Body*, 20th American Edition. Philadelphia, PA: Lea & Febiger, 1918]

neck to coccyx are innervated by dorsal nerves organized *segmentally*. Hypaxial dermis of the trunk is more intriguing. It has a central zone (t3-l3) that is quite standard, that is innervated by ventral nerves organized *segmentally*. But the hypaxial dermis of the neck (c2–4), upper extremity (c5-t2), and lower extremity (l4-s3) are supplied by ventral nerves organized into *plexuses* (cervical, brachial, and lumbosacral, respectively). Why should this take place?

The best way to understand these differences is the evolutionary model of the extremities—this can be stretched to include the neck. The limb buds are hypaxial structures located at fixed locations along neuraxis of all tetrapods. Thrusting outward like a fist through a flexible membrane, the extremities drag all their associated lateral plate mesoderm away from the body wall. The neurovascular supply to the limbs is excluded as well. The upper extremity represents an “envelope” of hypaxial skin and mesenchyme stolen from the neck-upper trunk interface. The lower extremity repeats the crime by stealing hypaxial tissue from the interface between caudal trunk and the sacrum.

Within the limb buds lateral plate mesoderm makes the appendicular skeleton of the arms and legs. These bones must be populated by paraxial mesoderm muscles arising from somites *from the same neuromeric levels*. Everybody needs to know where to go. In the case of the upper limb, LPM innervated by neuromeres c5-t2 is simply no longer represented in the body wall. Paraxial mesoderm supplied by c5-t2 makes up somites S9-S15. The ventral myotomes of these 8 somites send forth hypaxial muscles that are assigned to their counterpart LPM bone structures. Thus, hypaxial PAM muscles migrate out into the limb buds, accompanied by their respective motor nerves.

During development the limb buds rotate, flex, pronate. As a consequence, the migration paths of the various myoblasts cross one another to assume a position on either the flexor or extensor surface of the limb bones. In so doing, the pathways of the peripheral nerves merge and diverge, thus creating the brachial plexus. In both upper and lower extremities, *the spatial-temporal trajectories of each all muscles in sequence are faithfully recapitulated in the anatomy of the plexus that supplies that extremity.*

### The Old Neck Versus the New Neck: Neck 1.0 vs. Neck 1.1

The evolution of the neck is a fascinating topic that we shall consider in a separate chapter. For our purposes here, the rationale of the cervical plexus should be considered from an evolutionary standpoint. Fishes do not have necks. The



**Table 11.2** Developmental potential of somites

Somite	Neuromere	Sclerotome	hypaxial myotome	epaxial myotome	hypaxial dermatome	epaxial dermatome
S1	r8	+	+	–	–	
S2	r9	+	+	–	–	
S3	r10	+	+	–	–	
S4	r11	+	+	–	–	
S5	c1	+	+	+	+	–
S6	c2	+	+	+	+	+

vault and oropharynx. Somitic mesoderm is responsible for all the remaining dermis, that is, that of the neck and the posterior scalp. The epaxial dermatomes of cervical somites 2 and 3 produce the dermis of the posterior scalp and part of upper auricle. The hypaxial dermatomes of cervical plexus, c1-c4 produce the dermis of the neck and contribute to the lower auricle and earlobe as well. We shall examine each of the forms of dermis in sequence (Table 11.2).

## Sources of Dermis: Prosencephalic Neural Crest

### Components of Frontonasal Skin (Figs. 11.9 and 11.10)

#### Frontonasal Skin Comes from Two Sources: Telencephalon and Diencephalon

The neural folds of the prosencephalon (forebrain) have been mapped by LeDouarin et al. demonstrating two major zones. The rostral prosencephalic folds correspond to the *telencephalon*, *eye fields*, and *hypothalamus*. They are in register (in the old Puelles model) with prosomeres p6-p4. Even though these terms are no longer in use, it is useful to divide the rostral folds into three distinct zones. Zone p6 has adeno-hypophyseal placode, nasal placode, and internal nasal (vestibular) epithelium. Zone p5 has optic placode and external nasal epithelium. Zone p4 has calvarial ectoderm which will act to program the frontal bone complex.

The caudal prosencephalic folds correspond to the *diencephalon* which contains *prethalamie*, *thalamie*, and *post-thalamie nuclei*. They have three neural crest populations in register with prosomeres p3, p2, and p1. PNC flows forward beneath p6-p4 in a strict spatial-temporal sequence. Like water filling a glass PNC populates the frontonasal target areas in a distal-to-proximal fashion. Three vertical homeotic “stripes” of the dermis are created, probably from p1 medial to p3 lateral. Each one imposes a distinct genetic identity upon the overlying epidermis. *The neuromeric model of frontonasal skin is a “grid” of three developmental zones.* The supratrochlear, supraorbital, and lacrimal fields seen in the skin of the nose and forehead reflect this grid. We postu-

late that these fields represent p1, p2, and p3 dermis, respectively, but it could also be the reverse, as mapping has not been done. PNC skin, coming from forebrain per se, is devoid of the blood vessels and nerves required for its survival. Neither does it have the capacity to form bone or cartilage. The mesenchyme required for these roles must come from an external source.

#### Neurovascular Support for Frontonasal Skin Comes from r1 Neural Crest

The forebrain has three specific limitations. Prosencephalon cannot provide its own external coverage, is insensate, and has no means to create blood supply. The solution for all three problems is an external source of mesenchyme with neurovascular properties: mesencephalic (midbrain) neural crest. Although mesencephalon is composed of m1-m2, and r0-r1) we shall refer to mesencephalic neural crest as r1 or MNC interchangeably. They are distributed as follows: (1) r0-r1 produces forebrain dura, sphenethmoid complex, anterior cranial base, and frontal bone complex; (2) m1-m2 is assigned to cover the eye; and (3) a separate r1 population supports the upper eyelid and conjunctiva.

*Nature never produces a structure without immediately providing it with blood supply for survival.* Neural crest development and migration from the neural folds of the CNS follows the temporal sequence of the CNS: (1) rostral hindbrain and midbrain (2) hindbrain, (3) caudal forebrain, and (4) rostral forebrain. This makes perfect sense. Gastrulation starts at r1 and proceeds backward. Midbrain is almost simultaneously induced by r1. Forebrain induction is caudal to cranial so neural crest from the diencephalic folds (p1-p3) migrates prior to that from telencephalon (p5-p6). Thus, prior to the development of forebrain dermis from above downward, hindbrain mesenchyme has migrated from below-upward and midbrain mesenchyme is flowing in a bilaminar pattern—a deep layer (the future dura) ascending over the forebrain and a superficial layer passing through the orbit and upward as a second lamina over the deep layer. Bifurcation of the StV1 neurovascular pedicles into superficial and deep components reflects this migration pattern. Frontal bone is synthesized between the two lamina of MNC. It is thus bilaminar and contains a sinus.



Once the forebrain and midbrain neural crest layers are in place all individual neuroangiosomes of stapodial system (annexed by ophthalmic) become assigned to specific developmental fields according to the organization of prosencephalic skin. The stapodial trunk attached to primitive ophthalmic has two main branches. The nasociliary axis is medial and supplies dermis from p4 and p3. The supraorbital axis is lateral and supplies dermis of p2 and p1. Let's map out these developmental fields and see how the system works.

MNC has an additional vital function: *it is the source material for all the bones and cartilages of the frontonasal vault*. In so doing, it is programmed by PNC.

## Neuromeric Map of Frontonasal Skin

### The Nose (Figs. 11.10 and 11.11)

Nasal skin consists of p6 vestibular epidermis and p5 nasal epidermis supported by p1 dermis. This results in two distinct developmental fields. When the face flexes, this frontonasal skin-mucosa is rolled downward and backward 180 degrees beneath the developing brain, terminating at Rathke's pouch. As a result, when the nasal chambers develop, p6 mucosa becomes tucked inside to form the nasal lining, while p5 skin remains outside as the nasal dorsum, sidewalls, philtrum, and columella.

The developmental zones of external nasal skin, and internal lining have exactly the same design. They have medial and lateral zones supplied by separate branches of the nasociliary axis. Externally, nasal dorsum is supplied by anterior ethmoid artery while the external lateral nasal skin is supplied by infratrochlear artery. Internally, septal mucosa receives septal branches of anterior and posterior ethmoid arteries while the upper lateral nasal mucosa covering superior turbinate is irrigated directly from the same arteries. From a clinical standpoint, Tessier cleft zones 13–12 in the nose are perfused by the branches from the most medial StV1 arterial, nasociliary.

### The Forehead

Forehead skin consists of p5 epidermis supported by three zone of dermis (p3-p1). This creates three clinically relevant developmental fields, each with its respective arterial axis. These are medial (p1), supratrochlear, middle (p2) supraorbital, and lateral (p3), lacrimal. These fields correspond to Tessier cleft zones 13–12, 11–10, and 9.

Several lines of clinical evidence support the neuromeric model of frontonasal skin. Tessier zones 13–9 run from medial to lateral. Nasal pathology is limited to zones 13 and 12, whereas forehead pathology can be found in any of the

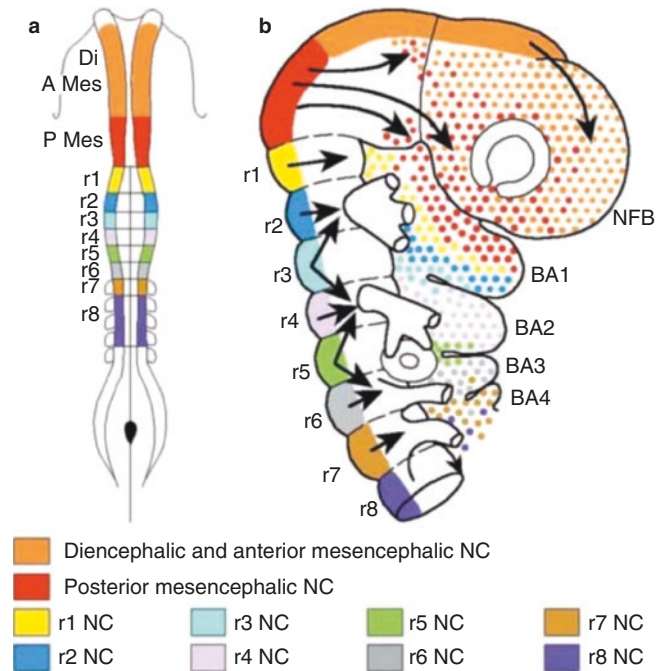


**Fig. 11.11** Neural crest migration begins at stages 10–11. Diencephalic NC (orange) from neural folds in register with p1–p3 makes frontonasal dermis. Midbrain NC (red) admixed with r1 (yellow) populates the entire frontonasal zone, especially the orbit, and forms anterior cranial base. Note that r1 does *not* participate in first arch derivatives; these are derived from r2–r3. The pattern of two rhombomeres per pharyngeal arch is maintained. Neural crest cells from certain rhombomeres are blocked and need to accompany a neighboring population to gain access to the arch. Note that r8 has four subdivisions. These have been recently demonstrated as separate homeotic entities corresponding to r8–r11 and assigned as pairs to the fourth and fifth pharyngeal arches. NC from r8–r11 also interacts with the four occipital somites (S1–S4). [Reprinted from Creuzet S, Couly G, Le Douarin NM. Patterning the neural crest derivatives during development of the vertebrate head: insights from avian studies. *J. Anat.* 2005; 207:447–459. John Wiley & Sons]

three zones. Developmental field excess/deficiency states follow a medial-lateral gradient with midline zones being more frequently affected. These pathologies are based on defects of individual branches of the V1 stapodial system.

The spectrum of holoprosencephaly is based on distinct branches of the StV1 system to the nose and orbit and branches of the anterior cerebral axis in the brain. Thus, the severity of HPE follows a gradient: mild hypotelorism, heminose, arhinia, cyclopia with presence of bilateral temporal globes in a single orbit, and complete absence of globe/orbit. The take-home message is that pathologies of the stapodial system tend to involve individual branches of StV1 with midline being more frequent, whereas HPE involves a progressive medial-lateral involvement of branches of prICA. More on this subject can be found in Chap. 6.

## Sources of Dermis: Mesencephalic Neural Crest

### The Mesencephalon and Isthmus

The midbrain (mesencephalon) is induced by the most forward zone of the hindbrain. Recall that the gastrulation takes place through the primitive streak. The cranial limit of the streak is also the cranial tip of the notochord, located forward at r0-r1r1. The functional hindbrain is associated with the pharyngeal arches runs backward from r2-r11. Genes produced at level r1 such as *Otx-2* are responsible for induction of the midbrain.

The midbrain consists of two mesomeres, m1 and m2. These contain the two nuclei of the oculomotor nerve complex. Somitomere 1 (inferior rectus, inferior oblique, and medial rectus) is supplied by m1. Somitomere 2 (superior rectus, levator palpebrae superioris) is supplied by m2. Just behind the midbrain proper, and separating it from the hindbrain, lies the isthmus, r0. This gives rise to anterior cerebellar peduncle and the decussation of trochlear nerve.

Immediately caudal to r0 lies the first rhombomere. Although r1 is anatomically part of hindbrain it is functionally closely related to midbrain. It gives rise to the inferior cerebellar peduncle and contains the nucleus of trochlear nerve. Sm3 (superior oblique) is supplied by r1. Furthermore, running all the way forward from r1 to the anterior limit of midbrain, sensory nucleus of trigeminal nerve (called the mesencephalic nucleus of trigeminal) receives all general somatic afferents (pain, temperature, etc.) from tissues innervated by V1. Sensory nucleus of V caudal to the mesencephalic zone extends all the way down the brain stem and receives information in a somatotopic manner from the rest of the head.

### The Isthmus and Hindbrain Clarified

Hindbrain technically begins with rhombomere 1. The nucleus of trochlear nerve resides in r1; it produces the posterior peduncle of cerebellum. Although the structure of hindbrain begins with r1, the functional hindbrain consists of two subunits. *Metaencephalon*, known as pons, is made up of rhombomeres 2–7. *Myelencephalon*, known as medulla, is composed of rhombomeres r8-r11.

## Cutaneous Representation of Midbrain Neural Crest

What about r1 and MNC? First off, we must re-emphasize that gastrulation takes place exclusively via the primitive node/streak, the cranial limit of which is r1. By logic, there must be a zone of epidermis that is “encoded” by r1 neural crest dermis? For reasons detailed below, a strict definition

of r1 “skin” is quite limited, *superior conjunctiva* being the most likely candidate.

### Mesenchymal Representations of m1, m2, and r1

Little has been described mapping neural crest derivatives of r0. For this reason, we shall arbitrarily refer to neural crest from r0 and r1 as one and the same (r1 for short).

Midbrain neural crest migrates almost immediately, beginning at stages 9–10. First to migrate is r1 which flows bidirectionally along the base of the brain, forward to the anterior cranial fossa, and backward to tentorium. After that m1-m2 localize around the developing eye. Because all three neuromeres contain V1, their migration pathways are defined by the individual branches of that nerve.

Accompanying these branches of V1 are the individual arteries of the StV1 stapodial complex, the stem of which is annexed by the primitive ophthalmic axis just behind the greater orbital fissure. Further clues as to the migration pathways of these three streams of MNC can be seen in the spatial positioning of the somitomeres with which they become associated. Sm1 is inferomedial, Sm2 and Sm3 is superolateral. Thus the *m1 and m2 define the insertion sites of the globe*, leaving only the lateral zone of the uncovered. This of course will receive lateral rectus originating from Sm5 and supplied by cranial nerve VI, abducens.

What we can induce from this is that MNC from m1 and m2 is buried inside the orbit where it produces non-ocular structures. Recall that the nuclei of oculomotor nerve reside in m1 and m2. Neural crest from these neuromeres is the logical source of fascia for 6 of the 7 extraocular muscles. They may well provide sclera for the globe. Thus the eye has an *internal lining of neural crest in the retina arising from the optic placode and an external lining of neural crest as sclera* originating from MNC. Finally, *m1 and m2 do not produce dermis*.

When we observe the physical position of r1 neural crest we can see that it is ideally positioned to provide the *substantia propria* of the upper conjunctiva and the subcutaneous tissue of the upper eyelid. This does not include the dermis of upper eyelid which is likely to come from r1.

On the other hand, the distribution of r1 neural crest (as revealed by the innervation of V1) is very extensive. All dura innervated by V1 is an r1 neural crest derivative. First rhombomere neural crest provides the subcutaneous tissue for the mucosa of the nasal cavity. As such r1 is the mesenchymal source for the frontal, nasal, lacrimal, ethmoid, and presphenoid bones. All mesenchymal structures of the orbit are r1 derivatives. These include the sclera, connective tissue structures such as Whitnall’s ligament and the septum orbitale, and intraorbital fat, and the substantia propria of the upper conjunctiva. Neural crest from the first rhombomere contributes to both upper, providing the tarsal plate and fat. Under the right circumstances, mesenchymal stem cells can convert

to muscle. This is the likely source for the intrinsic muscles of the eye controlling papillary size.

In sum, the destiny of r1 neural crest is to provide support for the frontal lobe, the surrounding structures of the nasal cavity, the orbit, and the nasolacrimal system. Note that none of these structures bears any biologic relationship to the first pharyngeal arch. This is important because of number of studies have mapped the physical distribution of r1 neural crest to the superior (dorsal) aspect of the maxillary prominence (Fig. 11.11). This has given rise to the concept that the first pharyngeal arch is constructed from three neuromeric levels: r1, r2, and r3. The ultimate format of PA1 excludes V1 innervation. A possible resolution of this contradiction could be the existence of a putative *premandibular arch*, as postulated by Kuratani. For the sake of simplicity, because r1 neural crest is so heavily distributed to the orbit, *we will use MNC and r1 interchangeably*.

The importance of MNC for three pathologies of the cranial base and face cannot be overemphasized. Mesenchyme from r1 flows forward in the midline from the presphenoid to create a block of mesenchyme that lies deep to the nasal placodes, separating them and surrounding them. In normal development, the nasal placodes sink into r1 mesenchyme and then medialize. The approximation of the nasal chambers toward the midline requires apoptosis of r1 mesenchyme that separates them. *Failure of apoptosis of internasal mesenchyme results in hypertelorism*, the surgical treatment of which requires resection of ethmoid mesenchyme and orbital approximation, the facial bipartition operation. A second pathology involves the temporary filling of the nasal chambers with mesenchyme. This takes place immediately after the invagination of the nasal placodes is complete. Once again, apoptosis is required. *Failure of intranasal apoptosis results in choanal atresia*. A third pathology involves inadequate supply of r1 mesenchyme to the midline. Neural crest from r1 is responsible for dividing prechordal plate mesoderm and driving each half laterally into the future orbits. *Reduction in amount of available r1 neural crest results in hypotelorism*, a quantitative reduction of interorbital distance. This is the external manifestation of *holoprosencephaly*. Inappropriate production of gene products from the prechordal plate and/or r0-r1 affects the formation of midline neural structures such as corpus callosum, a near-constant finding in holoprosencephaly.

### Sources of Dermis: Rhombencephalic Neural Crest

The hindbrain or rhombencephalon subdivides during development into two functional units. *Metaencephalon* or pons develops from rhombomeres 2–7. It supplies all derivatives of pharyngeal arches 1–3. Its floor plate contains the motor

nuclei of V, VI, VII, IX, and X. Somatic sensory afferents nuclei refer to the trigeminal nucleus.  $RNC_R$  is responsible for all facial dermis, the overwhelming source of which comes from r2 and r3, that is, from first pharyngeal arch. *Myelencephalon* or medulla develops from rhombomeres 8–11. Its floor plate contains the motor nuclei of X, XI, and XII.  $RNC_C$  plays no role whatsoever in the formation of craniofacial skin.

Let's consider facial skin: neuromere by neuromere. The contributions of r2-r3 are well known. V2 and V3 dermis of the first pharyngeal arch is hypaxial. Note: with the face downward the skin of lateral forehead and scalp supplied by V2 and V3 is still considered hypaxial (Fig. 11.12). A small part of posterior ear canal is innervated by the facial nerve (r4-r5). Because the taste nucleus of chorda tympani resides in r4, second arch neural crest dermis likely originates from r5. The dermis of the external posterior pinna is r6-r7, that is, third arch. Recall that IX and X cohabit together in r6-r7. Thus, sensory innervation via auricular branch of vagus, X with a possible contribution from IX. The salivatory control for parotid may reside in r6, hence third arch neural crest dermis likely originates from r7.

Next, let's consider the anatomy of dermis supplied by V2 and V3. Head and neck skin has two fundamental components, both of which are supplied in similar ways. The interface between forehead skin and scalp is the boundary between hypaxial r1-r3 and epaxial C2-C3. The interface between facial skin (non-forehead) and neck skin is the boundary between hypaxial r1-r3 versus hypaxial C1-C4 (the cervical plexus).

Ear skin has an interesting composition. The pinna is constructed from six cartilaginous hillocks (Fig. 11.13). The anterior three come from the first arch; they are covered by r3 skin supplied by V3 auriculotemporal nerve. The posterior three develop from the second arch. These are *not* covered by second arch skin because *there is none available*. Instead, the posterior external auricle is supplied by cervical nerves. Its upper zone is supplied by epaxial lesser occipital nerve (C2) which is *not* a part of the cervical plexus. The lower zone is supplied by hypaxial greater auricular nerve (C2, C3) from cervical plexus. Why the need for two distinct cervical nerves? The answer has to do, once again, with epaxial vs. hypaxial structures. Of the three posterior hillocks, the upper one is epaxial and the lower two are hypaxial. The territories of lesser occipital n. and greater auricular n. reflect this fact. Finally, the skin of posterior auricle comes from somites S6-S7, that is, C2-C3. As the pinna first developed, it was flat against the mastoid, it had no deep surface. With growth, as the pinna began to project away from the head, a sulcus developed. The same two neuroangiosomes extend posteriorly, with lesser occipital supplying the epaxial half and greater auricular the hypaxial half (Fig. 11.14).

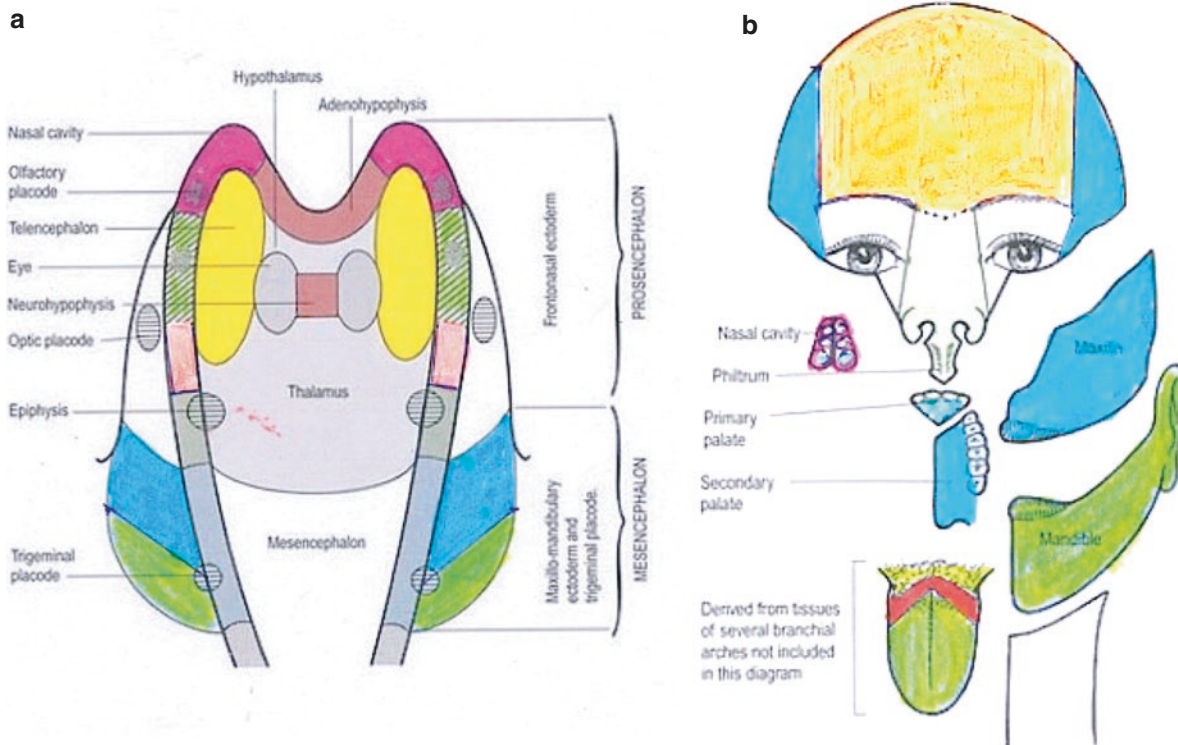


**Fig. 11.12** Formation of ectomeres from forebrain and midbrain. Neural folds are color coded with p6 (red), p5 (green), and p4 pink. Frontonasal ectoderm (white) sits astride the anterior neural folds. Posterior neural folds p3-p1 (gray) provide dermis. Derivatives are seen on the right with p6 vestibular tissues (red) seen within the nasal cavity.

Note that p1-p3 dermis is not sensate. Neurovascular supply of frontonasal skin depends upon V1 and V1 stapedial arteries. Source: Gray. [Reprinted from Williams PL. *Gray's Anatomy*, 38th edition. Philadelphia, PA: Churchill-Livingstone; 1997. with permission from Elsevier.]

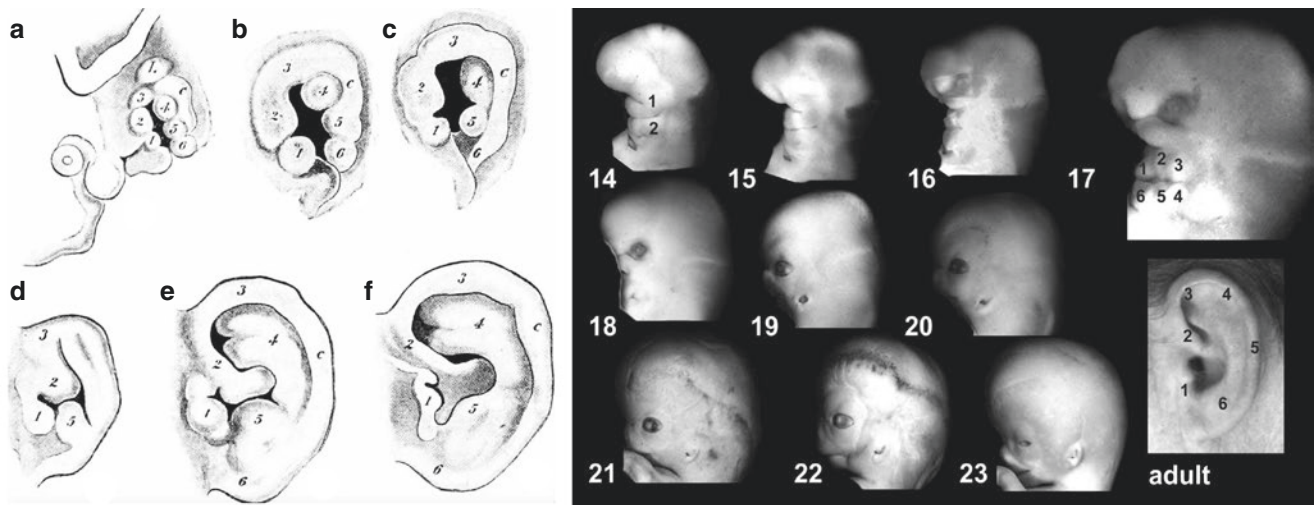


**Fig. 11.13** Development of the external ear LEFT: Six stages in the development of the external ear. 1, 2, 3, elevations on the mandibular arch; 4, 5, 6, elevations on the hyoid arch. 1, tragus; 2, 3, helix; 4, 5, antihelix; 6, antitragus. c, hyoid helix or auricular fold. A, 11 mm.; B, 13.6 mm.; C, 15 mm.; D, beginning of third month; E, fetus of 85 mm.; F, fetus at term. an ingrowth takes place from the ventral portion of the groove, to form a funnel-shaped canal. The lumen of this tube is temporarily closed during the fourth and fifth months, but later re-opens. During the third month a plate of cells at the extremity of the primary auditory meatus grows in and reaches the lower wall of the tympanic cavity. During the seventh month a space is formed by the splitting of this plate, and the secondary portion of the meatus is thus developed. The tympanic membrane is formed by a

thinning out of the tissue in the region where the wall of the external auditory meatus abuts upon the wall of the tympanic cavity. RIGHT: Auricular development by Carnegie stage. fifth week hillocks appear between first and second arches. sixth week six hillocks are present. seventh week development proceeds caudo-cranially (from neck upward). 12th week hillocks fuse. 20th week remodeling complete. Auriculotemporal nerve V3 covers hillocks 1-3, greater auricular (C2-C3) covers hillocks 5-6, and lesser occipital (C3) covers hillock 4. Left: [Reprinted from Charles W. Prentice Laboratory Manual and Textbook of Embryology. Philadelphia, PA: WB Saunders, 1922.]. Right: [Reprinted from The Kyoto Collection, Kyoto University Graduate School of Medicine. Courtesy of Prof. Kohei Shiota and Shigehito Yamada]

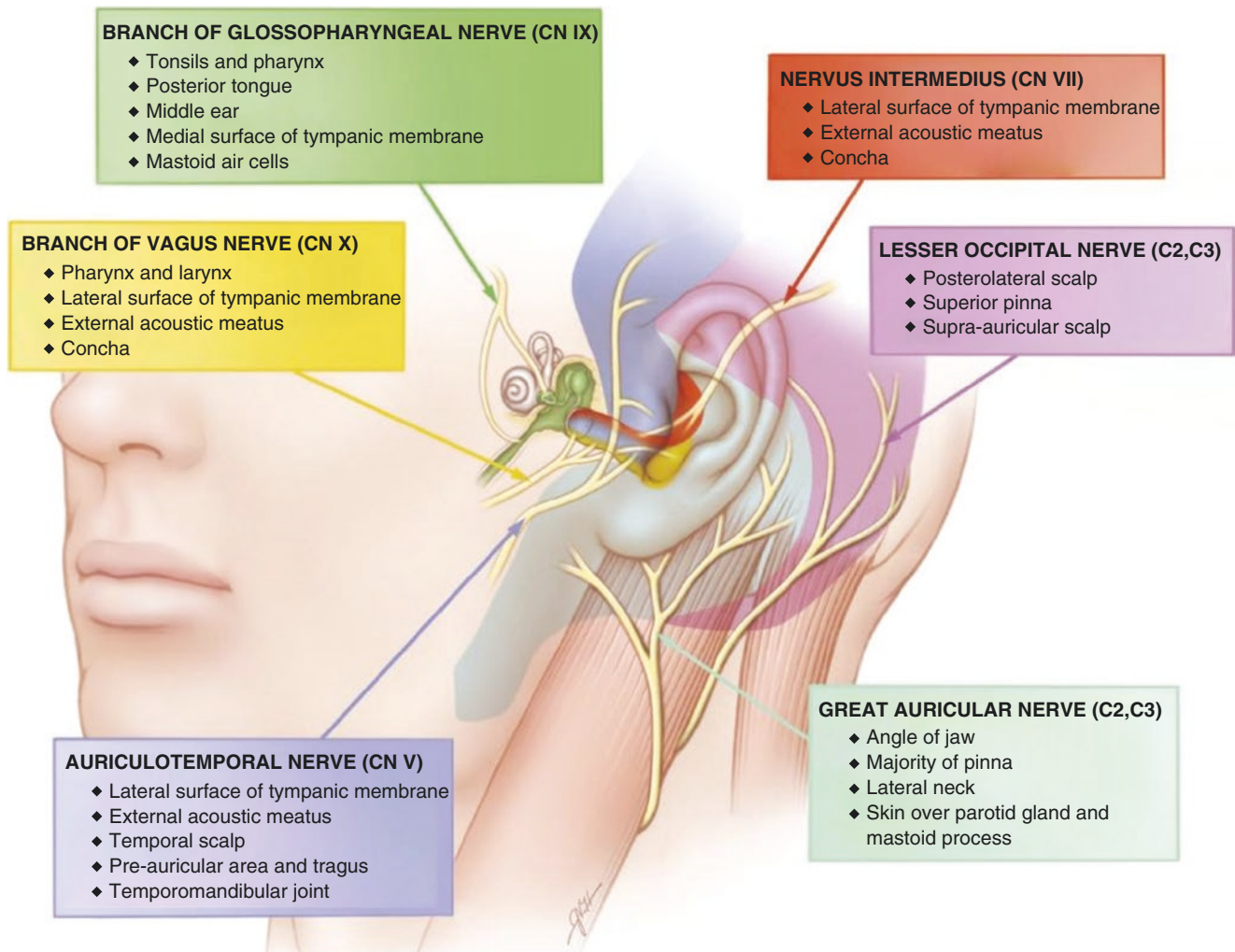


**Fig. 11.14 Sensory innervation of the ear and surrounding structures.** Sensory supply to the ear comes from 8 neuromeres (r2-r7 and c2-c3). Depiction of the sensory nerves shows the innervation of the ear and surrounding anatomy. Each box with its corresponding color illustrates each nerve's distribution. Sensory distributions may overlap.

Note the anterosuperior aspect of the Eustachian tube is auriculotemporal (first arch). [Reprinted from DeLange JM, Garza I, Robertson CE. Clinical Reasoning: A 50-year-old woman with deep stabbing ear pain. *Neurology* 2014; 83(16): e152-e157. With permission from Wolters Kluwer Health, Inc.]

What becomes of the remaining arches? That of the second arch is the most complex. It essentially submerges into the first arch. In the process, its ectodermal epithelium disappears. The same process takes place intraorally; second arch mucosa vanishes. First arch skin now abuts cervical skin. But second arch “gets even” as its fascia, myoblasts, and motor branches of VII insinuate themselves forward into PA1, splitting around the parotid into deep and superficial components. Thus buccinator is “assigned” to oral mucosa while the muscles of facial expression remain in a superficial location. The primary attachment (origin) of the superficial facial muscles is from the superficial musculo-aponeurotic system (the SMAS). The secondary attachment (insertion) is to the nearest available neighboring bone. second arch myoblasts migrate frontally beneath the skin overlying alisphenoid (zone 9) and continue beneath the

frontonasal skin overlying lateral frontal bone (zones 10 and 11). Backward migration takes place to the ear and beneath the mastoid skin to produce occipitalis. The latter muscle is located over membranous (r7) supraoccipital, inserting at the membranous-chondral boundary, that is, the highest nuchal line. In sum, PA2 is completed melded into PA1, overlies PA3, and travels deep to cervical and mastoid skin populating facial muscles available zones over membranous bones of the calvarium and clavicle. fourth arch and fifth arch develop successively in stages 13 and 14. They form successive concentric rings *internal* to third arch.

This melding of pharyngeal arch mesenchyme is illustrated by the sensory innervation of the ear. The external components of the ear arise as six hillocks, three from PA1 and 3 from PA2 (Figs. 11.13, 11.14 and 11.15). Deep to them both lies PA3. Thus cranial nerves arising from rhombo-

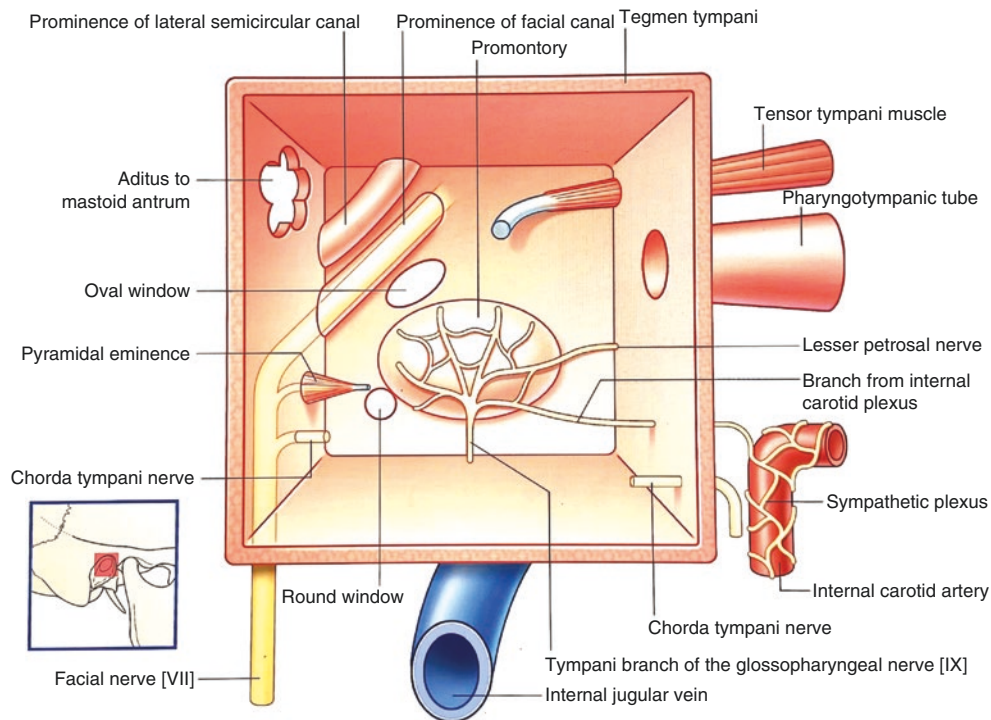


**Fig. 11.15** Innervation of the tympanic cavity. **Tympanic branch of IX** sensory to the lining of middle ear, antrum, and auditory tube. Its preganglionic PANS fibers are secretomotor to parotid gland. **Caroticotympanic nerves** (sup and inferior Vasosomotor—originate from SANS plexus around the internal carotid artery). **Facial nerve:** Runs in bony canal along the medial and posterior walls of tympanic cavity: three branches: *Chorda tympani nerve*: taste anterior 2/3 tongue (except vallate papillae and secretomotor to submandibular and sublingual salivary glands. *Greater petrosal nerve*: secretomotor to lacrimal, nasal and palatal mucous glands. *Nerve to stapedius muscle* dampens

down sound waves. **Mandibular nerve:** V3 to tensor tympani muscle. Note: chorda tympani, branch of facial nerve, enters across the tympanic membrane being located lateral to the long process of the incus and medial to the handle of the malleus. It enters the tympanic cavity via the posterior canaliculus in the posterior wall and leaves via the anterior canaliculus medial to the pterotympanic fissure. [Reprinted from Drake R, Vogel AW, Mitchell AWM. *Head and Neck*. In: Gray's Anatomy for Students, third edition. Philadelphia, PA: Churchill-Livingstone. 2015: 924–1052. With permission from Elsevier]

meres r3-r7 are represented by the innervation of the auricular and tympanic cavity, Finally, there is no further cutaneous representation of neuromeres r8-r11 and c1 the skin of the posterior pinna and occipital scalp is supplied by neuromeres c2 and c3.

- Evolution of adipose tissue.
- Pericytes: precursor cells for adipose tissue.
- Mesenchymal stromal and adipose-derived stromal vascular fraction (SVF).

## Adipose Tissue

Research interest in adipose tissue has undergone a metamorphosis in recent years with the original emphasis on metabolism and thermal regulation being supplemented by an intense focus on the biology of its cellular components as a source of reconstructive and regenerative cells. Despite this, concepts of its embryonic origins remain obscure. This section will outline a structural and functional model of adipose tissue as follows:

- White and brown fat: comparison and contrast.
- Pathologies of white fat.

## White Fat vs. Brown Fat: Energy and Endocrinology vs. Thermoregulation

**Histologic Considerations (Figs. 11.16, 11.17, 11.18, 11.19, 11.20, 11.21, 11.22, 11.23, 11.24, 11.25, 11.26, 11.27, 11.28, 11.29)**

White fat is the best-known form of adipose tissue. Ubiquitous throughout the body it comprises, on average, 20% of body mass in men and 25% in women. As insulation, it is distributed in two layers superficial and deep, being separated by the superficial fascia, otherwise known by various regional terms: Internally it forms the apron of the omentum and is intrinsic to tissues such as the thymus. Adipose tissue

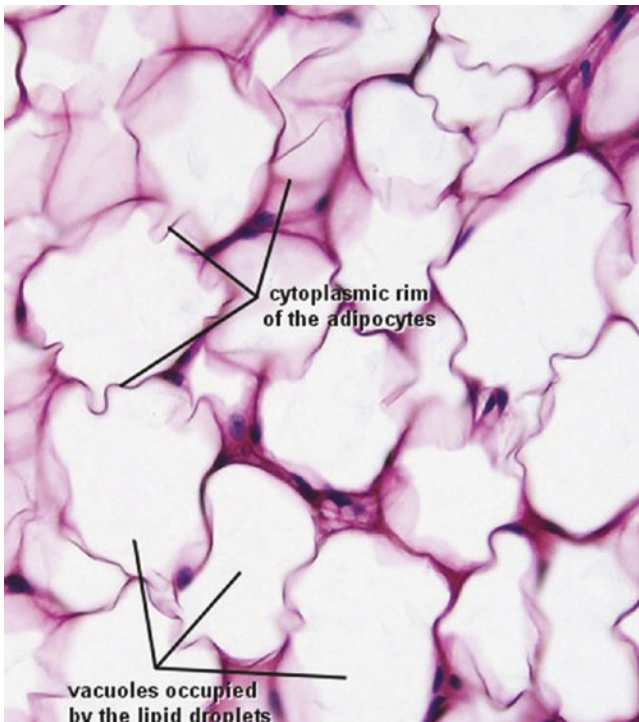


**Fig. 11.16** White adipose tissue. White fat (H&E stain) has a peripheral nucleus, low number of mitochondria, and is designed for energy storage. The single large vacuole accommodates lipid and can expand its volume. Under control by SANS via NE. [Courtesy of Michael Carstens, MD]

forms deposits external to solid organs such as heart and kidney but it is notably not an intrinsic element of their parenchyma. Of note is its association with vascular bundles throughout the body as part of a trifecta in which fat accompanies and encompasses a nerve and its accompanying artery. This vascular “leash” is of use for reconstructive surgeons tracing out the blood supply for composite tissue flaps as these pass along tissue planes and from deep to superficially through intermuscular septae.

The cells of white fat are made up of a single lipid droplet which displaces the nucleus to the periphery. Important receptors in the membrane are for norepinephrine, insulin, glucocorticoids, and sex hormones. White fat is under control by the sympathetic autonomic system. White adipocytes produce two hormones: *leptin*, which, acting at the level of the hypothalamus, acts as an appetite suppressant, and *asprosin*, which stimulates the liver to release glucose (Fig. 11.16).

White adipose tissue is both dynamic (diet related) and trophic (perhaps supported by the SANS?). Newborns, especially premature, have little to no fat stores and a very sensitive to ambient temperature changes. The knock-out mouse model for *lipodystrophy* is characterized by diabetes and hepatomegaly. Loss of white fat stores, as seen in *anorexia nervosa*, involves multiple systems including the brain (memory decline and depression), skin (hair loss), muscle weakness, skeleton (bone loss), kidney (stone), intestine

**Fig. 11.17** White fat is dynamic. Perry-Romberg syndrome represents an involutonal state of neural crest mesenchyme affecting dermis, fat, and membranous bone within a defined neuroanatomic distribution. It occurs in childhood and “burns out” in early adulthood. [Reprinted from Raposo-Amaral CE, Denadai R, Nunes Camargo D, et al. Parry-Romberg Syndrome: Severity of deformity does not correlate with quality of life. 2013; 37: 792–801. With permission from Springer Nature]





**Fig. 11.18** HIV-associated lipodystrophies. LEFT: Buffalo hump” associated with protease inhibitor treatment. RIGHT: Facial fat wasting is a tell-tale finding in treated HIV patients. Left: [Reprinted from Sharma D, Bitterly TJ. Buffalo hump in HIV patients: surgical reconstruction with liposuction. *Plast Reconstr Surg* 2009; 62(7): 946–949.

With permission from Springer Nature.]. Right: [Reprinted from Rauso R, Gherardini G, Greco M, et al. Is buffalo hump fat the perfect filler for facial wasting rehabilitation? Reflections on three cases. *Eur J Plast Surg* 2012;35(7):553–556. With permission from Springer Nature]



**Fig. 11.19** Acquired partial lipodystrophy and lipedema. A 37-year-old woman with acquired partial lipodystrophy. Note the loss of SAT from the upper body to the waist but obesity of the hips and legs. [Reprinted from Herbst K. Rare adipose diseases (RADs) masquerading as obesity. *Acta Pharmacologica Sinica* 2012; 33: 155–172. With permission from Springer Nature]

(constipation), and growth retardation. This condition, found in up to 1% of adolescent girls, if uncorrected can be lethal. Parry–Romberg disease, a progressive form of volume loss involving soft tissues and bone of the face has a common denominator derivation from neural crest populations associated with branches of the trigeminal nerve (Fig. 11.17).

Adipose tissue storage can be symmetrical or asymmetrical. Obesity (BMI  $\geq 30$ ) has two common forms of symmetrical distribution. Pear-shaped obesity is subcutaneous and centers around the midriff and thighs. It is a low-risk condition regarding diabetes and metabolic syndrome. Apple-shaped obesity has increased visceral fat and presents a high risk for diabetes and diseases associated with metabolic syndrome. Lipodystrophy, on the other hand is asymmetrical, favoring localized deposits of fat in the buttocks and/or thighs that are out of proportion to the overall body fat stores [5]. HIV-related treatment may be a characteristic cervical “buffalo hump” or sites of local atrophy in the face (Figs. 11.18 and 11.19). Lipomas arising from white fat can develop in many locations (Fig. 11.20). Although most lipomas are solitary they can be multiple, as in Madelung’s disease (Fig. 11.21).

**Brown fat cells** contain multiple lipid droplets arrayed around a central nucleus. Multiple mitochondria in the cytoplasm—which relate to the thermogenic function of this tissue—are responsible for its color. Capillary content is higher as well, perhaps reflecting the greater metabolic rate. Deposits of brown adipose tissue are found in highly vascularized sites such as the aorta, kidneys, paravertebral arteries and supraclavicular (thyrocervical, costovertebral, and thoracoacromial trunks). These arterial “switchyards” supply multiple distinct developmental fields, many of which



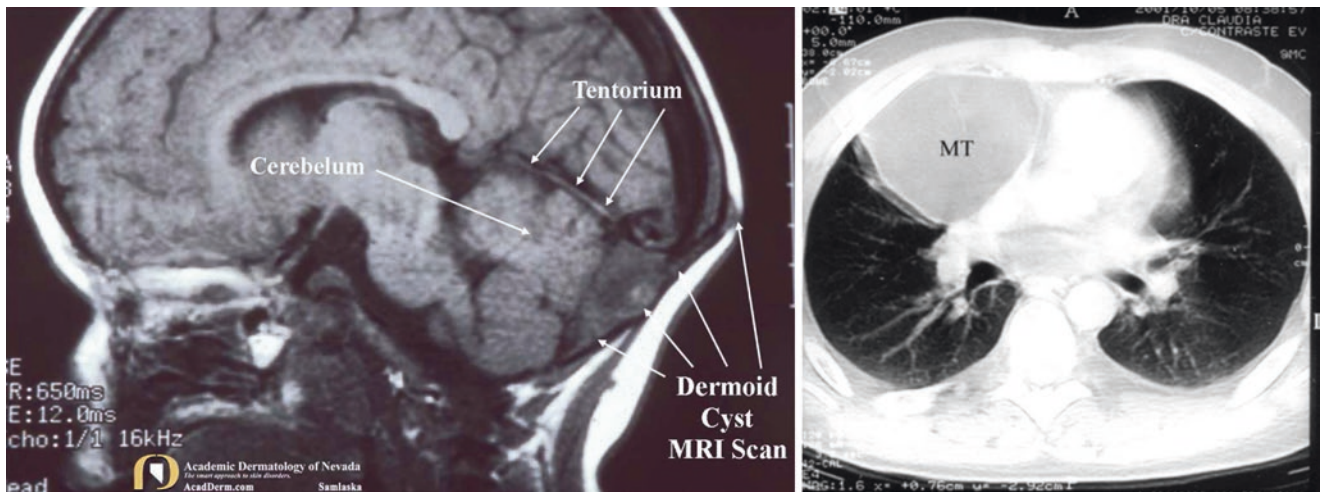


**Fig. 11.20 Solitary lipomas:** LEFT: Lipoma are typically found in the face and neck but they occur in many sites. MRI scan demonstrate dermoid Cyst pressing against the cerebellum and communicating through the occipital bone to the subcutaneous tissues of the scalp. RIGHT: intrathoracic thymolipoma. Left: [Courtesy of Curt Samlaska, MD, FACP, FAAD. Academic Dermatology of Nevada]. [Reprinted from

Ramos Filho J; Melo RF; de Macedo M; Fiorelli LA; Costa A, Isolatto RB. Chest pain due to right atrial compression caused by a thymolipoma. *Arq Bras Cardiol* 2004; 82(5):484–486. With permission from Creative Commons License 4.0: <https://creativecommons.org/licenses/by-nc/4.0/deed.en>]

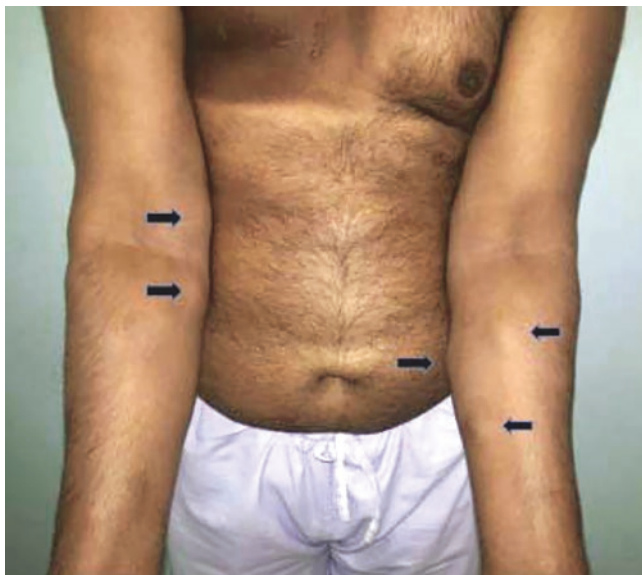


**Fig. 11.21 Multiple lipomas.** LEFT: [Reprinted from Reddy N, Malipatil B, Kumar S. A rare case of familial multiple subcutaneous lipomatosis with novel *PALB2* mutation and increased predilection for cancers. *Hematol Oncol Stem Cell Ther* 2016; 9(4):154–156. With permission from Elsevier.]. RIGHT: [Reprinted from Maximiano LF,

Gaspar MT, Nakahira ES. Madelung disease (multiple symmetric lipomatosis). *Autopsy Case Rep* [Internet]. 2018;8(3):e2018030. With permission from Creative Commons Attribution Non-Commercial License (CC-BY-NC)]

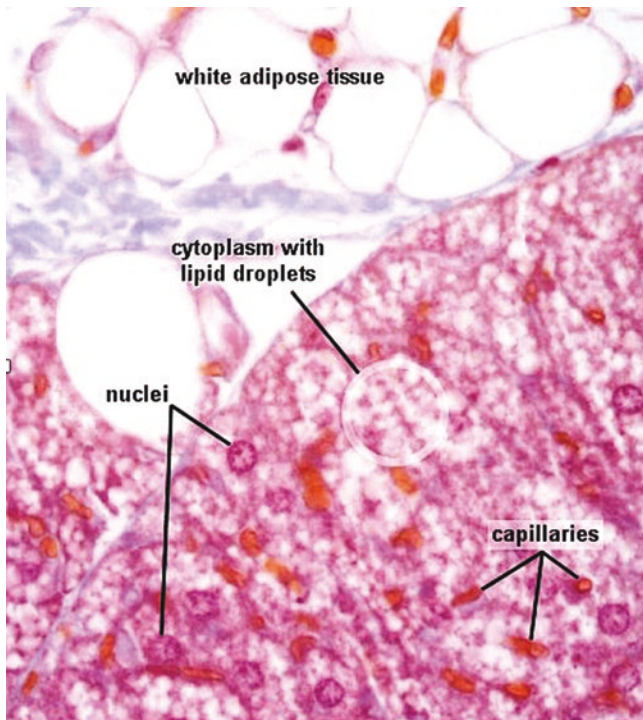


**Fig. 11.22** Brown fat. BAT (trichrome stain) related to paraxial mesoderm and if PRDM16- whereas somitic muscle is PRDM16+. BAT is designed for energy production with abundant mitochondria and multiple small lipid droplets of uniform size; these are non-expansile. Control is by SANS via NE. [Courtesy of Michael Carstens, MD]

are useful as reconstructive tissue sources. The segmental location of brown fat deposits along the para-aortic branches off the aorta indicate a somitic origin with likely distinct homeotic codes for each collection of fat (Figs. 11.20 and 11.21).

**Beige fat cells** constitute a separate type of brown fat that develops within white adipose tissue itself as an adrenergic induction of existing pre-adipocytes interspersed within the white fat. The color difference relates to the greater relation of fat droplets to mitochondria, hence a less red color. The existence of beige fat is of developmental significance (vide infra).

Like white fat, the function of brown fat is under the control of the SANS. Mitochondria produce ATP via the enzyme *ATP synthase* which makes use of a flow of protons along a gradient of internal membranes (chemiosmosis). Once the protons are used they are pumped out of the mitochondrion by the electron transport chain (ETC). An alternative mitochondrial enzyme, *thermogenin* (otherwise known as uncoupling protein 1) provides a return route for protons previously expelled by the ETS. This couples oxidative phosphorylation so the energy of the proton motive force (PMF) is channeled into heat rather into ATP. Mammals have a unique surface/volume ratio which translates this energy release into shivering. The existence of a superficial fatty insulation layer ensures that the heat will be conserved internally.

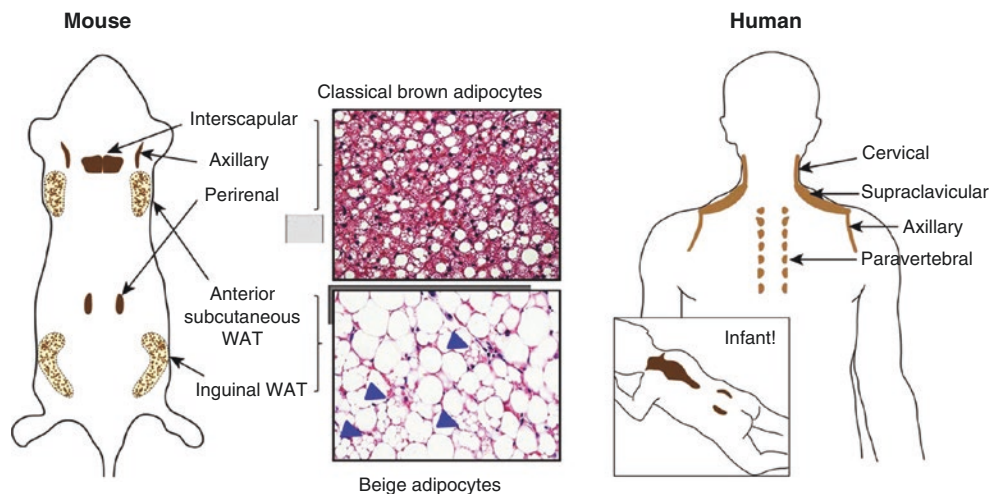


**Fig. 11.23** Beige fat: “good” fat. Anatomical Locations of Thermogenic Fat in Mice and Humans. Classical brown adipocytes reside in dedicated brown adipose tissue (BAT) depots, including interscapular, axillary, and perirenal BAT depots in mice and infants. Beige adipocytes sporadically reside in subcutaneous white adipose tissue (WAT) depots, such as the inguinal and anterior subcutaneous WAT in mice (arrowheads indicate the multilocular beige adipocytes). In adult humans, BAT is present in multiple locations, including cervical, supra-

clavicular, axillary, paravertebral, and abdominal subcutaneous regions. UCPI-positive adipocytes from the supraclavicular region show a molecular signature resembling that of mouse beige adipocytes, whereas the deep neck regions contain thermogenic fat that resembles classical brown adipocytes in mice. [Reprinted from Ikeda K, Maretich P, Kajimura S. Common and distinct features of brown and beige adipocytes. *Trends Endo Metab* 2018; 29(3): 191–200. With permission from Elsevier]

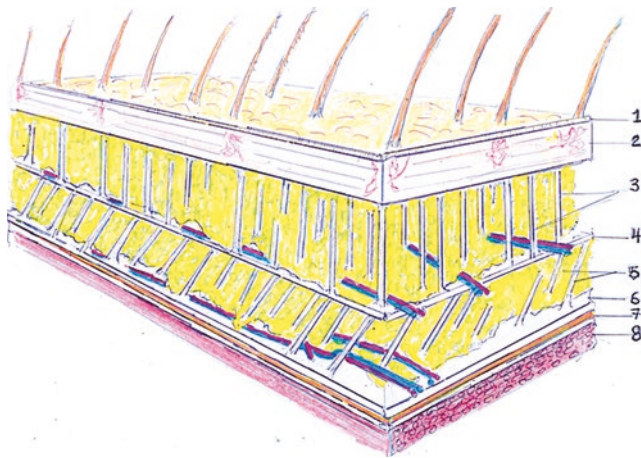


**Fig. 11.24** Gross anatomy of subcutaneous fat. Note two layers of fascia. Although the nomenclature may vary between craniofacial skin and non-craniofacial skin the concepts are the same. **Superficial fascia (SF)** divides subdermal fat from deep cutaneous fat. It may be the network associated with panniculus carnosus. Retinacula cutis fibers are vertical and extend from SF to the dermis, thus creating mini-compartments. These allow for flexibility and gliding of the skin over muscle (trauma protection). Accumulations of fat within these compartments causes unsightly “cellulite.” Loss of fibers allows for greater skin laxity and may be the cause of wrinkles. Key: (1) epidermis, (2) dermis, (3) superficial retinacular fibers, vertical, and superficial fat, (5) superficial or subcutaneous fascia, (6) retinacular fibers, oblique, and deep fat, (7) deep fascia, (8) hyaluronic acid layer, (9) epimysium, (10) muscle. **Note:** Within this adipose tissue complex (ATC) the fat cells make up 85% of the volume but, in terms of cell numbers, only 12–15% of the total count. The remaining cells are stromal and are found clustered around blood vessels and connective tissue fibers.

**Deep investing fascia** DIF invests voluntary muscle. DIF connects with SIF using *oblique fibers* but these are discontinuous with those of the overlying layer. The function of the superficial adipofascial plane is movement. The function of the deep adipofascial plane is energy storage and padding. Distinct vascular planes reveal different sources of embryogenesis.

Perhaps the fat layers are different embryologically?

- Superficial fat: pre-pericytes non-somitic population admixed with neural crest.
- Deep fat; prepericytes that enter the somites—perhaps later in development.

[Courtesy Michael Carstens, MD]

## Gross Anatomy

In non-facial skin, white adipose tissue exists in two distinct layers separated by an intervening layer of subcutaneous fascia, likely of neural crest derivation. Although it is referred to as an investing fascia in some mammals it is related to the *panniculus carnosus*. The upper-fat layer is thinner and is interspersed with thin vertically-oriented septae known as the superficial retinacula cutis. These fibers connect the superficial fascia with the overlying dermis, thus permitting the skin to glide. The superficial fascia is of neural crest derivation. Neurovascular structures run along its upper surface. Adipose hypertrophy in this zone creates a puckering effect

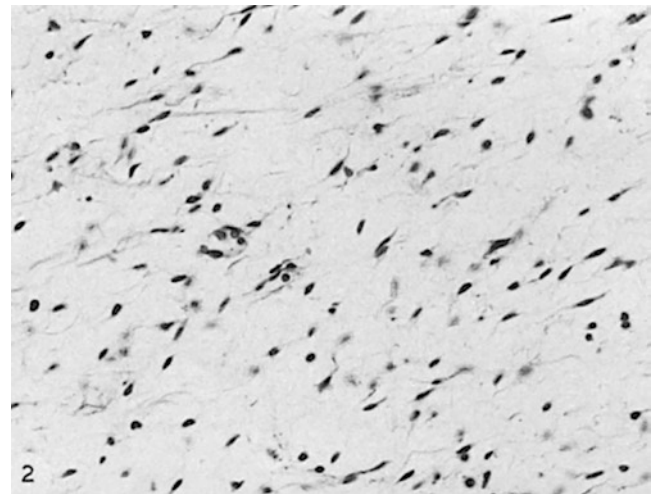


**Fig. 11.25** White fat development, stage 1. 14 weeks Undifferentiated mesenchyme, no obvious vascular invasion. [Reprinted from Poissonet CM, Burdi AR, Bookstein FL Growth and development of human adipose tissue during early gestation. Early human devel 1983; 8:1–11. With permission from Elsevier]

of the overlying skin known in the popular parlance as “cellulite.” (Fig. 11.24).

The lower layer is thicker; and is the site of subcutaneous fat storage. It rests on a deep (investing) fascia associated with the underlying muscle layer. In non-facial skin this fascia arises from paraxial mesoderm. Fibers of the deep reticulum cutis fibers, course obliquely upward to the superficial fascia. This layer provides insulation.

As previously stated, the neuromeric identity of skin is determined by its dermis. Outside the head and neck, skin is organized into dermatomes depending on the somitic origin of its dermis. But subcutaneous fat is not somitic. There is not dedicated “adipotome” compartment in somites. Instead, mammalian fat development follows the invasion of interposition of neural crest cells associated with neurovascular structures. As we shall now see, the true origin of white adipose tissue is vascular.

## Developmental Considerations (Figs. 11.25, 11.26, 11.27, 11.28 and 11.29)

The appearance of white adipose tissue follows a developmental sequence that appears to be neuromeric: head and neck (r0-r11 and c1-c8), thorax (t1-t12), abdominal (l1-l5) and extremities (c4-t1 and l4-s3) but is not somatic. Histologic development takes place in 5 stages, each strongly correlated with blood vessel formation (Poissonet 1983, 1984)

- Stage 1 (14 weeks) undifferentiated mesenchyme: non-condensed amorphous ground substance and stellate cells and ground substance.

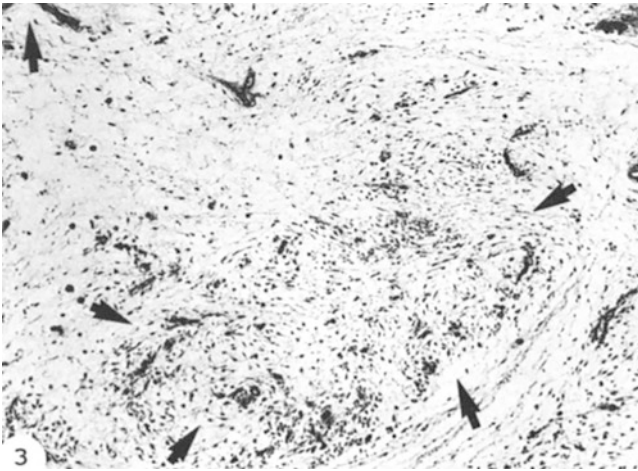


**Fig. 11.26** White fat development, stage 2. 14.5 weeks Mesenchymal condensation is taking place around blood vessels. No lobules are present. [Reprinted from [26, 27]. With permission from Elsevier]

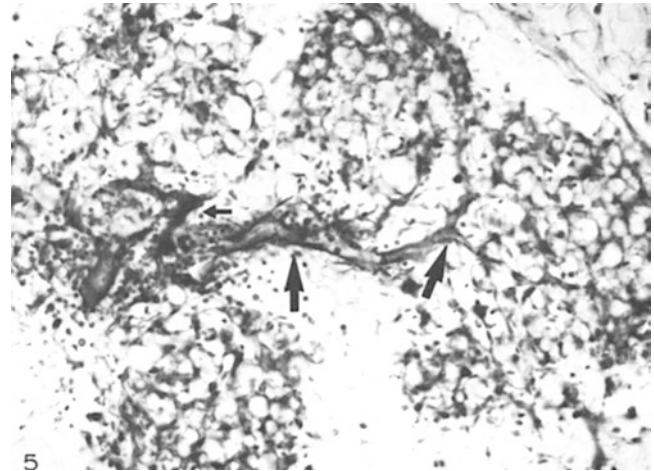


**Fig. 11.28** White fat development, stage 4. 22 weeks Primitive fat lobules. Intracellular fat droplets for storage. [Reprinted from [26, 27]. With permission from Elsevier]

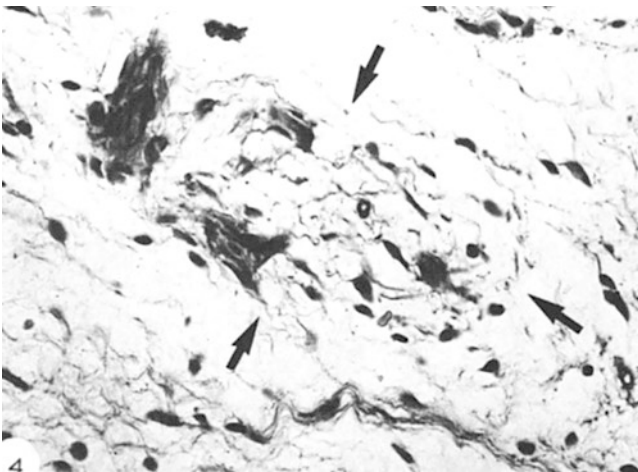


**Fig. 11.27** White fat development, stage 3. 16 weeks Mesenchymal lobules. No intracellular fat droplets. [Reprinted from [26, 27]. With permission from Elsevier]

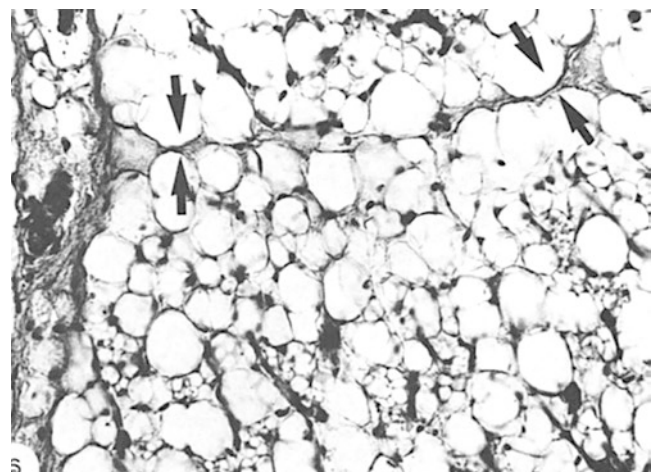


**Fig. 11.29** White fat development, stage 5. Adult configuration. 28 weeks shows fat lobules clearly separated by connective tissue septae. [Reprinted from [26, 27]. With permission from Elsevier]

- Stage 2 (14.5 weeks) angiogenesis: the proliferation of primitive vessels around which fat cells will organize around primitive vessels; no lobules are present.
- Stage 3 (16 weeks) mesenchymal lobules: stellate pre-adipocytes do not contain lipid droplets.
- Stage 4 (22 weeks) primitive fat lobules: each lobule has a vascular stalk that branches off the main vessel. After 23 week number of lobules stabilizes.
- Stage 5 (28 weeks) fat lobules are well separated by stromal septae of connective tissue. In weeks 23–29, lobules increase in size and stabilize.

White fat originates from a poorly characterized precursor cell, the *pre-pericyte* which differentiates either into mature pericytes (vide infra) or into adipose tissue. Furthermore, mesenchymal stromal cells derived either from

pre-pericytes or pericytes themselves have, by definition, the capacity to further differentiate into adipocytes. Pre-pericytes are likely ectomesenchymal in nature given that their pericyte offspring are responsible for SANS stimulation. Moreover, MSCs can be driven in vitro, into primitive neural tissue, indicating that pre-pericytes are NOT strictly mesodermal; more likely they share a common precursor with neural crest cells.

It is widely (and incorrectly) stated that brown fat comes from mesoderm. Pericytes and pre-pericytes are present in all somites as they are associated with the vascular axis of each neuromere. Apparently, pluripotential pre-pericytes that are physically located in a developing somite are committed by the presence of *myogenic factor 5* (*myf5*) into a binary choice depending on the subsequent expression of PRDM16, a zinc finger transcription factor that controls the fate of the cell to become muscle or adipose tissue. PRDM16+ cells become brown fat while PRDM16- cells are committed to myogenesis (Fig. 11.22).









Differentiation of beige fat provides clues about the embryologic origins of the precursor state. The fact that pericyte-derived pre-adipocytes can be driven to beige fat indicates that the number of mitochondria in the white fat cell line is adrenergic dependent as is the physical state of the fat droplet. In beige fat, the solitary droplet is broken down into smaller compartments to create the final histology (Fig. 11.23).

In sum, ectomesenchymal cells with multi-differentiation potential and related to neural crest, flow outward into mesenchymal environments both somitic and non-somitic. In either scenario, some of these will form pericytes and partici-

pate in the vascularization of the tissue. In the case of non-somitic environment adipocytes with a metabolic fate will develop. Within somites, the pre-pericytes are exposed to a sequential influence of *myf5*. Those that express PRDM16 will commit to brown fat.

### Evolution and Lineage of Adipose Tissue (Figs. 11.30 and 11.31)

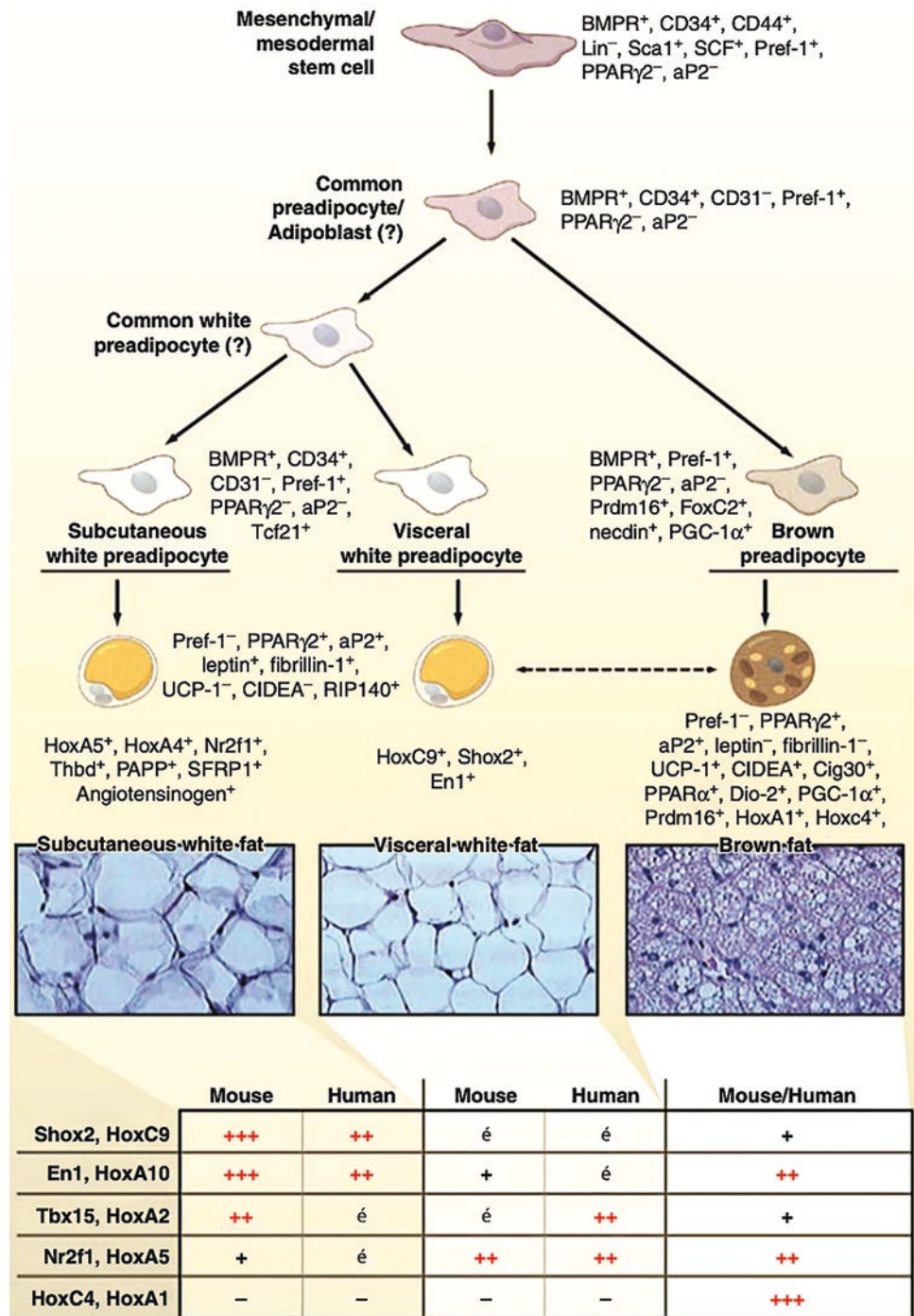
The evolution of adipose tissue is characterized by phylogenetic changes in distribution and fat storage. Worms, such as *C. elegans*, store fat in the intestine, whereas insects such as *Drosophila* have a defined deposition site, the “fat body”. Chondrichthyan fishes (sharks) are devoid of adipose tissue but store fat in the liver. Osteichthyan fishes such as the carp has intra-abdominal deposits of white adipose tissue (WAT) that become apparent, coinciding with the presence of leptin in bony fishes, such as carp (*Cyprinus carpio*). This pattern continues in their evolutionary derivatives, amphibians, and fast-moving reptiles. A branch point appears prior to the divergence of dinosaurs, as precursors of the avian line and the modern reptiles leading to mammals in which WAT is present both internally and subcutaneously. This fat pattern is exemplified by the chicken (*Gallus gallus domesticus*), mouse (*Mus musculus*), and human (*Homo sapiens*). Thermoregulation also appears in the course of evolution but independently of the appearance of brown adipose tissue (BAT). Estimated to have emerged 150 million years ago, BAT is only present in higher mammals, although UCP-1 expression appears independently of BAT in bony fish.

Species	 <i>Caenorhabditis elegans</i>	 <i>Drosophila melanogaster</i>	 <i>Carcharodon carcharias</i>	 <i>Cyprinus carpio</i>	 <i>Xenopus laevis</i>	 <i>Gallus gallus domesticus</i>	 <i>Mus musculus</i>	 <i>Homo sapiens</i>
Fat storage	Stored in intestinal cells	Stored in the “fat body”	Stored in liver	Stored in WAT	Intra-abdominal WAT (no subcutaneous WAT)	Subcutaneous and internal WAT	Subcutaneous and internal WAT	Subcutaneous and internal WAT
Leptin	No	No	No	Yes	Yes	Yes	Yes	Yes
BAT	No	No	No	No	No	No	Present throughout life	Present at birth; reduced in adults
UCP	UCP-like protein ( <i>ucp-4</i> )	No	?	UCP-1 in liver	UCP-4 in oocytes	Avian UCP in muscle	UCP-1 in BAT	UCP-1 in BAT
Thermoregulation	Ectotherm	Ectotherm	Ectotherm	Ectotherm	Ectotherm	Endotherm Shivering and nonshivering thermogenesis	Endotherm Shivering and nonshivering thermogenesis	Endotherm Shivering and nonshivering thermogenesis

**Fig. 11.30** Evolutionary phylogeny of adipose tissue. Note the sequential phylogenetic emergence of white fat (osteichthyes), leptin (tetrapods), and brown fat (mammals). [Reprinted from Gesta S, Tseng

Y-H, Kahn R. Developmental origin of fat: tracking obesity to its source. *Cell* 2007; 131(2): 242–256. With permission from Elsevier]

**Fig. 11.31** From ectomesenchymoblast/pre-pericyte to adipose lineages. Although some stages are still not clearly defined, this differentiation pathway presumably involves differentiation of the pre-pericyte to a common preadipocyte or adipoblast, which has the capacity to differentiate into either white or brown preadipocytes. The proteins and genes that represent potential molecular markers in cells within the adipocyte lineage are marked with a “+” or “-” sign, indicating the relative levels of expression of these markers. The table summarizes the relative ex-pression levels of various developmental and patterning genes in different fat depots in both humans and mice. The relative levels of expression have been graded from absent (-) to high (+++). [Reprinted from Gesta S, Tseng Y-H, Kahn R. Developmental origin of fat: tracking obesity to its source. *Cell* 2007; 131(2): 242–256. With permission from Elsevier]



Endotherm refers to an animal that produces its own heat from within versus ectotherm, an animal that does not. These terms are interchangeable with homeotherm, that is, an animal that can maintain a specific body temperature or are warm-blooded versus poikilotherm, that is, an animal that has a body temperature that varies with the ambient temperature or is cold-blooded.

The embryologic origins of adipose tissue are poorly understood. There certainly exists a mesenchymal precursor stem cell that gives rise to preadipocytes but also gives rise to pericytes. It is often assumed that this precursor arises from mesoderm but that model has developmental flaws. We will develop the argument (vide infra) that this primitive precursor cell can be better termed the **pre-pericyte** and that it is derived

from a lineage of non-neural ectodermal cells, including neural crest, which is *ectomesenchymal*. This cell line emerges from the very inception of gastrulation (stage 6), long before the intraembryonic mesodermal tissues have been defined. The derivatives of this ectomesenchymal cell line therefore contain carry genomic information which gives them the potential to differentiate, not only into mesodermal lines such as fat and cartilage but also to cells that retain a connection with the sympathetic autonomic nervous system.

For the moment, let's consider what we know about the differentiation process of fat. When triggered by appropriate developmental cues, the common pre-pericytes become committed to become pre-adipocytes (white versus brown) versus pericytes. A node exists between preadipocytes destined for white fat versus brown fat. The former carry CD34+ markers whereas the latter are Prdm16+. Note that myoblasts develop along the same line as brown pre-adipocytes but they are Prdm-. In their mature state, white and brown adipose tissues express distinct signatures Hox genes. Since brown fat deposits are associated with somites, future studies are needed to ascertain if there are distinct homeotic signatures of fat in register with specific neuromeric levels.

## Pericytes

### Definition (Fig. 11.32)

Pericytes (Rouget cells) are multi-functional *mural cells* of the *microcirculation* that wrap around the *endothelial cells* that comprise the “tubing” of all capillaries and *venules* throughout the body [6]. Pericytes are embedded in the *basement membrane*, where they communicate with endothelial cells of the body's smallest *blood vessels* by means of both direct physical contact and *paracrine signaling* to control *porosity* and *permeability* [7]. In the brain, they sustain the *blood–brain barrier*. Pericytes *regulate capillary blood flow* and dispose of cellular debris by *phagocytosis*. Pericytes *stabilize maturation of endothelial cells* which they monitor by means of direct communication between the cell membrane as well as through paracrine signaling. A deficiency of pericytes in the *central nervous system* can cause the blood–brain barrier to break down, leading to the leakage of high molecular weight protein down (Winkler, 2011).

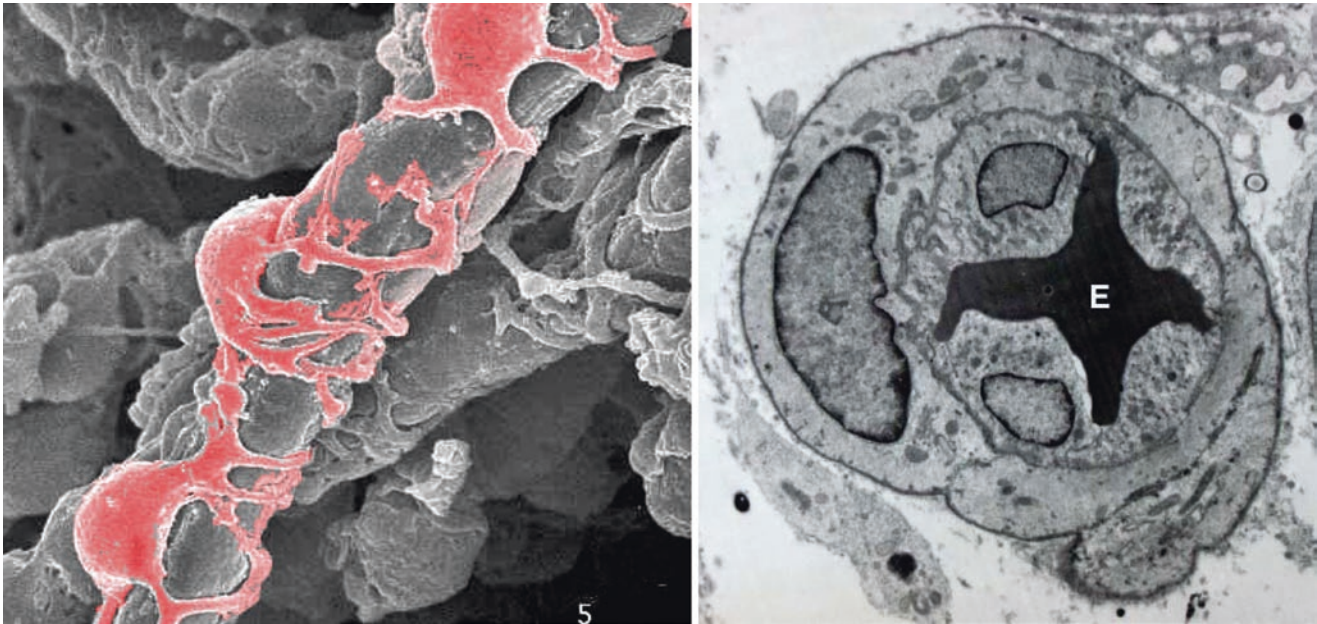


**Fig. 11.32** Pericyte relationship to endothelial cells in a capillary. Pericyte wraps around the circumference of the capillary. Erythrocyte (E) surrounded by two endothelial cells with a single pericyte (nucleus left) encircling the vessel. Left: [Reprinted from Alexander RW, Harrell DB. Autologous fat grafting: use of closed syringe microcannula system for enhanced autologous structural grafting. *Clinical,*

*Cosmetic and Investigational Dermatology*; 2013(6) 91–102. With permission from Dove Medical Press.] Right: [Reprinted from Wikimedia. Retrieved from: <https://en.wikipedia.org/wiki/Pericyte#/media/File:Microvessel.jpg>. With permission from Creative Commons License 3.0: <https://creativecommons.org/licenses/by/3.0/deed.en>]

## Structure

Pericytes wrap around the endothelial cells that line the inside of the capillary. These two types of cells can be easily distinguished: from one another based on the presence of the prominent round nucleus of the pericytes have a prominent round nucleus whereas endothelial cells have nuclei that are flat and elongated. Pericytes have finger-like extensions that wrap around the capillary wall; these extensions are contractile, allowing for regulation of capillary blood flow. Pericytes and endothelial cells share a common basement membrane where a variety of intercellular connections are made. They communicate by means of various types of integrin molecules. Although they are dispersed along the vessel walls pericytes can form direct connections with each other and with neighboring cells by forming peg and socket arrangements in which parts of the cells interlock. At these interlocking sites, [gap junctions](#) can be formed, which allow the pericytes and neighboring cells to exchange ions and low molecular weight compounds. Intercellular connections are mediated by [N-cadherin](#), [fibronectin](#), [connexin](#), and various integrins [8].

## Embryology of the Pericyte (Fig. 11.33)

In the developing embryo, the vascular system appears at stage 5 (of 23) well before all others. The reason is simple: ongoing growth requires mechanisms for nutritional supply and waste removal in order for the organism to survive. Although the endothelial cells of the vascular conduits are mesodermal in nature the pericyte may originate from an ectomesenchymal precursor cell related to neural crest. Pericytes are contractile and communicate. Their adipose progeny, as white and brown adipocytes, carry out neuroendocrine functions directly related to the sympathetic nervous system [8].

## Vascular Niche (Fig. 11.34)

Pericytes have a variety of mural cell types. These form a continuum along the vasculature. Smooth muscle cells form concentric rings on arterioles. Hybrid smooth muscle-pericyte cells reside on precapillary arterioles and interlock

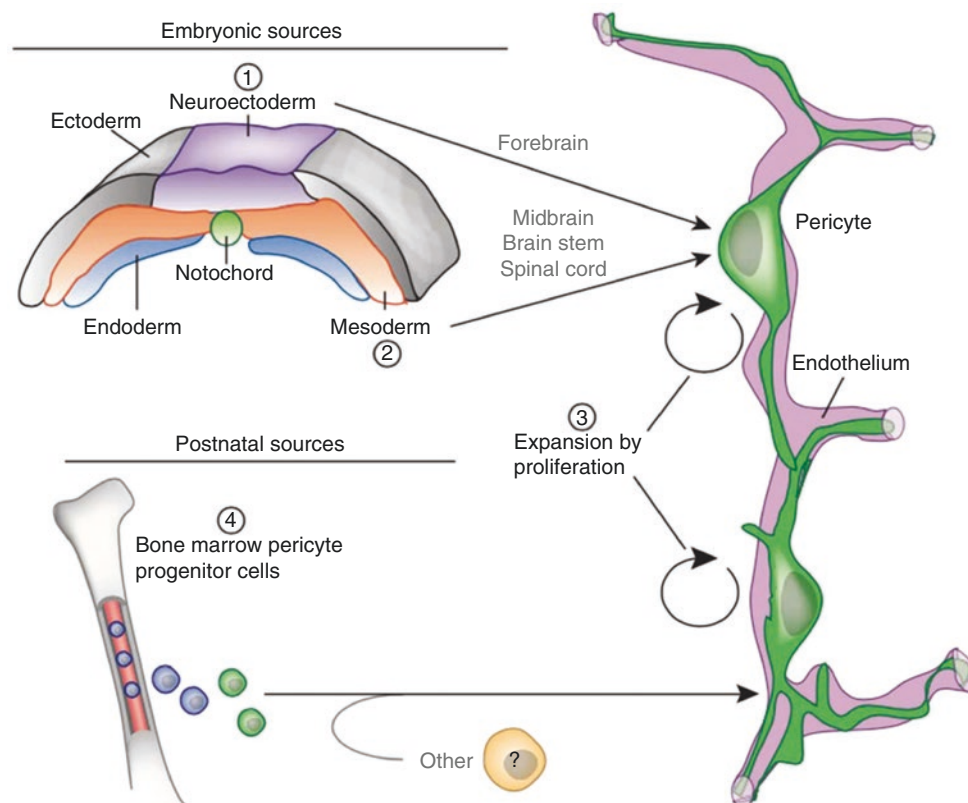


**Fig. 11.33** Origin of pericytes in the CNS. The embryonic sources of pericytes include (1) *neuroectoderm-derived neural crest* cells, which give rise to pericytes of the forebrain, (2) *mesoderm-derived mesenchymal stem cells* -probably originating from pre-pericytes within the mesoderm—which give rise to pericytes in the midbrain, brain stem and spinal cord, and (3) expansion by proliferation from the newly-established *pericyte pools*. Postnatal sources of pericytes include (3)

expansion by proliferation from the existing pericyte pools and (4) mesoderm-derived circulating mesenchymal stem cells (bone marrow pericyte progenitor cells) and presently undetermined ‘other’ sources. **Note:** *Neuroectoderm-derived pre-pericytes likely give rise to MSCs of (2) and (4).* [Reprinted from [28]. With permission from Springer Nature]



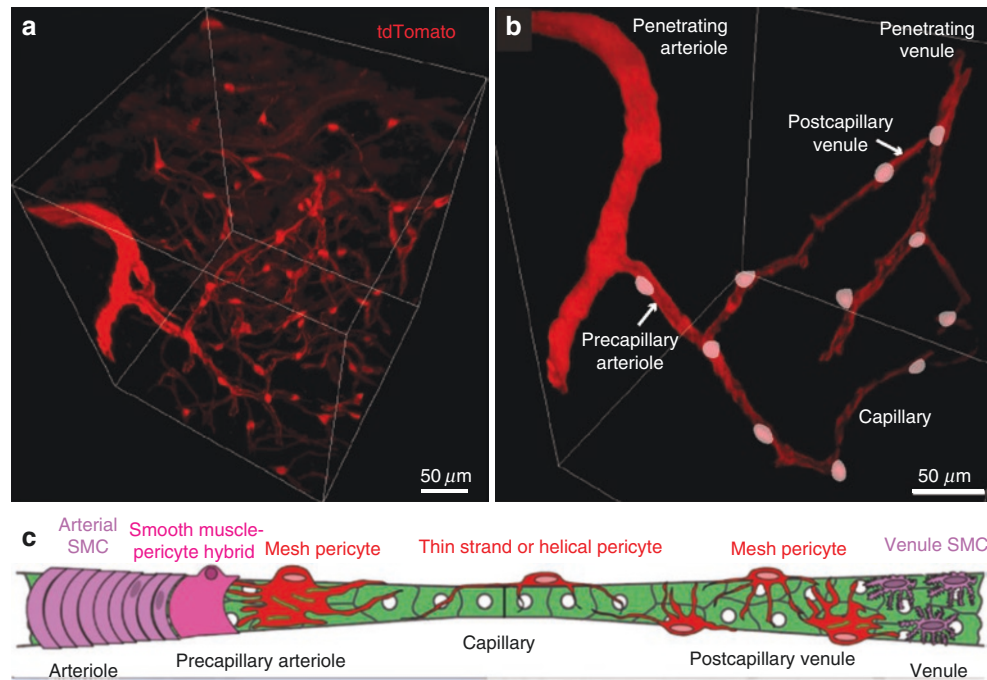


**Fig. 11.34** Pericytes assume different forms depending on their location in the vascular system. Summary of mural (pericyte) cell organization in the cerebrovasculature: (a) A tissue volume from a PDGFR $\beta$ -tdTomato mouse imaged after optical clearing. (b) Distribution of pericytes and pericyte-smooth muscle hybrids in an arteriole-capillary-venule loop. The cell bodies are labeled in white. (c) Schematic showing the continuum of mural cell types along the cerebral vasculature. Smooth muscle cells form concentric rings on arterioles. Hybrid smooth muscle-pericyte cells reside on precapillary arterioles and interlock with mesh pericytes at the arteriole-capillary interface, which occurs as penetrating arterioles ramify into the capil-

lary bed. Pericytes in capillary beds typically exhibit long processes that traverse the microvasculature in single strands or pairs that twist in a helical fashion. Mesh pericytes become more prevalent again as capillaries turn into postcapillary venules. Stellate-shaped smooth muscle cells cover the walls of parenchymal venules. [Reprinted from Hartman DA, Underly RG, Grant RI, et al. Pericyte structure and distribution in the cerebral cortex revealed by high-resolution imaging of transgenic mice. *Neurophotonics* 2015; 2(4): 041402. With permission from Creative Commons License 4.0: <https://creativecommons.org/licenses/by/4.0/>]

with mesh pericytes at the arteriole-capillary interface, which occurs as penetrating arterioles ramify into the capillary bed. Pericytes in capillary beds typically exhibit long processes that traverse the microvasculature in single strands or pairs that twist in a helical fashion. Mesh pericytes become more prevalent again as capillaries turn into postcapillary venules. Stellate-shaped smooth muscle cells cover the walls of parenchymal venules.

## Function

### Differentiation (Fig. 11.35)

Pericytes in the **skeletal striated muscle** are of two distinct populations, distinguished by their ability to express Nestin, their differentiation potential, and their responses to injury by glycerol and barium chloride (BaCl<sub>2</sub>).

#### Type-1

- Nestin negative (PDGFR $\beta$ +CD146 + Nes-).
- Differentiates from fat cells.

- Proliferates to glycerol and to BcCl<sub>2</sub> but differentiates only with glycerol.

#### Type-2

- Nestin positive (PDGFR $\beta$ +CD146 + Nes+).
- Differentiates from muscle cells.
- Proliferates to glycerol and to BcCl<sub>2</sub> and differentiates with both.

## Angiogenesis and Anti-Apoptosis

Pericytes are also associated with endothelial cell differentiation and multiplication, stimulate angiogenesis, promote survival of **apoptotic** signals, and travel. One subtype of pericytes, known as **microvascular pericytes**, develops around the walls of capillaries and helps to serve this function. Microvascular pericytes may not be contractile cells, as they lack **alpha-actin** isoforms, structures that are common amongst other contractile cells. These cells communicate with endothelial cells via **gap junctions**, and in turn, cause endothelial cells to proliferate or be selectively inhibited. If

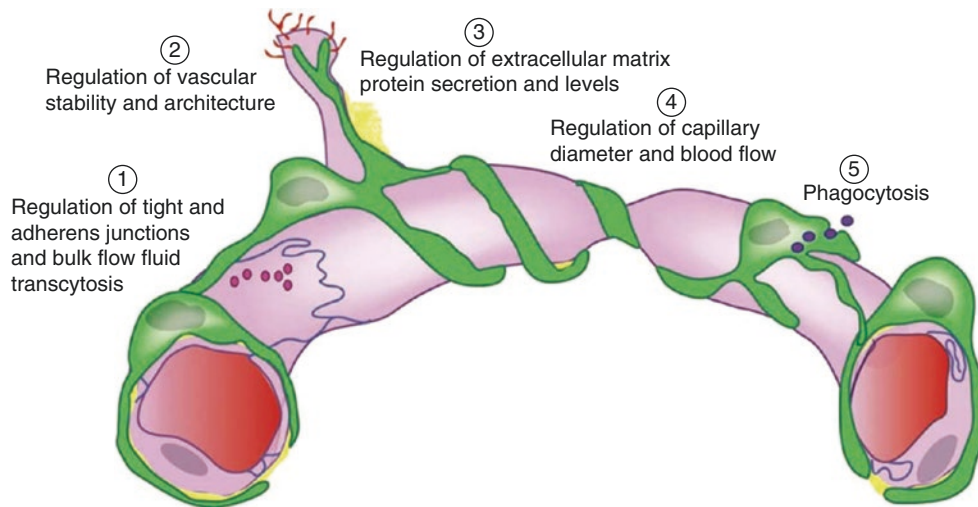


**Fig. 11.35** Pericyte functions. Pericytes are multi-functional members of the neurovascular unit. Pericytes (1) control BBB integrity by regulating the orientation and abundance of endothelial tight and adherens junction proteins, as well as the rate of bulk flow fluid transcytosis (transendothelial transport of fluid-filled vesicles); (2) regulate the stability and architecture of newly formed cerebral microvessels; (3) con-

tribute to secretion and regulate the levels of extracellular matrix proteins forming the basement membrane; (4) regulate capillary diameter and blood flow; and (5) provide clearance and phagocytotic functions in brain. [Reprinted from [28]. With permission from Springer Nature]

this process did not occur, **hyperplasia** and abnormal vascular **morphogenesis** could result. These types of pericytes can also **phagocytose** exogenous proteins. This suggests that the cell type might have been derived from microglia, an association that stems from their ectomesenchymal origin and thus relates them to neural crest.

Lineage relationships to other cell types have been proposed, including **smooth muscle cells**, neural cells, NG2 glia, muscle fibers, **adipocytes**, as well as fibroblasts and other **mesenchymal stem cells**. However, whether these cells differentiate into each other is an outstanding question in the field. Although aging affects pericytes' regenerative capacity, they remain functional throughout life. Such versatility is useful, as they actively remodel blood vessels throughout the body and can thereby blend homogeneously with the local **tissue** microenvironment.

Aside from creating and remodeling blood vessels, pericytes have been found to protect endothelial cells from death via apoptosis or **cytotoxic** elements. It has been shown *in vivo* that pericytes release a **hormone** known as *pericytic aminopeptidase N/pAPN* that may help to promote angiogenesis. When this hormone was mixed with **cerebral** endothelial cells as well as astrocytes, the pericytes grouped into structures that resembled capillaries. Furthermore, in the absence of pericytes, the endothelial cells would undergo apoptosis. Thus, proper angiogenesis depends on (1) the presence of pericytes to ensure the proper endothelial cell function, and (2) the presence of astrocytes, as these cells ensure that both other cell types remain in contact with each other. Pericytes contribute to the survival of endothelial cells,

as they secrete the protein **Bcl-w**, an instrumental protein in the pathway that enforces **VEGF-A** expression and discourages apoptosis, by inhibiting the activation of apoptosis-inducing **enzymes**. Two biochemical mechanisms utilized by VEGF to accomplish this would be the **phosphorylation** of **extracellular regulatory kinase 1** (ERK-1, also known as MAPK3), which sustains cell survival over time, and the inhibition of stress-activated protein kinase/c-jun-NH2 kinase, which also promotes apoptosis.

### Blood Flow

Increasing evidence suggests that pericytes can **regulate blood flow** at the capillary level. Retinal pericytes constrict capillaries when their membrane potential is altered to cause calcium influx. In the brain, it has been reported that neuronal activity increases local blood flow by inducing pericytes to dilate capillaries. Thus, different mechanisms regulate the constriction of capillaries by pericytes and of arterioles by smooth muscle cells. Pericytes are also important in **maintaining circulation**. In a study involving adult pericyte-deficient mice, cerebral blood flow was diminished with concurrent vascular regression due to loss of both endothelia and pericytes. Significantly greater hypoxia was reported in the hippocampus of pericyte-deficient mice as well as inflammation, learning, and memory.

### Selective Permeability: Blood–Brain Barrier

Pericytes play a crucial role in the formation and functionality of the **blood–brain barrier**. This barrier is composed of endothelial cells and ensures the protection and functional-

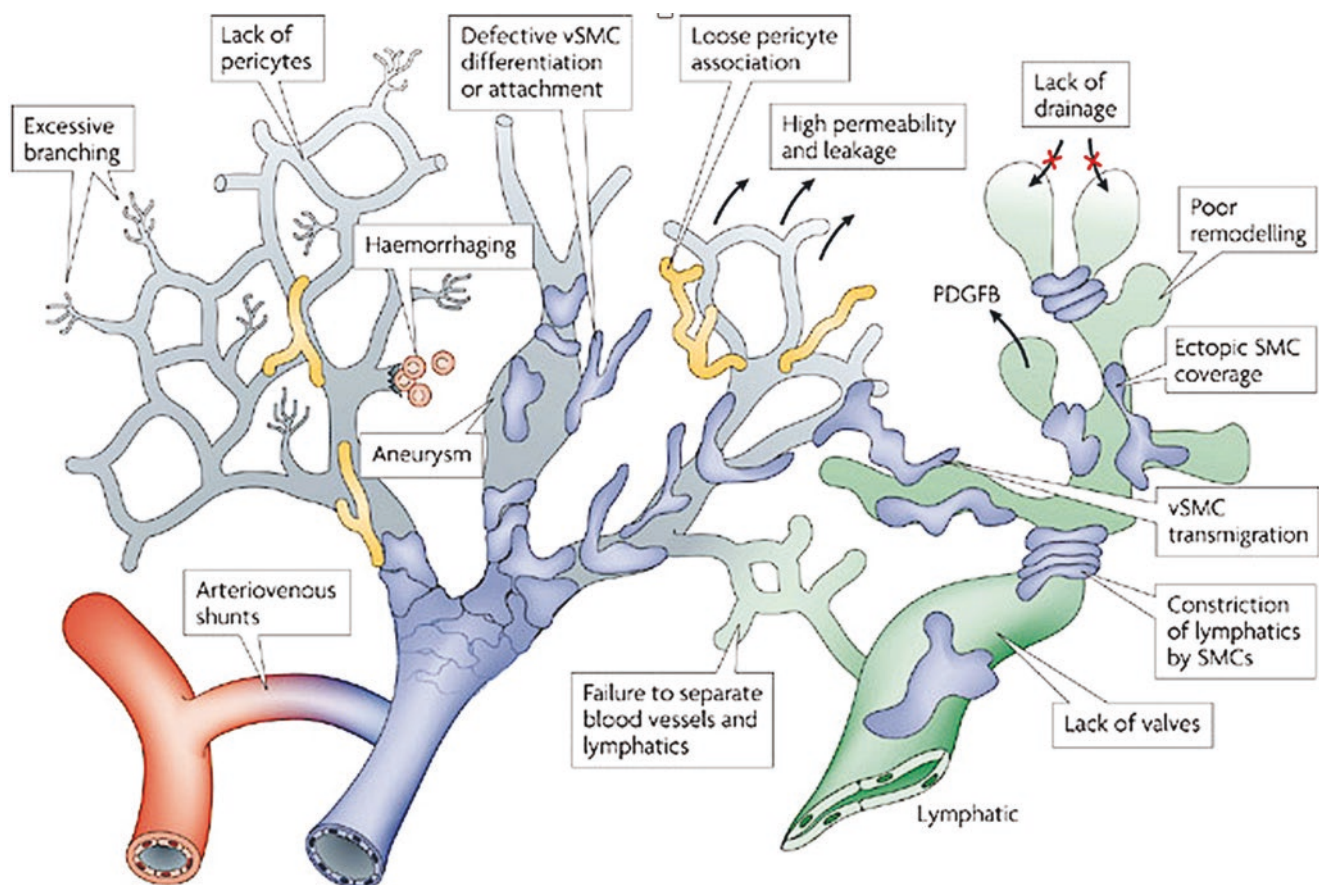
ity of the brain and central nervous system. It has been found that pericytes are crucial to the postnatal formation of this barrier. Pericytes are responsible for **tight junction** formation and **vesicle trafficking** amongst endothelial cells. Furthermore, they allow the formation of the blood–brain barrier by inhibiting the effects of CNS **immune cells** (which can damage the formation of the barrier) and by reducing the expression of molecules that increase vascular permeability [9].

Aside from blood–brain barrier formation, pericytes also play an active role in its functionality by controlling the flow within blood vessels and between blood vessels and the brain. In animal models with lower pericyte coverage, trafficking of molecules across endothelial cells occurs at a higher frequency, allowing proteins into the brain that would normally be excluded. Loss or dysfunction of pericytes is also theorized to contribute to neurodegenerative diseases such as **Alzheimer's**, **Parkinson's**, and **ALS** through the breakdown of the blood–brain barrier [7].

### Pathologies of Pericytes (Figs. 11.36 and 11.37)

*Hemangiopericytoma* is a rare vascular neoplasm, or abnormal growth, that may either be benign or malignant. In its malignant form, metastasis to the lungs, liver, brain, and extremities may occur. It most commonly manifests itself in the femur and proximal tibia as a bone sarcoma and is usually found in older individuals, though cases have been found in children. Hemangiopericytoma is caused by the excessive layering of sheets of pericytes around improperly formed blood vessels. Diagnosis of this tumor is difficult because of the inability to distinguish pericytes from other types of cells using light microscopy. Treatment may involve surgical removal and radiation therapy, depending on the level of bone penetration and stage in the tumor's development.

*Diabetic retinopathy* is commonly associated with a loss of pericytes. Pericytes are essential in diabetic patients as they protect the endothelial cells of retinal capillaries. With the loss of pericytes, microaneurysms form in the capillaries.



Nature Reviews | Molecular Cell Biology

**Fig. 11.36** Pericyte pathologies. Defective numbers of pericytes make the vessel walls unstable: resulting in aneurysm or hemorrhage. Smooth muscle may fail to attach properly to the vessel wall. Abortive attempts at new vessel formation or arteriovenous fistulae can occur. Shunting between the venous and lymphatic systems has been documented.

[Reprinted from Armulik A, Genové G, Betscholtz C. Pericytes: Developmental, physiological and pathological perspectives, problems and promises. *Developmental Cell* 2011; 21(2): 193–215. With permission from Elsevier]

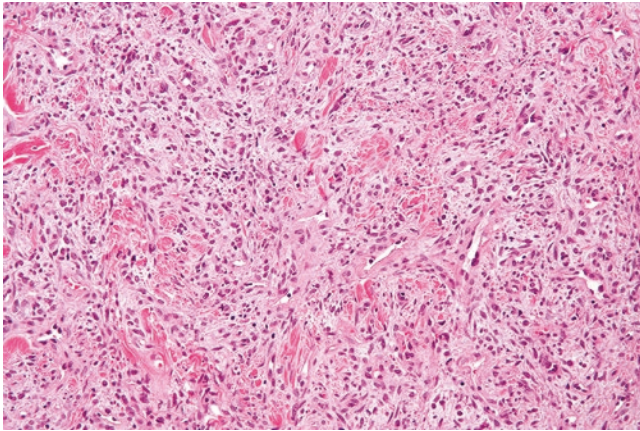


**Fig. 11.37** Hemangiopericytoma. Histologic Features: Cellular solitary fibrous tumors (hemangiopericytoma pattern) are composed of plump round or oval cells lacking atypia. The cells are arranged haphazardly or in short, intersecting fascicles around a network of sinusoidal vessels with staghorn configuration. The cells have moderate amount of eosinophilic cytoplasm with indistinct borders. Mitotic activity is not increased. [Reprinted from Wikimedia. Retrieved from: [https://commons.wikimedia.org/wiki/File:Solitary\\_fibrous\\_tumour\\_intermed\\_mag.jpg](https://commons.wikimedia.org/wiki/File:Solitary_fibrous_tumour_intermed_mag.jpg). With permission from Creative Commons License 3.0: <https://creativecommons.org/licenses/by-sa/3.0/deed.en>]

The retinal response with (1) increased vascular permeability and macular edema or with (2) neovascular vessels that penetrate into the vitreous membrane. Either of these processes leads to a reduction or loss of vision. Pericyte loss in diabetic patients has been attributed to the stimulation of the polyol pathway by elevated glucose levels. The intracellular accumulation of sorbitol, fructose, and advanced glycation products (AGEs) is toxic as it leads to osmotic imbalance, which results in cellular damage.

### Interactions between Endothelial Cells and Pericytes

There are several pathways of communication between endothelial cells and pericytes. Pericyte differentiation is dependent on transforming growth factor (TGF) signaling from endothelial cells. Pericyte recruitment depends on platelet-derived growth factor (PDGF) from the endothelial cells as it directs the pericytes to migrate toward and populate developing blood vessels. Blocks in this pathway lead to pericyte deficiency and instability of the blood vessel walls. Endothelial signaling with sphingosine-1-phosphate (S1P) promotes N-cadherin tracking signals in endothelial membranes; these strengthen endothelial contacts with pericytes. In turn, endothelial cells are themselves stabilized by pericyte production of angiopoietin 1 and Tie-2 signaling.

Communication defects between endothelial cells and pericytes result in vascular instability. Inhibiting the PDGF pathway leads to pericyte deficiency. This causes endothelial hyperplasia, abnormal junctions, and diabetic retinopathy. A lack of pericytes also causes an upregulation of vascular

endothelial growth factor (VEGF), leading to vascular leakage and microhemorrhage. Angiopoietin 2 is antagonistic to Tie-2, thereby destabilizing the endothelial cells, resulting. Less endothelial cell and pericyte interaction. This occasionally leads to a proliferative tumor state, hemangiopericytoma. Reduction in pericytes by angiopoietin 2 reduces levels of pericytes, leading to diabetic retinopathy.

### Neurodegeneration and Scarring

Studies have found that pericyte loss in the adult and aging brain leads to the disruption of proper cerebral perfusion and maintenance of the blood–brain barrier, which causes neurodegeneration and neuroinflammation. Pericyte apoptosis in the aging brain may result from failed communication between growth factors and pericyte receptors.

Immunohistochemical studies of human tissue from Alzheimer’s disease and amyotrophic lateral sclerosis show pericyte loss and breakdown of the blood–brain barrier. Pericyte-deficient mouse models (which lack genes encoding steps in the PDGFB:PDGFRB signaling cascade) and have an Alzheimer’s-causing mutation have exacerbated Alzheimer’s-like pathology compared to mice with normal pericyte coverage and an Alzheimer’s-causing mutation.

### Pericytes and Mesenchymal Stromal Cells

Bone marrow contains two lines of multipotent mesenchymal cells: The first to be described was the hematopoietic line, all with CD34+ markers and with differentiation into the various types of blood cells. In the 1970s Friedenstein reported that bone marrow stroma (non-osseous structural elements such as collagen fibers and blood vessels) harbored a distinct mesenchymal line of CD34- cells which were shown in vitro to differentiate into multiple mesodermal lineages such as chondrocytes, osteoblasts, myocytes, and adipocytes. This multilineage behavior gave rise to the term, *mesenchymal stem cells* (MSCs) which, however popular, is not accurate, as this differentiation does not take place in vivo. Instead, MSCs are best considered as mesenchymal stromal cells, mesenchymal signaling cells, or medicinal stromal cells [10]. In 2001 Zuk et al. described the existence of MSCs in adipose tissue. These cells have the same cell markers as those in bone marrow but exist in far greater numbers; being up to 500 times more frequent. CD marker analysis reveals that the pericyte is the likely precursor of both types of MSCs. Direct involvement of pre-pericytes in adipogenesis explains the high number of MSCs found in the stromal vascular fraction.

Comparison of cell membrane markers demonstrates a very close match between pericytes and MSCs such that pericytes can be considered the legitimate precursor cell line. Alternatively, these cell lines may represent related derivatives of a common precursor, putatively, the pre-pericyte.

[Caplan] Under conditions of stress, such as infection and inflammation, pericytes detach from their vascular niche and undergo transformation into MSCs. Furthermore, the two cell lines share an overlapping menu of documented clinical effects. From a clinical standpoint, they are literally “an injury drugstore.” [11].

### Adipose Tissue-Derived Reconstructive Materials

While the clinical applications of adipose-derived stem/stromal cell products are evolving rapidly, the terminology regarding fat and its reconstructive products is quite confusing; therefore, a clarification is necessary based on histology: (1) adipose tissue complex, (2) Coleman-type whole fat graft, (3) microfat whole fat graft, (4) tissue stroma graft, and (4) cellular stromal graft.

### Adipose Tissue Complex (ATC) (Fig. 11.38)

In histological terms, a tissue consists of a functional component, the parenchyma, and a supporting component, the stroma. *Parenchyma* refers to an aggregate of cells specifically organized to accomplish a function. *Stroma*, a word of Greek origin (“bed”), refers to cells or structures that are not specific, but rather perform a structural or nutritional support function (connective tissues, vessels, and lymphatics) or communicate between the parenchyma and another anatomical site (nerves and ducts).

The most primitive component in the embryo is the vascular system. It is the first system to be formed; of the 23 stages in the embryonic period, the vessels are only identifiable at stage 5. And it is to be assumed because the mere survival of the embryo depends on achieving a link that guarantees nutrition. Primitive vessels have only two components: a tube made up of endothelial cells, and a network of

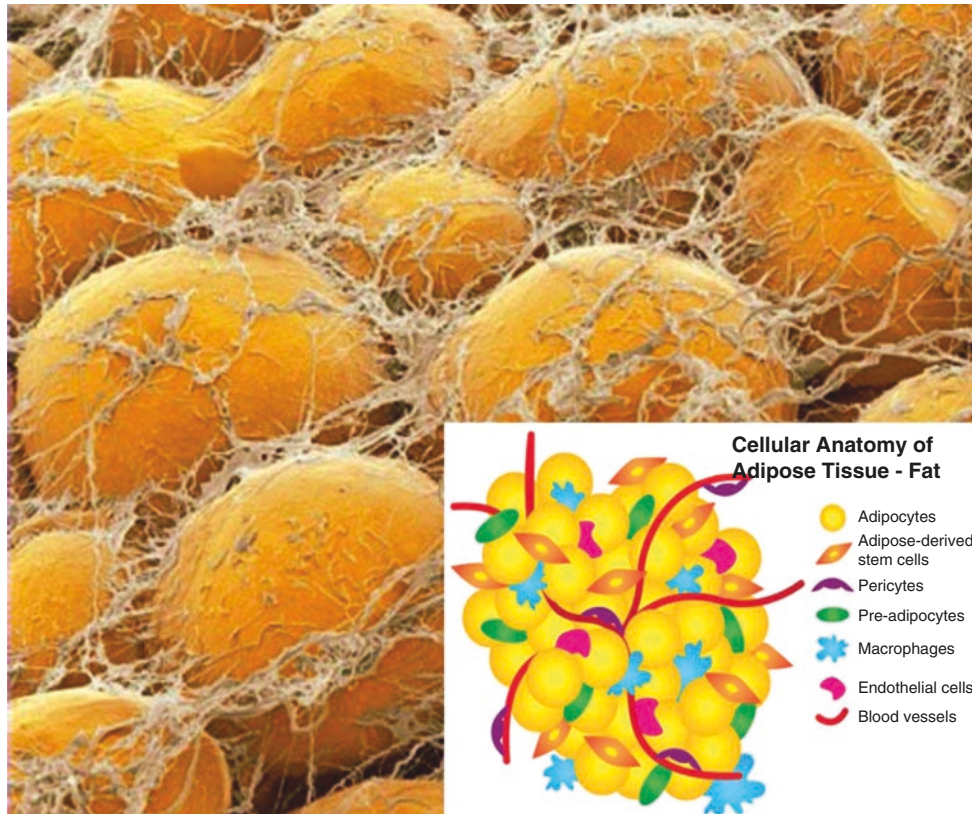


**Fig. 11.38** Adipose tissue. Parenchyma consists of the functional cells of the adipose organ (adipocytes) Stroma refers to the supporting cells for the adipose organ: blood vessels, nerves, lymphatics, and structural proteins. Composition of the adipose tissue complex is 85% adipocytes by volume only 12–15% adipocytes by total cell count.

- Adipocytes (yellow): terminally differentiated, endocrine-active
- Pre-adipocytes (green): progenitor cells, near terminal differentiated form, adherent to adipocytes
- Pericytes (purple): physically related to endothelial cells of the microvascular system; important in angiogenesis.

- Endothelial cells (pink).
- Mesenchymal stem cells (orange): derived from pericytes these constitute approximately 45% of nucleated cell counts in SVF.
- Macrophages (blue) in extracellular matrix: intrinsic versus extrinsic (blood).
- Extracellular matrix: fibroblastic elements.

[Reprinted from Alexander RW, Harrell DB. Autologous fat grafting: use of closed syringe microcannula system for enhanced autologous structural grafting. *Clinical, Cosmetic and Investigational Dermatology*; 2013(6) 91–102. With permission from Dove Medical Press.]



**Fig. 11.39** Density Gradient Separation. Left: Standard decantation; Right: Post-centrifugation (1000 g-force for 4 minutes) Note in the latter process the clear separation of the lipid supernatant layer and the aqueous infranatant layer. [Reprinted from Alexander RW, Harrell DB. Autologous fat grafting: use of closed syringe microcannula system for enhanced autologous structural grafting. *Clinical, Cosmetic and Investigational Dermatology*; 2013(6) 91–102. With permission from Dove Medical Press]

regulatory cells, the pericytes. These form a network outside the actual vessel and perform functions of controlling its porosity and diameter. Therefore, they have a future connection with the sympathetic nervous system. Hence, they have an embryonic relationship with their cousins, the neural crest cells.

Being a component of every vessel in the body, pericytes are found in all human tissues, where they represent the mere origin precursors of mesenchymal cells (MSCs), the so-called “stem cells.” Since the pericyte is also the precursor cell for white fat, the concentration of MSCs in fat is the richest in the body.

The adipose tissue complex (CTA) has, as its parenchymal component, adipocytes that constitute 90% of the volume plus 10% of its cellular content. These adipocyte aggregates are  $\geq 400$  microns in diameter and are supported by a multicellular stroma.

**ATC fat graft (Coleman):** atraumatic technique and graft placement near microvessels (Fig. 11.39).

For more than 100 years the use of whole-fat grafts has had a bad reputation. These tissue grafts had high levels of reabsorption, given the vulnerability of their parenchymal

component (adipocytes) to ischemia. In 1987 Syndey Coleman demonstrated better results using low-pressure atraumatic harvesting with smaller cannulae and graft placement in mini-rows in the circumference of the subcutaneous vascular network with greater nutritional support and greater graft retention. Thus, fat transplantation changed towards a less traumatic process with reproducible results.

The concept of separation by centrifugation, also introduced by Coleman, solved another fundamental problem: the variability in the real volume of the grafts. The aesthetic plastic surgery literature, a repository of extensive evidence regarding fat grafting, reports great variability in the rate of “resorption” observed in structural fat grafting procedures. Most of these reports do not account for the fact that these grafts *themselves* contain an appreciable amount of fluid (up to 30–40% of their total volume) due to the injection of serum with epinephrine prior to liposuction. These carrier fluid volumes have been described as a residual volume “load”, and when included in the injection constitutes a diluting factor that affects the actual cellular content of the graft.

In addition, Coleman documented the trophic effects that these grafts exert on receptor sites so. These observations revealed the importance of stromal elements in adipose tissue.

- Purpose: volumetric reconstruction.
- Tissue: parenchyma + stroma.
- Adipocyte content 80%.
- Diameter: 1–3 mm.
- Processing: washing and centrifugation @ 1000 rpm for 4 minutes.
- Placement: Mini-grafts placed in multiple parallel rows.

**ATC microfat graft:** size reduction for better graft survival (Fig. 11.40).

The purpose of microfat is to increase graft retention by harvesting to the smallest possible diameter to allow adipocyte survival.

- Purpose: volumetric reconstruction.
- Tissue: parenchyma + stroma.
- Adipocyte content 80%.
- Diameter: 700 nm to 1.0 mm via harvest using small diameter cannulae.
- Processing and placement: similar to Coleman.

**AD-tSVF graft:** adipose-derived tissue SVF (Figs. 11.41, 11.42 and 11.43).

**Mechanical dissociation:** This technique eliminates adipocytes using a traumatic disruption, leaving as a product an emulsion in which there is a matrix of fibers, vessels, cells

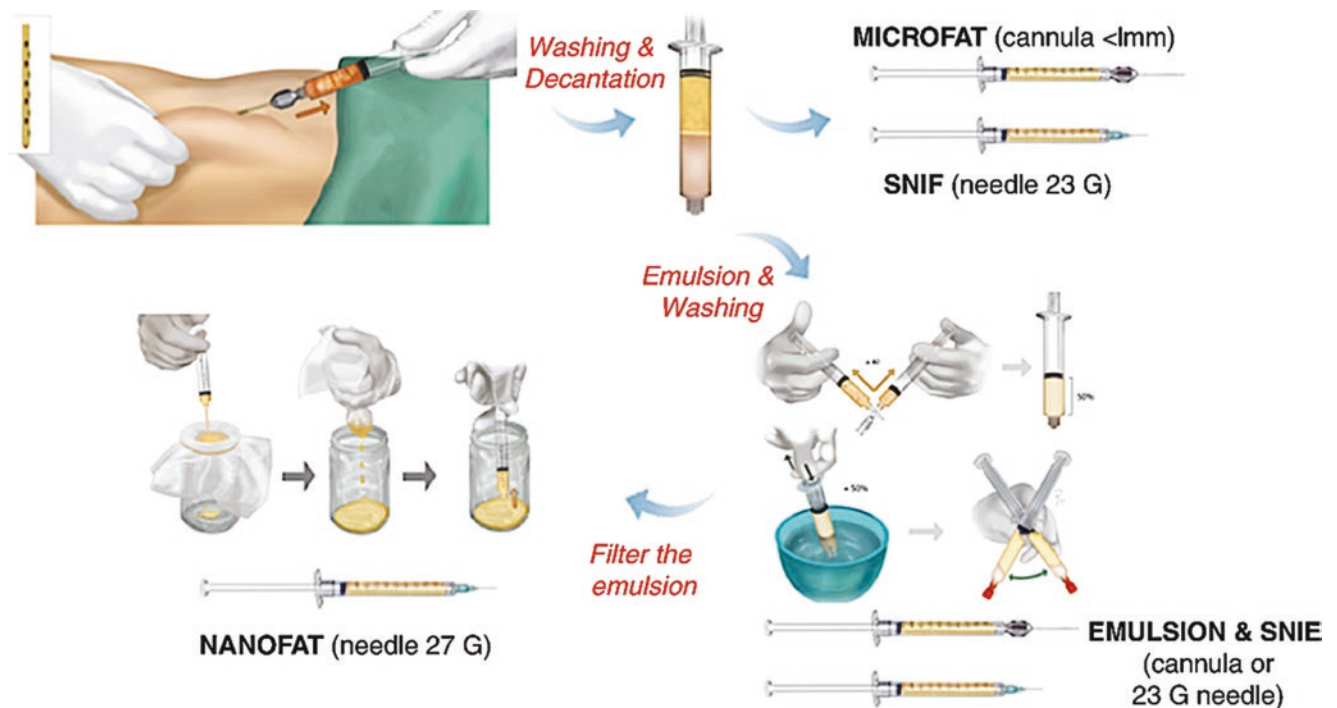


**Fig. 11.40 Microfat.** Microfat is produced from a mechanical separation method that maintains the viability of the adipocytes using: (1) saline wash, (2) mesh filter, (3) sedimentation by gravity vs centrifuge, (4) reduction to 1 mm Adipocytes are 400 nm so they survive. [Reprinted from Serra-Mestre J, Serra-Ramon JM. Variants of Fat Grafting: from

Structural Fat Grafting to Microfat, Sharp-Needle Intradermal Fat (SNIF), Nanofat. In: Pinto H, Fontdevila J. (ed). Regenerative Medicine Procedures for Aesthetic Physicians. Springer, Cham; 2018: 81–85. With permission from Springer Nature]



**Fig. 11.41 Mechanical reduction system to produce Nanofat (AD-tSVF).** 1. Tissue harvest with cannulae  $\leq 3.0$  mm 2. tissue is washed for pH control and reduction of inflammatory cells 3. centrifugation of capped (red) syringes @ 200 gm 4. serial passage of dry fat through reducing Leur-Leur connectors (3.0 mm, 2.5 mm, 2.0 mm, 1.5 mm) 5. Final pass through a nanofat filtration chamber (purple) containing 400 nm mesh. [Courtesy of Michael Carstens, MD]

connected with those elements, and loose cells. Although the crude number of stem cells released in this emulsion is less than their count in a pure solution, they nevertheless maintain similar biological actions.

- Purpose: trophic effects.
- Tissue: emulsion: predominantly stroma.
- Adipocyte content 15% adipocytes.
- Diameter: 400 nm (some adipocytes survive).
- Processing: mechanical disruption of adipocytes.

The cellular composition of AD-tSVF is:

- Cell proportions do not have good characterization.

**AD-cSVF graft:** adipose-derived cellular SVF (Figs. 11.44, 11.45, 11.46 and 11.47).

**Enzymatic dissociation:** This technique removes adipocytes using enzymatic digestion by collagenases, leaving a cellular liquor as a product. AD-cSVF is a pure liquid without fibrotic structures, such as collagen fibers. Therefore, SVF of enzymatic origin is pure enough that it allows its use intravascular, but at the same time, the viable mononuclear cells in that solution lack native structures (such as elastic fibers, collagen networks, tubes) with which they previously maintained a physiological relationship:

- Purpose: trophic effects.
- Tissue: purely cellular concentrate derived from stroma.
- Adipocyte content 0%.

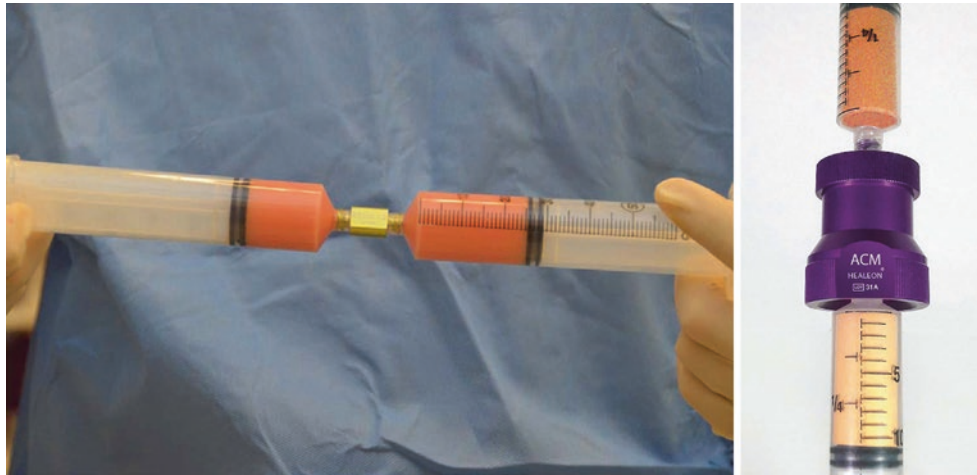


**Fig. 11.42** Mechanical dissociation. Consecutive reductions (4) by Leur-Leur connector: from 3.0 mm to 1.5 mm. Each connector reduction requires 30 passes. Single-pass reduction via mesh filter: 0.4 mm. Note color change from the delivery port (left) to the recipient port (right). [Reprinted from Alexander RW, Harrell DB. Autologous fat

grafting: use of closed syringe microcannula system for enhanced autologous structural grafting. *Clinical, Cosmetic and Investigational Dermatology*; 2013(6) 91–102. With permission from Dove Medical Press]

Microfat (emulsion, dense / color orange)  
 Nanofat (emulsion, creamy / color white)

Microfat 700-1000 nm non-homogeneous  
 Nanofat 400 nm es homogeneous

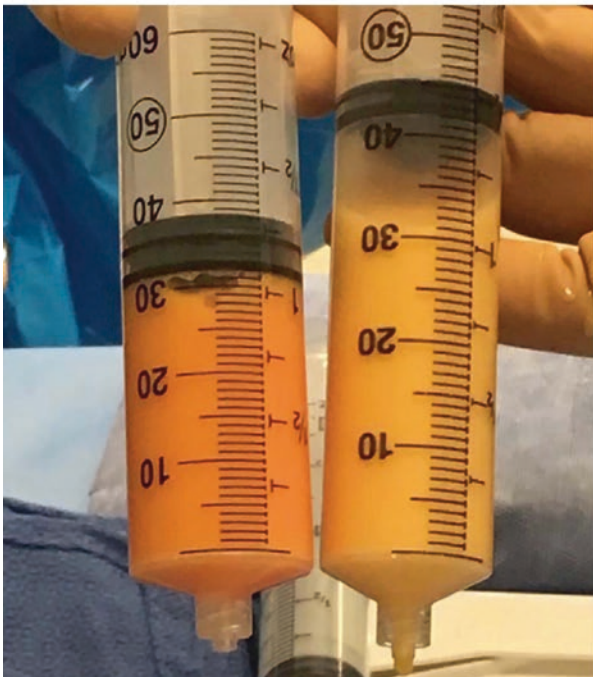


**Fig. 11.43** Microfat vs Nanofat: 700 nm vs 400 nm. LEFT: microfat is a dense orange emulsion whereas nano fat is a creamy, white emulsion. RIGHT: When applied to gauze, the lumpy nature of 700 nm diameter microfat is compared with the homogeneous appearance of 400 nm nanofat. Left: [Reprinted from Rihani J. Microfat and nanofat: when and where these treatments work. *Fac Plast Surg Clin North America*

2019; 27(3): 321–330.with permission from Elsevier.]. Right: [Reprinted from Dong Seok Oh, Dae Hwa Kim, Tai Suk Roh, In Sik Yun, Young Seok Kim Correction of Dark Coloration of the Lower Eyelid Skin with Nanofat Grafting. *Arch Aesthetic Plast Surg* 2014;20(2):92–96. With permission from Creative Commons License 3.0: <https://creativecommons.org/licenses/by-nc/3.0/>]



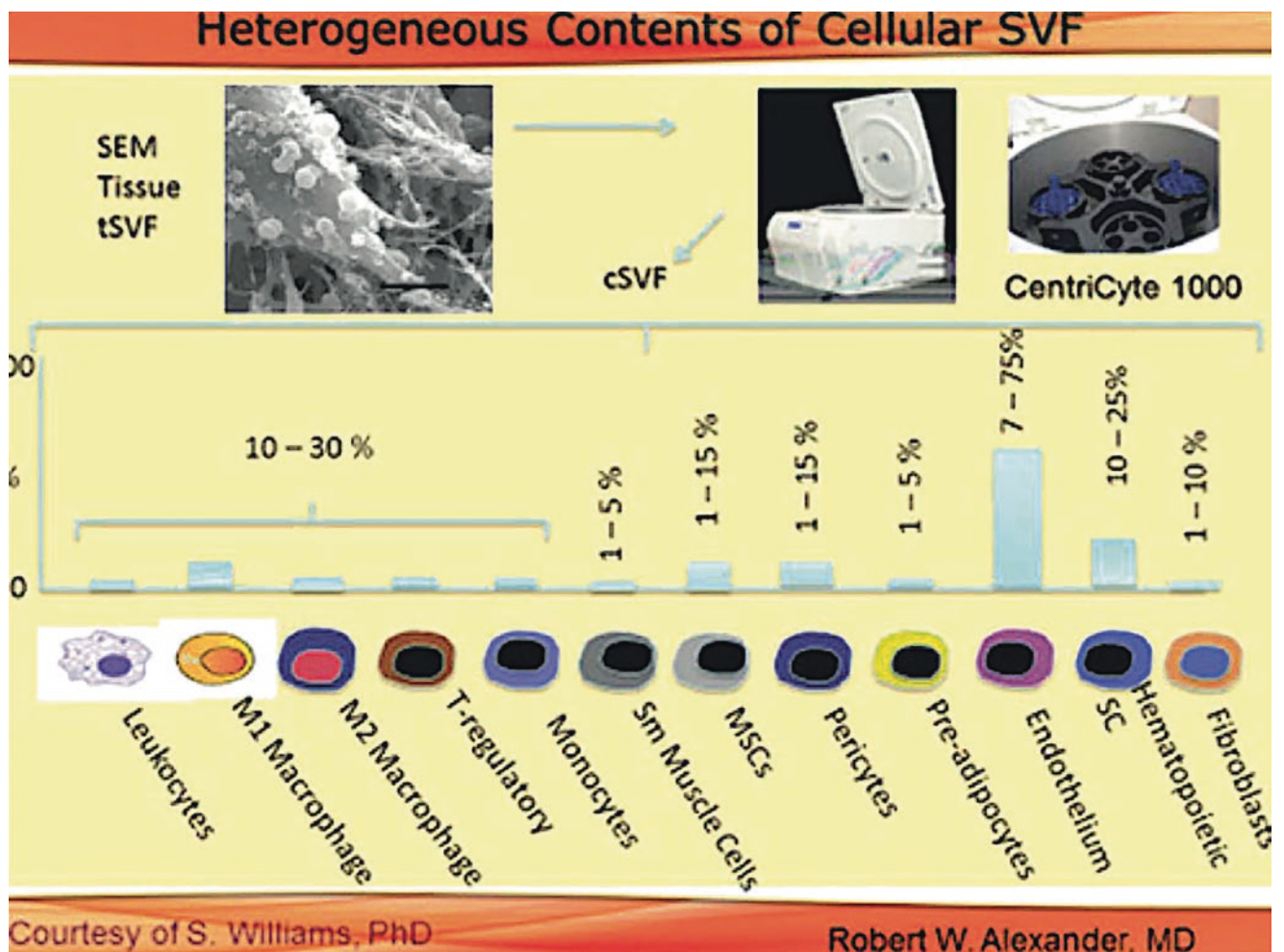


**Fig. 11.44** Cell profile of adipose-derived SVF after digestion (adipocytes removed). [Reprinted from Alexander RW, Harrell DB. Autologous fat grafting: use of closed syringe microcannula system for enhanced

autologous structural grafting. *Clinical, Cosmetic and Investigational Dermatology*; 2013(6) 91-102. With permission from Dove Medical Press]

- Diameter: less than  $\leq 400$  nm (no adipocytes).
- Processing: enzymatic digestion of adipocytes.

The cellular characterization of AD-cSVF is:

- 10-30% leukocytes, M1 and M2 macrophages, regulatory T cells, monocytes
- 1-5% myocytes (smooth type)
- 1-15% MSCs signaling mesenchymal cells/stem cells
- 1-15% pericytes
- 1-5% preadipocytes
- 7-70% endothelial cells
- 10-25% hematopoietic stem cells
- 1-10% fibroblasts.

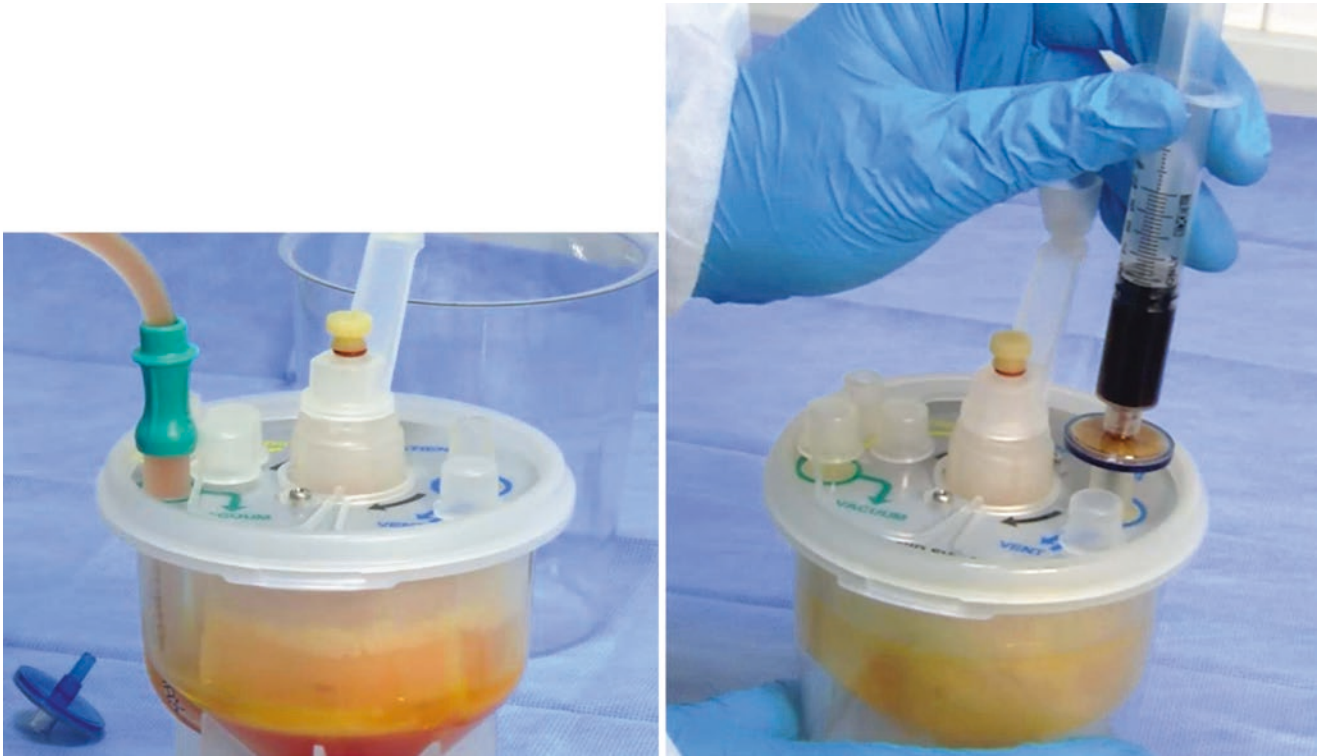


**Fig. 11.45** Enzymatic reduction system to produce AD-cSVF. 1. harvest 2. wash to normalize pH and decrease inflammatory (CD 45+) cells from 60% > 10% 3. collagenase (blue) digestion 4. centrifugation 5. extraction of pellet. [Courtesy of Michael Carstens, MD]

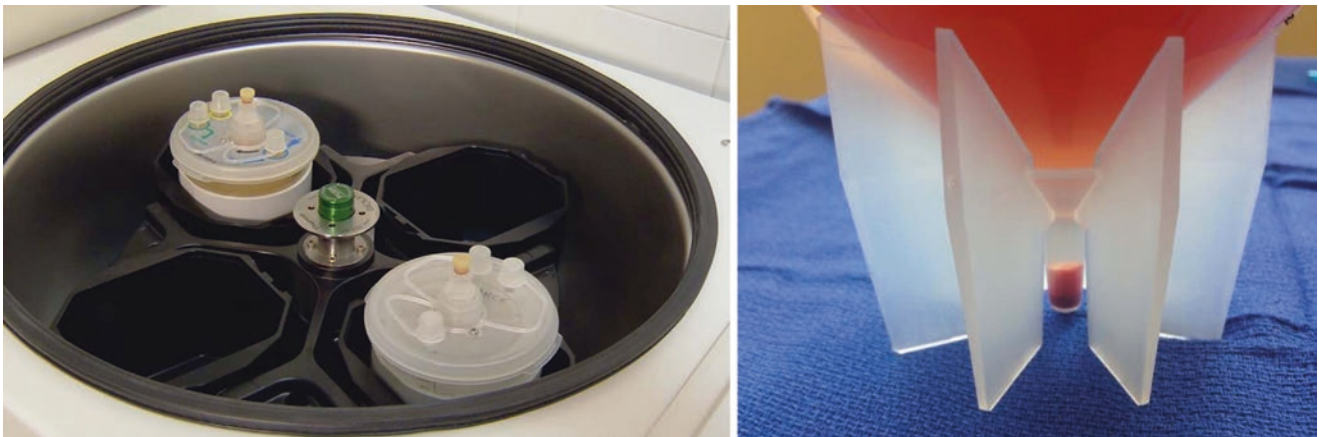


**Fig. 11.46** Lipoaspirate post-digestion is a slurry of stromal tissue suspended in a slurry of ruptured adipocytes. Centrifugation at 600 g drives the stroma against the 400 nm mesh with SVF cells forced down-

ward into a collection chamber to create a cellular concentrate or pellet. [Courtesy of Michael Carstens, MD]

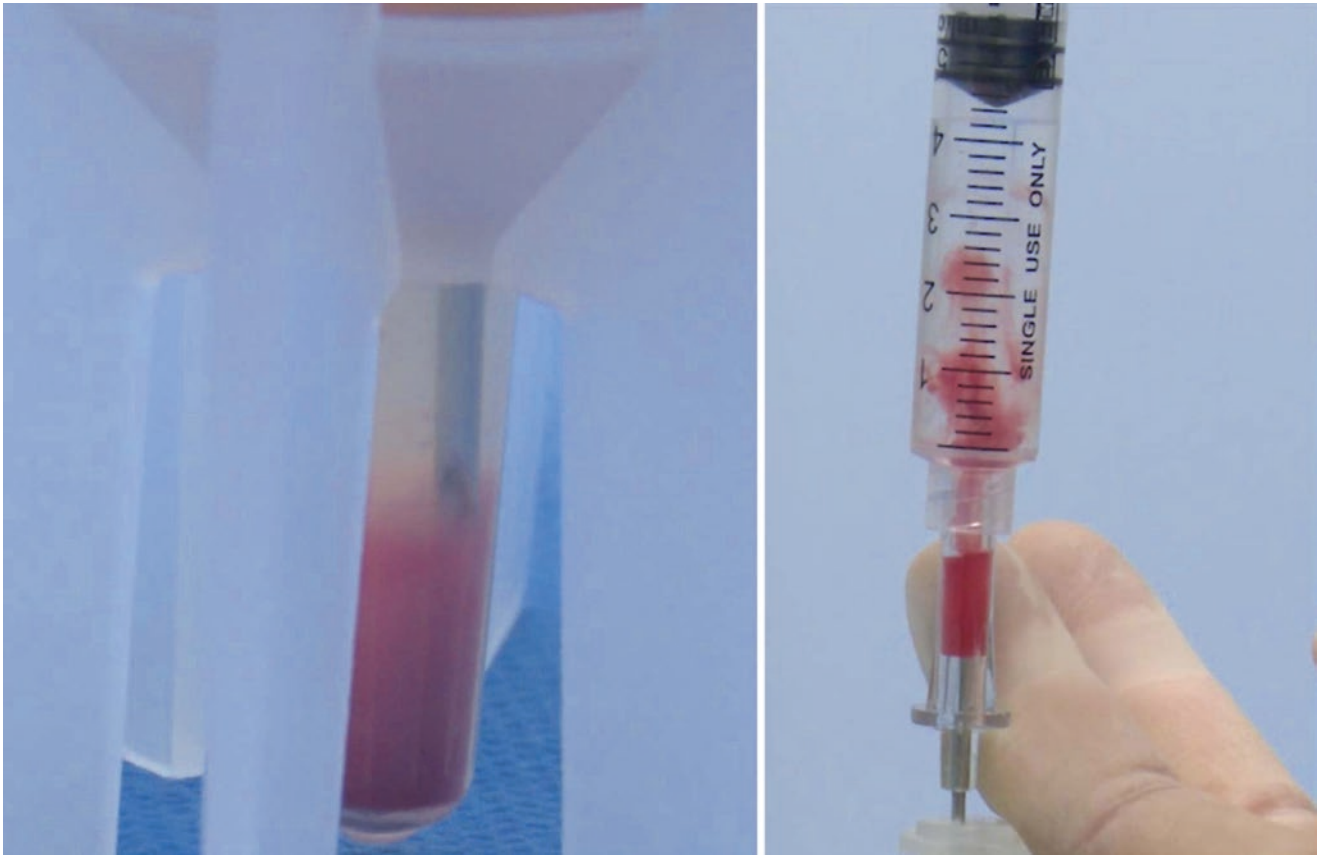


**Fig. 11.47** Resuspension of the pellet. Pellet containing SVF stromal drawn upward and suspended in solution ready for administration into tissues (directly) or the intravascular space (via blood filter). [Courtesy of Michael Carstens, MD]

## Stromal Vascular Fraction: AD-cSVF as Therapy

### Concepts and Components

Adipose tissue, when digested with collagenase, yields an oily supernatant fluid of dissolved adipocytes and a precipitate of stromal tissue, the fibers, and blood vessels that constitute the structural framework for the adipocyte population. Clustered around the vascular component of the stromal are cells representing, adipose-derived mesenchymal signaling cells (stem cells) or ASCs, their embryologic precursors, pericytes, endothelial cell precursors capable of forming blood vessel walls, embryonic pre-adipocytes, macrophages, and other cell types. When the stromal fluid is spun down, the cellular components are separated from the fibers to form the stromal vascular fraction or SVF [12].

As polycellular mixture, SVF has multiple properties which represent the sum of its component parts. The individual characteristics of these cells are well-summarized by Nguyen and Gao. Adipose tissue contains intrinsic cells derived from an original embryologic anlage and extrinsic

cells that originate from a secondary (hematogenous) source. Intrinsic cells are categorized on the basis of molecular structures of their surface membranes known as cluster of differentiation (CD) markers; these can be positive or negative. The components of SVF are as follows:

#### Pericytes (CD34+, CD31-, CD146+)

- 5% of SVF
- Original component of primitive vascular system; ensheath all blood vessels.
- In the embryonic state pericytes are the precursor cells of adipocytes, fibroblasts, and MSC stem cell precursors.
- Interact with endothelial cell precursors to produce new blood vessels.
- In vivo Pericytes under stress can differentiate into mesenchymal stromal cells.
- In vitro (2 weeks of cell culture) pericytes can differentiate into MSCs.

#### Mesenchymal stromal cells (CD34+, CD31-, CD146+)

- 30% of SVF
- MSCs have multiple broad biologic functions.

- In vivo mesenchymal stromal cells are **not** capable of differentiation.
- In vitro (2 weeks of cell culture) mesenchymal stromal cells differentiate into **true** mesenchymal stem cells (capable of multiple pathways of differentiation).

#### Endothelial cell precursors (CD34+ weak, CD31+)

- 5–10%
- Original component of primitive vascular system; forms lining of all blood vessels.
- Interact with pericytes to produce new blood vessels.

#### Fibroblasts (CD34-)

- 45–50%
- Derived from pericytes but lose the CD34+ marker.
- Fibroblasts of SVF have a physiologic role: produce normal collagen.
- Type III (organized) > type I (disorganized).

---

## SVF: Mechanisms of Action

Autologous stromal vascular fraction constitutes the first known form of comprehensive management for the body's response to trauma, with actions impacting pathologies in both the acute and chronic states. We can summarize these as follows.

Inflammation SVF cells block or attenuate pro-inflammatory cytokines (acute products of injury) such as interleukins (IL-6, IL-12, and IL-17) and tumor necrosis factor. They also produce anti-inflammatory cytokines, such as IL-4 and IL-10. Finally, they antagonize pathologic growth factors in a yin-yang fashion. For example, the highly inflammatory transforming growth factor beta (TGF-*b*) is opposed by hepatic growth factor (HGF), and transforming growth factor alpha (TGF-*a*).

Immune system modulation SVF affects both cell lines of the immune response. The B cell (humoral) arm is modulated via dendritic cells the "present antigens for processing. The T cell (cellular) arm is influenced via (1) the Induction of regulatory T cells (Tregs), and (2) a phenotype shift of helper T cells from the Th1 (inflammatory) state to Th2 (anti-inflammatory) state, and (3) paracrine cytokines indirectly influence immune cells.

Anti-bacterial/viral action This property is poorly understood. SVF cells have been observed to survive and function under hostile conditions, such as cellulitis. They exercise an adjunctive role in microbial control. Direct clearance by MSCs eliminates microbes using IL-37, beta-defensin. MSCs perform indirect clearance by increasing the phagocytic (cell-eating) properties of existing macrophages. Viral control by MSCs involves: (1) suppression of viral replication and shedding, (2) production of anti-viral products: indoleamine 2,3-dioxygenase (IDO), and (3) promotion of Tregs to attack virus.

Anti-apoptosis Prevention of cell death is another property of MSCs. They stabilize cell membranes and decrease levels of attack molecules. They produce bio-active factors such insulin growth factor (IGF) which gives protection for mitochondria (the energy-producing organelles of cells) and, by improving blood supply (VEGF), provide better metabolic support.

Tissue regeneration MSCs interact with and support regenerative cell populations that are intrinsic to every tissue. Under conditions of injury MSCS (1) reduce or prevent ongoing injury to this cell population, (2) stimulate mitosis of local cell populations, thereby replenishing tissues that are non-functional or lost due to injury. The multitude of interactions observed with MSCs in the presence of tissue trauma can be categorized as: immunomodulation and trophic effects [13].

Anti-fibrosis The common endpoint of pathologic wound healing is the production of scar tissue, the mechanical strength of which for any given never exceeds 70% of its baseline. Adipose tissue fibroblasts are a normal component of the stroma.

Non-adipose tissue fibroblasts are recruited (1) from local sources such as muscle or epithelium via epithelial-mesenchymal transformation o (2) from blood: monocyte > macrophages > fibroblasts > myofibroblasts. Under the condition of inflammation: platelets recruit large numbers of monocytes to the site of injury. Accumulation of myofibroblasts leads to abnormal collagen and contraction [14–17].

Matrix metalloproteinases (MMPs) control collagen production/degradation. Collagen has two primary forms: collagen I (disorganized) and collagen III (organized). In the normal state, III > I; physiologic fibers predominate. With inflammation, I > III; this indicates pathologic fibers (scar). MMPs are controlled by two main growth factors. TGF-B1 from platelets (first responders) is inflammatory whereas HGF from SVF is anti-inflammatory. In sum, the anti-fibrotic activity of MSCs takes two forms: (1) control of the number of myofibroblasts by inhibiting their proliferation and promoting their elimination by favoring apoptosis; and (2) prevention and/or reversal of pathologic fibrosis. [Pardo].

Pro-angiogenesis Vascular endothelial growth factor (VEGF) produced by MSCS and endothelial precursor cells (EPCs) has several effects. VEGF induces the sprouting of new blood vessels in which the EPCs form the substrate for new vessel walls. This represents a feedback response of MSCs to states of ischemia.

---

## Wound Healing in the Presence of MSCs: Returning Tissues to the Fetal State

One of the most critical applications for therapy with MSCs, be they from adipose tissue, bone marrow or umbilical cord or placenta is to understand that the transition from the fetal state to the natal state involves a paradigm shift in the way

tissues respond to injury. It is a transition from regeneration to repair. Regeneration involves the reconstitution of normal tissue, like replaces like, with all cellular components in place and functional. Repair inevitably involves so form of permanent tissue loss and its replacement with scar: like is not replaced by like but with a material that provides structural support but lacks function.

Why does this transition occur in the first place? As a first pass, let us consider the primary function of MSCs (1) homeostatic and therefore (2) regenerative. They act much as conductors for a complex orchestra of biological responders, directing the response to injury and/or inflammation in such a way as to restore structure and function. To this end all cell populations must be replaced, and the order of tissue micro-anatomy returned to its original state. An extreme example of this is regeneration of complex structures in lower orders of vertebrates such as the salamander which can replace a lost tail. Let us further postulate that, **in order for regeneration to take place within a given tissue environment, the concentration of healing cells [MSCs], that is, the number of cells per cm<sup>3</sup> of tissue exceeds a critical threshold.**

In sum: the difference between regeneration and repair is a binary choice between healing cells and inflammatory cells:

**Inflammatory cells low/healing cells high** = before 24 weeks: scar-less healing.

**Inflammatory cells high/healing cells low** = after 24 weeks: healing with scar.

**Adult (inflammatory) state versus the fetal (regenerative) state.**

	Adult wound healing	Fetal wound healing
Collagen content	Type I collagen blocks migration	Type III collagen stim migration
Hyaluronic acid	Low hyaluronic acid blocks cellular movement	High hyaluronic acid: Favors hydration and cell movement
Metalloproteinases to tissue inhibitors	Low MMP/TIMP favors the accumulation of scar	High MMP/TIMP favors fibrosis turnover
Inflammatory cells	High population	Low population
	Proinflammatory cytokines Il-6 and Il-8	Anti-inflammatory Il-10 decreases Il-6 and Il-8
Transforming growth factor	High levels b-TGF1 and b-TG-F3	Low bTGF1-2, high bTGF3
Gene expression	Delayed upregulation of genes for growth and differentiation	Upregulates genes cell driving growth & differentiation
Progenitor cells	Insufficient # to prevent scar	Sufficient # for scar-less healing

### What Causes the Change in the Wound Healing Paradigm?

The answer to this may well be quite simple and is embedded in the basic difference between the embryonic period and the fetal period. As we have seen throughout this book, the 23 stages of embryogenesis involve a choreographic sequence in which tissues are induced, differentiate, and assembled into organ systems. In this scenario, the first system to arise at stage 5 is the vascular system...for upon this, the survival of the embryo depends. The primitive blood vessels of the embryo represent a marriage between two cell sources. (1) Endothelial cells arise at stage 5 from the extraembryonic mesoderm within the blood islands of yolk sac; and (2) Pre-pericytes arise at stage 6 from ectomesenchyme of the neural crest (or nearby cells). During gastrulation at stages 6 and 7, these two cell lines unite during vasculogenesis, thereby ensuring a source of oxygen and nutrition for the organism. Note: a semantic difference exists regarding the ectomesenchymal source for pericytes of craniofacial vessels versus those of non-craniofacial vessels. The former is classified as a formal derivative of neural crest, the latter are derivatives of cells related to the neural crest but without formal characterization.

At the start of the fetal period blood vessels have been distributed throughout the organism and an explosive period of mesenchymal growth occurs. In this process, the number of non-MSc cells expands exponentially in comparison with the number of MSCs cells. Thus [MSC], that is, #MSCs/cm<sup>3</sup> fetal tissue continues to drop until a critical threshold is reached at about the sixth month of life. After this threshold is passed, the biological potential of the resident MSC population within a tissue is no longer sufficient to maintain the healing potential of the early fetal period.

### The Clinical Effect of MSC Transplantation: Recapitulation of the Early Fetal State

When MSCs are harvested and concentrated, either in the form of enzymatically derived SV cells delivered at the point-of-care or in the form of cultured cells produced by in vitro expansion, what is accomplished is the creation of a critical mass of regenerative cells. When transplanted into a recipient site either prior to, or consequent to, an inflammatory event, the effect of this increased [MSC] is to return the target tissue to the fetal state, one in which a sufficient number of MSCs is present such that their cytokines and growth factors are able to change the clinical behavior of the surrounding tissues.

## Clinical Applications of SVF: Restoration of Homeostasis (Adult > Fetal)

Given a knowledge of the cellular components of SVF, and of their mechanisms of action, therapy with SVF cells/MSC cells can be applied to a number of clinical conditions.

**Acute inflammatory states** Cell therapy can counter the acute reaction of tissues to trauma, surgery, and perhaps infection. Not only are tissues under stress addressed but “innocent bystander” injury can be averted. Examples would include safer wound healing after surgery, improved local blood supply, less inflammation, and better scars. By reducing the inflammatory response faster rehabilitation can occur post-orthopedic surgery.

**Chronic inflammatory states** These take various forms depending on the tissues involved. *Musculoskeletal conditions* include the arthritides, both degenerative (osteoarthritis) and immunologic (rheumatoid arthritis). *Chronic kidney disease* can involve tubulointerstitial inflammation (Mesoamerican nephropathy) and glomerulonephropathies, both metabolic (diabetes) and immunologic (lupus). *Skin conditions* with inflammation managed with topic therapy such as eczema and psoriasis or immune complex attack (hair loss) may respond.

**Fibrotic states** *Pathologic fibrosing conditions* can include, liver fibrosis, scleroderma, and post-pneumonic scarring such as post-COVID. *Pathologic scars*: cell treatment can permit revision without recurrence for surgical scars at high-risk sites such as knees, sternum, and c-section and for keloids (almost 100% recurrence). *Periarticular soft tissue mobilization* after complex fracture surgery, or disuse (stroke). *Modulation of burn scar tissue* for better elasticity [17–19].

**Ischemic states** SVF cells can improve damaged microcirculation in diabetic patients for lower extremity ulcers, peripheral neuropathy, and diabetic kidney disease [20]. Angina pectoris in non-surgical candidates could benefit via neoangiogenesis Macrocirculation as in arteriosclerosis by benefiting by external application of SVF around the vessel walls affected by plaque formation. Given the extensive damage exacted by COVID-19 on pulmonary microcirculation [21, 22].

---

### In Summation

- The origins of adipose tissue can be traced to the cell lines emerging at the earliest stages of embryogenesis during the formation of extraembryonic tissues (stage 5) and gastrulation (stages 6–7).

- Of all embryonic systems, the vascular system is the most primitive consisting of a mesodermal component, endothelial cells, and an ectomesenchymal component, the pre-pericyte.
- Pre-pericytes are a cell line synonymous with, or closely related to, neural crest.
- The ectomesenchymal derivation of pericytes explains the broad range of clinical properties they possess, both for differentiation and for the production of many bioactive molecules.
- Pre-pericytes are the precursors of pre-adipocytes and white fat.
- The biologic properties of mesenchymal stromal cells reflect their origins from the pre-pericyte/pericyte line.
- Adipose MSCs and bone marrow MSCs originate from a common source but display the difference in cell markers and relative clinical properties.
- The niche of pericytes and their MSC progeny is vascular.
- MSCs constitute a cell line dedicated to homeostasis.
- The biology of tissue response to injury prior to 6 months of intrauterine life is regenerative and reflects the high number of MSCs/cc<sup>3</sup> of parenchyma relative to the population of inflammatory cell populations.
- With growth the high [MSC] declines.
- The biology of tissue response to injury after 6 months of intrauterine life is reparative reflecting lesser number of MSCs/cc<sup>3</sup> of parenchyma with respect to inflammatory cell populations.

Reconstructive procedures that concentrate large numbers of regenerative cells either as SVF or MSCs in any form and then implant them in a recipient tissue result in a recapitulation by that tissue of its fetal state, thereby changing its healing potential from one of inflammation and fibrosis to one of regeneration.

---

## Fascia and Blood Supply of the Head

All craniofacial fascia develops from neural crest. Dura of the forebrain and midbrain (including r1) develops from a combination of neural crest and paraxial mesoderm; the dura covering the hindbrain and spinal cord is exclusively mesodermal. This section will examine the embryologic rationale of the fascial layers and their functional significance. We shall see that the organization of craniofacial arteries is also functional and follows the same planes.

Let's make a quick summary to get oriented (Table 11.3).

**Table 11.3** Fascial planes of the head and neck

Plane	Fascia	Artery	Function
CNS, deep	Pia/arachnoid	Head plexus	Blood-brain barrier
CNS, superficial FNO, palatoquadrate	Dura mucoperiosteum	Stapedial-intracranial stapedial-extracranial	Protect brain support cranial base
ECA-deep plane	Deep investing	Ext carotid-deep	Arches, oral mucosa
ECA-superficial plane	Superficial investing	Ext carotid-superficial	Facial mm, skin, scalp

### Blood Supply Runs in Four Planes

The tissues that will comprise CNS deep layer of leptomeninges are in place as soon as the neural tube begins to round up. These consist of neural crest from the *local neural folds* and head mesoderm. Although the pia and arachnoid are not yet visible at stage 9, formation of the head plexus is immediate. Eventually, this will connect to the internal carotid. The spatial organization of the external carotid system is very rational, reflecting its function to supply the derivatives of pharyngeal arches 1–4 (Fig. 11.48).

At stages 12 events take place which are critical for the formation of the fascia covering the brain, the eye, and the structures that support the neurocranium (neural crest bones of the skull). By that time, the third pharyngeal arch has formed, and dramatic changes have taken place in the structure of the first and second arches. Their arterial axes have disintegrated, in each case leaving an arterial stump behind, hanging off from the dorsal aorta. The remnant of AA1 is the *primitive mandibular artery*. The remnant of AA2 is the *hyoid artery*, a critical intermediate structure that morphs into the *stem of the stapedial system*. Stapedial is the very first branch of the internal carotid before it enters the skull. Note formation of the stapedial takes place slightly before the formation of the external carotid and in a plane deep to it.

In the meantime, first and second pharyngeal arches undergo a merger into a single large entity. The bulk of PA2 is internalized within the epithelial envelope of PA1. In so doing, PA2 *loses all of its epithelial representation* save a small contribution to the external auditory meatus. The original arterial supply of the two arches, which came from the first and second aortic arch arteries, falls apart, leaving behind a tangle of comingled blood vessels. These are saved from ischemic death by a timely connecting branch sent forth from the third aortic arch artery, which comes into existence at this exact same time.

The spatial location of AA3 with the third pharyngeal arch is analogous to the arterial supply of the first two arches: runs right up the center. Unlike the first two aortic arches, AA3 does not break down—it remains connected with the dorsal aorta to form the common carotid and the external carotid system.

External carotid comes into existence at stage 12 when AA3 sends out a stem that projects forward into the 1st/second arch amalgam, where it encounters the plexus and makes an anastomosis. This intermediate vessel formed is known as the *ventral pharyngeal artery*. As it produces multiple branches VPA morphs into the external carotid system. ECA will divide into two functional units in two distinct planes.

- **Deep plane** branches of ECA supply all the *pharyngeal arch muscles* (except the facial series) and the *oral (non-maxillary) mucosa*. These muscles lie within the deep investing fascia, the arteries being external to the DIF (Figs. 11.49 and 11.50).
- **Superficial plane** branches of the ECA will supply the second arch *muscles of facial expression* and *skin and scalp*. These muscles lie are within the superficial investing fascia, or SMAS; the arteries being external to the SIF (Fig. 11.48).

External carotid artery terminates with two branches, one for each plane. Superficial temporal artery runs in the SIF/SMAS. It courses upward to supply the galea and skin of the scalp. Maxillary artery runs in the DIF to supply muscles of mastication but it is quickly joined by the external division of stapedial. The result is a composite structure, part ECA and part stapedial. It is rightly named the *maxillo-mandibular artery* (MMA) and has three parts. In the first part, stapedial contributes four arteries that enter the skull. The second part has a single stapedial branch supplying the mandible. ECA terminates here. The third part of MMA is exclusively stapedial. It supplies the maxilla and part of the oral-nasal cavity.

It will be seen that the stapedial branches of the first part of MMA do not follow a fascial plane, but run along the pterygoid plate and into the skull. In the third part of MMA, V2 stapedial plunges into the pterygopalatine fossa from whence its various branches connect with those of the V1 stapedial system that have exited the skull. Note the stapedial system occupies the *pericranial—FNO plane* to supply the dura. For this reason, terminal branches of stapedial that access the face through foramina proceed along two planes. Deep branches course along the surface of the bone and superficial branches connecting with SMAS and skin. And in the frontonasal skin envelope, superficial branches develop. These take over for ECA, running superficial to the plane of the SMAS to supply the muscles and make anastomoses with ECA vessels such as the angular. The nose is a perfect exam-

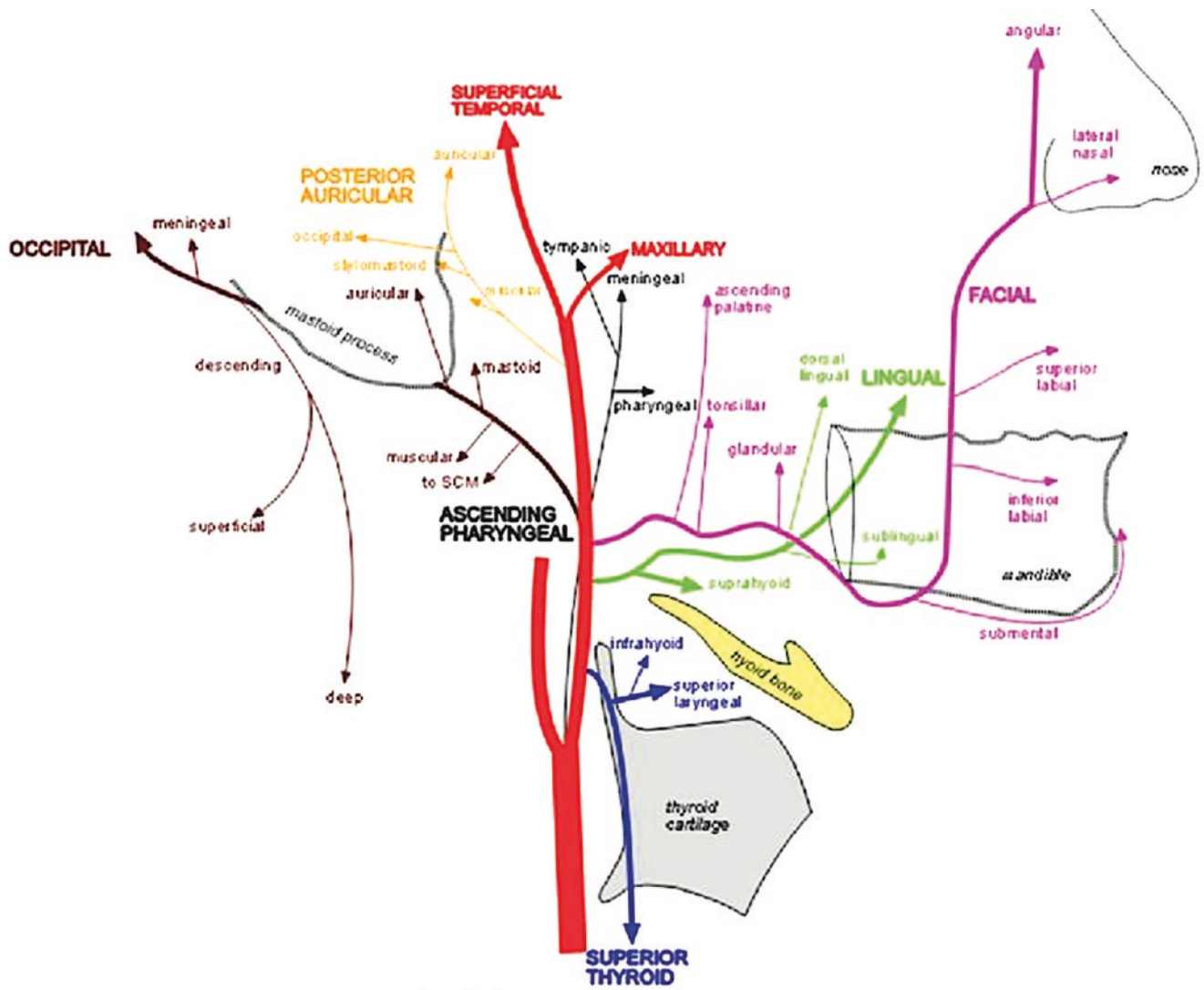


**Fig. 11.48** Blood supply to *non-FNO* skin: external carotid system. SThA, superior thyroid; LA, lingual; FA, facial; APA, ascending palatine; OA, occipital; PAA, posterior auricular; STA, superficial temporal; TFA, transverse facial artery; MMA, middle meningeal; AMA, accessory meningeal; IDA, inferior dental; MDTA, middle deep temporal; Max, maxillary; ADTA, anterior deep temporal; DPA deep palatine;

PSDA, posterior superior dental; IOA, inferior orbital; SPA, sphenopalatine; 1, artery of superior orbital fissure; 2, artery of foramen rotunda; 3, artery of pterygoid canal; 4, pharyngeal (pterygovaginal). [Reprinted Kiyosue H. External Carotid Artery. In: Kiyosue H. (eds) External Carotid Artery. Singapore: Springer Nature; 2020: 1–5. With permission from Springer Nature]



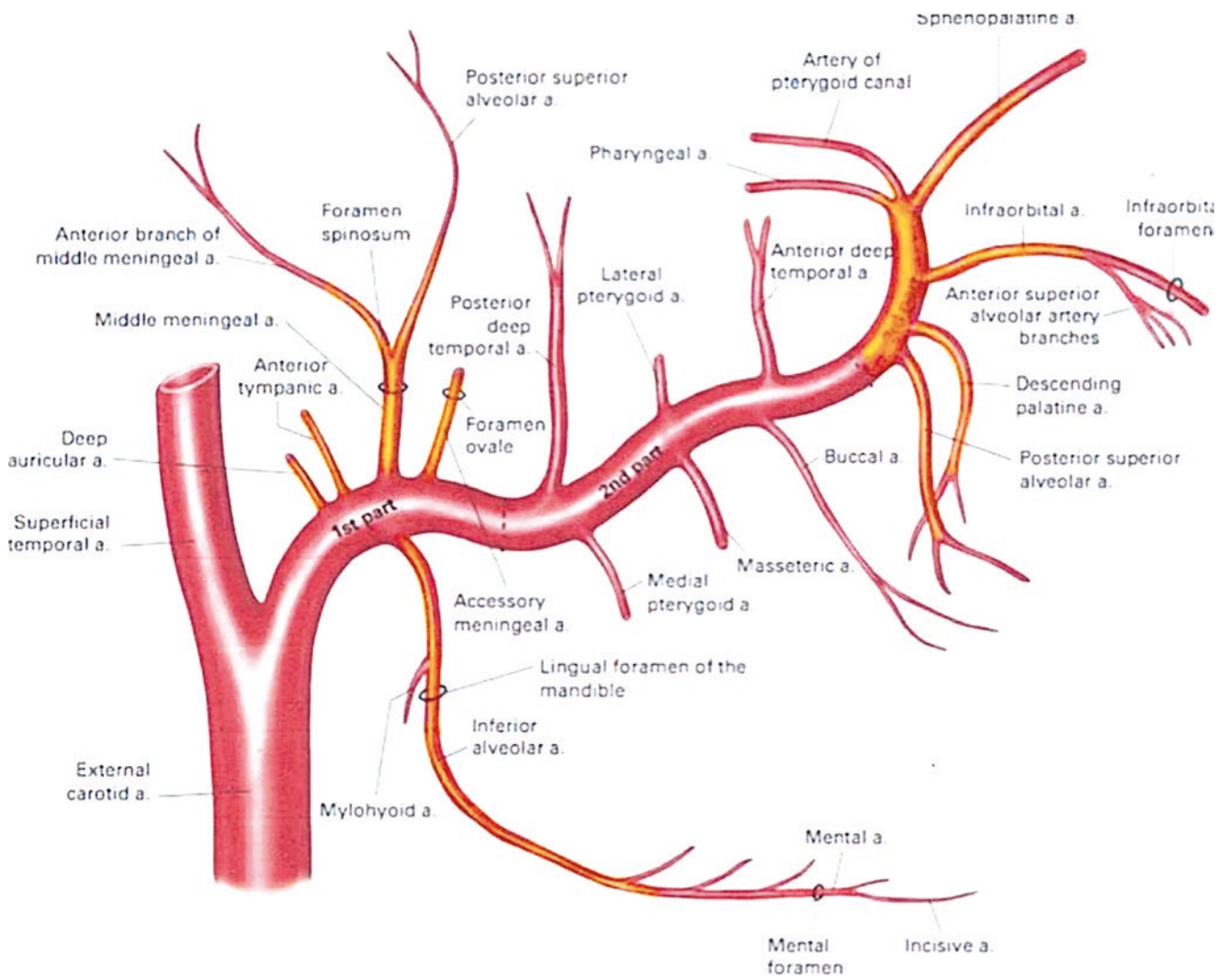
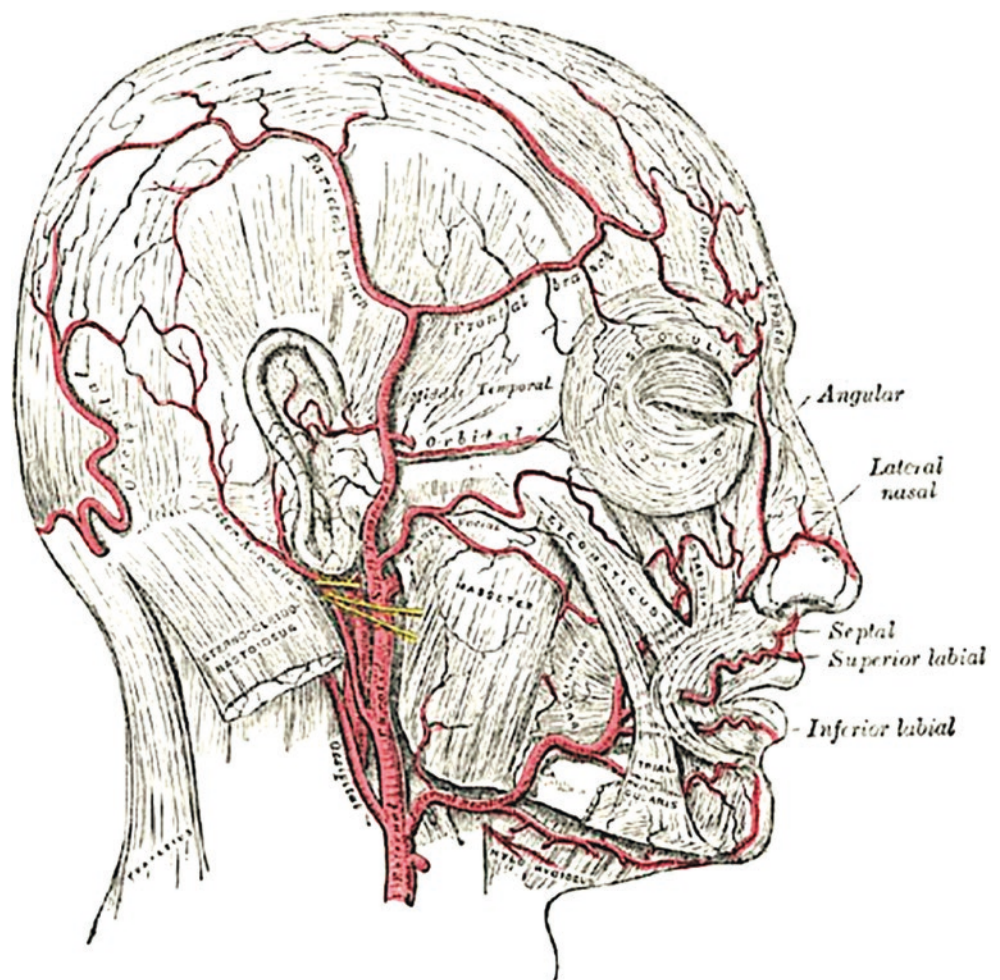


**Fig. 11.49** ECA skin: IMMA system. The internal maxillo-mandibular system has three functional zones. IMMA is direct branch of ECA. Original components (red) predate the stapedal system (orange). Zone 1: stapedal branches to tympanic cavity and meninges (except: mylohyoid artery off the inferior alveolar). Zone 2: exclusively for Sm4

muscles of mastication, including Sm6 buccinator. Zone 3 exclusively for neural crest bones of midface. [Reprinted from Lewis, Warren H (ed). Gray's Anatomy of the Human Body, 20th American Edition. Philadelphia, PA: Lea & Febiger, 1918]

**Fig. 11.50** ECA skin: transverse facial artery distribution. TFA is one of two terminal branches of ECA distal to internal maxillomandibular (the other being superficial temporal). It supplies infrazygomatic and lateral orbital SMAS. TFA emerges out of parotid gland and runs above the duct and below the zygomatic arch. It supplies the gland and masseter as well as SMAS. [Reprinted from Lewis, Warren H (ed). *Gray's Anatomy of the Human Body*, 20th American Edition. Philadelphia, PA: Lea & Febiger, 1918]



ple of this anatomy. StV1 external nasal runs deep to SMAS to access the columella and also superficial the SMAS of nasalis to supply the skin.

Thus, by the end of stage 12 two completely separate craniofacial vascular systems have been initiated. The *stapedial system* supplies all the V1-innervated fronto-nasal-orbital tissues, the zygomaticomaxillary complex, and all dura. The

*external carotid system* supplies all structures of all the pharyngeal arches (skin, mucosa, muscles, fascia, and bones) and the epaxial structures of the scalp innervated by V2-V3. It also supplies all muscles originating from the second arch including auricular and occipitalis—but *none of the muscles of the forehead* (frontalis, procerus, and corrugator) (Fig. 11.51).

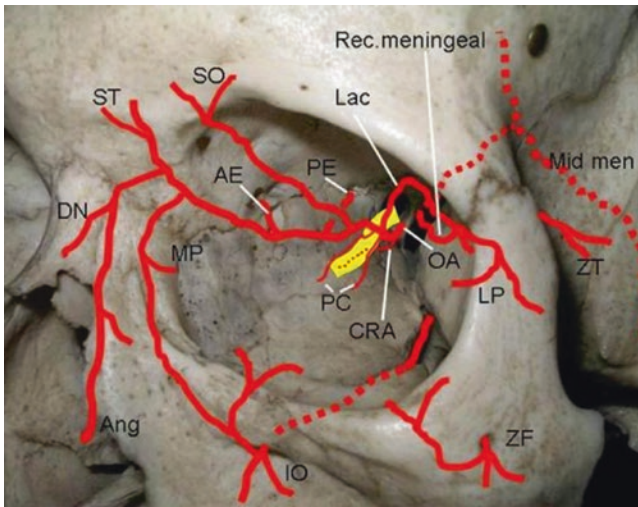


**Fig. 11.51** Stapedial supply to skin: ophthalmic distribution. StV1 branches connected secondarily to the ophthalmic axis supply all V1-innervated skin. Note the role of the lacrimal artery axis in zone 9 and the anastomosis with transverse cervical branch from the external carotid. The muscular branches, short posterior ciliary, long posterior ciliary, and anterior ciliary arteries are not depicted. The yellow structure is the optic nerve. Key: OA, ophthalmic artery; CRA, central retinal artery; PC, posterior ciliary artery; Lac, lacrimal artery; LP, lateral palpebral artery; IO, infraorbital artery; ZT, zygomaticotemporal artery; ZF, zygomaticofacial artery; Mid men, middle meningeal artery; Rec meningeal, recurrent meningeal artery; Ang, angular artery; MP, medial palpebral artery; DN, dorsal nasal artery; ST, supratrochlear artery; SO, supraorbital artery; AE, anterior ethmoidal artery; PE, posterior ethmoidal artery. [Reprinted from Rene C. Update on orbital anatomy. *Eye* 2006; 20:1119–1129. with permission from Springer Nature]

### Why Do we Need the Stapedial System in the First Place?

There are developmental reasons for why external carotid does not invade the forehead territory of V1 stapedial. Facial muscles migrate according to SMAS neural crest fascia “pathways” that follow a fixed spatiotemporal sequence: deep-to-superficial, lateral-to-medial, and ventral-to-dorsal. For this reason, frontalis will be one of the final muscles to migrate into position. By the time it does so, StV1 supply to FNO tissues is already fully established. The muscles are already supplied. There is no need for ECA to proceed further.

Why should these systems be so different? The distinct nature of V1-supplied FNO tissues makes sense. But have we not always considered the zygomaticomaxillary complex and mandible to be part of the first arch? Why should dura from r1-r3 neural crest be supplied by one system, whereas dermis and fascia (also from hindbrain neural crest) require a completely different source of blood supply? The answers are both (1) spatiotemporal, due to differential migrations of neural crest populations and (2) evolutionary, due to two critical inventions that revolutionized the first two branchial arches—jaws and facial muscles.

### (1). Structural considerations

The structural design of the stapedial and external carotid systems reflects the anatomy of the tissues they serve. Stapedial arteries supply structures derived from the *earliest* forward migrations of MNC and RNC<sub>R</sub> (r1–3). These are *deep plane* migrations, skimming along the surface of the brain, which are dedicated to the orbit and to the creation of FNO mesenchyme from which the upper third of the face is constructed. Thus, stapedial supplies the dural protection of the brain as well as the bone fields that support the anterior cranial base and coverage of the brain itself. For this reason, in the cranium, stapedial occupies plane deep to that of external carotid. ECA arteries represent a more superficial migration, supporting tissues of the middle and lower thirds of the face as well as the pharynx. Since the brain is already enclosed with dura, the skin and subcutaneous tissues supplied by the ECA will provide the external coverage epithelial coverage of the brain. They are also essential for the synthesis of the membranous calvarium.

External carotid also matures in a temporal sequence. Pharyngeal arch muscles mature in cranial-caudal sequence. In the PA1-PA2 complex, the muscles of mastication are in place prior to those of facial expression. Thus, DIF structures precede those of the SIF. They occupy a deeper plane and are supplied by the deep branches of external carotid artery.

### (2). Evolutionary Changes in the First and Second Arches.

#### The Invention of Jaws

Changes in oral anatomy facilitating increased efficiency of food acquisition have been favored by evolution. Transformation of the first two arches into jaws were accompanied changes in the number of respiratory organs and their arterial anatomy. Primitive *agnathic* (jawless) fishes, as represented by the lamprey, taken in food through a simple stoma. The fishes have 7 branchial arches, each of which is equipped for extracting air from water and each has its own aortic arch artery. The first *gnathic* (jawed) fishes, *chondrichthyes*, had an exclusively cartilaginous skeleton, as in sharks. In these species, the first two branchial arches stopped being gills. Their cartilaginous cores were converted into tooth-bearing jaws capable of capturing prey. The remaining five arches continued to have gill structures. Thus, sharks have **five** branchial arches. In modern bony fishes, *osteichthyes*, the last two branchial arches have morphed into primitive lungs called swim bladders. They have 3 branchial arches. Tetrapods retained jaws but, with the advent of lungs, the branchial arches (gills), no longer needed for oxygenation, were converted to pharyngeal arches. In so doing, the need for aortic arch arteries to supply the gills was also elim-

inated. Modern tetrapods, now with **three** pharyngeal arches, thus settled upon a revised vascular system.

Jaw-based predation demanded an innovation in the arterial supply for branchial arches 1 and 2. The result was a conversion of second aortic arch breakdown products into a new iteration: the stapedal system. Both upper and lower jaws had articulations with the skull. The relationship of the zygoma to maxilla—such that both are supplied by stapedal—stems from their derivation from a common palatoquadrate cartilage hinged with the skull. The mandible is attached indirectly to the skull via a second arch hyoid bone, itself suspended from the skull. All remaining structures of the first arch, *retain their supply from the external carotid system*.

### The Invention of Facial Mimetic Muscles

All the muscles of the first arch plus the hyoid series of second arch transitioned from gills to mastication without change in their blood supply or their neurology. In tetrapods, the pharyngeal arches underwent radical forms of reassignment as well. Muscles formerly involved in movements of the gills became elevators and depressors of the jaws, including the hyoid. With the exception of posterior digastric these originate from first arch because they act upon first arch.

In mammals, the evolution of facial skin and hair was accompanied by the creation, from the second arch hyoid mass, of an entirely new layer of muscles and fascia accompanied by the reiteration of the facial nerve to produce the SMAS. This layer, consisting of neural crest from r4 to r5, encircles the entire face and skull and extends to the clavicles. The SMAS system functions to control movements of the skin, permit suckling, and raise the hair on one head. Note that the buccinator is part of the oral sphincter; it is not a muscle of facial expression. For this reason, the plane of the SMAS does not subdivide, it remains superficial at all times to the muscles of mastication, and, perforce to the deep plane of the stapedal system.

The anatomy of external carotid reflects these evolutionary changes. It consists of a *deep plane*, supplying all non-

SMAS structures and oral mucosa and a *superficial plane* supplying the facial musculature and skin. FNO mesenchyme is the sole exception. Although SMAS is present over the nose and forehead, the muscle masses flow around, and are supplied by, V1 stapedal neurovascular pedicles; ECA is excluded.

External carotid and its branches can be categorized by their neurologic targets.

---

### Superficial Investing Fascia (SIF): Muscles of Facial Expression and the Scalp

In 1976, a superficial musculoaponeurotic system (SMAS) was originally described in the parotid and cheek regions of the face, dividing superficial and deep adipose tissue into superficial and deep layers and constituting a surgically useful structure for enhancing results of face lift [Mitz]. Because SMAS has a regional connotation, this later is referred to as the superficial investing fascia (SIF). SIF is a second arch neural crest structure that provides primary insertion for the Sm6 muscles of facial expression. Over parotid gland, it exists as a separate layer. SIF and its muscles are supplied by the four branches of ECA derived from the original second aortic arch artery: facial, superficial temporal, posterior auricular, and occipital. Work by Carstens and Tolhurst confirmed between SIF with the galeal and subgaleal fascia over the entire skull as an enveloping epicranial layer. [23, 24] should be noted that SIF sends out retaining ligaments to the skin of the face. These divide facial fat compartments associated with specific neuroangiosomes (Figs. 11.52, 11.53 and 11.54).

Note SIF targets muscles derived from the second arch and supplied by the superficial plane of the facial nerve (deep plane of VII goes to buccinator, posterior digastric, and stapedius). The individual branches of this system are patterned upon the motor branches of the facial nerve. Although SIF is dedicated to Sm6 muscles it can be dissected even from muscle-free areas. It is a layer over the entire skull (Table 11.4).

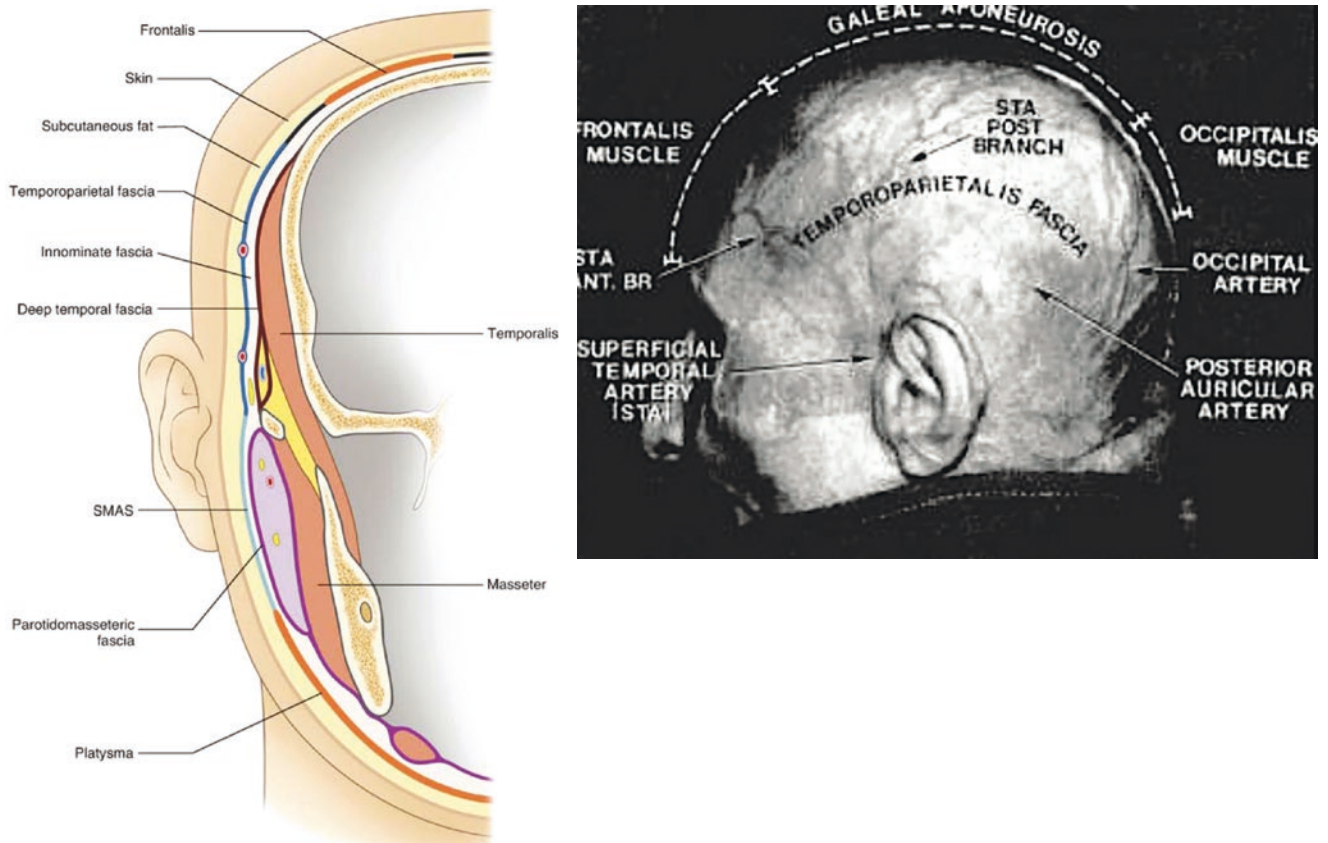


**Fig. 11.52** Superficial investing fascia (SIF). LEFT: Superficial investing fascia of the face (SIF) is known as submusculoaponeurotic system (SMAS). Beneath the SMAS is an *areolar sub-SMAS* separating it from the parotidomasseteric fascia below zygomatic arch and from the temporalis muscle fascia above zygomatic arch. SMAS over the cranium is truly a global layer, known in nomina anatomica as the **epi-cranium**; in common parlance this layer is referred to as the **galea aponeurotica**. The areolar tissue beneath it is the **subgaleal fascia** (SGF) or innominate fascia. RIGHT: Superficial musculoaponeurotic system is

covered with an external layer of fascia which is continuous with the galea, that is, the epicranium. Left: [Reprinted from Kim B, Oh S, Jung W. Anatomy for Absorbable Thread Lifting. In: The Art and Science of Thread Lifting. Singapore: Springer; 2019: 13–29. With permission from Springer Nature.] Right: [Reprinted from Tolhurst DE, Carstens MC, Greco RJ, Hurwitz DJ. Surgical anatomy of the scalp. *Plast Reconstr Surg* 1991; 87(4):603–612. With permission from Wolters Kluwer Health, Inc.]

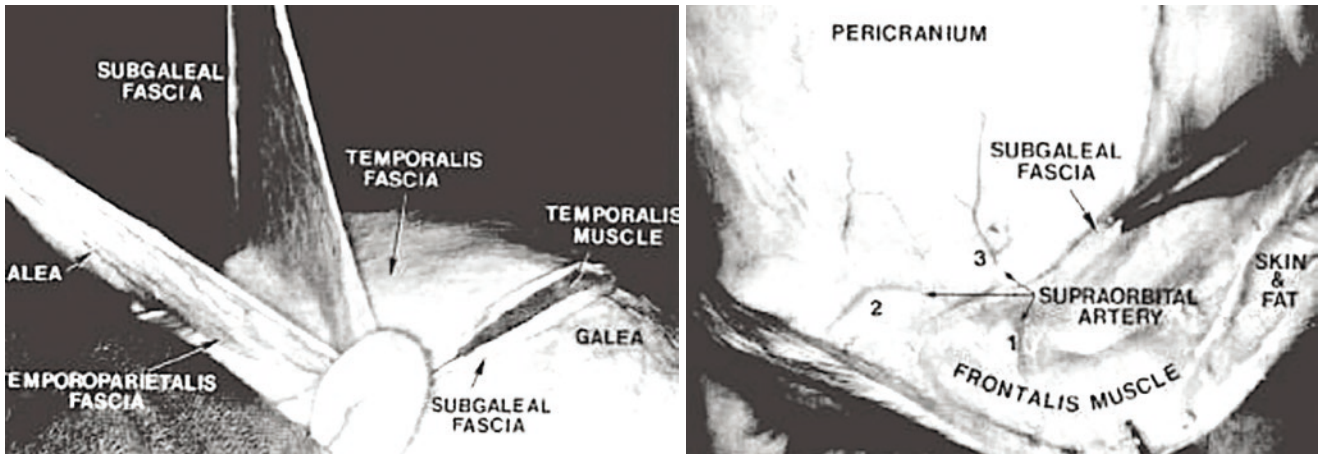


**Fig. 11.53** Subgaleal fascia (SGF). Anterior and lateral dissections of the scalp demonstrating the subgaleal fascia and its relationship to other layers of fascia. Arteries were injected with orange Microfil. LEFT: SGF is sharply dissected from the underlying temporalis fascia. RIGHT: In the view over the supraorbital rim, the artery is shown trifur-

cating to supply the overlying muscle, the SGF, and the periosteum. [Reprinted from Tolhurst DE, Carstens MC, Greco RJ, Hurwitz DJ. Surgical anatomy of the scalp. *Plast Reconstr Surg* 1991; 87(4):603–612. With permission from Wolters Kluwer Health, Inc.]

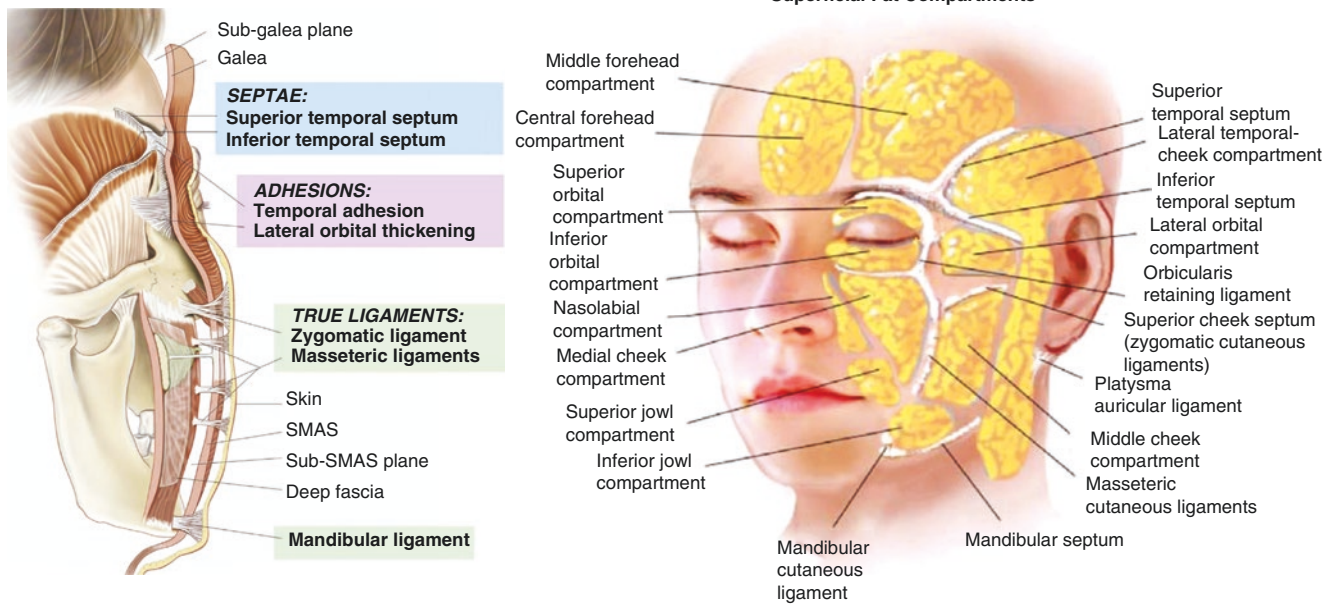


**Fig. 11.54** Retaining ligaments of the face. LEFT: In the face, DIF ligaments pass through the SIF to the skin connect first arch fascia/bone to first arch skin; adhesions and septae connect DIF to SIF. Surgical management of these ligaments is an important concept in facelift. RIGHT: Note that septae divide facial fat into distinct compartments with specific neurovascular definition...another example of relationship between adipose tissue and vascular development. Left: [Reprinted

from Moss CJ, Mendelson BC, Taylor GI. Surgical anatomy of the ligamentous attachments in the temple and periorbital regions. *Plast Reconstr Surg* 2000;105: 1475. With permission from Wolters Kluwer Health, Inc.]. Right: [Reprinted from Alghoul M, Codner MA. Retaining ligaments of the face: review of anatomy and clinical applications. *AesthSurg J* 2013; 33(6): 769–782. With permission from Oxford University Press]

**Table 11.4** Arterial supply of the skin

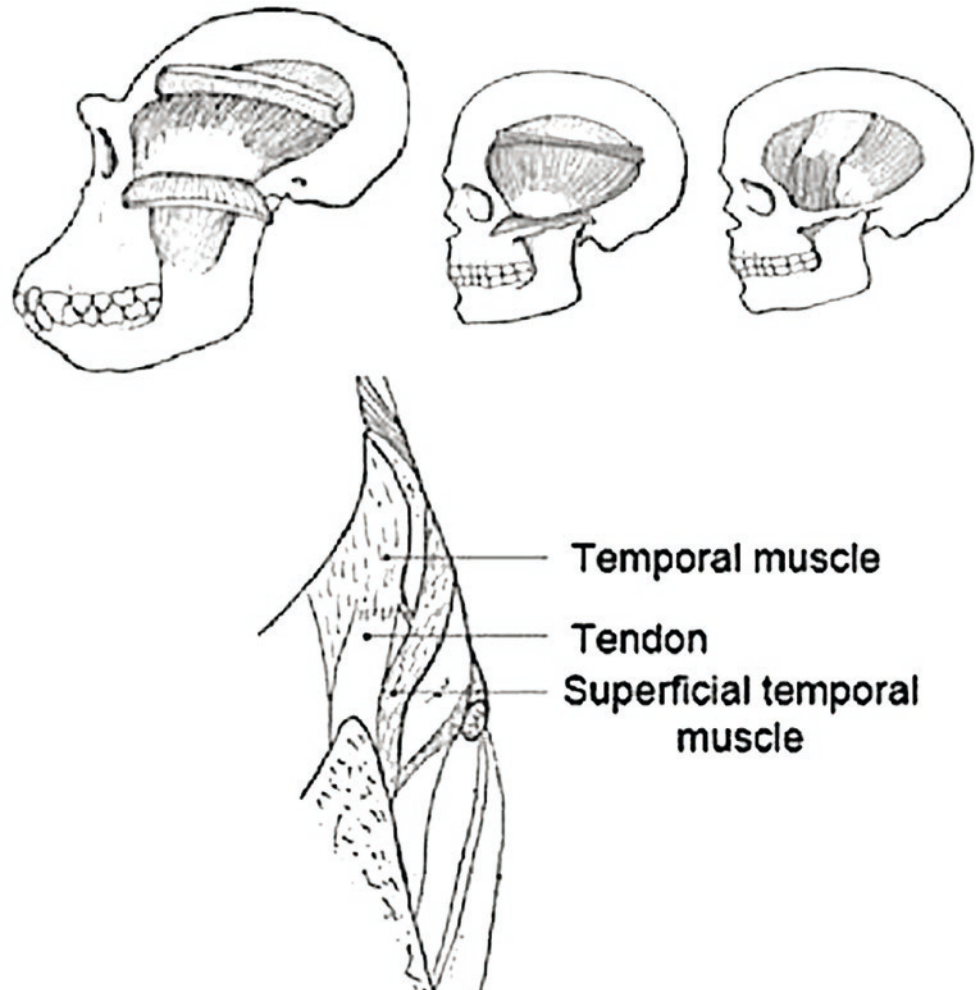
Anterior SMAS	
Superficial temporal	r4 temporal branch: V2-V3 scalp
Transverse facial	r4 zygomatic branch: V2 middle 1/3 face
Facial, superficial	r4 buccal branch: V2 cheek r5 marginal mandibular branch: V3 jaw r5 cervical branch: C1-C2 upper neck
Posterior SMAS	
Posterior auricular	r4-r5 ear Mastoid, occipitalis, skin over membranous occipital bone
Occipital	occipital bone
Anterior	
Maxillary, non-stapedial	r3 cranial (PA1): muscles of mastication
Facial, deep	r3 caudal (PA1): Mucosa, masseter, ant digastric r4-r5 (PA2): Buccinator, stylohyoid, soft palate
Lingual	r3 (PA1): Mucosa ant 2/3 tongue r8-r11 (S1-S4) tongue mm. Occipital somites
Occipital, muscular	r4-r5 (PA2): Post digastric
Ascending pharyngeal	r6-r7(PA3): Mucosa post 1/3 tongue, soft palate & upper pharynx, superior/middle constrictors
Superior thyroid	r8-r11 (PA4-PA5): Mucosa larynx, hypopharynx Laryngeal mm., inferior constrictor
Posterior/epaxial	
Occipital, muscular	r8-r11 (S1-S4): sternocleidomastoid, trapezius skin over chondral occipital bone, C2-C4 neck skin

### Deep Investing Fascia: Muscles of Mastication, Oral Mucosa

DIF targets all remaining muscles and mucosa of all pharyngeal arches (Sm4, Sm6-Sm11). DIF is readily apparent over the muscles of mastication but it extends backward and downward to cover the pharyngeal constrictors as well. The relationships between SIF and DIF are particularly evident at the temporal arch. As the facial nerve ascends over the zygomatic arch, it is vulnerable to injury. Subperiosteal plane exposures for trauma and deep-plane rhytidectomy take advantage of entry through the superficial temporal fat pad to encounter the dorsal rim of the arch, and from there, proceed in the subperiosteal plane, with the facial nerve preserved from injury (Figs. 11.55, 11.56 and 11.57) (Table 11.4).

In summation, we have discussed the developmental rationale of the major territories of craniofacial skin can be understood on the basis of their innervation. Fronto-naso-orbital skin and mucosa innervated by V1 are supplied by stapedial arteries associated with the nerve. Facial and scalp skin supplied by all remaining cranial nerves is supplied by external carotid, SMAS.

**Fig. 11.55** Superficial temporalis muscle in primates. The DIF covers all the muscles of mastication. As such, temporalis muscle is covered by a cranial extension of the DIF of the face and neck. Primates have a two-layer masseter. In humans STM may be the homolog of the intermediated fat pad. Note fascia arrangement with an oblique connection between STM and DTM. [Reprinted from Guerrissi JO, Cotroneo GG. Developmental Anomalies of Temporal Muscle. *Surgery Curr Res* 2014;4: 199. doi: 10.4172/2161-1076.1000199. With permission from Creative Commons Attribution License]



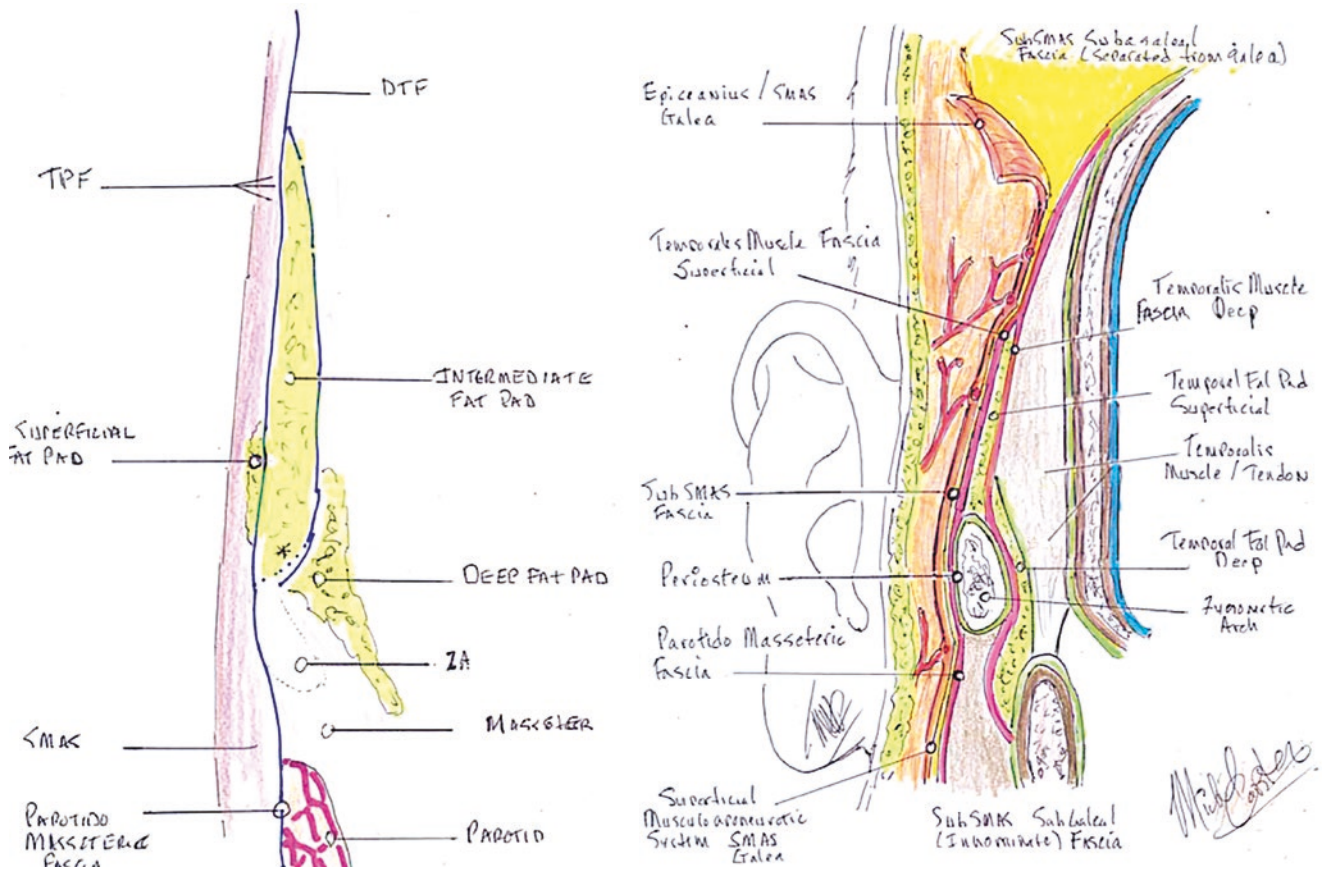


**Fig. 11.56** Overview of Temporal fasciae. LEFT: Preferred names of the anatomic structures. The asterisk marks where the deep layer of the deep temporal fascia (D-DTF) abuts the posterosuperior surface of the zygomatic arch (ZA) on both sides (external and internal). The superficial layers and the deep layers of the deep temporal fascia (DTF) fuse at the anterosuperior surface of the Zygomatic Arch. DTF indicates deep fat pad; IFP, intermediate fat pad; MM, masseter muscle; PG, parotid gland; PMF, parotidomasseterica fascia; S, skin; S-DTF, superficial layer of the DTF; SFP, superficial fat pad; SMAS, superficial musculo-aponeurotic system; TM, temporal muscle; TPF, temporoparietal fascia. RIGHT: Management of the relationship of facial nerve to

zygomatic arch. Protection of the facial nerve at the arch is a critical point for surgeons for facial dissection. Continuity of SMAS over the zygomatic arch. SMAS has two layers: (1) an organized fascial layer (the SMAS proper) which becomes the fibrous substance of the galea and abuts directly beneath the skin of the scalp; and (2) an areolar layer (the subgaleal fascia) which, above the temporal line, received penetrating branches from the superficial temporal arterial system. Although these two layers are fused at the level of the zygomatic arch, and developmentally distinctive from the periosteum, they are biologically distinct. [Courtesy Michael Carstens, MD]



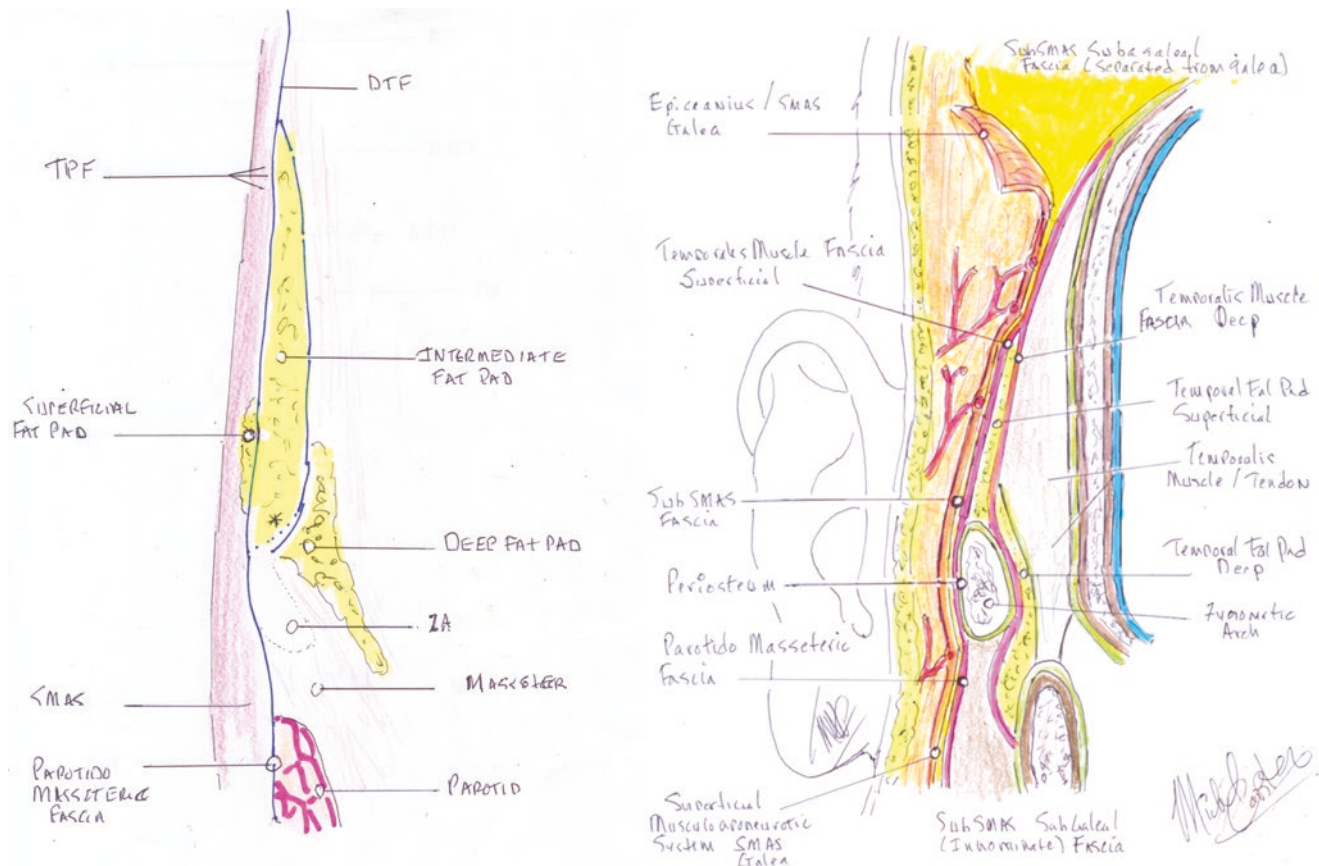


**Fig. 11.57** Pathway of facial nerve: from below DIF to above SIF. The frontal branch of the facial nerve is shown exiting the superior border of parotid gland. It continues coursing superiorly before traversing from a sub-SMAS plane to a supra-SMAS plane both above the zygomatic arch and posterior to Pitanguy's line (blue line). Arrows indicate the specific region where the frontal nerve transitions from the sub-SMAS plane to an intra-SMAS plane relative to Pitanguy's line (left arrow) and the zygomatic arch (right arrow). Measurements for these arrows

are in the same plane. The left arrow indicates a mean distance of  $12.2 \pm 4.77$  mm posterior to Pitanguy's line. The right arrow indicates a mean distance of  $9.6 \pm 5.08$  mm superior to the zygomatic arch. [Reprinted from Pankratz, J, Baer J, Mayer C, Rana V, Stephens R, Segars L, Surek CC Depth Transitions of the Frontal Branch of the Facial Nerve: Implications in SMAS rhytidectomy *J Plast Reconstr Aesth Surg Open*. <https://doi.org/10.1016/j.jpra.2019.11.00>. with permission from Elsevier]

## Fascia and Blood Supply of the Neck

### Blood Supply to Neck Skin

The skin of the neck is supplied by two different kinds of systems, reflecting the origins of its dermis (Figs. 11.58 and 11.59).

Epaxial skin consists of seven dermatomes (c2–c8), each supplied by paired dorsal and lateral arteries directed from the aorta.

Hypaxial skin consists of four dermatomes (C1–C4) of the cervical plexus. It consists of four zones.

POSTERIOR SUPERIOR (C2–C3): descending cervical branch from occipital artery. Occipital is the distal

extension of external carotid covering posterior derivatives of occipital somites, specifically sternocleidomastoid and trapezius. Both of these muscles are hypaxial in design but, with evolutionary migration of the scapula from ventral to dorsal, trapezius has assumed an apparently epaxial position. Nonetheless, its motor innervation, from hypaxial cranial nerve XI and its blood supply from hypaxial external carotid, betray its true evolutionary baseline state.

POSTERIOR INFERIOR (C3–C4): costocervical trunk

ANTERIOR SUPERIOR (C1–C2): facial artery to the level of the hyoid bone.

ANTERIOR INFERIOR (C3–C4): thyrocervical trunk.

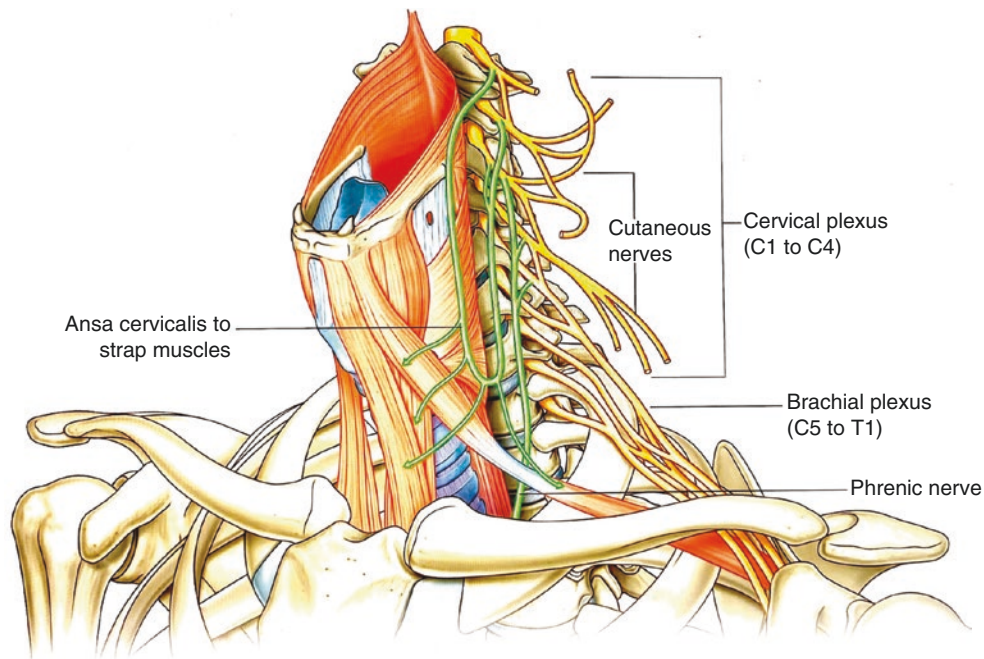


**Fig. 11.58** Neural zones of the neck: plan of the cervical plexus. Cervical plexus is composed of nerves originating from the first 4 spinal segments. Its branches supply hypaxial structures originally associated with the forefin. These are in three functional groups.

(1) Motor nerves (green) supply the strap muscles associated with the ancient coracomandibularis.

(2) Sensory branches (yellow) innervate 4 zones of hypaxial skin.

- Anterior superior zone: facial artery, submandibular branch
- Posterior superior zone: occipital artery, sternocleidomastoid branch

- Anterior inferior zone: thyrocervical trunk, inferior thyroid branch
- Posterior inferior zone: thyrocervical trunk, transverse cervical branch.

(3) Mixed motor and sensory: phrenic nerve is motor to the muscular diaphragm and sensory for associated fasciae.

[Reprinted from Drake R, Vogel AW, Mitchell AWM. Gray's Anatomy for Students, third edition. Philadelphia, PA: Churchill-Livingstone. 2015. With permission from Elsevier]



**Fig. 11.59** Erb's point: nerve blocks. Named for German neurologist Wilhelm Heinrich Erb, renowned for his research on muscular dystrophies. Erb's point is located at midpoint of the posterior border of sternocleidomastoids where 4 sensory nerves of the cervical plexus emerge: greater auricular, lesser occipital, transverse cervical and supraclavicular. The point is located superficial to the junction of C5-C6 nerve roots. Spinal accessory nerve is located 1 cm above Erb's point. Local anesthesia here (red circle) can block cutaneous sensation for virtually the

entire ipsilateral neck. Left: [Modified from Wikimedia. Retrieved from: [https://commons.wikimedia.org/wiki/File:Wilhelm\\_Heinrich\\_Erb\\_\(HeidICON\\_53028\)\\_cropped.jpg](https://commons.wikimedia.org/wiki/File:Wilhelm_Heinrich_Erb_(HeidICON_53028)_cropped.jpg). with permission from Creative Commons License 4.0: <https://creativecommons.org/licenses/by-sa/4.0/deed.en>]. Right: [Reprinted from Lewis, Warren H (ed). Gray's Anatomy of the Human Body, 20th American Edition. Philadelphia, PA: Lea & Febiger, 1918]

**Table 11.5** Embryologic zones of the skin

Zone	Tissue source of epidermis	Tissue source of dermis	Neuromere of origin	Innervation
Fronto-nasal	NNE rostral p6-p4	PNC caudal p4-p1		Segmental V1
Eyelid, upper conjunctiva	Hypaxial Ectoderm	Hypaxial Neural crest	r1	Segmental V1
Eyelid, lower	Hypaxial Ectoderm	Hypaxial Neural crest	r2	Segmental V2
Face	Hypaxial ectoderm	Hypaxial neural crest	r2-r3	Segmental V2-V3
Scalp, lateral	Epaxial ectoderm	Epaxial Neural crest	r2-r3	Segmental V2-V3
Scalp, postauricular	Hypaxial ectoderm	Hypaxial Mesoderm	c2-c3	Plexus C2-C3
Scalp, posterior	Epaxial ectoderm	Epaxial Mesoderm	c2-c4	Segmental C2
Neck, anterior	Hypaxial ectoderm	Hypaxial Mesoderm	c1-c4	Plexus C1-C4
Neck, posterior	Epaxial ectoderm	Epaxial Mesoderm	c2-c8	Segmental C2-C8

## Zones of Craniofacial Skin

Craniofacial skin zones are classified by the source of epidermis and dermis. Bear in mind that all craniofacial skin is supported by superficial investing fascia/SMAS and vascularized by branches of the superficial division of the external carotid artery (Table 11.5).

## Classification of Head and Neck Skin and an Evolutionary Aside

Type 1 epidermis—neural crest//dermis—neural crest.

The unique source of frontonasal skin, these tissue derivations explain various pathologic states such as frontonasal dysplasia.

Type 2 epidermis—ectoderm//dermis—neural crest.

Lateral scalp dermis arises from small sector of epaxial V2 in the postorbital zone and large sector of epaxial V3 extensively distributed to the vertex where it has a direct interface with ascending branches of C2 and C3.

Type 3 epidermis—ectoderm//dermis—mesoderm.

For neck skin and posterior scalp there is little to add other than that the *dorsal and ventral zones have differences in innervation*. Epaxial skin is served by *segmental* sensory nerves. Hypaxial skin is served by sensory nerves that intermingle in a cervical *plexus*.

The take-home message of this section is not to add pointless trivia but to answer an important anatomic question.

Why is the neuromeric representation of craniofacial skin discontinuous? Why should we find dermis originating from the rostral hindbrain, r3 abutting directly up against dermis from the second cervical somite? And why is first cervical somite not represented?

Probably the simplest explanation is that both neural crest dermis is only produced at r1-r3. Paraxial mesoderm is incapable of producing dermis until Sm13, C2. By default, post-occipital skin will come from the first somite of the trunk. The piscine head-trunk interface is immobile. The process of resegmentation, in which the cranial half of somite merges with the caudal half of the preceding somite, did not extend forward into the occipital somites. Evolution of tetrapods involved a redefinition of the first three body somites into the primitive proatlas, which, as mentioned before, remained unincorporated into the cranial base. Incorporation of the first cervical somite into the occipital bone in reptiles permitted head flexion but eliminated its capacity to form dermis.

Several zones of mammalian skin demonstrate this evolutionary legacy. In hypaxial anterior neck, the V3/C2 interface takes place along the margin of the mandible. The ear has an anterior hypaxial zone with V3 abutting the C2-C3 greater auricular nerve from cervical plexus. It also has an epaxial posterior zone supplied by the segmental C2 lesser occipital nerve. In posterior scalp, V3 apposes that supplied by segmental C2 greater occipital nerve all the way to the vertex. The spatial positioning of C2 skin over the occipito-parietal skull occurs because of tissue expansion due to growth of the braincase.

## Fasciae of the Neck

### Superficial Investing Fascia (SIF) (Figs. 11.60, 11.61, 11.62 and 11.63)

SIF, as previously described, is a product of the second arch and is derived from neural crest from rhombomeres r4-r5. It covers platysma which sweeps down over the clavicles to neuromeric level c4. Platysma and the SIF sweep backward over sternocleidomastoid where with the termination of the muscle SIF blends into but is not continuous with the superficial fascia of the neck. Platysma has an anomalous relationship with the remainder of the facial muscles. It is the only one not supplied

by the second arch facial arterial system, being instead supplied from the first arch. It is explicable because the blastema of the platysma, being the most caudal and posterior develops prior to the other facial muscles and thus picks up its arterial axis of the inferior alveolar. The inferior supply reflects its extension beyond its “home base.”

- SIF in relationship to pharyngeal arches: submental artery from inferior alveolar, a derivative of StV3. This is the instance of a first arch artery supplying a second arch muscle.
- SIF in relationship to neck: penetrating branches of supra-scapular artery, a branch of thyrocervical trunk.

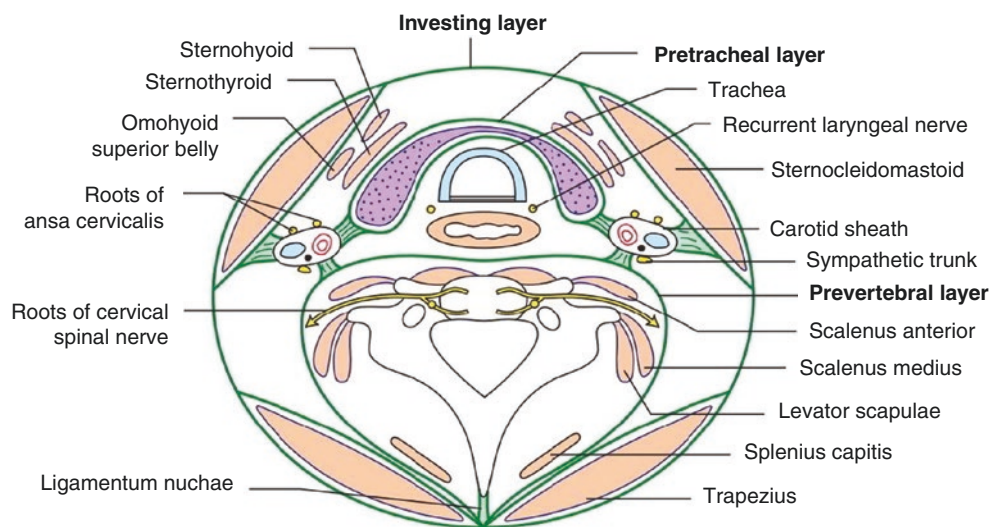


**Fig. 11.60** Cervical fascia (axial at vertebra C6) SCF and SIF not labeled. Subcutaneous fascia (SCF):

- Neural crest.
- Panniculus carnosus for skin contraction.
- Arrector pili muscles—connect to hair shafts—relation.
- Platysma sometimes considered a remnant of panniculus carnosus.

#### Superficial investing fascia (SIF)

- Neural crest.
- Mammals only.
- Originates from r4-r5.
- Branchiomic second arch muscles, superficial layer (muscles of facial expression).

#### Deep investing layer (DIF):

- Neural crest in anterior neck and PAM everywhere else.
- All non-mimetic pharyngeal arch muscles.
- Splits to enclose submandibular gland: superficial lamina to mandible border, deep lamina mylohyoid line.
- Splits to enclose parotid gland.

- Splits to enclose sternocleidomastoid/trapezius.
- Pretracheal fascia (PTF):
- Neural crest.
  - Encloses straps.
  - Lateral extension to carotid sheath: connects laterally to DIF and posteriorly to the PVF.
- Buccopharyngeal fascia (BPF):
- Neural crest.
  - Branchiomic constrictors of oropharynx.
  - Continuous with buccinator fascia (DIF).
  - Muscle function: swallowing.
  - BFP (neural crest) continuous with esophageal fascia (LPM).
- Pre vertebral fascia (PVF):
- PAM.
  - Somitic muscles with primary insertions into cervical spine.
  - Muscle function: spin-spine, spine, scapular (c4) and first rib.
  - PVF continuous with c4.

[Courtesy of Instant Anatomy ([www.instantanatomy.net](http://www.instantanatomy.net))]

**Fig. 11.61** Cervical Fascia (sagittal).

Subdermal fascia (SDF) not shown:

- Arrector pili muscles in the scalp.

Superficial investing fascia (SIF): not shown.

Deep investing fascia (DIF):

- Superior: to superior nuchal line, mastoid, mandible.
- Inferior: jugular notch, upper clavicle (note split over manubrium and clavicle—indicating embryologic relationship).
- Anterior: symphysis, hyoid, jugular notch.
- Posterior: cervical sternocleidomastoid/trapezius.

Pretracheal fascia (PTF) lies deep in DIF:

- Sagittal extent (mandible, hyoid, thyroid, thyroid gland, pericardium).

- Reproduces migration of tongue, thyroid, and thymus.

Buccopharyngeal fascia (BPF):

- Functionally related to oropharyngeal mucosa.
- Covers constrictors r2-r11.
- Changes at esophagus to LPM.

Prevertebral fascia (PVF):

- Extends downward from the skull base far as T3/T4 the upper level of pericardium.

Danger zone: spread of oral infection into the chest.

- Extends outward as axillary sheath.

[Courtesy of Instant Anatomy ([www.instantanatomy.net](http://www.instantanatomy.net))]

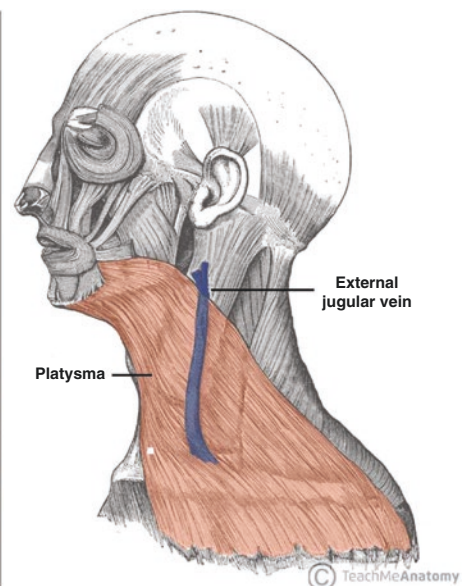
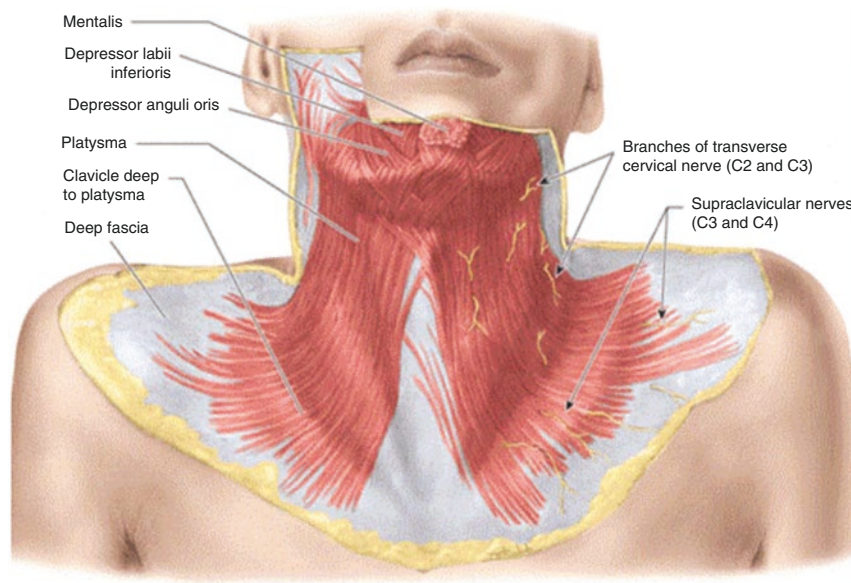
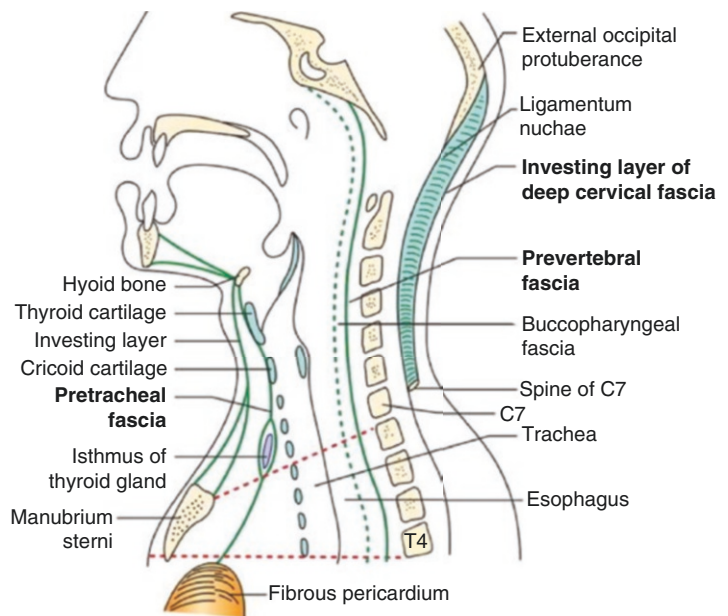
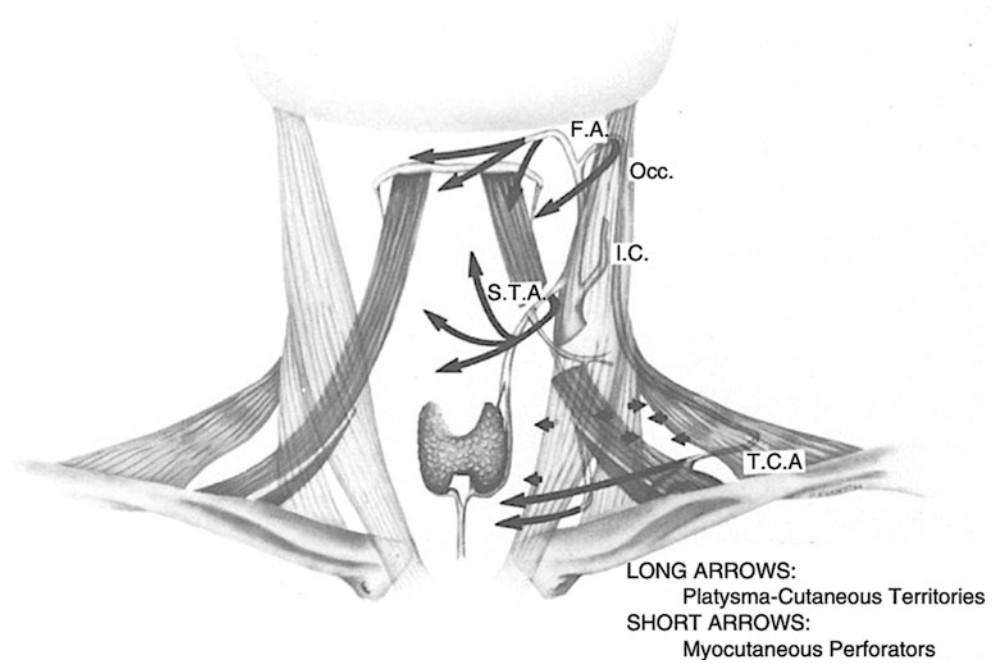


**Fig. 11.62** Superficial investing fascia: branchiomeric second arch. Platysma is a hypaxial branchiomeric muscle from Sm4-Sm5 with motor supply from the cervical branch of cranial nerve VII. It passes downward from angle of mandible beneath dermis supplied by C2-C4. Platysma exists within superficial investing fascia (SIF) or submusculo-aponeurotic fascia (SMAS), a neural crest structure from r4-r5. It advances over branchiomeric territory of deep investing fascia involving straps and sternocleidomastoid because these muscles develop neu-

romeres c1-c4, which were *originally branchiomeric*. Sensory nerves C2-C3 (transverse cervical) and C3-C4 (supraclavicular) supplying their respective quadrants of skin pre-date myogenesis so platysma mesenchyme flows around them. Left: [Reprinted from JC Boileau Grant. Atlas of Human Anatomy Philadelphia: Williams & Wilkins; 1943.]. Right: [Reprinted from TeachMeAnatomy, courtesy of Dr. Oliver Jones]

**Fig. 11.63** Blood supply to neck skin. Platysma is perforated by branches from facial artery (FA), superior thyroid artery (STA), occipital artery (occ), and transverse cervical artery (TCA). These penetrate platysma to supply the subdermal-dermal plexus of the skin. Musculo-cutaneous perforators (small arrows) reach the skin from sternocleidomastoid, the straps, and trapezius (small arrows). [Reprinted from Rabson JA, Hurwitz DJ, Futrell JW. The cutaneous blood supply of the neck: relevance to incision planning and surgical reconstruction. *Br J Plast Surg* 1985; 38:208–219. With permission from Elsevier]



### Deep Investing Fascia (DIF) (Figs. 11.64, 11.65 and 11.66)

DIF follows the same rules. This fascia remains dedicated to pharyngeal arch muscle derivatives of the ancient branchial arch system, sternocleidomastoid, and trapezius. DIF splits to enclose them and therefore encircles the neck. Recall that both these muscles are branchiomic and descend from the ancient cucullaris muscle complex. As such they have neuromeric elements extending from the r10 to r11 segment of the nucleus ambiguus to c4 for SCM and c8 for trapezius. Their blood supply and that of their overlying fasciae are likewise regional.

Sternocleidomastoid connects the r6-r7 mastoid process with the c1 portion of the clavicle. Its mesenchyme originates from seven neuromeric levels: somitomeres 6–7, occipital somites 1–4 and the first cervical somite. Its blood supply reflects this neuromeric trifecta: its upper third is supplied by occipital branch of ECA representing third arch (r6-r7), the middle third receives superior thyroid from fourth arch (r7-r8), and the lower third is irrigated from the supra-scapular branch of the thyrocervical trunk (the second branch of the subclavian). The arteries reflect three distinct blocks of mesenchyme that produce this muscle.

As previously discussed, clavicular mesenchyme originates from the first four spinal somites, sp1-sp4. its physical

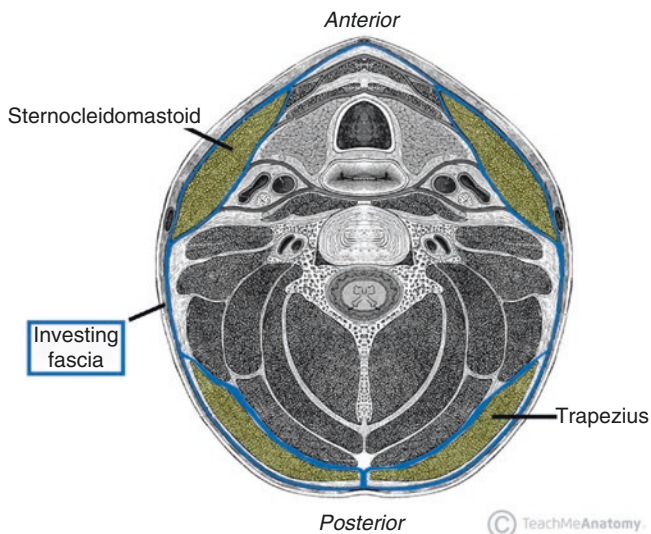


**Fig. 11.64** Deep investing fascia (DIF): branchiomic muscles. Sternocleidomastoid and trapezius originate from the ancient cucularis, a branchiomic derivative of arches B4-BA7 in register with neuromeres r8-r11 and Sp1-Sp4 with mesoderm derived from the first 8 somites (4 occipital and 4 spinal). [Reprinted from TeachMeAnatomy, courtesy of Dr. Oliver Jones]

disconnection from the skull reflects the changes wrought by the evolution of the neck itself. These initial spinal somites undergo a name change from sp1-sp4 to c1-c4 as clavicle migrates downward relationship to the skull migrating c1-c4/sp1-sp4) to the base of the skull, specifically the mastoid process that relates neuromerically to r6-r7. Thus, sternocleidomastoid spans from r6 to c1, that is from Sm6-

Trapezius has an extensive territory extending from the posterior skull base at level c1/sp1 down to the scapula as low as its tip, level c7/sp7. The muscle is irrigated from the transverse cervical branch of the thyrocervical trunk. It can be elevated upward as a flap based on this arterial axis. TCA has an ascending branch supplying the branchiomic (cucularis) mesenchyme from levels sp1-sp4 (BA6-BA7) and a descending branch to mesenchyme from sp5-sp8 (BA8-BA9). Recall that the prototypical branchial arch system as in placoderms contains 9 arches.

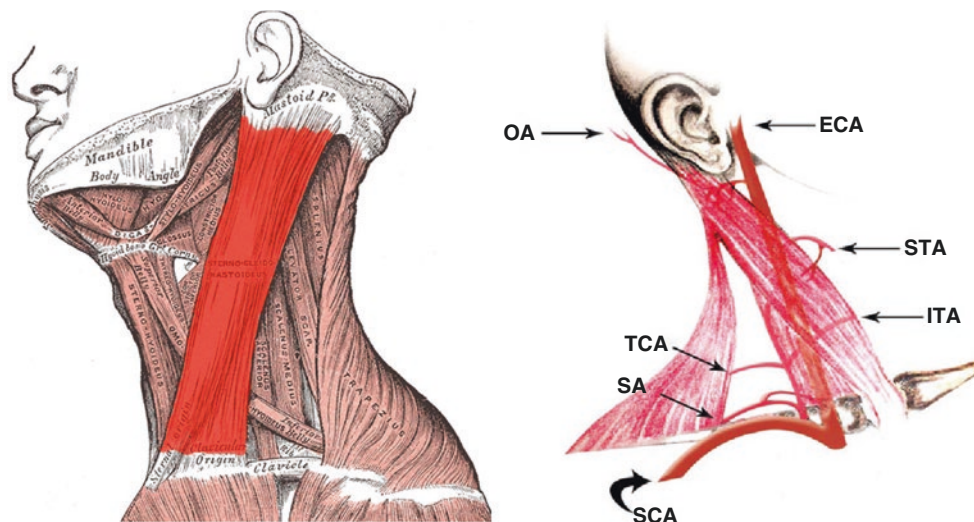


**Fig. 11.65** DIF: Sternocleidomastoid. Branchiomic muscle from multiple levels with three levels of blood supply. Left: [Reprinted from Lewis, Warren H (ed). Gray's Anatomy of the Human Body, 20th American Edition. Philadelphia, PA: Lea & Febiger, 1918.]. Right: [Reprinted from Khazaeni K, Rajati M, Shahabi A, Mashadi L. Use of

sternocleidomastoid myocutaneous flap based on the sternocleidomastoid branch of the inferior thyroid artery to reconstruct extensive cheek defects. Aesth Plast Surg 2013; 37(6): 1167-1170. With permission from Springer Nature]



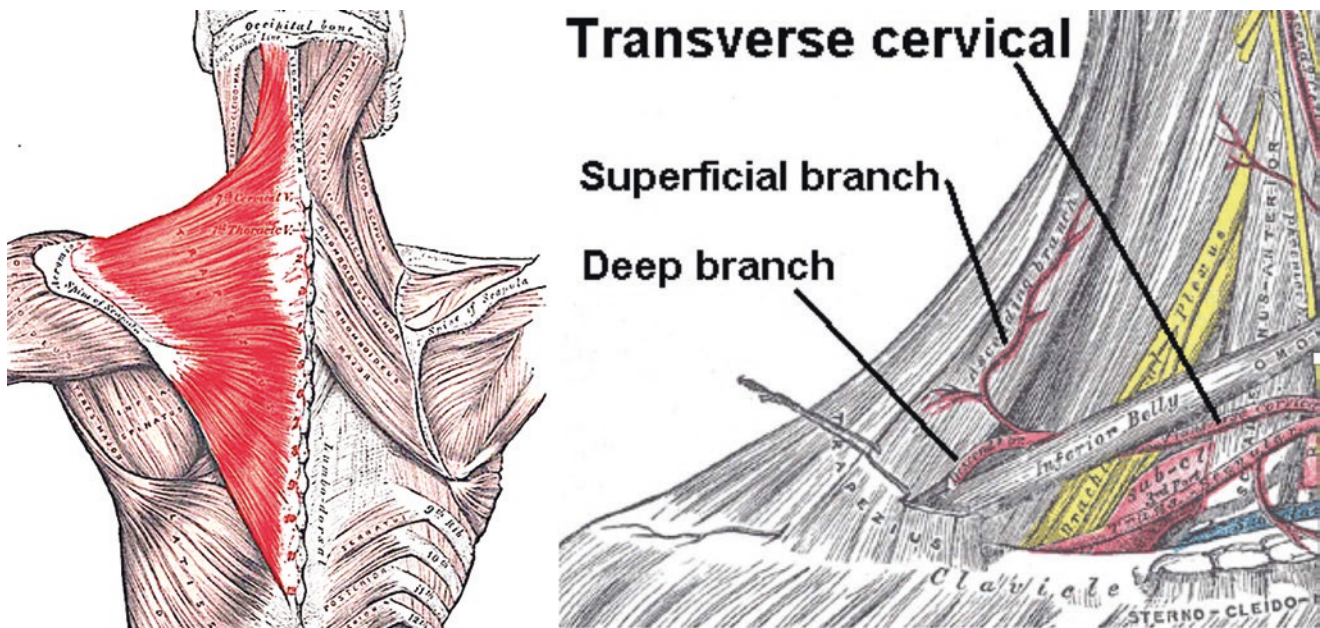


**Fig. 11.66** DIF: Trapezius. Transverse cervical artery (TCA) is one of the four branches of thyrocervical trunk. It travels laterally in the posterior triangle, in front of phrenic nerve, the scalene muscles, and brachial plexus. It slides beneath omohyoid (inferior belly) and reaches anterior border of levator scapulae. There it divides into superficial and deep branches. Superficial branch (1) ascends to supply upper 1/3 of trapezius where it anastomoses with occipital; and (2) descends to supply middle 1/3 and lower 1/3 of trapezius. Deep branch supplies levator scapulae and the rhomboids; it contributes to trapezius. Phylogenetically, superficial branch is dedicated to a branchiomic muscle (cucullaris) at

levels sp1-sp4 and deep branch is dedicated to non-branchiomic muscles connected to levels sp5-sp8 and the rhomboids; it contributes to trapezius. Phylogenetically, superficial branch is dedicated to a branchiomic muscle (cucullaris) at levels sp1-sp4 and deep branch is dedicated to non-branchiomic muscles connected to levels sp5-sp8. Left: [Reprinted from Lewis, Warren H (ed). Gray's Anatomy of the Human Body, 20th American Edition. Philadelphia, PA: Lea & Febiger, 1918.]. Right: [Modified from Lewis, Warren H (ed). Gray's Anatomy of the Human Body, 20th American Edition. Philadelphia, PA: Lea & Febiger, 1918]

### Prevertebral Fascia (Figs. 11.67, 11.68, 11.69 and 11.70)

Prevertebral fascia (PVF) encircles the spine and contains muscles on both the epaxial and hypaxial aspects of the vertebral column.

- PVF horizontal: fascia of posterior triangle, non-branchiomic muscles (scalenes, levator scapulae, splenius capitis). PVF lies ventral to roots of brachial plexus. As the trunks of the brachial plexus move into the upper extremity, they carry with them an extension of PVF, the axillary sheath. Note that the subclavian artery and vein are outside the sheath.
- PVF vertical: skull base in front of longus colli down to anterior ligament of t1. Neuromeric relationship with cervical neuromeres.

The epaxial (extensor) group is segmentally supplied from the vertebral system and from the ascending cervical branch of the costocervical trunk, the third dorsal derivative of subclavian. Recall that longitudinal nature of the ascending cervical artery is (like vertebral) really the sum of original transverse segmental branches from the dorsal aortae. There are two functional groups of hypaxial muscles. A medial vertebral group includes those muscles, such as longus capitis that are flexors; these relate segmentally to the anterior vertebrae. A lateral vertebral group consists of the three scaleni which connect the cervical spine to the first rib and levator scapulae which attach to the c4 medial superior angle. The blood supply to these two groups of muscles comes from a single axis, the thyrocervical trunk along with its overlying fascia is spatial and neuromeric. Inferior thyroid while going up to the r11-c1 junction below the cricoid ascending cervical gives off a separate ascending cervical branch. Together these two vessels supply the midline muscles.

**Fig. 11.67** Prevertebral fascia (PVF): axial. PVF covers axial somitic muscles (S5-S13) from the skull base to the pericardium. [Reprinted from TeachMeAnatomy, courtesy of Dr. Oliver Jones]

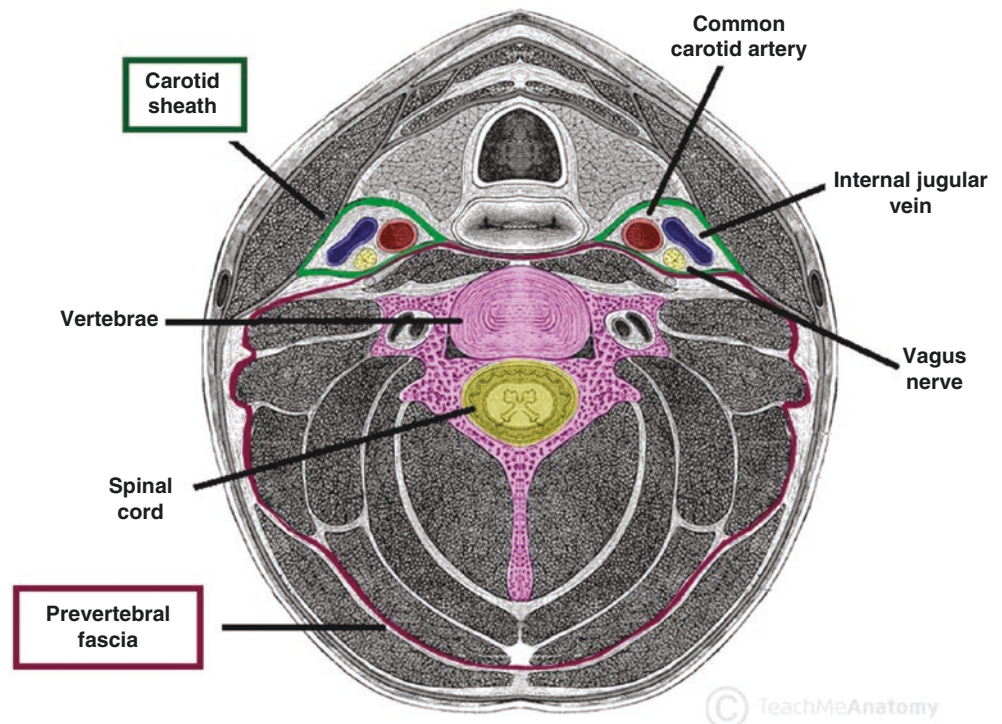


**Fig. 11.68** PVF: coronal. **PVF horizontal:** fascia of posterior triangle, non-branchiomic muscles (scalenes, levator scapulae, splenius capitis).

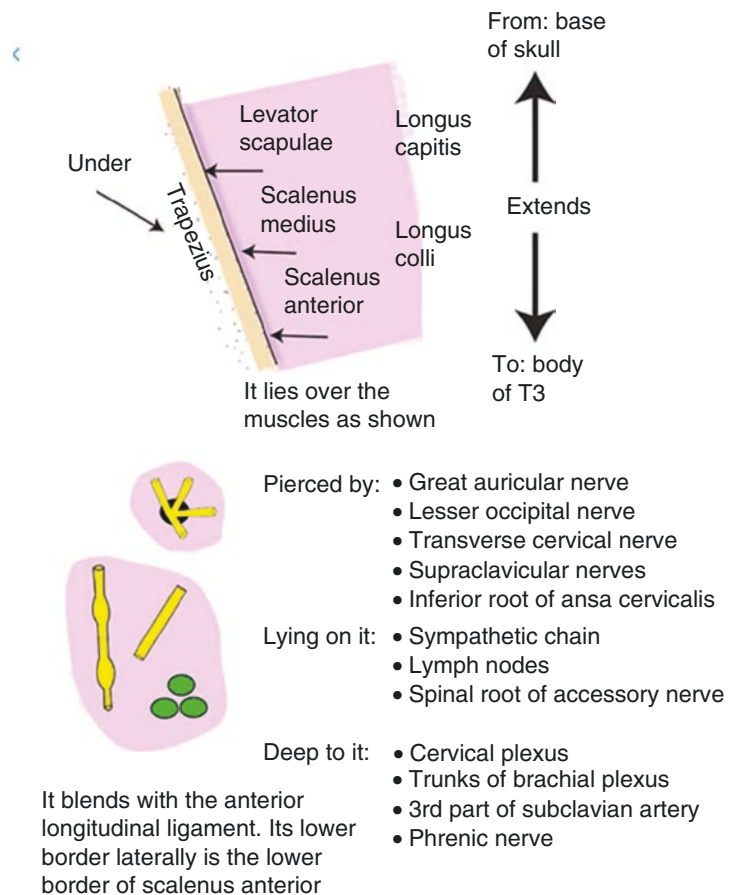
Lies ventral to roots of brachial plexus.

- As trunks move into upper extremity, they carry an extension of PVF, the axillary sheath.
- Subclavian artery and vein are outside the sheath.

**PVF vertical:** skull base in front of longus colli down to anterior ligament of t1

- Neuromeric relationship with cervical neuromeres.
- [Courtesy of Instant Anatomy ([www.instantanatomy.net](http://www.instantanatomy.net)). Retrieved from: <https://www.instantanatomy.net/headneck/areas/fasprevertebral.html>.]

**PREVERTEBRAL PART OF DEEP FASCIA OF NECK**



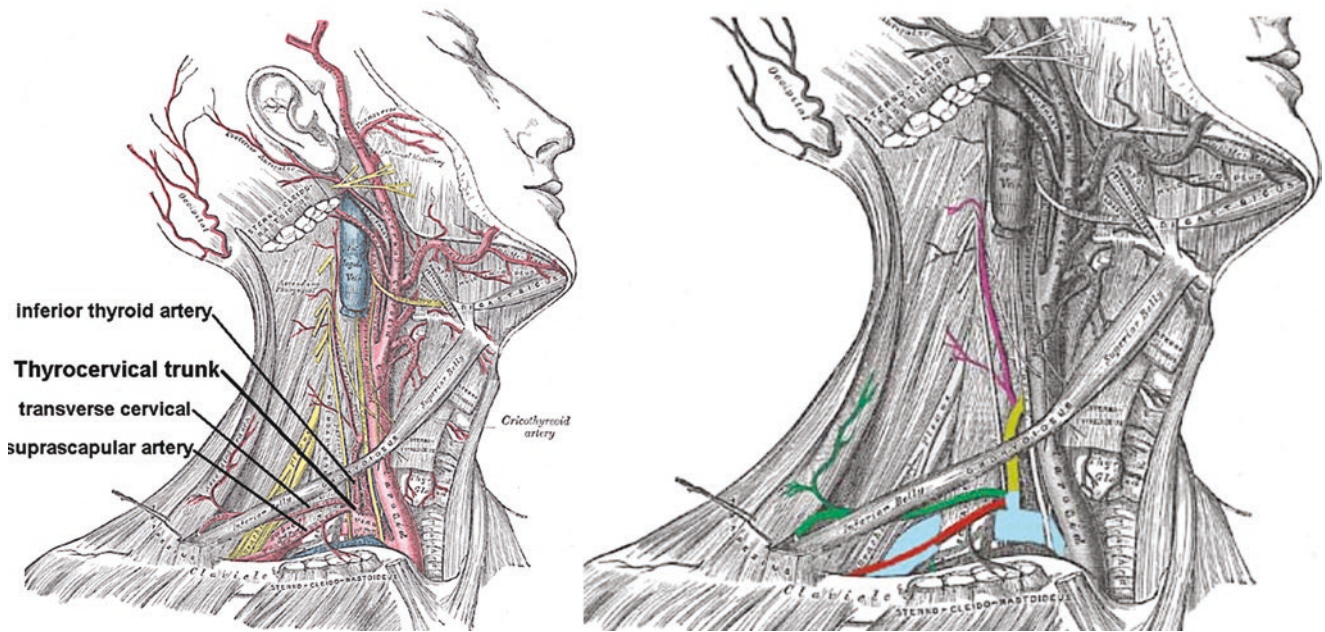


**Fig. 11.69** Thyrocervical trunk: muscular relations. Thyrocervical trunk (TCT) is the predominant source of blood supply to the neck. TCT (aqua) arises from second part of subclavian (aqua). It gives off *inferior thyroid* (yellow), *ascending cervical* (magenta), *transverse cervical* (green), and *suprascapular* (red). *Dorsal scapular artery* not

shown—it arises as a branch from transverse cervical or just lateral to thyrocervical trunk. Suprascapular also can arise from transverse cervical. [Reprinted from Lewis, Warren H (ed). *Gray’s Anatomy of the Human Body*, 20th American Edition. Philadelphia, PA: Lea & Febiger, 1918.]

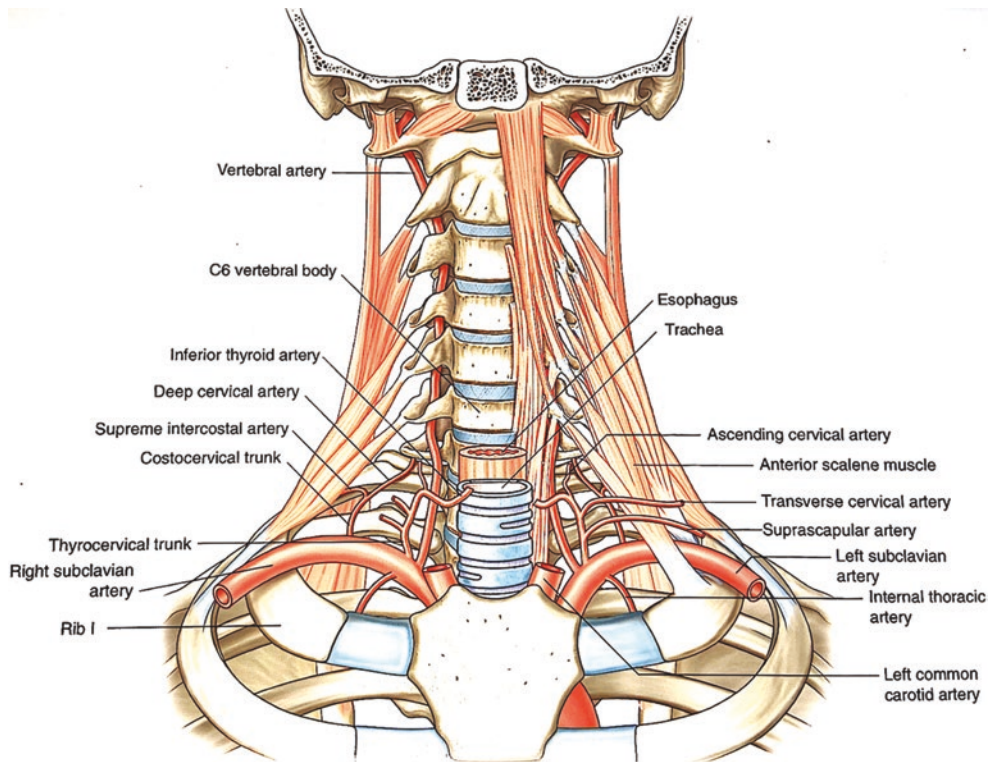


**Fig. 11.70** Thyrocervical trunk: skeletal relations. TCT has 3 main branches and supplies the hypaxial muscles enclosed by all 3 cervical fasciae. (1) Inferior thyroid a. supplies the pretracheal fascia and the overlying strap muscles of ancient coracohyoideus enclosed within the deep investing fascia. It gives off a deeper ascending cervical br. to the prevertebral fascia. (2) Transverse cervical branch a. supplies the deep investing fascia of the anterolateral neck. (3) Suprascapular a. supplies deep investing fascia and muscles of the scapula. Although scapula is

located dorsally the muscles which control it from both the neck and trunk are all hypaxial representing its evolutionary origin as a ventral bone of the limb girdle. All branches of TCT three provide perforating branches to the overlying platysma within the superficial investing fascia. [Reprinted from Drake R, Vogel AW, Mitchell AWM. *Head and Neck*. In: *Gray’s Anatomy for Students*, third edition. Philadelphia, PA: Churchill-Livingstone. 2015: 924–1052. With permission from Elsevier]

### Buccopharyngeal Fascia (BPF) (Fig. 11.71)

BPF is a neural crest structure that covers the branchiomic muscles of the pharynx (r4-r5) and the three pharyngeal constrictors (r6-r11). It extends from the skull base downward to the esophagus. This fascia is supplied by arterial branches representing each of the arches.

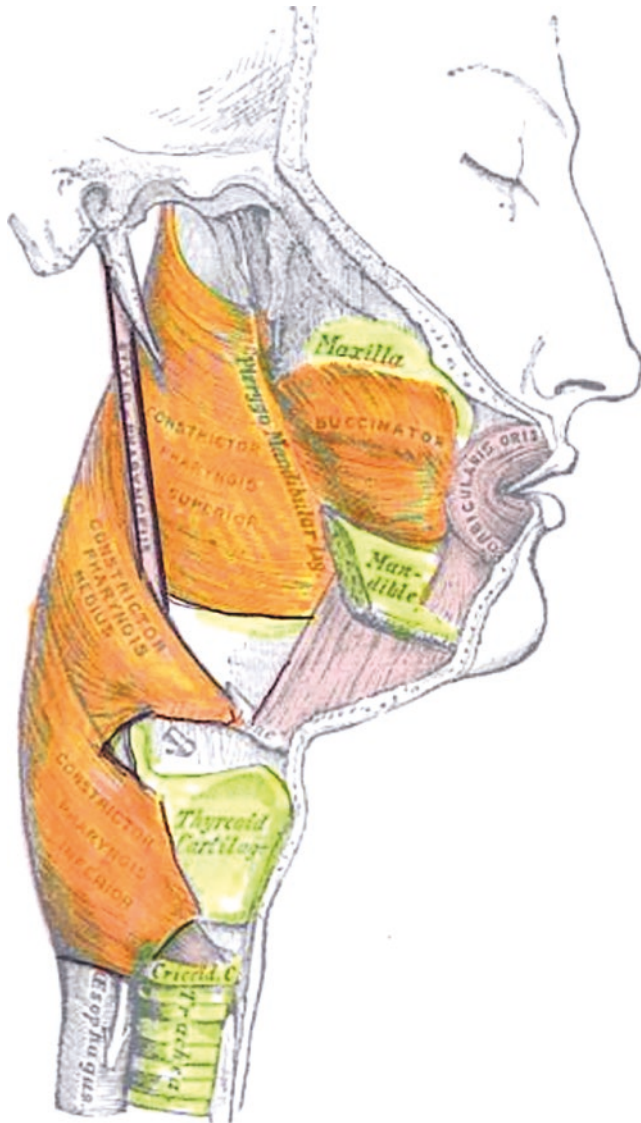


**Fig. 11.71** Buccopharyngeal fascia (BPF). Neural crest structure extends from C1 down to esophagus. Covers branchiomic all muscles lining the pharynx: buccinator (r4-r5) and pharyngeal constrictors (r6-r-11). Joined in the midline with prevertebral fascia. [Reprinted from Lewis, Warren H (ed). *Gray's Anatomy of the Human Body*, 20th American Edition. Philadelphia, PA: Lea & Febiger, 1918]

### Pretracheal Fascia (PTF) (Figs. 11.72, 11.73, 11.74, 11.75, 11.76, 11.77, 11.78, 11.79, 11.80, 11.81, 11.82, 11.83, 11.84, 11.85, 11.86, 11.87, 11.88, 11.89, 11.90, 11.91 and 11.92)

PTF is a thin layer that begins at the anterior margin of hyoid bone and extends downward to ensheath the thyroid, the infrahyoid strap muscles, and, ultimately the strap muscles. PTF recapitulates the fascia associated with coracohyoideus. Recall from our discussion of the neck that the chondrichthyan clavicle is connected to the mandible using two successive muscles coracohyoideus and geniohyoideus. Together these trace the ventral margins of branchial arches 1–7. This tract provides a guidance system for the descent of the thyroid and thymus. Furthermore, since it terminates at neuromeric level c4 (the termination of BA7), that is, at pericardium it represents the pathway by which thyroid can stay undescended in the tongue or thymus can find itself in the mediastinum.

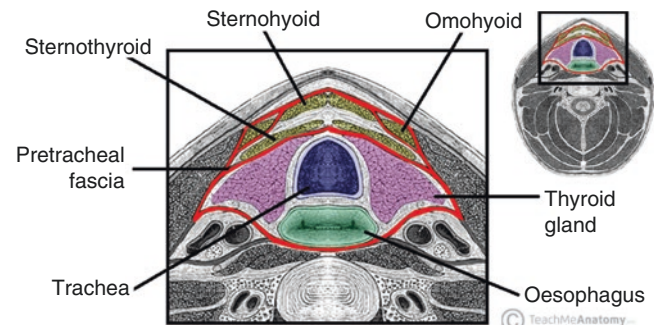


**Fig. 11.72** Pretracheal fascia (PTF): infrahyoid strap muscles (C1-C3). Infrahyoid muscles (C1-C4) innervated from the cervical plexus. 4/5 muscles related phylogenetically from coracomandibularis. Innervation by the cervical plexus to hypaxial branchiomic muscle belies ancient position of the forefin. Perhaps a remnant of more anteriorly positioned forefin? Refer to Fig. 11.57. [Courtesy of Instant Anatomy ([www.instantanatomy.net](http://www.instantanatomy.net)). Retrieved from: <https://www.instantanatomy.net/headneck/areas/faspretracheal.html>]





**Fig. 11.74** Blood supply to PTF. Diagram of the superior and inferior blood supply to the infrahyoid muscles. *LA* lingual artery, *HA* hyoid artery, *STA* superior thyroid artery, *ITA* inferior thyroid artery, *IMA* internal mammary artery, *OH* omohyoid muscle, *SH* sternohyoid muscle, *ST* sternothyroid muscle, *TH* thyrohyoid muscle, *scn br* sternocleidomastoid branch. [Reprinted from Eliachar I, Marcovich A, HarShai Y, Lindbaum E. Arterial blood supply to the infrahyoid muscles: an anatomical study. *Head & Neck Surg* 1984; 7:8–14. With permission from John Wiley & Sons, Inc.]

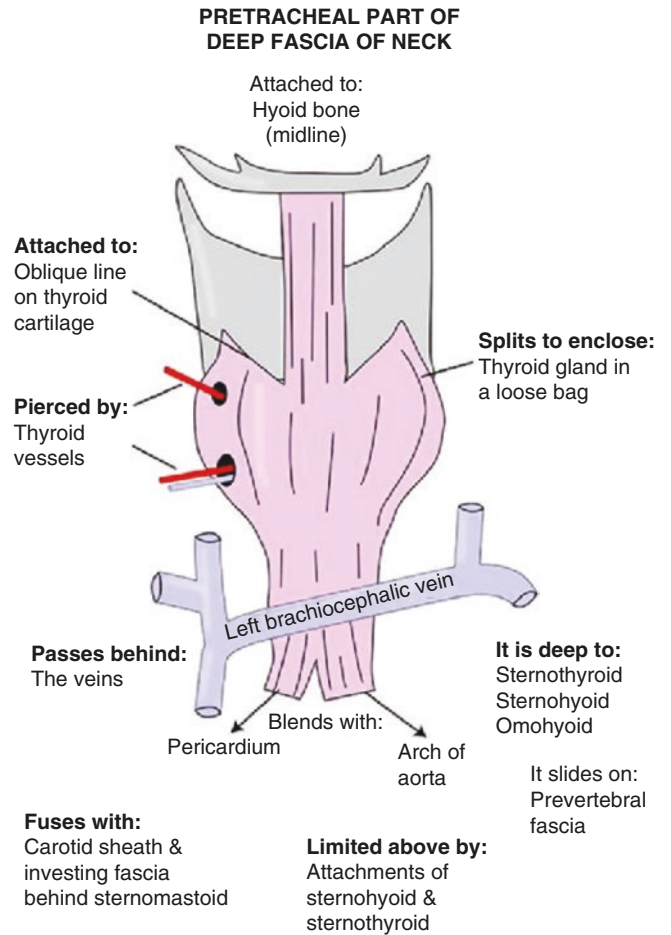


**Fig. 11.75** Pretracheal fascia. Coronal: PTF is attached on its under-surface to thyroid cartilage oblique line indicating its developmental relationship with the larynx. Because it splits to enclose thyroid, PTF constitutes a potential space in which the gland descend. Thyroid neuromuscular pedicles constitute primary structures of the fourth arch anlage, around which the PTF must condense. Were this the reverse the pedicles would traverse around the fascia. PTF is narrowed by the homologs of coracomandicularis muscles, being limited by the infrahyoid strap muscles and by the paired bellies of the suprahyoid geniohyoideus. [Courtesy of Instant Anatomy ([www.instantanatomy.net](http://www.instantanatomy.net))]

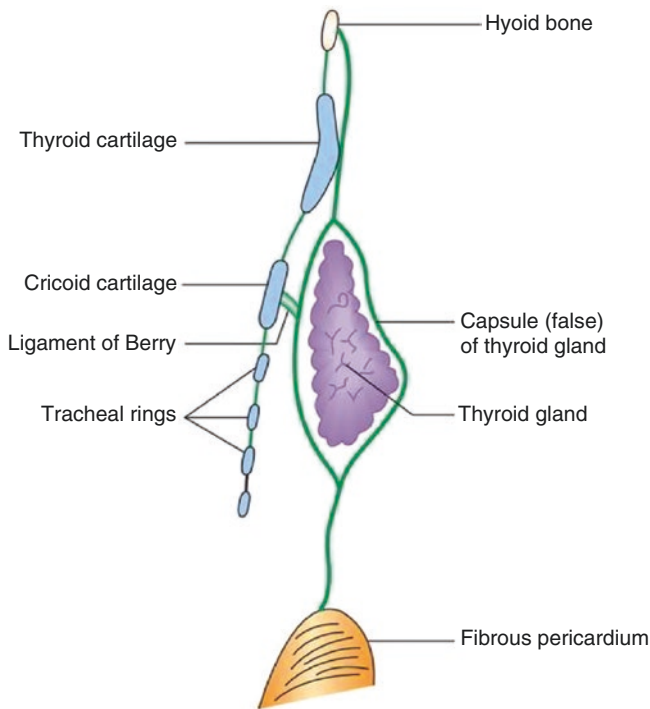


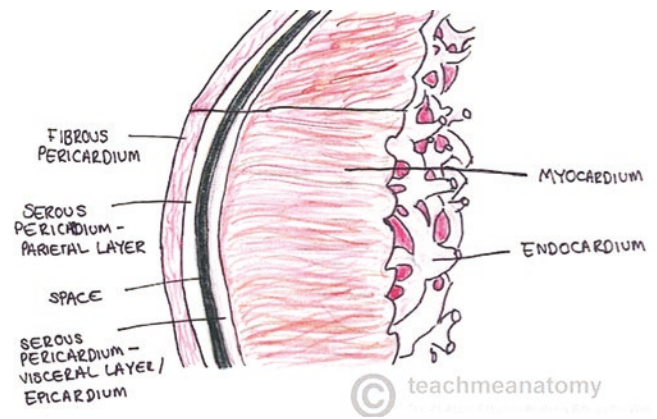
**Fig. 11.76** Pretracheal fascia.

Axial: Unites with all DIF enclosing the sternocleidomastoid and the anterior wall of the carotid sheath.

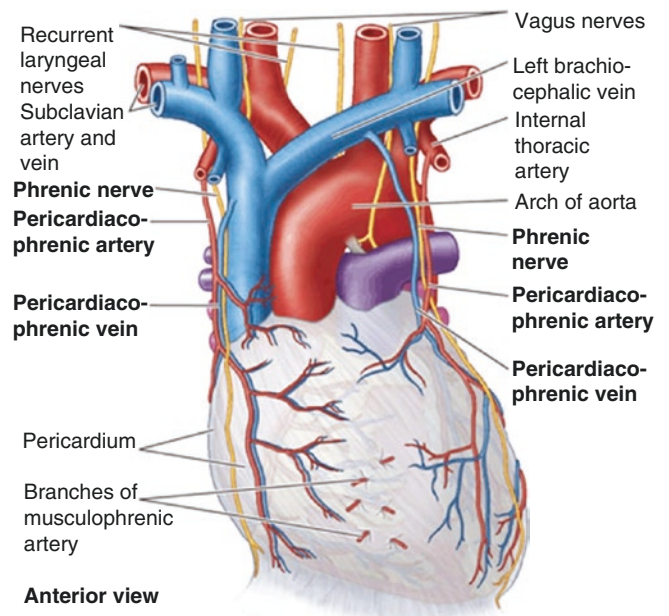
Sagittal: Connected to the hyoid bone, enters thorax, fuses with the apex of the fibrous pericardium.

- PTF connects hyoid bone with thyroid and cricoid cartilages.
- Conduit for migration of tongue myoblasts, thyroid, and thymus.
- Gliding surface between trachea and esophagus during swallowing.
- Layer posterior to thyroid is thin and permits goitre to compress esophagus (dysphagia).

[Courtesy of Instant Anatomy ([www.instantanatomy.net](http://www.instantanatomy.net))]

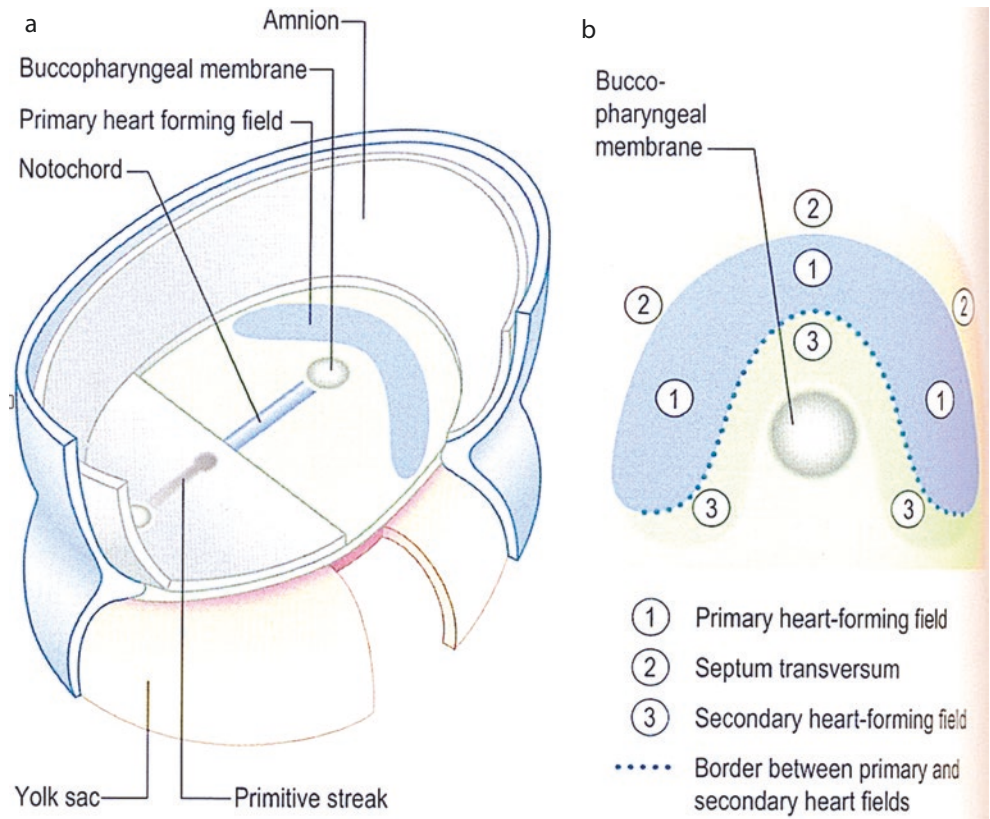


**Fig. 11.77** Pericardium and endocardium. Pericardium: fibrous (cervical LPM<sub>S</sub>) + serous (prechordal LPM<sub>S</sub>). Epicardium: serous and fibroadipose (prechordal LPM<sub>V</sub>). [Reprinted from TeachMeAnatomy courtesy of Dr. Oliver Jones]

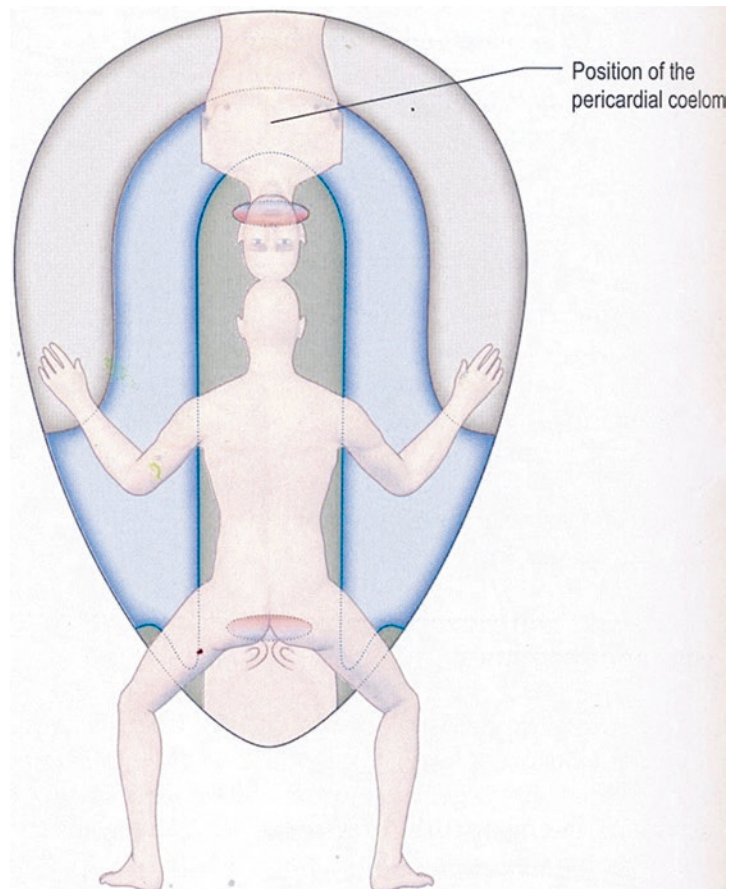


**Fig. 11.78** Blood supply to pericardium. Cervical LPM<sub>S</sub> fibrous layer of pericardium: *pericardiophrenic arteries* accompany phrenic nerves and are distributed to the Prechordal LPM<sub>S</sub> parietal serous layer of pericardium: *internal thoracic arteries* note *musculophrenic* branches connect with anterior intercostal arteries 7–9 and supply lower pericardium. LPM<sub>V</sub> epicardium (visceral serous layer + fat): *coronary arteries* supply prechordal cardiogenic mesoderm. [Reprinted from Drake R, Vogel AW, Mitchell AWM. Gray’s Anatomy for Students, third edition. Philadelphia, PA: Churchill-Livingstone. 2015. With permission from Elsevier]

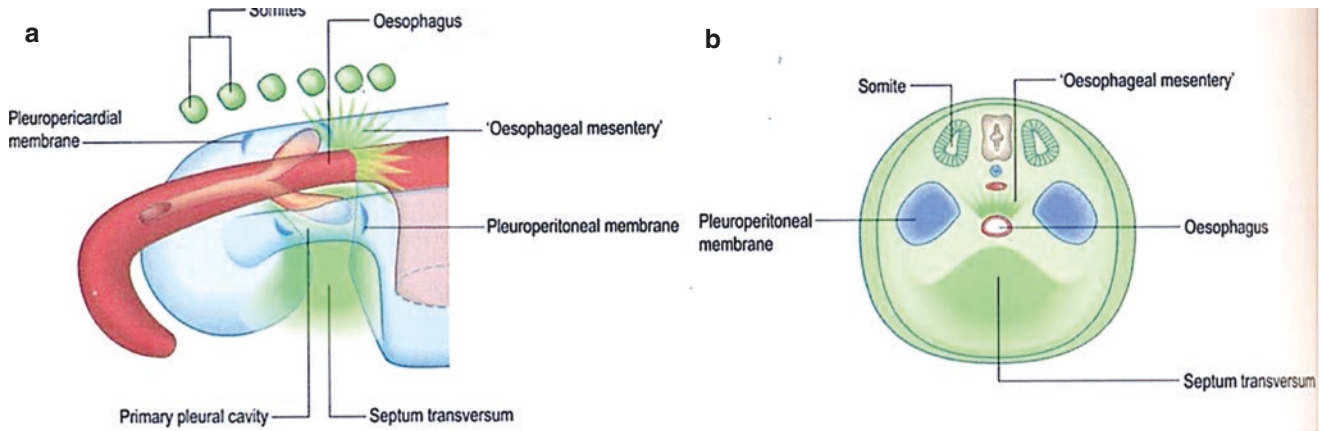
**Fig. 11.79** Folding of the embryo 1; heart fields and septum transversum. Prechordal plate mesoderm extends forward from the primitive node to the primary heart field. Thus, when first aortic arches develop in LPM they are in intimate contact with PCM. [Reprinted from Standring S. The Back. In: Gray's Anatomy, 40th edition. Philadelphia, PA: Churchill-Livingstone; 2008: 763–774. With permission from Elsevier]



**Fig. 11.80** Folding of the embryo 2: origins of dermis. Note that lateral plate mesoderm forms all ventral dermis from T2 to L1. Note that the upper extremities, although hypaxial, are PAM. The PAM/LPM interface runs down the sides of the trunk as the mid-axillary line. Key: somatic LPM, blue; visceral LPM, grey. [Reprinted from Standring S. The Back. In: Gray's Anatomy, 40th edition. Philadelphia, PA: Churchill-Livingstone; 2008: 763–774. With permission from Elsevier]



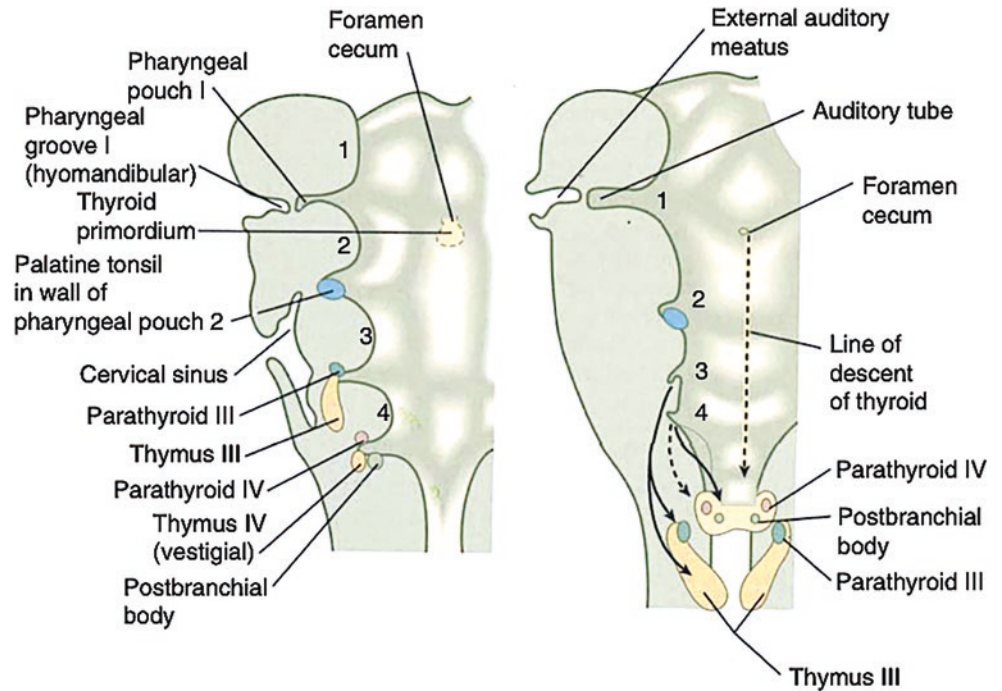




**Fig. 11.81** Folding of the embryo 3. PCM comes to lie directly dorsal to the first aortic arches and is ideally positioned to contribute to the cranial base at the r1 level. Pleuroperitoneal membranes define a cavity but are an important source of tissue in their own right. They contribute to the diaphragm and provide an means by which, in mammals, the C4

supracoracoideus muscle invades the chest wall to form the bulk of muscle in the diaphragm. [Reprinted from Standing S. The Back. In: Gray's Anatomy, 40th edition. Philadelphia, PA: Churchill-Livingstone; 2008: 763–774. With permission from Elsevier]

**Fig. 11.82** Thyroid migration. Note association of thymus with third pharyngeal pouch and with parathyroid III. [Reprinted from Carlson BM. Human Embryology and Developmental Biology, sixth edition. St. Louis, MO: Elsevier; 2019. With permission from Elsevier]



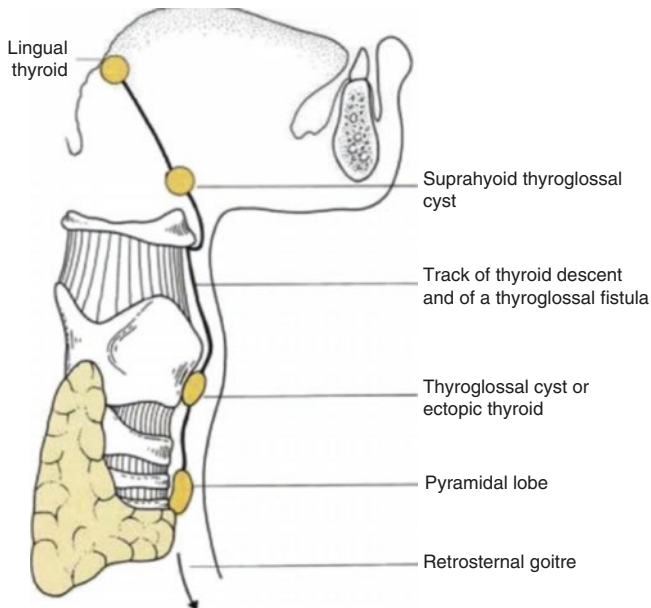


**Fig. 11.83** Ectopic thyroid tissue. Thyroid tissue has been found within the trachea, substernal and with intra-abdominal sites reported as well. Thyroid follows the tract of PTF from the site of origin in the tongue through the hyoid bone, remaining immediately anterior to the PTF and reaching as far as level c4. [Reprinted from Fiaschetti V, Claroni G, Scarano AL, Schillaci O, Floris R. Diagnostic evaluation of a case of lingual thyroid ectopia. *Radiology Case Reports* 2016; 11:165–170. With permission from Elsevier]



**Fig. 11.84** Lingual thyroid. [Reprinted from Amr B, Monib S. Lingual thyroid: A case report. *International Journal of Surgery Case Reports* 2013; 2:313–315. With permission from Elsevier]

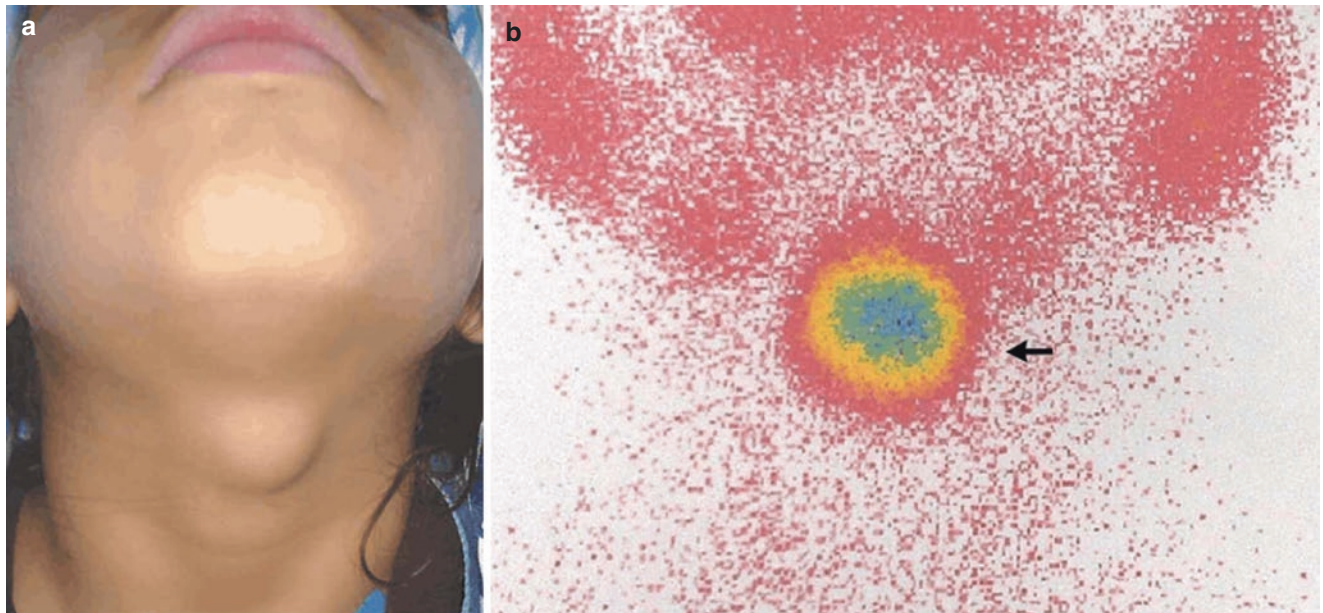


**Fig. 11.85** Thyroid gland in the thyroglossal tract. A 12-year-old girl presented with a lump situated high in her neck at the midline (Panel A). She had previously been found to have hypothyroidism and had been treated with levothyroxine. There were no signs of infection. An ultrasoundogram showed a solid midline mass. A technetium-99 thyroid scan showed uptake in the region of the mass but no uptake in the area of the

thyroid gland (Panel B, arrow). A fine-needle aspiration biopsy did not reveal any evidence of a malignant condition. The diagnosis was an ectopic thyroid gland in a thyroglossal tract. [Reprinted from Aalaa M, Mohajeri-Tehrani MR. Ectopic Thyroid Gland. *New Eng J Med* 2012; 366:943. With permission from Massachusetts Medical Society]

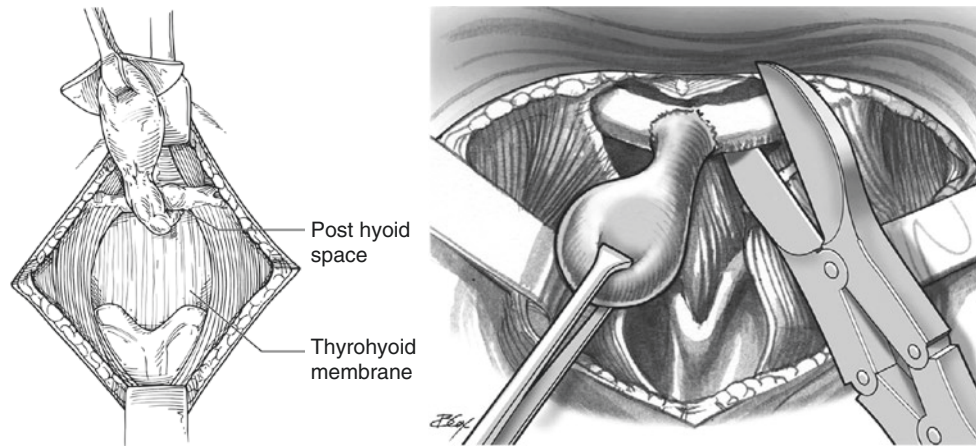


**Fig. 11.86** Surgical management of thyroglossal duct cyst. LEFT: Descent of the thyroid track through the anlage of the developing hyoid bone. The cyst and duct are being elevated with a cuff of surrounding tissue off the thyrohyoid membrane. The posthyoid space is entered with blunt dissection to ensure the tract is not truncated with hyoid resection. RIGHT: Thyroglossal duct management requires at times surgical section of the hyoid bone at the anterior midline: the Sistrunk procedure. Note how fibers of the sternohyoid and mylohyoid have been

detached from the hyoid bone to allow for exposure of the bone. The cuts of the hyoid have been made medial to the attachment of the digastric tendon and with sufficient length so as not to cut the duct. Left: [Reprinted from Newton SS. Thyroglossal duct cyst. *Op Tech Otolaryngol* 2017; 28: 173–178. With permission from Elsevier.]. Right: [Reprinted from Goldstein H, Khan A, Pereira KD Thyroglossal duct excision—The Sistrunk Procedure *Op Techn Otolaryngol* 2009; 20 (4): 256–259. With permission from Elsevier]

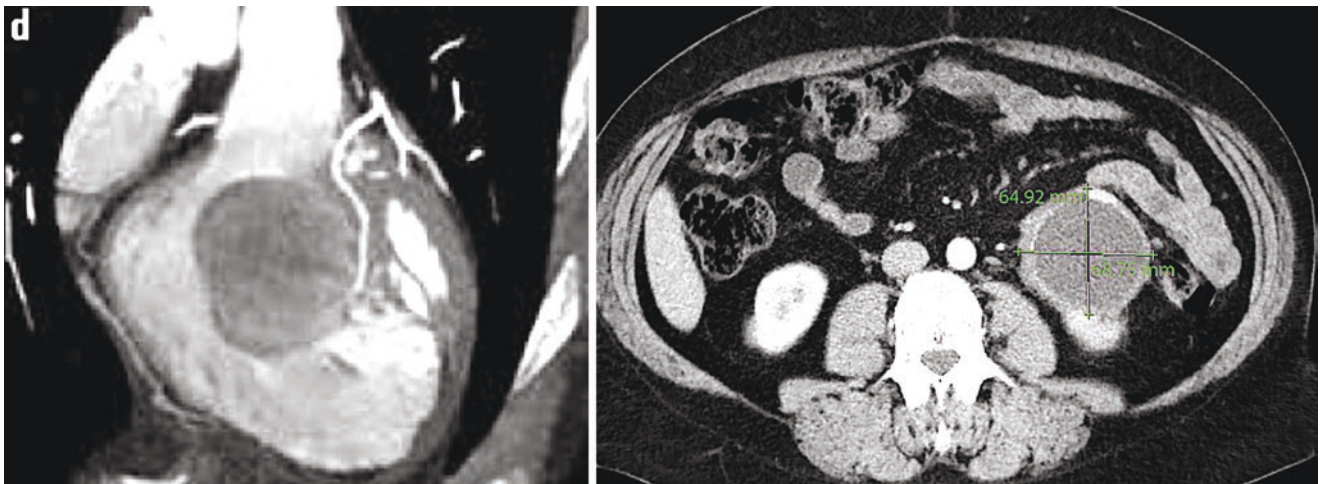


**Fig. 11.87** Ectopic thyroid in viscera: right ventricle and left kidney. LEFT This case shows the neuromeric pathway of fascia connecting the anterior margins of the pharyngeal arches and the pericardial sac. It is associated with the sensory innervation of the pericardium from neuromeres c3–c5. RIGHT First-in-man report of ectopic thyroid found in the left kidney. The first iteration of renal blastema, the pronephros, develops in the intermediate mesoderm at the level of the cervical neuromeres. The close association of kidney anomalies with congenital heart disease arises from this common embryonic connection. In the same

way thyroid tissue tracking along the pre-tracheal fascial plane may become incorporated into the pronephric anlage. Left: [Reprinted from Sun Y, Wang J, Cao D. Uncommon right ventricular mass: Ectopic thyroid. *Anatol J Cardiol*. 2018 May; 19(5): E8–E9. With permission from AJC Publications]. Right: [Reprinted from Mata Mera C, Kreutzer N, Lorenzen J, Truss M. Der setene Nierentumor: Renales ektopes Schilddrüssgewebe. *Urologe* 2018; 57: 944–946. With permission from Springer Nature]

**Fig. 11.88** Thymus development (mouse model). Stage 10 (E9.5) positioning thymic epithelial cells arise in third pouch. Stage 13 (E11) (CS 13) initiation. Stages 14–16 (E11.5–E12.5) outgrowth and patterning. Stages 15–18 (E 12–E13.5) separation. Stage 15 to birth (12–birth) differentiation. [Reprinted from Blackburn CC, Manley NR. Developing a new paradigm for thymus organogenesis. *Nature Reviews Immunology* 2004; 4:278–289. With permission from Springer Nature]

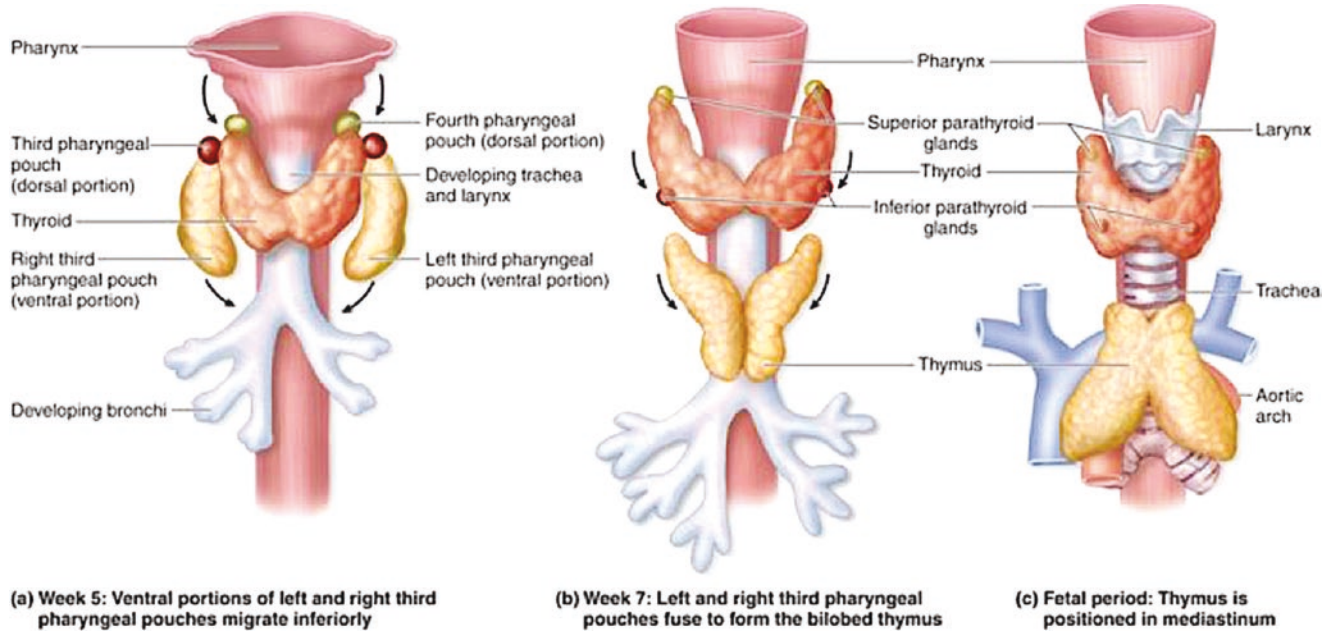
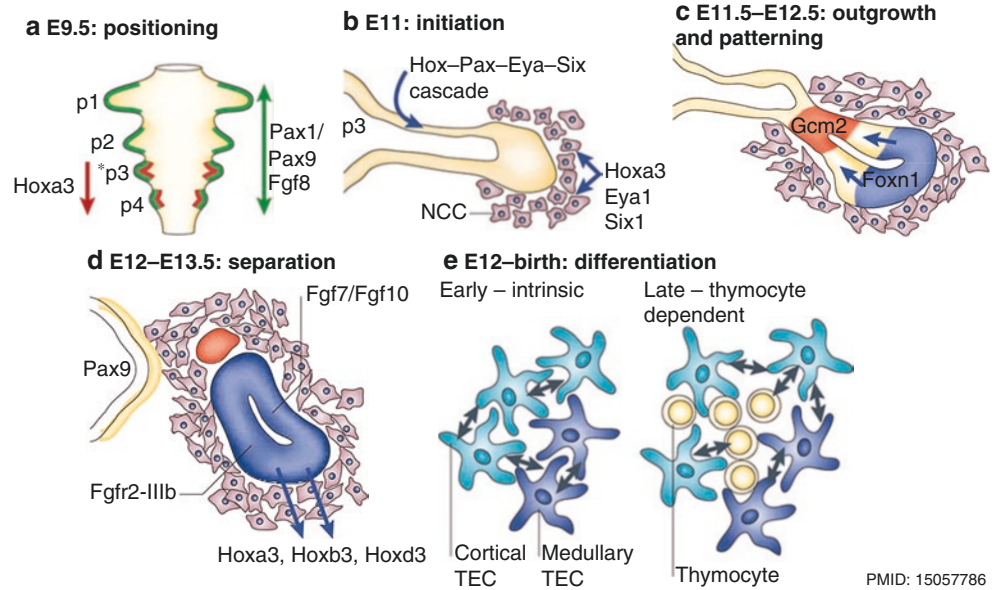


**Fig. 11.89** Descent of the thymus. Stage (6 weeks). Stage (7 weeks). [Reprinted from O’Laughlin V, McKinley M. *Anatomy & Physiology: An Integrative Approach*. New York, NY: McGraw-Hill Education; 2017. With permission from McGraw-Hill LLC]

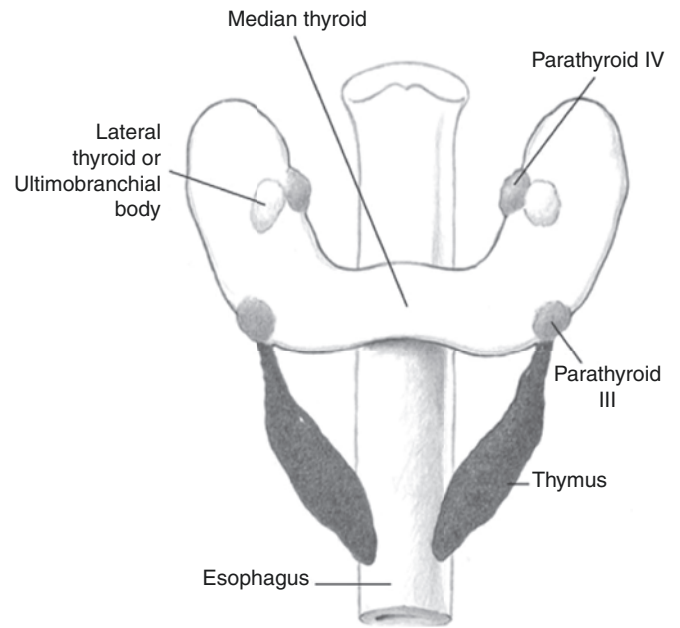
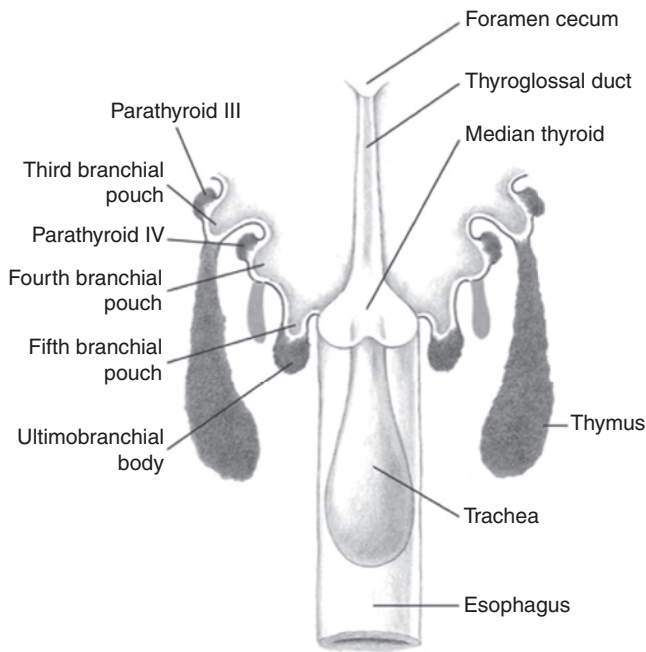


**Fig. 11.90** Parathyroid displacement during thymus descent  
Diagrammatic representation of routes of descent of thymus, parathyroid glands, and “ last branchial body “ during fetal life. Parathyroid glands originating more cranially in third branchial pouch migrate in close association with thymus to reach final position more caudally with respect to parathyroid glands originating in fourth branchial pouch. Final location of last branchial body is intimately embedded in thyroid gland, to constitute parafollicular C-cells producing calcitonin. Thyroid gland originates at “ blind foramen “ along midline and migrates down to first tracheal ring.

- Third pouch contains thymus and parathyroid 3.
  - Fourth pouch contains parathyroid 4.
  - Thymus moves past thyroid dragging PT3 with it, distal to PT4.
  - Thymus can occasionally get stuck in thyroid gland.
- [Reprinted from Scharpf J, Kyriazidis N, Karmani D, Randolph G. Anatomy and embryology of the parathyroid gland. *Op Tech Otolaryngol Head Neck Surg* 2016; 27(3): 117–121. With permission from Elsevier.]

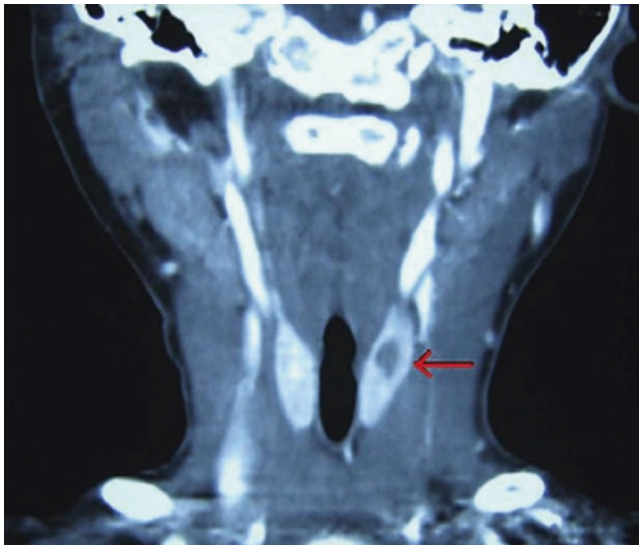


**Fig. 11.91** Thymic tissue in left lobe of thyroid. [Reprinted from Huang Y, Sheng S, Xio X. Ectopic intrathyroidal thymus in children: Two case reports and review of the literature. *J Ped Surg Case Reports* 2013; 1(11): 386–390. With permission from Creative Commons License 3.0: <https://creativecommons.org/licenses/by-nc-sa/3.0/>]

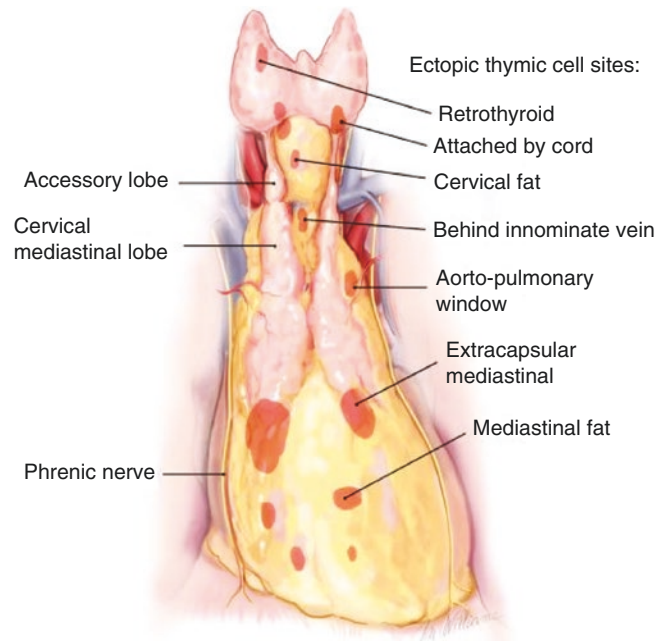


**Fig. 11.92** Mediastinal thymus. Thymic remnants can reach the pericardium. Note the physical position of descent does not permit intracardiac migration of the thymus. [Reprinted from Argote-Green LM, Jaklitsch MT, Surgarbaker DJ. Thoroscopic approach to thymectomy with advice on patients with myasthenia gravis. In: Sugarbaker DJ, Bueno R, Krasna MJ, Mentzer SJ, Zellos L (eds). *Adult Chest Surgery*. McGraw Hill; 2015: 1260–1265. With permission from McGraw-Hill Education]

## Evolution of Skin and Appendages

### Fishes

The epidermis of living fishes is not keratinized; it is alive with a pattern of microridges that retain mucous. This mucous cuticle provides lubrication for swimming, is a barrier layer for bacteria, and can include defensive chemicals. Three unicellular glands found in fish epidermis contribute to the mucous cuticle. Club cells can produce chemicals, that once diffused into the environment constitute alarm signals. Granular cells and goblet cells also contribute to the cuticle. The latter cell is phylogenetically more recent, as it is not found in lamprey skin.

Fish dermis is very elastic allowing for bending of the body during swimming and storing energy during unbending. It produces dermal bone which in turn gives rise to scales. Fish scales have structural characteristics similar to teeth: the outer layer is made of hard acellular enamel produced by the epidermis whilst the inner layer, produced by the dermis, is dentin.

Primitive fishes The ostracoderms and placoderms lived within an exoskeleton of dermal armor. In the cranial region, these dermal bones amalgamated into a head shield; those in the caudal regions remained distinct. Ostracoderm scales, *tubercles*, resemble teeth spread over dermal bone with a deep lamellar layer and a superficial reticular vascular layer, reminiscent of dental pulp chambers. In transitional forms, hagfish, and lamprey, dermal bone generation is lost. The skin becomes smooth without scales. Pigment cells make their appearance in the dermis. Finally, the hypodermis has adipose tissue (Fig. 11.93a).

Chondrichthyes Cartilaginous fishes, not surprisingly, do not make dermal bone. The dermis has large numbers of collagen and elastic fibers for swimming and it produces *placoid scales*, which project upward through the epidermis. Sharks use these scales to reduce drag while swimming (Fig. 11.93b).

Osteichthyes Bony fishes, ultimately ancestral to us, have two layers of dermis, the upper layer being loose and the lower layer being dense. Here dermal scales are produced; although they do not actually fully penetrate through the epidermis they make the skin hard (Fig. 11.94).

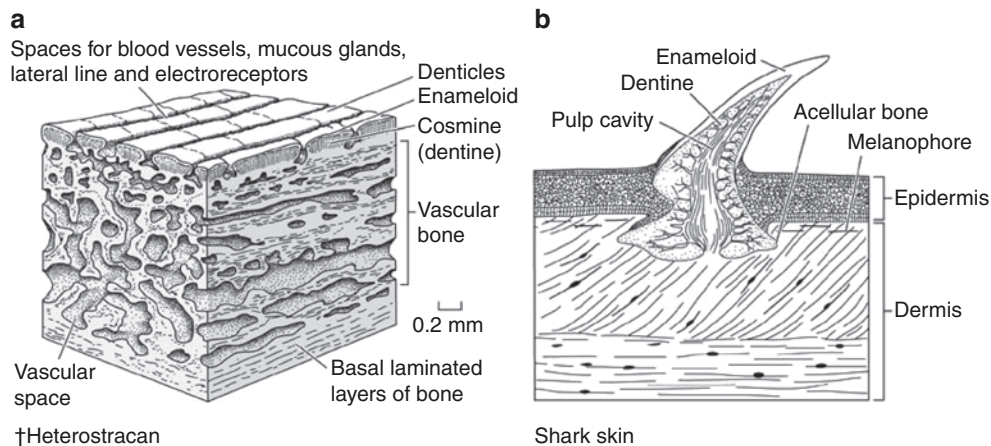
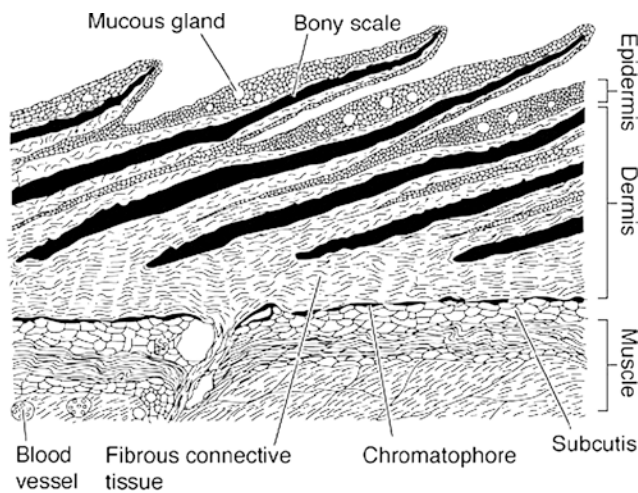


**Fig. 11.93** Evolution of fish skin 1. (a) Cosmoid plate of jawless fish (†heterostraca) showing cosmoid plate. Cosmine is a form of dentin with well-organized dental tubules. Enameloid (sic) is a hardened form of cosmine but is dermal in origin. (b) Chondrichthyan fish (shark) showing adaptation of dermal denticles become placoid scales

become spiny lacoid scales made of dentin covered by an unknown hard substance. [Reprinted from Kardong K. *Vertebrates: Comparative Anatomy, Function, Evolution*, seventh ed. New York, NY: McGraw-Hill; 2015. With permission from McGraw-Hill Education]



#### D. Teleost skin

**Fig. 11.94** Evolution of fish skin 2. (a) Early bony fish had rhomboidal adenticulate cosmoid scales. These are our ancestors. (b) Derived teleost fishes have imbricating cycloid scales with mucus glands and growth rings. [Reprinted from Kardong K. *Vertebrates: Comparative Anatomy, Function, Evolution*, seventh ed. New York, NY: McGraw-Hill; 2015. With permission from McGraw-Hill Education]

## Tetrapods

### Differences between Fish Skin and Tetrapod Skin

Rise of keratinization (present in fishes but to a minor degree).

Addition of lipids to the surface layer.

Increased complexity of epidermal layers.

Evolution of the pharyngeal arches: repositioning of the second arch

- Redistribution of second arch neural crest into the subcutaneous tissues.
- subcutaneous white fat (birds and mammals),
- sympathetic innervation,
- Dermal glands become multicellular and reach the surface via ducts.

Innervation of the dermis.

Subcutaneous adipose layer.

Evolution of the SMAS.

Skin appendages: feathers and hair.

## Amphibians

Amphibian skin represents a radical departure from the integument of fishes. It has a multi-layer corneum adapted to terrestrial life to prevent desiccation. Amphibians shed their

skins en masse under endocrine control from the pituitary and thyroid. Amphibians consist of three orders. *Anura* or frogs (Gk. *an* “without” + *oura* “tail”) have smooth skins. *Caudata*, the salamanders (Lt. +*cauda* “tail”), have skins with bumps. *Gymnophiona* (Gk *gymnos* “naked” + *ophis* “serpant”), known more commonly as caecilians, are limbless, wormlike creatures with skin bearing transverse folds and scales embedded in the furrows, a retention of the ancestral condition in which tetrapods had scales like the fishes from which they evolved (Fig. 11.95).

Amphibian skin is adapted to life underwater. It is delicate and permeable to water. Gas exchange can take place through the skin (**cutaneous respiration**). Allowing for long-term submergence, e.g. hibernation. Frogs and salamanders have two cutaneous glands, both located in the dermis and connected to the surface using ducts. **Mucous glands** keep the skin moist and prevent dehydration. **Poison (granular) glands** or parotoids are larger and store up their contents for release as needed; These foul-tasting products serve for protection.

Amphibian skin displays colors produced by three layers of pigment cells called **chromatophores** arranged in three layers in the dermis. Lipophores (yellow) are superficial, guanophores (blue-green) are intermediate and melanophores (brown-black) are deepest. Note that chromatophores are sometimes found in epidermis. Brightly-colored amphibians are often poisonous. Unlike fishes, whose skin color is under nervous system control and can change quickly amphibian skin color is under pituitary control and therefore changes slowly. Unlike bony fish, there is no direct control of the pigment cells by the nervous system, and this results in the color change taking place more slowly than happens in fish. Amphibians do not possess a subcutaneous adipose layer (Figs. 11.96 and 11.97).

## Reptiles

Reptile integument is similar to that of mammals in that it has two layers, epidermis and dermis, but is decidedly different, due to the presence of scales. Like amphibians, periodic shedding of the skin, ecdysis, or moulting serve to allow for growth and get rid of parasites.

The skin of reptiles demonstrates a greater commitment to life on land. The **epidermis** is characterized by a complete covering of keratin. The keratin is composed of many layers of very thin, flat cells. Cells closer to the surface become more compacted as they respond to pressure from beneath by new keratin cells being formed in the stratum germinativum. Reptilian skin has three keratin layers: (1) The *stratum corneum* is heavily keratinized and referred to as the *Oberhäutchen layer*; (2) The *intermediate zone* contains beta-keratin and is composed of stratum germinativum cells in differing stages of development; and (3) the deepest layer, *stratum germinativum*, consists of cuboidal cells containing alpha-keratin.

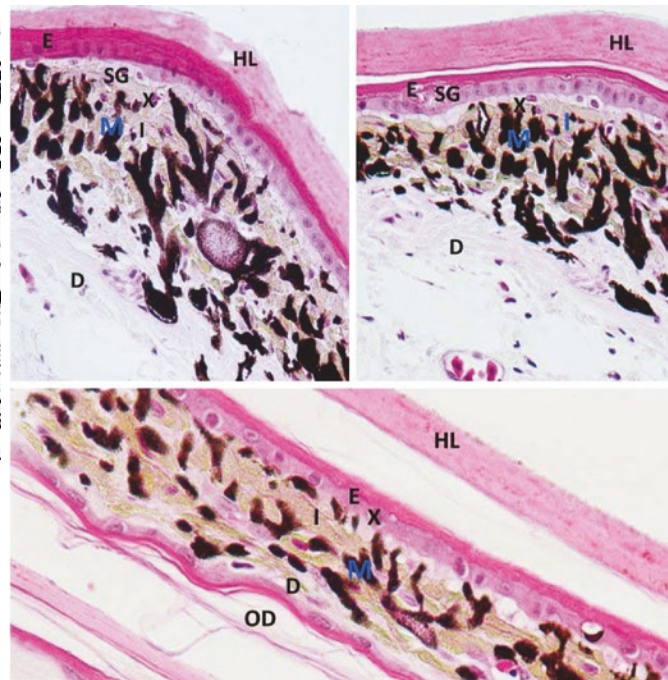
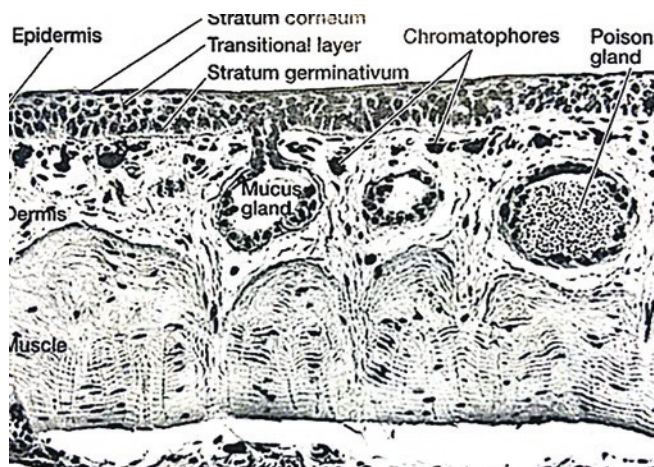


**Fig. 11.95** Histology of amphibian skin. Left: Mucous cell in dermis emptying on the epidermal surface. Right: These pigment cells were observed in vertical combination, with an uppermost layer of xanthophores, an intermediate layer of iridophores and a basal layer of melanophores. The ultrastructure of the melanophore is characterized by oval nucleus and numerous pigment granules, the melanosomes of different stages that remain scattered in the cytoplasm. The chromatophores of this species contain significant information of anatomical

similarity with lower as well as higher vertebrates. Left: [Reprinted from Kardong K. *Vertebrates: Comparative Anatomy, Function, Evolution*, seventh ed. New York, NY: McGraw-Hill; 2015. With permission from McGraw-Hill Education.]. Right: [Reprinted from Paray BA, Al-Sadoon MK. Ultrastructure of the dermal chromatophores in the Fringe-toed lizard, *Acanthodactylus orientalis* *Zoologia* 34: e11923 | DOI: 10.3897/zoologia.34.e11923. With permission from Creative Commons License 4.0: <https://creativecommons.org/licenses/by/4.0/>]



**Fig. 11.96** Reptilian skin is notable for several types of scales, a wide variety of colors and the phenomenon of shedding. [Reprinted from Freepik.com. image: [https://www.freepik.com/free-photo/closeup-shot-green-iguana\\_9991089.htm#page=1&query=reptile%20skin&position=10](https://www.freepik.com/free-photo/closeup-shot-green-iguana_9991089.htm#page=1&query=reptile%20skin&position=10). Nature photo created by wirestock—[www.freepik.com](http://www.freepik.com)]

The epidermis of reptiles lacks supporting elements from the dermis. Dermis in reptiles consists of connective tissue. In some, there may be small bones called *osteoderms*. These are what form the distinctive specialized scales on savannah

monitors and crocodylians. Glands are dermal and localized to areas such as the underside of the hindlimb. Their products serve for protection or reproduction. Reptiles do not possess a subcutaneous adipose layer. Of note: reptilian skin heals much more slowly than mammalian skin, often taking about 6 weeks for the defect to be fully restored.

## Birds

Recall once again the branch point just before dinosaurs at which the lines that would eventually produce birds and mammals diverged. This is the juncture at which several analogous innovations take place; although avian and mammalian skin differ, these commonalities are what count. Avian epidermis is thin and pliable. It has 4 well-defined layers: stratum basale, stratum intermedium, transitional layer, and the stratum corneum. In mammals, the two middle layers become stratum spinosum and stratum granulosum. The epidermis is lipogenic. The degree of keratinization is less than in mammal. This facilitates rapid cooling while still maintaining facultative waterproofing...i.e. the preening of feathers to distribute oil. This relatively “leaky” epidermis is because of the high metabolic rate, increased heat production



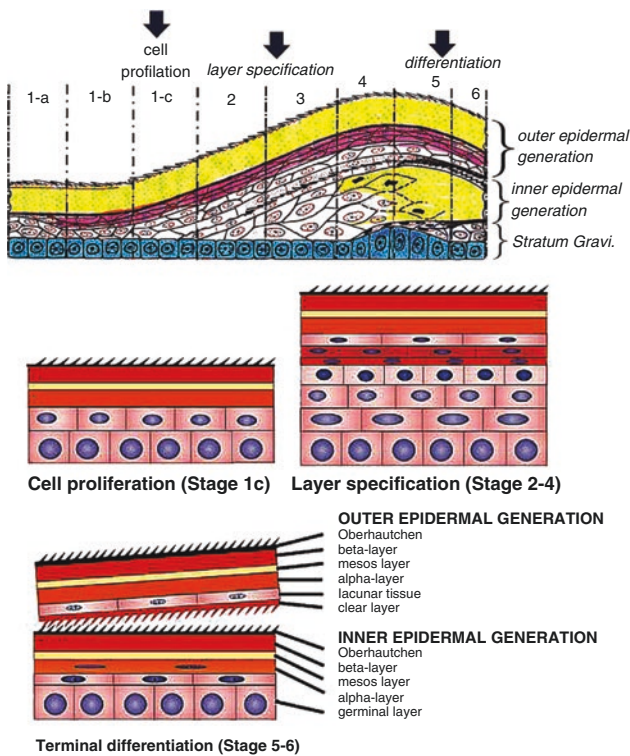


**Fig. 11.97** RIGHT: Shedding of reptilian skin involves a reduplication of the layers and a separation plane of lacunar tissue plus a clear layer. LEFT: Scales (resting phase) are shown in multiple layers with names labeled in panel B. (A) Non-overlapping tuberculate type scales. (B) Overlapping scales commonly seen in squamates. (C) Variations of microstructures from the *Oberhautchen* layer illustrating short spines in a, b and long setae in c (such as those in the adhesive pad lamellae in geckos, Fig. 4B). (D) Pits on the scales of anole, gecko and iguana (mainly epidermal sensory organs; Fig. 4E, F). (E) Tactile sensory organ on the hinge side of a scale in Agama. Some follicle-like structures have clustered dermal cells associated to their base; Fig. 4G). (F) Scales with ridges are seen on the back of skink or the neck of anole. (G) Frills, or very elongated scales, are seen on the back of iguana

during flight, and insulation by feathers. There are neither sweat glands nor sebaceous glands.

Birds have subdermal white fat. The overlying dermis layer is thicker than the epidermis and more complex than in amphibians or reptiles, having sensory nerves, blood vessels, and smooth muscle. The extension of neural control implies a proliferation of neural crest cells, required for sympathetic control. This is accompanied by the differentiation of neural crest-related pre-pericytes into smooth muscle cells. The crowning characteristic of bird skin is the presence of feathers with a highly vascularized dermal core and control via dermal muscle. Although birds do not have a SMAS layer for second arch controlled muscles, these findings indicate the dermal and subdermal anatomy of birds may be due to the subcutaneous spread of embryologic elements (from the second arch?) superficial to the underlying muscle layer (Fig. 11.98).

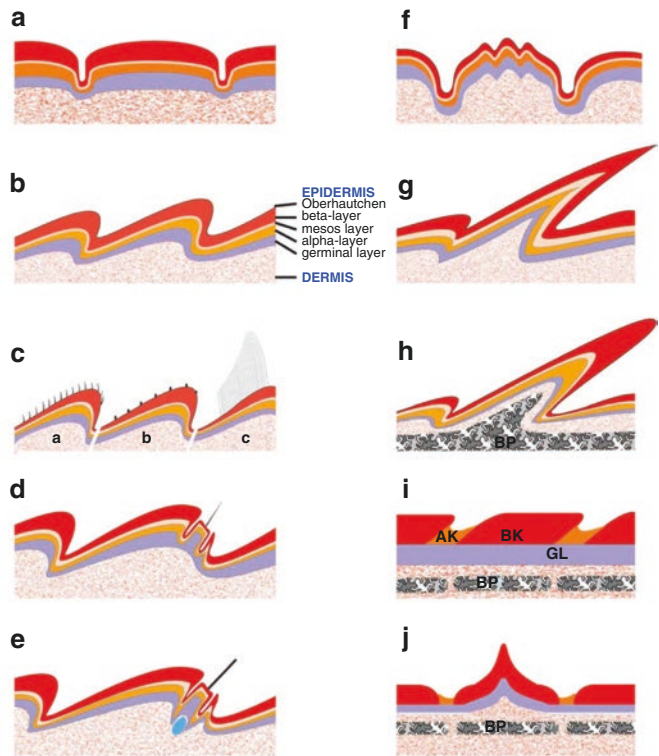


(Fig. 3B). (H) The horn on the head of chameleon contains a bony element core (osteoderm). (I) Scales on the limb of crocodilians show only minor overlapping. (J) Keeled scales with a central, elevated corneous ridge are seen on the dorsal body of crocodilians and some armored agamid lizards (e.g. Australian spiny desert lizard or molok). Legends: a, fine 'hair' on scales of anoles; b, Micro-ornamentation on scales of snakes; c, Toe pad of anole or gecko;\*, dermal cells clustered at the base of sensory organs in Agama; AK, beta-keratin; BK, beta-keratin; BP, bone element. [Reprinted from Chang C Wu P, Baker R E. Reptile scale paradigm: Evo-devo, pattern formation and regeneration. *Int J Devel Biol* 2009; 53(5-6): 813-826. With permission from The International Journal of Developmental Biology]

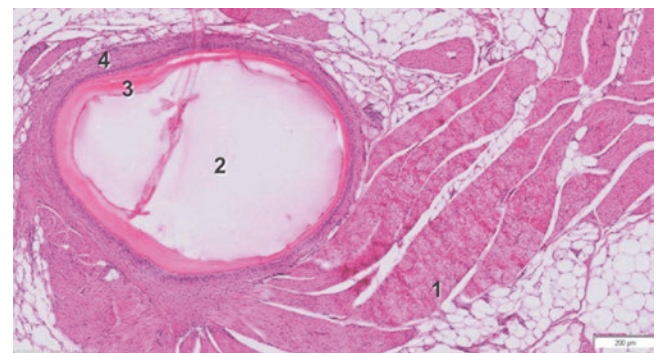


**Fig. 11.98** Feathers are produced in feather follicles. The hollow basal part of the feather shaft that is implanted within the follicle is called the calamus. 1. Musculus pennarum 2. air space 3. Calamus wall 4. feather follicle wall. [Reprinted from Histology of Birds. Retrieved from <http://www.histology-of-birds.com/galleries.php?id=32&v=>. with permission from Ghent University]

## Mammals (Figs. 11.99, 11.100 and 11.101)

Integument of mammals the multiple innovations that appear to recapitulate what happened in the avian line with greater overall complexity. Mammalian epidermis has five distinct layers with new cell types including Langerhans cells for antigen processing and neural crest-derived Merkel



**Fig. 11.99** Cutis anserina, “goosebumps”. Pilomotor response indicates diffuse location of *epidermal placodes*. [Reprinted from Wikimedia. Retrieved from [https://commons.wikimedia.org/wiki/File:2003-09-17\\_Goose\\_bumps.jpg](https://commons.wikimedia.org/wiki/File:2003-09-17_Goose_bumps.jpg). With permission from Creative Commons License 3.0: <https://creativecommons.org/licenses/by-sa/3.0/deed.en>]

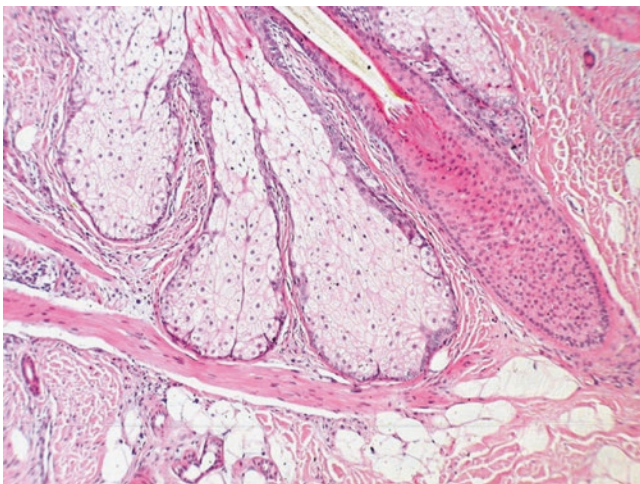


**Fig. 11.100** arrector pili. Arrector pili muscle can be seen coming in from the left and inserting into the hair shaft. Its relationship to the pilosebaceous unit explains how contraction of the muscle can cause sebum to be expressed. Arrector pili is under SANS control. [Reprinted from Wikimedia. Retrieved from: [https://commons.wikimedia.org/wiki/File:Base\\_of\\_Pilosebaceous\\_Unit\\_10x.JPG](https://commons.wikimedia.org/wiki/File:Base_of_Pilosebaceous_Unit_10x.JPG)]



**Fig. 11.101** Chimpanzees display with arrector pili. [de Waal, Frans. Chimpanzee Politics: Power and Sex among Apes. pp. 130. © 2007 Frans de Waal. Reprinted with permission of Johns Hopkins University Press]

cells that function as mechanoreceptors. Chromatophores also arise from neural crest and populate the deeper strata of the epidermis producing pigment that is passed directly up to the surface or into the hair shafts. Dermis in mammals has two distinct layers: the papillary dermis which projects into the overlying epidermis and the reticular dermis. Blood vessels within the mammalian dermis form a subepidermal rete but do not extend into the epidermis itself. Mammals have a trilecta of glands for temperature control, waterproofing, lubrication, and lactation. Finally, dermal bone formation is retained in mammals and is used to synthesize the membranous bones of the skull, the scapula, and part of the clavicle.

The evolution of hair is a defining characteristic of mammals. The actual impetus for this innovation is unknown. One hypothesis for hair is for temperature control via insulation, as the presence of turbinates in synapsids during the late Permian is considered as evidence for endothermy. Another model considers whether small “protohairs” emerged between scales as tactile sensory devices. Therapsids, as direct precursors to the mammalian line, show evidence of pitting in the facial zones of the skull potentially associated with vibrissae.

### Innovations in Skin Evolution: Strategies for Replacing the Epidermis

Among amniotes, the epidermis interacts with the harsh terrestrial environment, which can produce much wear and tear. A single-layered epithelium cannot accommodate this treatment. How to maintain an intact integument via epidermal homeostasis of stem cells, transient amplifying cells, and differentiated cells was an evolutionary challenge. The solution

was a multi-layered stratified epithelium. But this layer would inevitably have to be replaced. To this end, early reptiles have developed two different strategies.

- Episodic shedding as seen in snakes and lizards (also seen in crustaceans, among invertebrates).
- Continuous renewal as seen in mammalian epidermis. This model has also been adopted by most chelonians and crocodylians.

Episodic shedding: How to replace the epidermis.

Snakes and lizards achieve epidermal replacement using an episodic strategy. This allows the formation of multiple different layers which offer different and more complete protection. Thus, the basal layer gives rise to different supra-basal layers at different times. The cost is that at a particular point, the old epidermis has to be shed, leaving the animals vulnerable. In snakes, this usually occurs simultaneously across the whole body, so the molted skin can be in one sheet. In lizards, this can occur in patches.

In the perfect resting phase, the reptilian epidermis is typically composed of four layers of keratinocytes, which have fully differentiated. Cells are dead but the mechanically strong keratin scaffolds remain. In order, from outside in, these layers are known as the *Oberhäutchen* layer,  $\beta$ -layer, mesos layer, and  $\alpha$ -layer. At the base is one layer of live cells, that is, the basal layer or (germinal layer). In the lizard epidermis, these different layers are generated and specified in the temporal order. A keratinocyte will become one layer or the other. This contrasts with the mammalian epidermis where a keratinocyte must go through successive stages before being sloughed.

Birds and mammals also use this episodic strategy to generate complex cell types in feathers and hairs in cycles. Since stem cells and actively proliferating cells reside in the follicle, which is open to the external surface only via a small orifice, this does not lead to the problem of vulnerability during shedding. In the inter-follicular epidermis, the continuous replacement strategy is still used. Thus, by combining continuous and episodic strategies and by positioning each appendage with proper spacing, the integument is well protected. Furthermore, different skin regions can display appendages with different characteristics, lengths, and colors, depending on need.

## Continuous Renewal

In mammals, the basal epidermal layer generates cells that make up the spinous, granular, and corneal layers. These different layers represent different stages of keratinocyte life, and a single keratinocyte develops through all these stages in.

In mammals, the basal epidermal layer generates cells that make up the spinous, granular, and corneal layers. These different layers represent different stages of keratinocyte life, and a single keratinocyte develops through all these stages in succession. The basal layer, therefore, generates new cells, which then differentiate and become supra-basal cells (basal layer  $\rightarrow$  different supra-basal layers sequentially). As cells become more differentiated, they are displaced more externally to serve as the first line of defense. Eventually, they are worn and sloughed off. This same strategy is seen in alligator scales.

## The Invention of Hair

The tongue is considered as one of the integuments. By comparing the topology and keratin types of scales and hairs with those of filiform papillary taste buds, gradual changes in the expression of keratins in the inner surface of the scale epidermis might have led to a transformation of the scale structure from a hemicylindrical form to the more completely cylindrical structure found in hairs. This progression could have been the origin of hair follicle invagination.

Another view focuses on the dermal side [25]. The variation in areas of dermal-epidermal interactions in the skin during evolution in different amniotes has been hypothesized to have led to the origins of scales, hairs, and feathers. According to this hypothesis, based on extensive comparative observations in reptiles, birds, and mammals, reptilian scales show extended papillae beneath the outer scale surface where the hard,  $\beta$ -keratin layer is formed. Therefore, no dermal condensation is generally seen during scale morphogenesis in reptiles. Based on the supposed derivation of feathers from scales, it is hypothesized that the progressive reduction of the outer surface of reptilian scales has restricted the morphogenetically active dermis previously associated with these areas, into smaller “niches”, forming cell condensations. These have become dermal papillae. Hairs are hypothesized to have evolved when morphogenetically active mesenchyme invaginated near hinge regions of scales of reptilian ancestors (synapsids), a development that led to the formation of the dermal papilla.

---

## Mammalian Skin Appendages: Hair Development Provides Evidence for the Embryonic Ectomesenchymal Precursor Cells in the Evolution of Mammalian Skin

Consider the phenomenon of “gooseflesh,” the sudden elevation of body hair and scalp in response to sudden stress. The erection of the hair shafts is accompanied by a myriad of small

swellings, one beneath each shaft (Fig. 11.99). This condition reveals the action of small fibers of smooth muscle, the *arrector piliae*, which span from the hair bulb to the undersurface of the overlying dermis. The muscle fibers are under SANS control (Fig. 11.100). They differentiate from ectomesenchymal precursor cells that will give rise to pericytes and white fat. Recall from our previous discussion that these cells arise from the same region of the neural fold as the neural crest. It is likely that the two cell types are cousins, sharing common surface markers but having different developmental fates. Hair erection is used to great effect by animals, such as chimpanzees, to display aggression (Fig. 11.101).

Piloerection reveals the presence of another structure: each hair shaft emerges from an individual epidermal prominence; these “bumps” arise fossils of the ancient ectodermal placodes that are to the hair. The superficial fascia in some mammals is associated with a striated muscle layer, the pan-

niculus carnosus. In humans, this is considered homologous to platysma and the dartos muscle of the scrotum. The muscle-bearing nature of SIF is limited to SMAS (Fig. 11.102). In horses, this layer is useful for shaking off those pesky flies.

Placodes are actually fundamental for hair formation. These non-neural ectodermal cells are distributed throughout the hair-bearing epidermis. In the development of craniofacial skin and sensory organs, craniofacial placodes occupy specific locations along the neural fold and constitute populations distinct from those of neural crest (Fig. 11.103). But what can be said about the existence of placodes in skin? One model can postulate that non-neural ectoderm has two distinct populations which are admixed: garden-variety epidermal cells and placodal cells. A second model is one in which the epidermis contains a single type of non-neural ectodermal cell. Signals from mesenchymal cells in the evel-

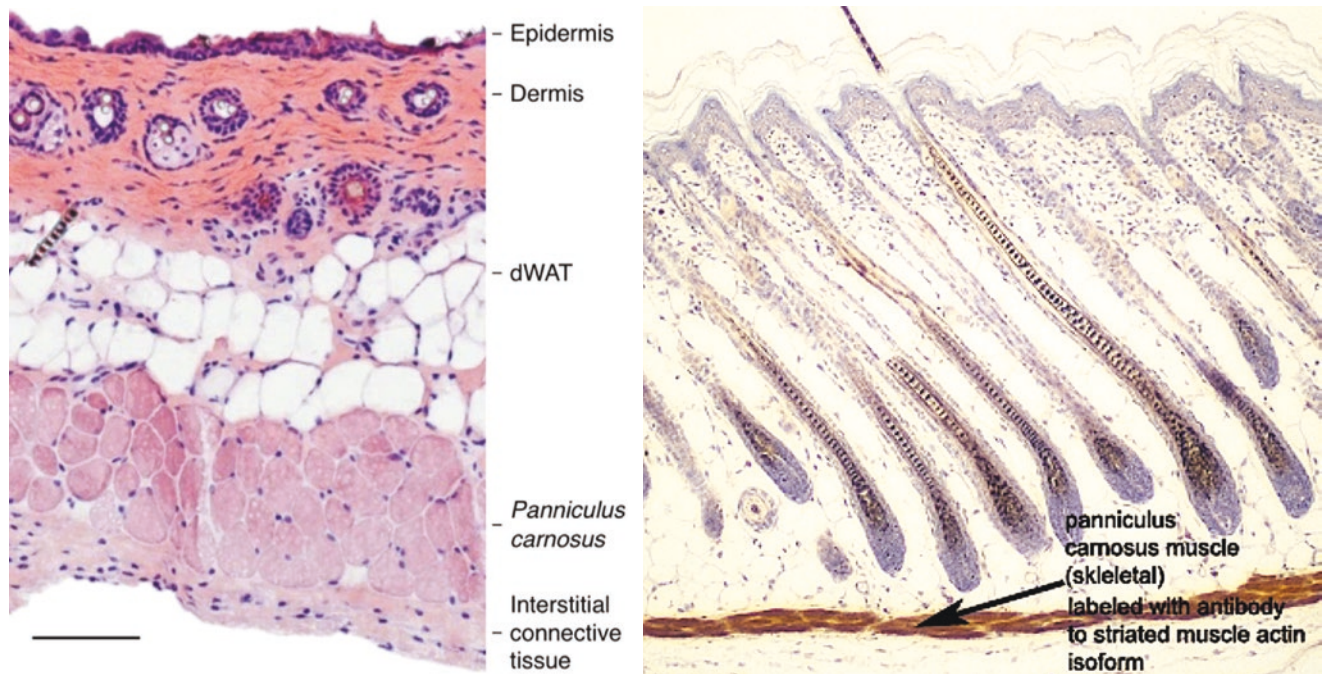


**Fig. 11.102** Panniculus carnosus. Immunohistochemical labeling of newborn mouse skin for the striated muscle actin isoform only labels the panniculus carnosus muscle (PC) below the fat layer. PC is the likely precursor of superficial fascia in humans. It is not the source of arrector pili muscles. Left: [Reprinted from Izeta A, McCullagh KJA, López de Munain A, et al. The panniculus carnosus muscle: an evolu-

tionary enigma at the intersection of distinct research fields. *J Anat* 2018; 233: 275–288. With permission from John Wiley & Sons.] Right: [Reprinted from Pathbase: [http://eulep.pdn.cam.ac.uk/~skinbase/Hair\\_cycle/PANNICULUS\\_CARNOSUS\\_ANNOTAT.jpg](http://eulep.pdn.cam.ac.uk/~skinbase/Hair_cycle/PANNICULUS_CARNOSUS_ANNOTAT.jpg) with permission from Creative Commons License 3.0: <https://creativecommons.org/licenses/by-nc-sa/3.0/>]

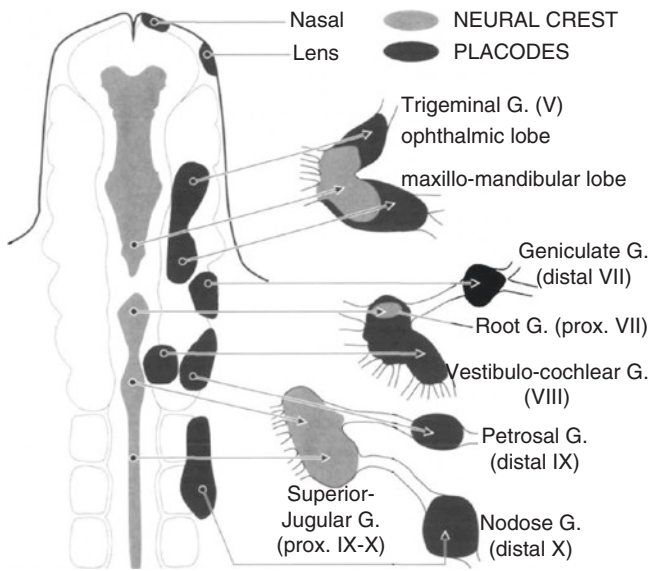


**Fig. 11.103** Sensory ganglia develop from neural crest and placodes. Note that ectoderm within which placodes develop is *lateral* to that of the neural crest. V1 neurons arise from the ancient profundus placode which is in register with r1. In fishes, ancient tetrapods, amphibians and some reptiles, profundus is spatially distinct. It is exclusively sensory; but its function varies phylogenetically. In snakes V1 provides infrared thermoreception for locating prey by body temperature. In mammals the profundus placode merges with the trigeminal placode as the ophthalmic lobe of trigeminal ganglion. Thus, V1 skin is embryologically distinct from all other facial skin. It is devoid of facial hair. Boundary zones between V1 skin and neighboring territories such as V2 skin and V1 nasal mucosa are demarcated by hair-bearing structures, such as eyebrows and nasal hairs. [Reprinted from D'amico-Martel A, Noden D. Contributions of placodal and neural crest to avian cranial peripheral ganglia. *Am J Anat* 1983; 166(4): 445–468. With permission from John Wiley & Sons]

oping dermis seem more plausible. These cells are randomly distributed in the subepidermal plane and they produce induction signals that convert non-neural ectodermal cells from an epidermal to a placodal fate. These chemical signals from a multitude of mesenchymal sources compete with one another creating an evenly spaced pattern of placodes. This model seems well-supported by the sequence of events by which hair develops which takes place in four steps (Fig. 11.104).

- **Specification** Ectomesenchymal cells in the subepidermal tissues differentiate into fibroblasts.
- **First dermal induction** Subepidermal fibroblasts produce Wnt-11 and fibroblast growth factor (FGF); these, along with local BMPs induce a localized thickening of the epidermis, the placode. The location of these placodes may reflect the physical location of the ectomesenchymal-inducing cells or is simply a reflection of competing chemical concentration gradients.
- **Epidermal induction** Signals produced by the placode, such as Shh, cause subplacodal dermal cells to clump together into a dermal papilla.
- **Second dermal induction** Signals directed upward induce a downward proliferation of epidermal placodal cells into the papilla itself.

It should be noted that this process is not unique to hair formation. Non-neurogenic placodes are also involved in the formation of teeth, mammary glands, the lens, and feathers. Local matrix metalloproteinases produced in the dermis determine the ultimate fate of the

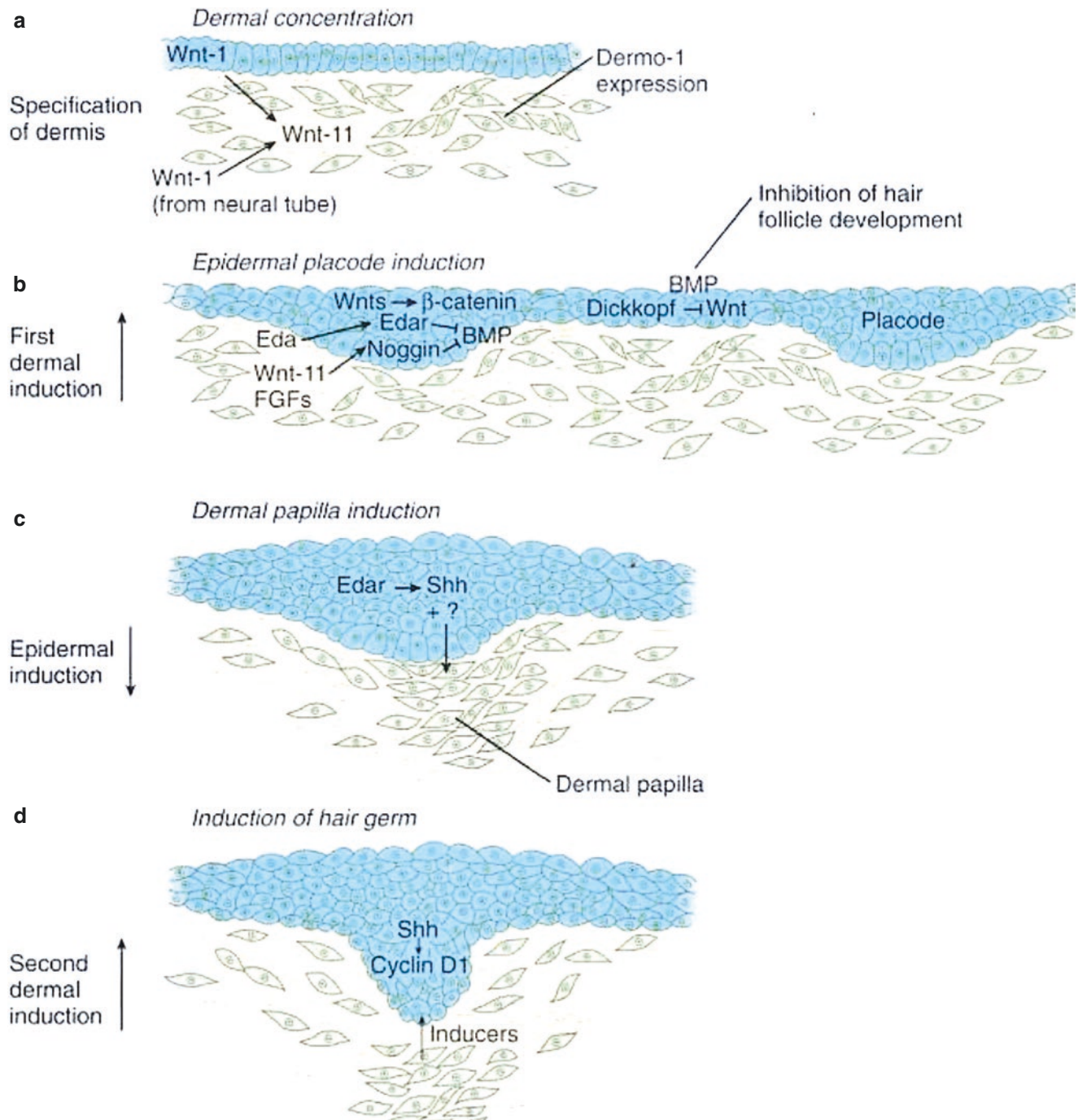


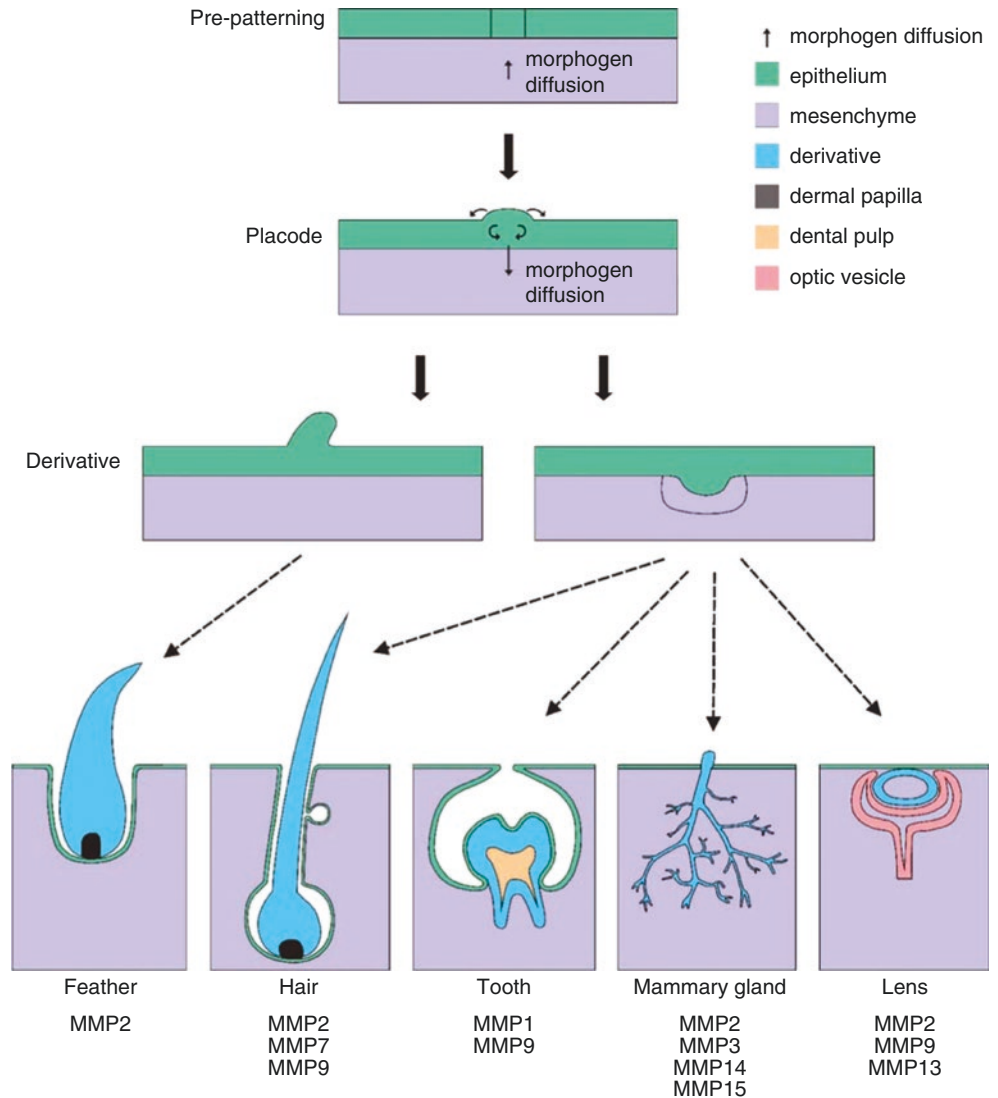
**Fig. 11.104** Formation of hair follicle. Epidermal placodes the ectodermal source of hair shafts. The process involves 4 steps: (1) specification of subcutaneous tissue into dermis by Wnt1 inducing Wnt11; (2) primary dermal induction of placodes by dermal MSCs; (3) epidermal response via Shh to induce a papillary condensation in the dermis; and (4) production by the dermal papilla of factors inducing epidermal down-growth in the papilla in a “bell and cap” configuration. Key:

BMP, bone morphogenetic protein, FGF, fibroblast growth factor; Wnt, *Wingless* genes; Eda, *ectodysplasin*; Edar, *ectodysplasin* receptor Cyclin D, controls cell cycle—initiated at G1 and drives the G1/S transition. [Reprinted from Carlson BM. *Human Embryology and Developmental Biology*, sixth edition. St. Louis, MO: Elsevier; 2019. With permission from Elsevier]

placodal structure. It should be noted that mesenchymal stromal cells derived from pericytes, including adipose-derived stromal vascular fraction cells produce a variety of MMPs (Fig. 11.105). In the case of hair development.

Interaction between the hair sheath with local MSCs results in the formation of an individual arrector muscle which extends upward to find an attachment site in the dermis (Fig. 11.106).

**Fig. 11.105** Placode-derived structures begin development with pre-patterning of the epithelium, which involves morphogen diffusion from the mesenchyme to the epithelium. Next, a thickening of the epithelium forms a placode structure. Following the formation of a placode, morphogen signaling from the epithelium down to the mesenchyme leads to the formation of a derivative structure. Some MMPs are involved in some of these processes. [Reprinted from Drake PM, Franz-Odenaal TA. A potential role for MMPs during the formation of non-neurogenic placodes. *J Developmental Biol* 2018; 6: 20–33. With permission from Creative Commons License 4.0: <https://creativecommons.org/licenses/by/4.0/>]



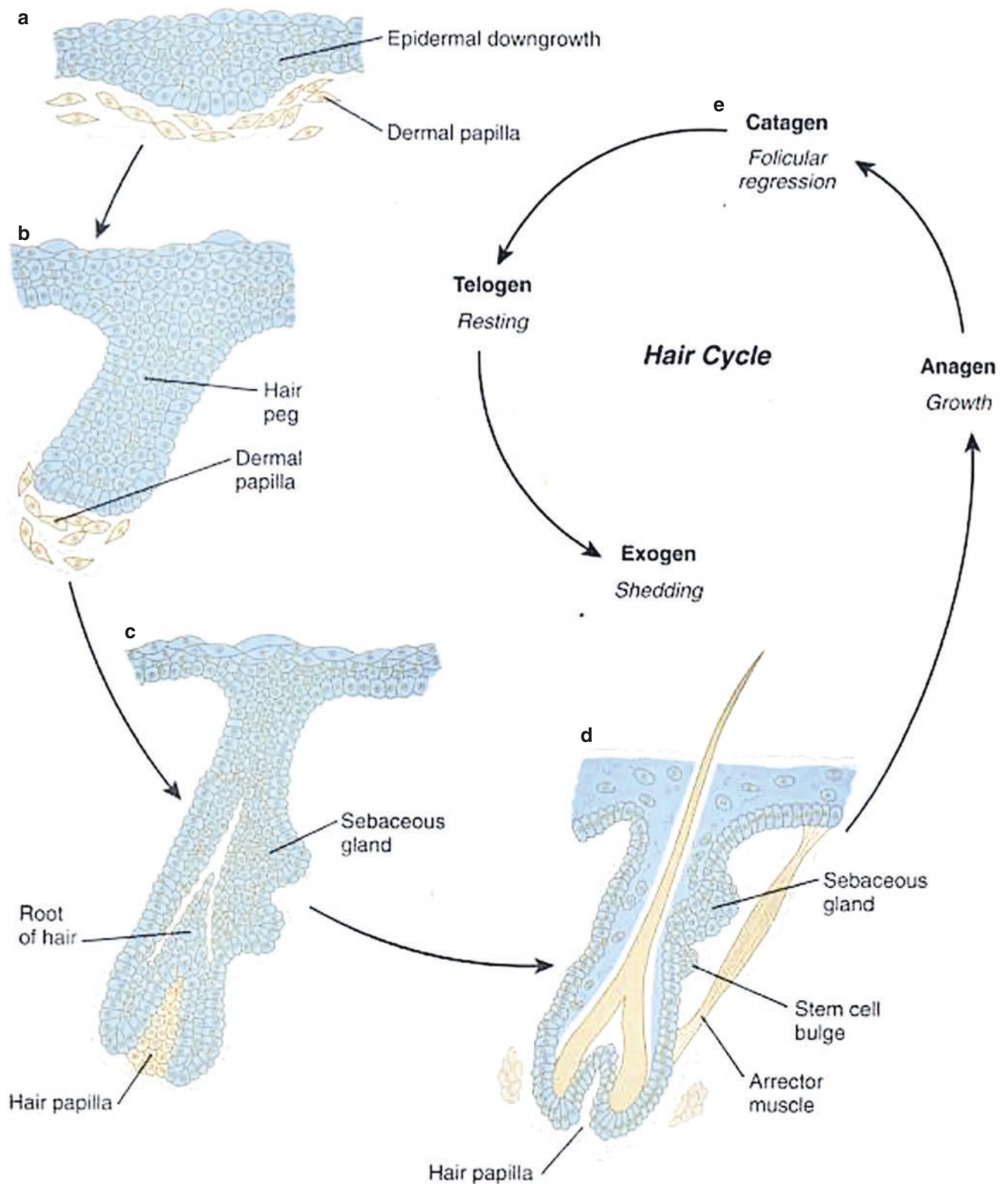


**Fig. 11.106** Hair follicle differentiation. (a) 12 weeks; (b) hair primordium; (c) 16 weeks, hair peg; (d) 18 weeks, bulbous follicle; maturity; (e) hair cycle: anagen, catagen, telogen, exogen. Matrix metalloproteinases produced by dermal MSCs derived from prepericytes help induce the final hair structure. The smooth muscle arrec-

tor pili are of MSCs differentiation. Hair development is inseparable from the surrounding adipose tissue. [Reprinted from Carlson BM. Human Embryology and Developmental Biology, sixth edition. St. Louis, MO: Elsevier; 2019. With permission from Elsevier]



## Coda: Evolutionary Aspects of Skin Appendages

Different appendages likely evolved from a primitive type of patterned skin. Odontodes (Od) are derived from both epidermis (E) and dermis (D) and are found in living chondrichthyans. Teleost scales (DSC) are mostly dermally derived and are commonly likely related to odontodes. Epidermal scales (ESCs), protofeathers (pF), feathers (F), and hairs

(HFG) are proposed to be epidermally derived from a *common placodal stage*. The integument of sauropsids differs from that of synapsids by the presence of  $\beta$ -proteins and by the distribution of glands. Sebaceous glands are a critical element of the hair follicle: their proteolytic enzymes allow for the hair shaft to erupt. Differences between plantar and body integument are controlled by an ancient interaction between Shh and BMPs dating back to the emergence onto land (Figs. 11.107, 11.108, 11.109 and 11.110).

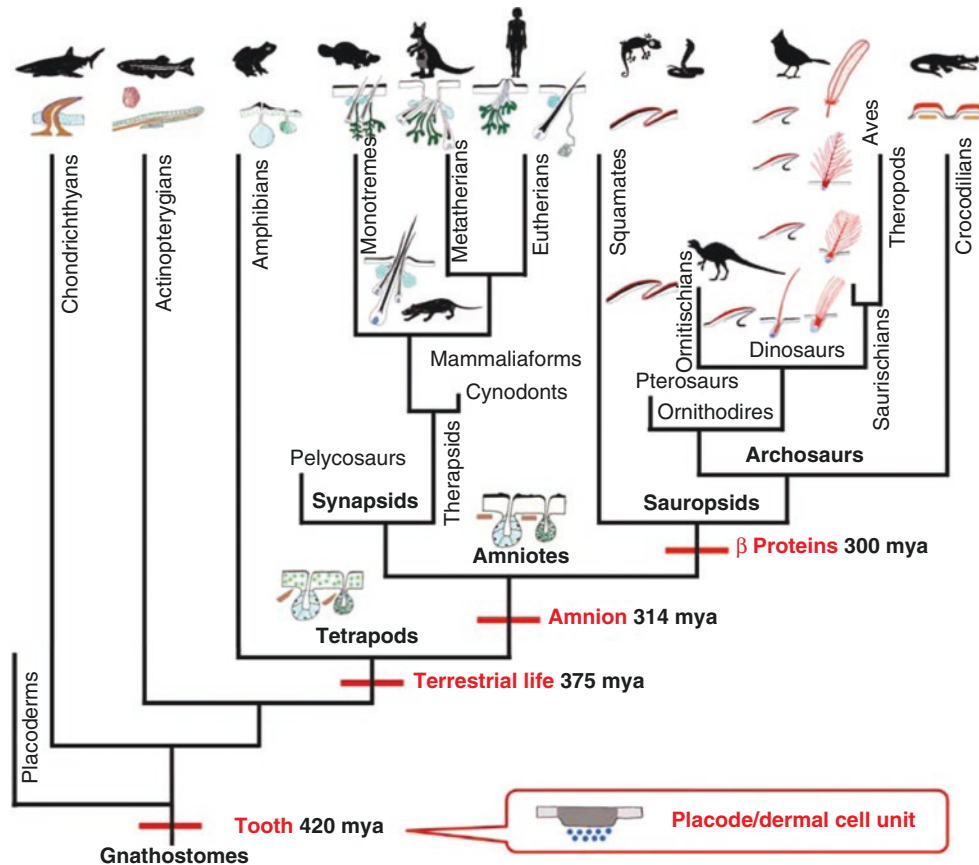


**Fig. 11.107** Phylogeny of skin. Cladogram of the major groups of vertebrates. The unit composed of a placode and its associated dermal cells is ancestral and has been conserved during evolution. It represents the initial step for every type of cutaneous appendage in living vertebrates. Note that fossilized hair, primitive feathers, and epidermal scales were found dating back to the Mesozoic era (252–66 mya). A number of clades have been omitted for simplicity, and the timescale is not accu-

rate. Red bars indicate evolutionary novelty. Note that beta-proteins (formerly beta-keratins) are an evolutionary novelty of sauropsids, while alpha-keratins appeared with the first vertebrates. [Reprinted from Dhouailly D, Godefroit P, Martin T, et al. Getting to the root of scales, feathers and hair: As deep as odontodes? *Exp Derm* 2017; 28(4): 503–508. With permission from John Wiley & Sons]

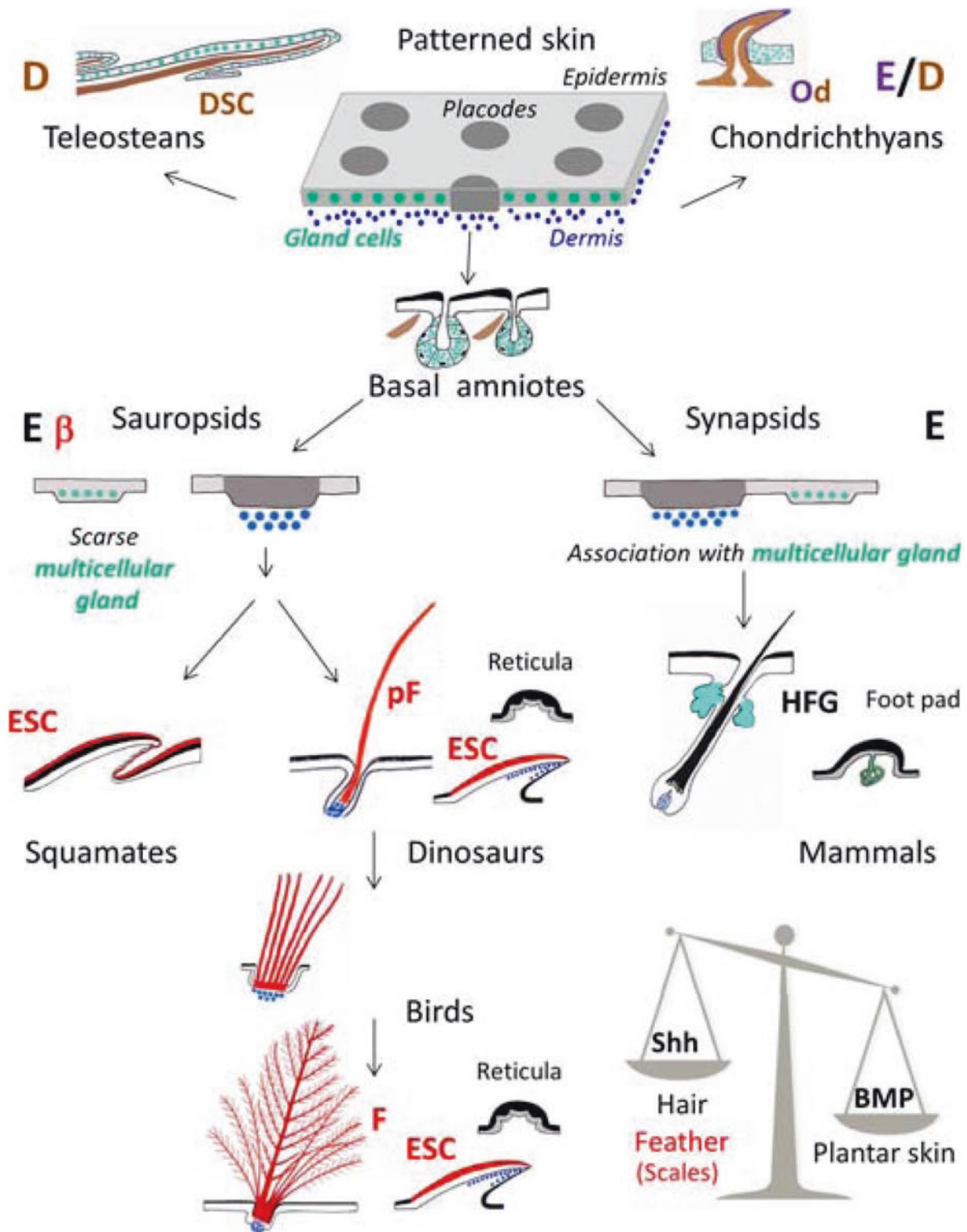


**Fig. 11.108** Evolutionary relationships between vertebrate integument appendages. The different appendages might have evolved from a primitive patterned skin. Odontodes (Od) are derived from both epidermis (E) and dermis (D). This type of appendage is still present in living chondrichthyans. Teleost scales (DSC) are mostly dermally derived and are commonly believed to be related to odontodes. Epidermal scales (ESCs), protofeathers (pF), feathers (F), and hairs (HFG) are proposed to be epidermally derived from a common placodal stage. The integument of sauropsids differs from that of synapsids by the presence of

$\beta$ -proteins (red) and by the distribution of glands (green). Sebaceous glands are an integral part of hair follicle as their proteolytic enzymes are required for the hair shaft to emerge (see text and supporting information Data S9). A balance between Shh and BMP signaling, probably established at the onset of terrestrial life, controls the difference between plantar and body integument. [Reprinted from Dhouailly D, Godefroit P, Martin T, et al. Getting to the root of scales, feathers and hair: As deep as odontodes? *Exp Derm* 2017; 28(4): 503–508. With permission from John Wiley & Sons]

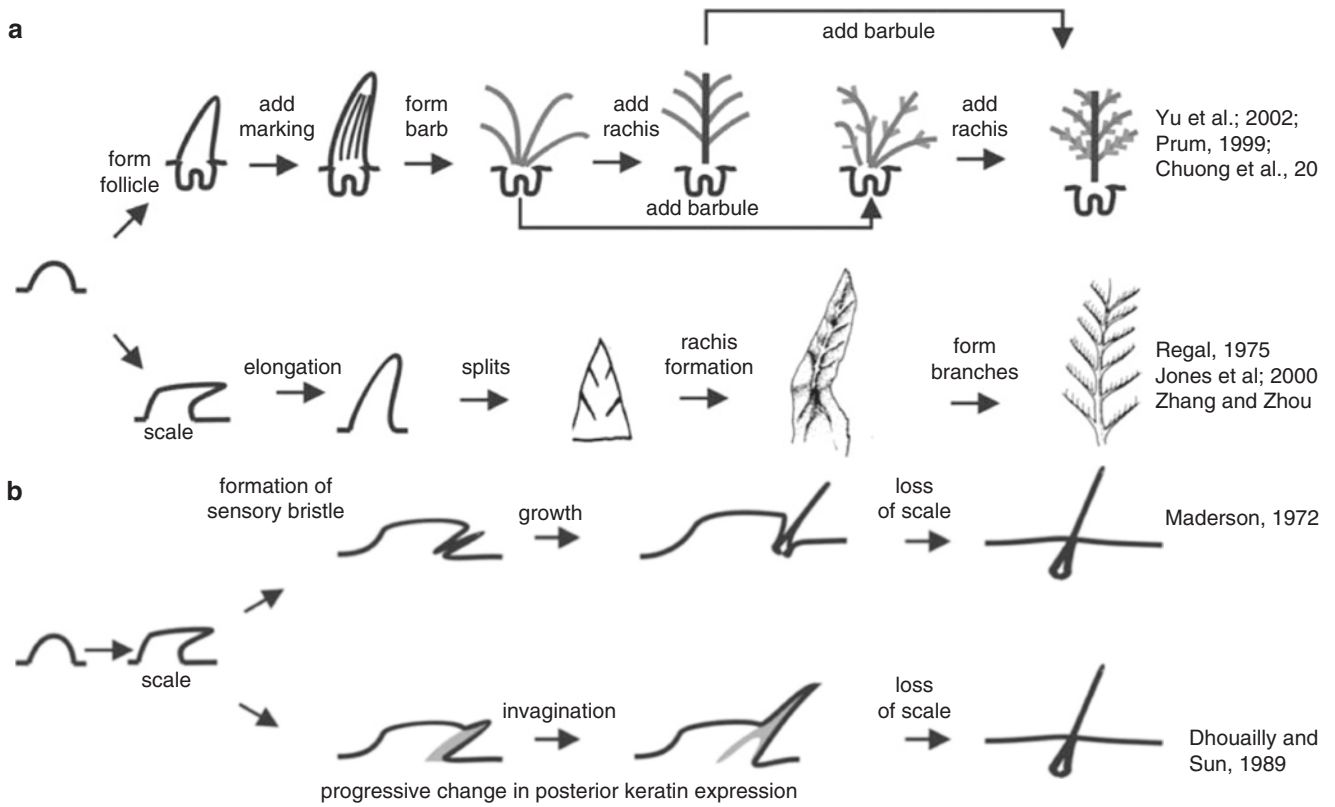
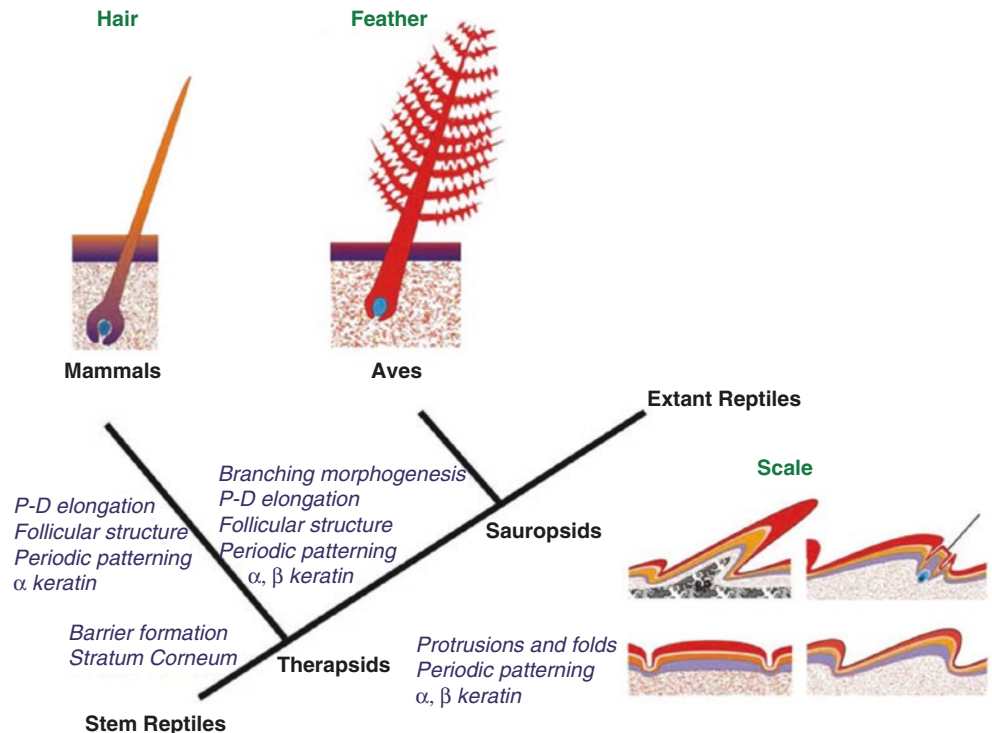


**Fig. 11.109** Possible models for feather and hair evolution. (a) Evolution of feathers. Experiments show that the barb—rachis model is correct. (b) Possible models for the evolution of hairs. [Reproduced

with the permission of UPV/EHU Press from Wu P, Hou L, Plikus M, et al. *Evo-Devo of amniote integuments and appendages*. *Int. J. Dev. Biol* 2004;48:249–270]

**Fig. 11.110** Potential relationship among amniote skin appendages and key evolutionary novel events. The reptilian integument shows some basal characteristics in comparison to mammalian and avian integuments. Mammals evolved about 225 million years ago from Therapsid-type reptiles, while birds evolved about 175 million years ago from archosaurian Sauropsids-type reptiles. Key events that led to evolutionary novelty are shown in blue italic characters. [Reproduced with the permission of UPV/EHU Press from Chang C, Wu P, Baker RE, Maini PK, Alibardi L, Chuong C-M. *Reptile scale paradigm: Evo-devel, pattern formation, and regeneration*. In *J Devel Biol* 2009; 53(5–6): 813–826]



## Speculation: Hair Distribution and Baldness

From time immemorial hair loss in males has been recognized to follow fixed anatomic patterns, as can be seen by models such as the modified Norwood scale, (Fig. 11.111) Note the following types: (1) isolated V2 expanding in the anterior temple, (2), isolated V1 extending posteriorly, (3) isolated V3, (4) V1-V3 extending back to C2-C3 territory. It is productive to view these from the standpoint of neural crest distribution patterns according to scalp innervation (Fig. 11.112). The ectomesenchymal cells responsible for placode induction are themselves likely to follow the same pattern as neural crest cells. Furthermore, as the follicles are maintained by interactions with the dermal environment changes in trophic signals in localized populations can explain patterns of hair loss.

The sensory neuroanatomy of the scalp faithfully reflects developmental distinctions between hypaxial and epaxial mesenchyme. The ear is a good case in point as it demonstrates these boundaries quite clearly (Figs. 11.12, 11.56). Posterior pinna is mainly hypaxial but its upper 1/3 contains cartilage #4 of the second arch.

A useful way to think about scalp is to visualize the person in the prone position. We note the breaking point of the retroauricular hairline beginning with epaxial C3 lesser occipital nerve. The anterior temple is V2 with a ventral part being hairless and the dorsal section hair-bearing. These observations do not fit with definitions of the first arch as its derivatives are considered strictly hypaxial. But V2 and V3 in the scalp are clearly supplying non-arch r2-r3 struc-

tures. Furthermore, V1 bears no relationship to first arch. Once again, we are reminded that facial and scalp skin develops from elements that do not participate in pharyngeal arch development. The more superficial contents of the

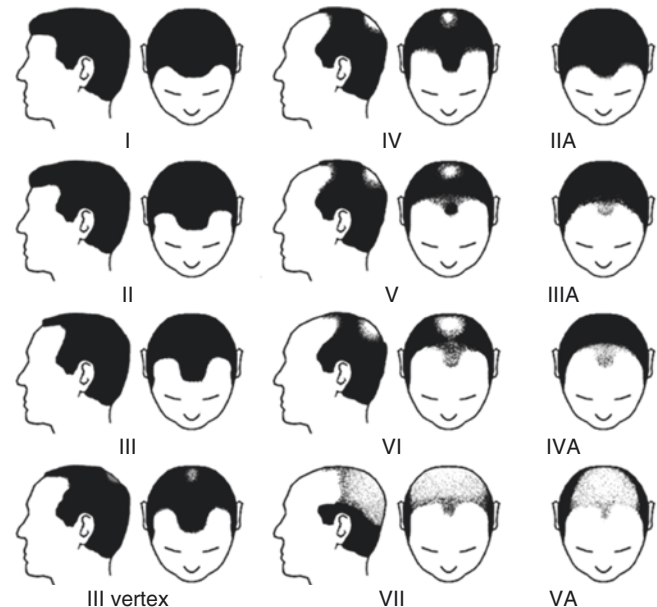
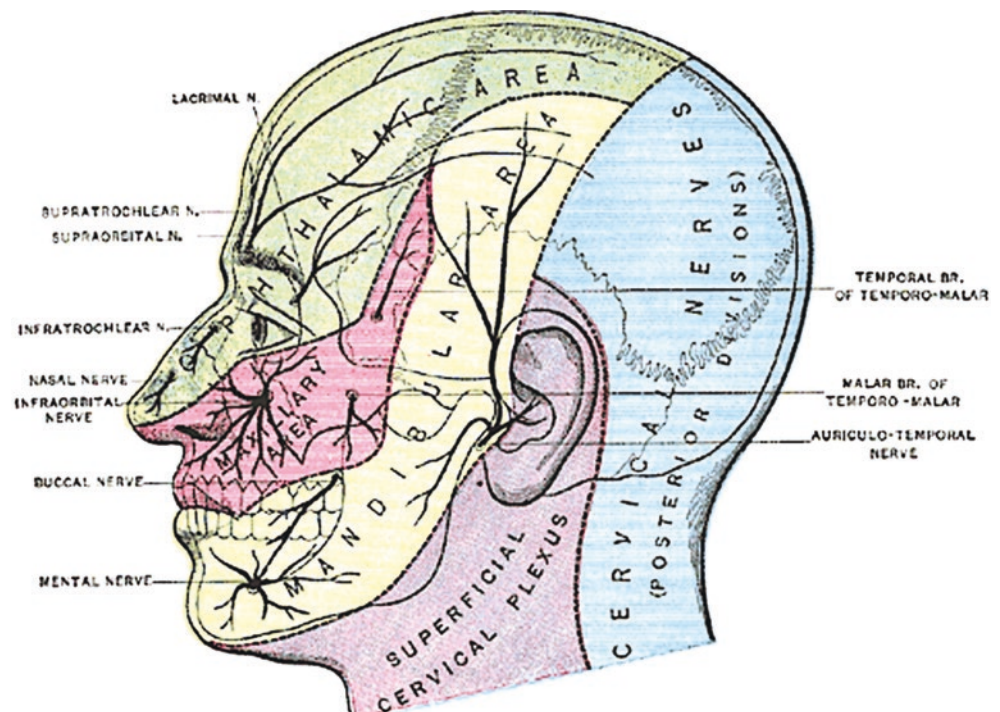


**Fig. 11.111** Male pattern baldness. All 4 patterns shown here represent degrees of failure of r2 and/or r3 neural crest cells to advance to the apex of the scalp. Skin with r1 neural crest alone cannot manufacture hair. This property may pertain to c2-c3 skin as well. [Reprinted from Koo S-H, Chung H-S, Yoo E-S, Park S-H. A new classification of male pattern baldness and a clinical study of the anterior hairline. *Aesth Plast Surg* 2000; 24(10): 46-51. With permission from Springer Nature]

**Fig. 11.112** Innervation of facial skin and scalp. The presence or absence of hair, the defining characteristic of forehead skin versus scalp may have to do with intermingling of r1 neural crest precursors in the V1 zone with those from r2 and r3. This may mean that central pattern baldness is a problem affecting the extensions of r2/r3 into r1. If the population becomes exclusively r1 it can no longer support scalp hair and central pattern baldness appears. This places the blame for other patterns of baldness upon those specific populations. [Reprinted from Lewis, Warren H (ed). *Gray's Anatomy of the Human Body*, 20th American Edition. Philadelphia, PA: Lea & Febiger, 1918]



arches (muscle and fascia) merely fill in the space below a skin envelope.

We can get some further clues to this biology by looking at the position of eyebrows and nasal hairs. Eyebrows are positioned over the prefrontal and postfrontal bone fields. Recall that formed the upper tetrapod orbit but became absorbed into the frontal bone complex. Eyebrows have a distinct neuromeric zone with distinct behaviors. Hypothyroidism produces hair loss localized to the lateral third of the eyebrow, the zone perfused by StV1 lacrimal artery (Fig. 11.113). At either extreme of the eyebrows, that

is, at the sutures of the ancient pre- and postfrontal bone fields, dermoids can occur, indicating a pinching off of periosteum filled with mesenchyme at those sites. Furthermore, the skin of the upper eyelids is distinct from that of the forehead. The former is strictly r1 whereas the latter is frontonasal skin. In certain individuals, the medial margins of the brow come together in the midline over the nose. This can be ethnic or seen in syndromes such as Waardenburg and Cornelia de Lange. Hair growth seems disorganized over the glabella (Fig. 11.114).

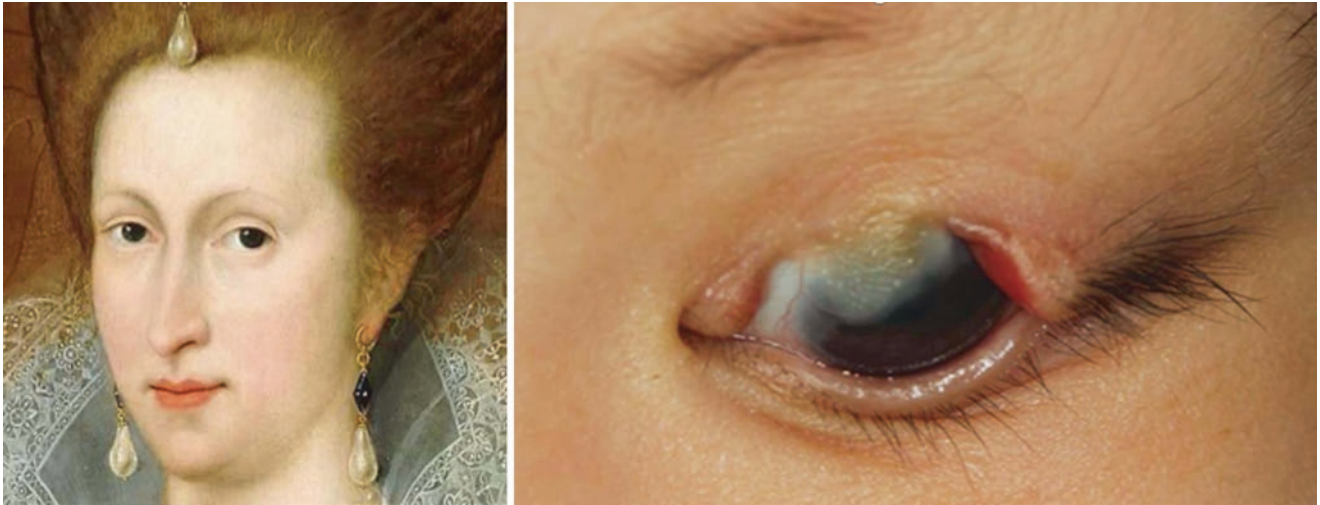


**Fig. 11.113** Eyebrow pathologies reveal neuromeric boundary zones. LEFT: Loss of thinning out of eyebrows can be from system disease. The lateral margin is selectively affected in hypothyroidism, atopic dermatitis, or leprosy. Selective hair loss with hypothyroidism affects the #9 zone based on the StV1 lacrimal neurovascular pedicle. This finding, described by the pioneer Belgian endocrinologist Ludovic Christian Hertoghe, bears his name and has been putatively associated with Queen Anne of Denmark has been (uncertainly) reputed to have suffered from hypothyroidism. RIGHT: Loss of eyebrow hair may be congenital as well and can be associated with dysplasia of eyelashes in the same zone. It is seen here in the medial margin of the #10 cleft zone. The mid zone of the eyelid is also cleft and a cutaneous pterygium is

present. The #10 cleft zone centers around the StV1 supraorbital neurovascular pedicle. It affects the center of the eyebrow and upper eyelid. The lower lid is supplied by the distal branches of StV2 anterior superior alveolar artery, that is, the infraorbital n/v pedicle. Note in the upper eyelid the accumulation of soft tissue, the abnormally long and coarse eyelashes, and the atrophic soft tissue leading upward from the eyelid to the eyebrow. Left: [Reprinted from Wikimedia. Retrieved from: [https://en.wikipedia.org/wiki/Anne\\_of\\_Denmark#/media/File:Anne\\_of\\_Denmark\\_1605.jpg](https://en.wikipedia.org/wiki/Anne_of_Denmark#/media/File:Anne_of_Denmark_1605.jpg)]. Right: [Reprinted from Shao C, Lu W, Li J, Yao Q, Fan X, Fu Y. Manifestations and grading of ocular involvement with Tessier number 10 clefts. *Eye* 2017; 31(8): 1140–1145. With permission from Springer Nature]



**Fig. 11.114** Waardenberg syndrome. *Synophrys* (unibrow) is highly regarded in Iran. This condition is also seen in Waardenburg and Cornelia de Lange syndromes. Note the disorganized directionality of the hairs. Eyebrows demarcate two different embryologic zones of skin, forehead and upper eyelid. Top Left: [Reprinted from Wikimedia. Retrieved from: [https://en.wikipedia.org/wiki/Unibrow#/media/File:Unibrow\\_Close\\_Up.jpg](https://en.wikipedia.org/wiki/Unibrow#/media/File:Unibrow_Close_Up.jpg). With permission from Creative Commons License 3.0: <https://creativecommons.org/licenses/by-sa/3.0/deed.en>].

Bottom Left: [Reprinted from Ghosh SK, Bandyopadhyay D, Ghosh A, Biswas SK, Mandal RK. Waardenburg Syndrome: a report of three cases. *Indian J Dermatol, Venerol Leprol* 2010; 76(5):550–552. With permission from Wolters Kluwer Medknow Publications.]. Right: [Reprinted from Wikimedia. Retrieved from: [https://en.wikipedia.org/wiki/Cornelia\\_de\\_Lange\\_Syndrome#/media/File:Eli\\_CDLS.JPG](https://en.wikipedia.org/wiki/Cornelia_de_Lange_Syndrome#/media/File:Eli_CDLS.JPG). With permission from Creative Commons License 3.0: <https://creativecommons.org/licenses/by-sa/3.0/deed.en>]

Nasal hairs occur precisely at the external nasal valve between the nostril introitus and the caudal margin of the lower lateral cartilage. This marks the junction between nasal skin of the p5 zone and vestibular skin of the p6 zone. Due to V1 innervation, plucking these hairs induces tears (Fig. 11.115). Ear hairs can be vellus within the external auditory canal or coarse outside of the canal. Hypertrichosis is concentrated at the hypaxial c2-c3 lobule and involves the external surface and helical rim, spacing the internal skin of the auricle. This can reach extreme dimensions, referred to as *hypertrichosis lanuginosa acquisita* and is found more frequently in men from India.

## Final Thoughts

In this chapter we have explored the soft tissue coverage of the head and neck based on the neuromeric origins of its epidermis, dermis, and adipose tissue. This has necessitated some detail regarding details of innervation and blood supply. Care has been given to describe the fascial layers clearly, to define their neuromeric basis, and to rationalize the organization of the arterial systems internal and external carotid, stapedia, and subclavian which supply these regions. Attention has been given to the organization and biology of adipose tissue. Finally, phylogenetic and evolutionary aspects of mammalian skin are outlined.



**Fig. 11.115** Eyebrows and nasal hairs as boundary markers. Left: Reprinted from Wikimedia. Retrieved from: [https://commons.wikimedia.org/wiki/File:Nasal\\_hair.jpg](https://commons.wikimedia.org/wiki/File:Nasal_hair.jpg). With permission from Creative Commons License 3.0: <https://creativecommons.org/licenses/by-sa/3.0/deed.en>. Right: Reprinted from Wikimedia. Retrieved from: [https://en.wikipedia.org/wiki/File:Long\\_ear\\_hair\\_on\\_man.png](https://en.wikipedia.org/wiki/File:Long_ear_hair_on_man.png). With permission from Creative Commons License 1.0: <https://creativecommons.org/publicdomain/zero/1.0/deed.en>

## References

- Jennet JP, Moody SA. Establishing the pre-placodal region and breaking it into placodes with distinct identities. *Dev Biol*. 2014;389(1):13–27.
- Patthey C, Schlosser G, Shimeld SM. The evolutionary history of vertebrate placodes I: cell type evolution. *Dev Biol*. 2014;389(1):82–97.
- Pieper M, Ahrens K, Rink E, Peter A, Schlosser G. Differential distribution of competence for neural crest induction to non-neural and neural ectoderm. *Development*. 2012;139:1175–87. <https://doi.org/10.1242/dev.074468>.
- Schlosser G, Patthey C, Shimeld SM. The evolutionary history of vertebrate placodes II. Evolution of ectodermal patterning *Dev Biol*. 2014;389(1):98–119.
- Herbst K. Rare adipose diseases (RADs) masquerading as obesity. *Acta Pharmacol Sin*. 2012;33:155–72. <https://doi.org/10.1038/aps.2011.153>.
- Attwell D, Mishra A, Hall CN, O’Ferrell FM, Dalkarra T. What is a pericyte? *J Cereb Blood Flow Metab*. 2016;36(2):451–5.
- Armulik A, Genové G, Betsholtz C. Pericytes: developmental, physiological, and pathological perspectives, problems, and promises. *Dev Cell*. 2011;21(2):193–216.
- Dore-Duffy P, Morphology CK, properties of pericytes. The blood-brain and other neural barriers. *Methods Mol Biol*. 2011;686:49–68. [https://doi.org/10.1007/978-1-60761-938-3\\_2](https://doi.org/10.1007/978-1-60761-938-3_2).
- Daneman R, Zhou L, Kebede AA, Barnes BA. Pericytes are required for blood-brain barrier during embryogenesis. *Nature*. 2010;468(723):562–6. <https://doi.org/10.1038/nature09513>.
- Caplan AI. Mesenchymal stem cells: time to change the name! *Stem Cells Transl Med*. 2017;6(6):1445–51. <https://doi.org/10.1002/sctm.17-0051>.
- Caplan AI, Correa D. The MSC: an injury drugstore. *Cell Stem Cell*. 2011;9(1):11–5.
- Brown S, Katz AJ. Adipose-derived stem cells. In: Atala A (ed). *Textbook of regenerative medicine* Elsevier, 3<sup>rd</sup> ed. 2019.
- Caplan AI, Dennis C. Mesenchymal cells as trophic mediators. *J Cell Biochem*. 2006;98:1076–84.
- Cahill EF, Kennelly H, Carty F, Mahon BP, English K. Hepatocyte growth factor is required for mesenchymal stromal cell protection against bleomycin-induced pulmonary fibrosis. *Stem Cells Transl Med*. 2016;5:1307–8.
- Cristani B, Marchand-Adam S, Quesnel C, et al. Hepatocyte growth factor and the lung. *Proc Am Thorac Soc*. 2012;9(3):158–63. <https://doi.org/10.1513/pats.201-202-018AW>.
- Ejaz A, Epperly MW, Hou W, et al. Adipose-derived stem cell therapy ameliorates ionizing irradiation fibrosis via hepatocyte growth factor-mediated transforming growth factor *B* down-regulation and recruitment of bone marrow cells. *Stem Cells*. 2019;37:791–802.
- Kapur SK, Dos-Anjos Vilaboa S, Llull R, Katz AJ. Adipose tissue and stem progenitor cells. *Clin Plast Surg*. 2015;42(2):155–67.
- Carstens MH, Correa D, Llull R, Gomez A, Turner E, Valladares LS. Subcutaneous reconstruction of hand dorsum and fingers for late sequelae of burn scars using adipose-derived stromal vascular fraction (SVF). *CellR4* 2015; 3(5): e1675-e1684.
- Carstens MH, Perz M, Briceño H, Valladares S, Correa D. Treatment of late sequelae of burn scar fibrosis with adipose-derived stromal vascular fraction (SVF) cells: a case series. *CellR4*. 2017b;5(3):e204–20.
- Zakhari JS, Zabonick J, Gettler B, Williams SK. Vasculogenic and angiogenic potential of adipose stromal vascular fraction cell populations in vitro. *In Vitro Cell Dev Biol Anim*. 2018;54:32–40. <https://doi.org/10.1007/s11626-017-0213-7>.
- Leng Z, Zhu R, Hou W, et al. Transplantation of ACE2- mesenchymal stem cells improves the outcome of patients with COVID-19 pneumonia. *Aging Dis*. 2020;11(2):216. <https://doi.org/10.14336/AD.2020.0228>.
- Rogers CJ, Harman RJ, Bunnell BA, et al. Rationale for clinical use of adipose-derived mesenchymal stem cells for COVID-19 patients. *Int J Mol Sci*. 2020;19:2532–45.
- Carstens MH, Greco RJ, Hurwitz DJ, Tolhurst DE. Clinical applications of the subgaleal fascia. *Plast Reconstr Surg*. 1991;87(4):615–26.
- Tolhurst DE, Carstens MC, Greco RJ, Hurwitz DJ. Surgical anatomy of the scalp. *Plast Reconstr Surg*. 1991;87(4):603–12.
- Alibardi L. Perspectives on hair evolution based on some comparative studies on vertebrate cornification. *J Exp Zool B Mol Dev Evol*. 2012;318(5):325–43. <https://doi.org/10.1002/jez.b.22447>.
- Poissonet CM, Burdi AR, Bookstein FL. Growth and development of human adipose tissue during gestation. *Early Hum Dev*. 1983;8:1–11.
- Poissonet CM, Burdi AR, Garn SM. Chronology of adipose tissue and its appearance in the human fetus. *Early Hum Dev*. 1984;10:1–11.
- Winkler E, Bull RD, Zlokovic BV. Central nervous systems pericytes in health and disease. *Nat Neurosci*. 2011;14(11):1398–405.

## Suggested Readings

- Ailhaud G. Development of white adipose tissue and adipocytes differentiation. In: Klaus S, editor. *Adipose tissues*. Georgetown: Landes Bioscience; 2001. p. 27–55.
- Alexander RW, Harrell DB. Autologous fat grafting: use of closed syringe microcannula system for enhanced autologous structural grafting. *Clin Cosmet Investig Dermatol*. 2013;6:91–102.
- Alexander RW. Understanding mechanical emulsification (Nanofat) versus enzymatic isolation of tissue stromal vascular fraction (tSVF) cells from adipose tissue: potential uses in biocellular regeneration medicine. *J Prolother*. 2016;8:e947–60.
- Borrelli MR, Shen A, Lee GK, et al. Radiation-induced skin fibrosis: pathogenesis, current treatment options, and emerging therapies. *Ann Plast Surg*. 2019;83:S59–64.
- Broughton M, Fyfe GM. The superficial musculoaponeurotic system of the face: a model explored. *Anat Res Int*. 2013;794682:5. <https://doi.org/10.1155/2013/794682>.
- Caplan AI. Are MSCs pericytes? *Cell Stem Cell*. 2008;3(3):229–30. <https://doi.org/10.1016/j.stem.2008.08.008>.
- Carstens MH, Gomez A, Correa D, et al. Non-reconstructable peripheral vascular disease of the lower extremity in ten patients treated with adipose-derived stromal vascular fraction cells. *Stem Cell Res*. 2017a;18:14–21.
- Chang C, Wu P, Baker RE, Maini PK, Alibardi L, Chuong CM. Reptile scale paradigm: evo-devo, pattern formation and regeneration. *Int J Dev Biol*. 2009a;53(5–6):813–26.
- Chang C, Wu P, Baker RE, Maini PK, Alibardi L, Chuong C-M. Reptile scale paradigm: evo-devel, pattern formation, and regeneration. In *J Dev Biol*. 2009b;53(5–6):813–26. <https://doi.org/10.1387/ijdb.072556cc>.
- Dhouailly D, Godefroit P, Martin T, Nonchev S, Carguel F, Oftedal O. Getting to the root of scales, feather and hair: as deep as odontodes? *Exp Dermatol*. 2019;28:503–8. <https://doi.org/10.1111/exd.13391>.
- Drake PM, Franz-Odenaall T. A potential role for MMPs during the formation of non-neurogenic placodes. *J Dev Biol*. 2018;6:20. <https://doi.org/10.33090/jdb6030020>.
- Friedenstein AJ, Deriglasova UF, Kulagina NN, Panasuk AF, Rudakowa SF, Luriá EA, Ruadkow IA. Precursors for fibroblasts in different populations of hematopoietic cells as detected by the in vitro colony assay method. *Exp Hematol*. 1974;2(2):83–92.
- Gesta S, Tseng Y-H, Kahn CR. Developmental origins of fat: tracking obesity to its source. *Cell*. 2007;131:242–56. <https://doi.org/10.1016/j.cell.2007.10.004>.
- Giannandrea M, Parks WC. Diverse functions of matrix metalloproteinases during fibrosis. *Dis Model Mech*. 2014;7:193–203.
- Guarrera M, Cardo P, Arrigo P, Rebora A. Reliability of Hamilton-Norwood classification. *Int J Trichol*. 2009;1(2):120–2.
- Guo J, Nguyen A, Banyard DA, et al. Stromal vascular fraction: a regenerative reality? Part 2: mechanisms of regenerative action. *J Plast Reconstr Aesthet Surg*. 2016;69:180–8.
- Hartman DA, Underly RG, Grant RI, et al. Pericyte structure and distribution in the cerebral cortex revealed by high-resolution imaging of transgenic mice. *Neurophotonics*. 2015;2(4):041402. <https://doi.org/10.1117/1.NPh.2.4.041402>.
- Isaka Y. Targeting TGF- $\beta$  signaling in kidney fibrosis. *Int J Mol Sci*. 2018;19:2532–45.
- Kalev-Altman R, Monsonegro-Oman E, Sela-Donnenfeld D. The role of matrix metalloproteinases MMP2 and MMP9 in embryonic neural crest cells and their derivatives. In: Chakraborti S, Dhalla NS, editors. *Proteases in physiology and pathology*. Springer; 2017. p. 27–48. [https://doi.org/10.1007/978-981-10-2513-6\\_2](https://doi.org/10.1007/978-981-10-2513-6_2).
- Khazaeni K, Rajati M, Shahabi A, Mashadi L. Use of sternocleidomastoid myocutaneous flap based on the sternocleidomastoid branch of the inferior thyroid artery to reconstruct extensive cheek defects. *Aesthet Plast Surg*. 2013;37(6):1167–70. <https://doi.org/10.1007/s00266-013-0216-z>.
- Ligia L, et al. Multiple doses of adipose tissue-derived mesenchymal stromal cells induce immunosuppression in experimental asthma. *Stem Cells Transl Med*. 2020;9:250–60. <https://doi.org/10.1002/sctm.19-0120>.
- Mitz V, Peyronie M. The superficial musculo-aponeurotic system (SMAS) in the parotid and cheek area. *Plast Reconstr Surg*. 1976;58(1):80–8.
- Nguyen A, Guo J, Banyard DA, et al. Stromal vascular fraction: a regenerative reality? Part 1: current concepts and review of the literature. *J Plast Reconstr Aesthet Surg*. 2016;69:170–9.
- Mok K-W, Saxena N, Heitman N, et al. Dermal concentrate niche specification occurs prior to formation and is placode progenitor dependent. *Dev Cell*. 2019;48:32–48. <https://doi.org/10.1016/devcel.2018.11.034>.
- Pispa J, Thesleff I. Mechanisms of ectodermal organogenesis. *Dev Biol*. 2003;262:195–205. [https://doi.org/10.1016/S0012-1606\(03\)00325-7](https://doi.org/10.1016/S0012-1606(03)00325-7).
- Pardo A, Cabrera S, Maldonado M, Selman M. Role of matrix metalloproteinases in the pathogenesis of pulmonary fibrosis. *Respir Res*. 2016;17:23–33.
- Stout AP, Murray MR. Hemangiopericytoma: a vascular tumor featuring Zimmermann's pericytes. *Ann Surg*. 1942;116(1):26–33. <https://doi.org/10.1097/0000658-194207000-00004>.
- Tonnard P, Verpaele A, Peeters G, Hamdi M, Cornelissen M, Declercq H. Nanofat grafting: basic research and clinical applications. *Plast Reconstr Surg*. 2013;132(4):1017–26. <https://doi.org/10.1097/PRS.0b013e31829fe1b0>.
- Wu P, Hou L, Plikus M, Hughes M, Scehnet J, Suksaweang S, Wideltz RW, Chuong C-M. Evo-devo of amniote integuments and appendages. *Int J Dev Biol* 2004;48:249–270. [PubMed: 15272390].
- Xu S, Liu C, Ji H-L. Concise review: therapeutic potential of the mesenchymal stem cell derived secretome and extracellular vesicles for radiation-induced lung injury: progress and hypotheses. *Stem Cells Transl Med*. 2019;8:344–54.
- Yagi LH, Watanuki LM, Issac C, et al. Human fetal wound healing: a review of molecular and cellular aspects. *Eur J Plast Surg*. 2016;39:239–46.
- Zuk PA, Zhu M, Mizuno H, Huang J, Futrell JW, Katz AJ, Benhaim P, Lorenz HP, Hedrick MH. Multilineage cells from human adipose tissue: implications for cell-based therapies. *Tissue Eng*. 2001;7:211–28.